Modulus-Based Construction Specification for Compaction of Earthwork and Unbound Aggregate

DRAFT FINAL REPORT

Prepared for
National Cooperative Highway Research Program
NCHRP Project 10-84

Transportation Research Board
of
The National Academics

Submitted by:

Soheil Nazarian, PhD, PE, Mehran Mazari, PhD, and Imad Abdallah, PhD
Center for Transportation Infrastructure Systems
The University of Texas at El Paso
500 West University Avenue, El Paso, TX 79968

Anand J. Puppala, PhD, PE
Department of Civil and Environmental Engineering
The University of Texas at Arlington, Arlington, Texas 76019

Louay N. Mohammad, PhD and Murad Y Abu-Farsakh, PhD
Louisiana Transportation Research Center
Louisiana State University
4101 Gourrier Ave., Baton Rouge, LA 70808

August 2014

ACKNOWLEDGEMENT OF SPONSORSHIP AND DISCLAIMER

This work was sponsored by the American Association of State Highway and Transportation Officials, in cooperation with the Federal Highway Administration, and was conducted in the National Cooperative Highway Research Program, which is administered by the Transportation Research Board of the National Academies.

TABLE OF CONTENTS

LIST OF FIGURES

LIST OF TABLES

CHAPTER 1 - INTRODUCTION

1.1 Problem Statement

The performance of a pavement depends on many factors such as its structural adequacy, the properties of the materials used, the construction method, and climatic conditions. Earthwork and unbound aggregates, collectively called compacted geomaterials hereafter, generally represent a significant portion of the construction of pavements. Pavement distress, particularly for flexible pavements, can be traced to problems in those materials. The performance of a pavement can only be assured with appropriate process control to ensure the material used is similar to the one selected, proper processing of the material to ensure that the material is uniformly mixed and contains an appropriate amount of moisture before compaction, and adequate compaction equipment to ensure proper density and stiffness. The primary tool for quality management—to ensure that appropriate density is achieved—is currently a nuclear density gauge (NDG). Despite the importance of the moisture content at the time of compaction to the quality of the final product, a number of highway agencies have not included moisture content in their specifications.

1.2 Objectives

The objective of this research was to develop a modulus-based construction specification for acceptance of compacted geomaterials that considers the following constraints:

1- The specification should be based on field measurement of modulus and moisture content.
2- Acceptance criteria should be correlated with design moduli.
3- The specification should be compatible with a variety of compacted geomaterials.
4- The specification should consider the principles of unsaturated soil mechanics.
5- Available models, devices, and methods should be incorporated in the specification.
6- The validity and practicality of the proposed specification should be documented by its use as a shadow specification for a number of actual construction projects.

1.3 Ideal Quality Management Process

Adequate in-place density and moisture content and their uniformity during compaction are vital to the success of compacted geomaterials. However, satisfying these criteria may not necessarily yield adequate modulus. To provide continuity among the design, construction, and laboratory testing, it is desirable to migrate from the traditional specifications to a rigorous modulus-based approach. This approach may ideally follow the flow chart in Figure 1.3.1.

Several inter-related parameters have to be considered in such a specification. Structural design software should be considered from the beginning so that the level of sophistication of the pavement design, laboratory testing, and field testing can be balanced. The construction specification should be ideally tied to a mechanistic-empirical design algorithm.

Achieving adequate modulus will not assure the constructability and durability of a compacted geomaterial. The source of the material for each layer, either in-place or imported, should be identified, and its suitability for a durable layer should be ascertained.

A design modulus of each layer should be estimated preferably based on modulus measurements considering field compaction effort and moisture conditions. Depending on the level of sophistication of the analysis and budgetary constraints, moduli can be estimated from either empirical relations, or presumptive default values, or a catalog of values established for common local geomaterials. Target modulus should be set in conjunction with establishing the design modulus considering the moisture content at the time of compaction and moisture content and density at the time of testing.

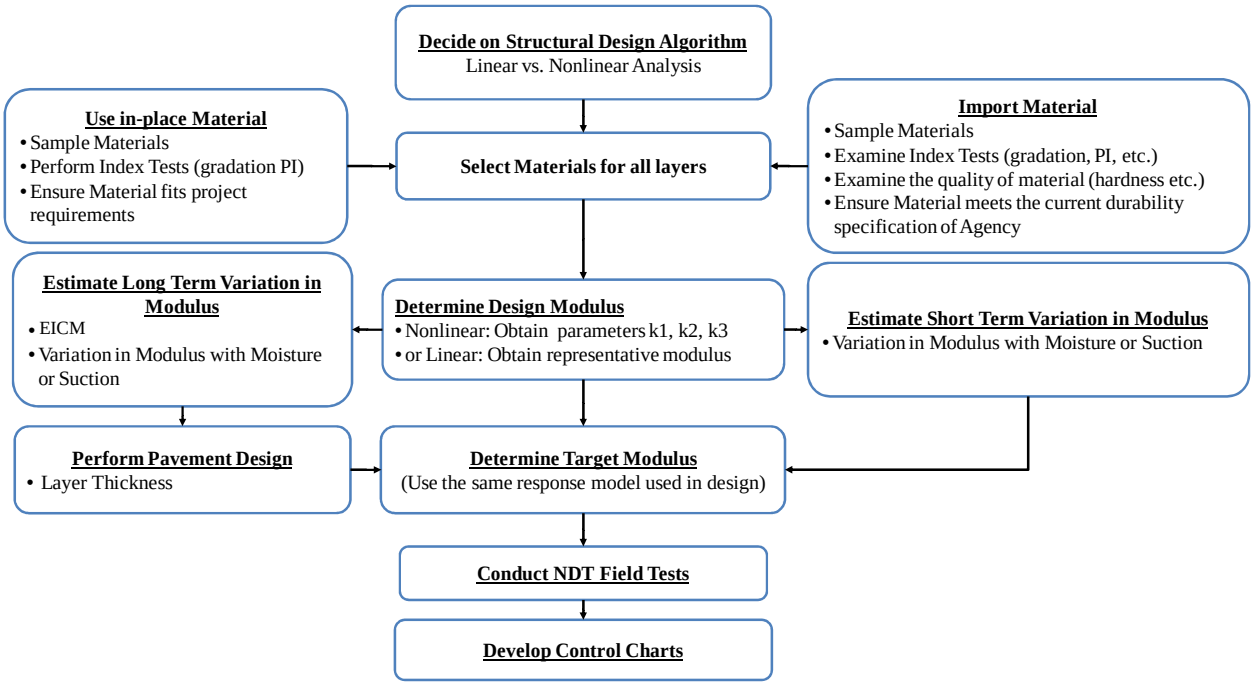

Figure 1.3.1 - An Ideal Flowchart of Modulus-based Specification

Field moduli should be measured during construction with an appropriate device to ensure that the target modulus has been achieved. The appropriate equipment for this purpose should have the following four attributes:

1. measure fundamental properties of materials (i.e., modulus),
2. sensitive enough so that poor and high quality materials can be readily delineated,
3. accurate enough to provide feedback to the pavement designer, and
4. precise enough so that it can be confidently used in the acceptance process.

Appropriate statistical analysis (e.g., using control charts) should be carried out to ensure that the modulus and its variability along the project are in control. Appropriate tolerances should be allowed based on the uncertainties in establishing the target modulus and measurement device to minimize any disputes between the contractor and the highway agency.

The process described above sets the theme for different activities carried out in this study in order to develop a specification.

1.4 Overview of Research Activities

The flow chart in Figure 1.3.1 and the results of a survey of highway agencies were used as the guiding principles in developing a modulus-based specification. The major issues requiring further study are discussed below.

1.4.1 Estimating Modulus of Geomaterial for Design

Ideally, the modulus of the material should be determined by conducting laboratory resilient modulus tests before the structural design of the pavement, as proposed for the Level 1 design with the MEPDG. Most highway agencies may not have the resources to conduct these tests routinely, and may choose to estimate those parameters. Accurate determination of the variation in modulus with moisture content is also important. It would be more cost effective to utilize empirical models rather than measuring the variation in modulus with moisture content. The concerns that were addressed in this project include the following items:

- Representative models for estimating the moduli of different geomaterials, and
- Representative models for estimating the variations in modulus with moisture content of different geomaterials.

1.4.2 Selecting Target Field Moduli

Most modulus-based devices measure the stiffness of the pavement system. The estimated moduli with these devices are based on single-layer Boussinesq theory. The target modulus should be set considering the following parameters:

- Structural analysis model utilized (linear or nonlinear),
- Thickness of the layer being tested and the subsequent layers below it, and
- Design moduli of the layer being tested and the layers below it.

Furthermore, the modulus of the layer being tested should be adjusted for relative compactions other that 100% and allowable tolerances in field moisture contents permitted by different highway agencies. The concerns that were addressed in this project include the following items:

- Best approach for determining target moduli based on structural analysis model and layer thicknesses,
- Representative models for estimating the variation in modulus with density, and
- Representative models for estimating the variation in modulus with moisture content.

1.4.3 Field Quality Control

Field quality control consists of conducting modulus-based tests with an appropriate tool at a number of points for a specified lot. A moisture measuring device should be used concurrent with the modulus measuring device to obtain the in-place moisture content. The measured moisture content can be used to adjust the measured modulus to a common moisture content (say optimum moisture content). The field and laboratory moduli may be different at the same moisture content and density due to differences in compaction processes. The concerns that were addressed in this project include the following items:

- Appropriate tools for measuring modulus and moisture content,
- Representative models for adjusting the measured field modulus based on in situ moisture content and density, and
- Appropriate models to relate field and laboratory moduli at the same moisture content and density.

1.4.4 Acceptance Process

A fair and equitable acceptance process requires appropriate tolerances based on the uncertainties in establishing the target modulus and the measuring devices. The topics that were researched are the following:

- Verifying the accuracy and versatility of candidate moisture and suction prediction models,
- Verifying the accuracy, applicability, and versatility of the candidate moisture and modulus devices selected,
- Developing and validating algorithms for estimating the target modulus as a function of the design modulus, loading characteristics of the device, thickness of the layer, moduli of underlying layers, and a transfer function between the laboratory and field measured moduli, and
- Generating adequate data for developing practical acceptance tolerances to accommodate the inevitable variability in the moisture content and degree of compaction by even conscientious contractors.

1.5 Research Approach

To address the objectives and goal of this project, the research was divided into three phases. Phase I (Documentation) consisted of documenting, synthesizing, prioritizing and conducting gap analyses on the following topics:

1. National and international state of practice in modulus-based quality management.
2. Devices for rapidly measuring relevant field parameters for a modulus-based specification.
3. Site variability in terms of material, moisture, thickness and compaction inconsistencies
4. Long-term moisture content variation models, and
5. Modulus-moisture content prediction models.

The main outcome of Phase I activities, was a systematic work plan for developing and validating a practical yet scientifically sound specification with the following characteristics:

- Identifying the most relevant parameters that should be included in the specification,
- Recommending the practical and desirable tolerances for relevant parameters,
- Suggesting the most appropriate device(s) for rapidly measuring relevant parameters, and
- Establishing the optimum frequency of measurement of each parameter that balances the risks of highway agencies and contractors.

Phase II activities primarily consisted of implementing the Phase I work plan to develop the specification. A draft copy of the proposed specification is provided in Appendix A. The focus of that phase was on describing the process and results obtained in support of the proposed preliminary specification.

Phase II work contained laboratory, small-scale and field testing programs. This three-prong approach was followed to separate a number of complex and inter-related issues into several well-defined hypotheses that, when combined, can provide a practical and scientifically sound specification.

1.5.1 Laboratory Study

Laboratory tests were conducted under precise moisture contents and densities on half-dozen geomaterials. The tests carried out and the anticipated outcomes are shown in Table 1.5.1. These results provided a database that was used to respond to a number of questions that are included in the table.

1.5.2 Small-Scale Study

Four 3-ft-diameter by 2-ft-deep specimens were constructed from each geomaterial (see Figure 4.2.1). The moisture contents and densities of all layers were strictly controlled as discussed in Chapter 4. The characteristics of specimens and the reasons for selecting them are shown in Table 1.5.2. Through these experiments, the impacts of a number of construction-related parameters were established. In addition, the specimens were used for the following purposes:

- Establishing characteristics (repeatability and reproducibility) of modulus and moisture devices,
- Establishing direct relationship between field and laboratory moduli at the same moisture and density conditions, and
- Calibrating the structural models with data collected from sensors embedded in the specimens.

1.5.3 Field Study

Field variability during actual construction processes brings another level of uncertainty that cannot be considered in the small-scale specimens. To incorporate such variability in the development of the specification, a 180-ft-long section was constructed and divided into three subsections with nominal moisture contents of OMC, OMC-2% and OMC+2%. The variability in the in-situ density and moisture content of each subsection was compared with the corresponding variability of modulus-based tests. In addition, the utility of the specifications in Appendix A was evaluated.

Table 1.5.1 - Experiment Design for Laboratory Tests

Test Method/Samples	Outcome
1. Modulus tests at • OMC • OMC±1% or OMC±10%OMC (if OMC>10%) • OMC±2% or OMC±20%OMC (if OMC>10%)	• Determine moduli and their variations with moisture under constant compaction energy. • Validate selected moisture modulus relationships
2. Modulus tests on specimens that are ***compacted to MDD*** by varying compaction energy through trial and error to simulate the construction process at • OMC±1% or OMC±10%OMC (if OMC>10%) • OMC±2% or OMC±20%OMC (if OMC>10%)	• Compare results from Items 1 and 2 to evaluate impact of moisture content at the time of compaction on modulus. • Develop relationships between moduli at the same moisture content from Items 1 and 2 in an attempt to explain differences between traditional compaction and a process that is more representative of the field • Document significance of moisture content on modulus for setting tolerances for moisture control during compaction. • Validate selected moisture modulus relationships
3. Place specimens similar to Item 1 in a 100°F oven and dry back to OMC-3% and test daily to establish modulus variation with time and moisture 4. Place specimens similar to Item 1 under capillary moisture conditioning and test daily until saturation to establish modulus variation with moisture	• Compare results from Items 1, 2 and 3 to evaluate impact of moisture content at the time of testing relative to the moisture content at compaction on modulus for setting tolerances for time to perform acceptance tests • Compare results from Items 1 and 4 to validate long-term moisture modulus relationships
5. Prepare specimens at ***relative compaction of 98% and 96% all at OMC*** and perform modulus tests	• Compare results from Items 1 and 5 to evaluate impact of density on modulus for setting tolerances on modulus considering current density requirements of DOT's
6. Repeat Item 1 but with suction control tests. 7. Determine soil water characteristic curve for each soil.	• Analyze effects of suction and moisture content on modulus • Evaluate feasibility of using moisture content or degree of saturation as a surrogate for suction

MDD = maximum dry density, OMC = optimum moisture content

Table 1.5.2 - Experiment Design for Small-Scale Tests

Item	Experiment Goal	Specimen Characteristics*		When to Perform Evaluation Tests
		Moisture	Density	
1	Determine impact of compaction moisture content at constant density on modulus	**OMC**	**MDD**	after 24, 48 hrs
		OMC+2%**	**MDD**	
		OMC-2%**	**MDD**	
2	Determine impact of moisture content at time of testing relative to moisture content at compaction on modulus (same specimens as Item 1)	OMC+2%	MDD	at OMC+1%, OMC, OMC–1% and OMC–2%
		OMC	MDD	at OMC–1% & OMC–2%
3	Determine impact of density on modulus	OMC	MDD	at OMC–1% & OMC–2%
		OMC	**96% MDD**	
4	Determine impact of subgrade stiffness on modulus	**OMC**	**MDD**	24, 48 hrs after saturation of subgrade

* Highlighted cells represent unique specimens; four specimens per selected geomaterial were prepared.
** For materials with OMC greater than 10%, used OMC+ 20%OMC or OMC – 20%OMC

Phase III consisted of implementing a work plan for validating and fine-tuning the proposed specification. Six sites distributed in the four environmental regions of the US were visited to obtain as many different geomaterial types, environmental conditions and construction and quality control procedures as possible. Phase III activities were carried out in two stages.

Stage I consisted of documenting the shortcomings and improving the specification at three sites. The research team collected relevant field data, conducted proposed laboratory tests, performed appropriate analyses and compared the results with the proposed specifications.

Stage II consisted of validating the specification as a shadow specification at three sites. The research team worked hand-in-hand with highway agencies to implement the specification by training agency personnel to conduct the tests (if needed), leaving the equipment with them to collect the data and interpret the results as well as obtain the opinion of the agency personnel on the practicality and complications of the proposed specification.

1.6 Organization of the Report

Aside from this chapter, this report contains nine chapters. *Chapter 2* contains a general background on definitions of moduli and factors that affect the modulus. Different modulus and moisture measurement devices are also introduced in that chapter. In addition, different structural and material models that can be used are discussed. This chapter also contains the results of a survey distributed among DOT's, and a discussion of the issues that were considered important and the approaches taken to address them.

Chapter 3 contains the results and analyses of laboratory work related to selecting of the appropriate material models and incorporating appropriate moisture/suction prediction models in the specification.

The results and analyses of small-scale tests are included in *Chapter 4*. Material and moisture models obtained from these tests are also related to those from the laboratory activities to develop appropriate transfer functions among them.

The modulus and moisture measurement devices are evaluated in *Chapter 5* to establish the uncertainties in their measurements and their practicality for day-to-day use.

Various structural models are evaluated and validated in *Chapter 6*. The process of estimating the target moduli in harmony with the pavement design parameters is also provided.

Chapter 7 contains the results and analyses of a field evaluation program to understand the implications of moisture and density variations associated with actual construction projects on the robustness of the specification.

Chapter 8 includes a summary of findings from implementation of the proposed specification in order to validate the practicality of the draft specification.

Chapter 9 summarizes the conclusion, remarks and recommendations drawn from different stages of the study. It includes the proposed modulus-based quality management process along with the rationale for incorporating different items in the draft specification. This chapter also discusses the limitations of the proposed process and suggestions for smooth implementation of the specification.

CHAPTER 2 - BACKGROUND

2.1 Introduction

This chapter contains a summary of the information gathered from the literature on the processes and tools for modulus-based quality management of compacted geomaterials. *In situ* test devices, which provide rapid stiffness/modulus measurements, have been studied extensively. Puppala (2008) and Nazzal (2014) contain a synthesis of the existing tools. Tutumluer (2013) includes a synthesis of practices for unbound aggregate pavement layers. Von Quintus et al. (2009), as part of NCHRP Project 10-65, investigated the application of existing nondestructive testing (NDT) technologies for measuring the quality of flexible pavements. That project suggested NDT technologies appropriate for implementation in routine and practical quality control/quality assurance (QC/QA) operations. A synopsis of the most common tools used for quality management of compacted geomaterials is included in Appendix B.

2.2 Modulus of Compacted Geomaterials

It is beneficial to distinguish between the terms "modulus" and "stiffness." As reflected in Figure 2.2.1, modulus is the ratio of a measured strain and an applied stress. Modulus of a material can vary between an initial tangent modulus, E_{max}, to a secant modulus (E_1 through E_3) depending on the magnitude of stresses applied. Stiffness, which is defined as the deformation of a material under an applied load, is not a unique material property but the response of a pavement system to load. With different levels of approximation, the modulus can be estimated from the stiffness given the layer properties, the dimensions of applied load, and a model that estimates the response of the pavement system.

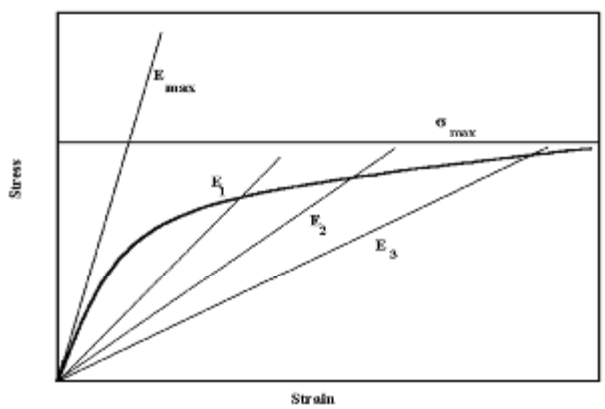

Figure 2.2.1 - Definitions of Modulus

The modulus of a layer can either be measured with field or laboratory testing, or can be estimated based on empirical relationships. Empirical relationships, which are typically based on the index properties of geomaterials, can be used in the design stages as a first approximation. Due to the general nature of these relationships and inherent variability in the geomaterials, the level of uncertainty in these estimated values is rather high.

Modulus measurement tests are essential for studying the parameters that affect the properties of materials. The behavior of a material in terms of variation in modulus with stress level, strain amplitude, and the strain rate is best established by conducting laboratory tests such as the resilient modulus test. However, moduli from laboratory tests are moderately to significantly different from the in situ results (e.g. the moduli from FWD test). An example of such variations is demonstrated in Table 2.2.1 from data extracted from the long-term pavement performance (LTPP) database. These differences can be due to sampling disturbance, differences in the state-of-stress between the specimen and in-place material, long-term time effects, and inherent errors in the field and laboratory test procedures (Anderson and Woods, 1975).

Since the resilient modulus tests are perceived as complex and time-consuming, simple methods (such as the free-free resonant column and bender elements) have been proposed for estimating the moduli of geomaterials in the laboratory (Puppala, 2008). It is also not uncommon to estimate the modulus from strength test results, such as the unconfined compressive strength or California Bearing Ratio (CBR).

Table 2.2.1 - Typical Differences between Laboratory Resilient Modulus and Field FWD Moduli (Von Quintus and Killingworth, 1998)

Layer Description	Ratio of Laboratory Resilient Modulus and Field FWD Modulus		
	Mean	Standard Deviation	Coefficient of Variation, %
Granular Base/Subbase under a PCC Surface	1.32	0.98	74.1
Granular Base/Subbase above a Stabilized Material	1.43	1.14	79.9
Granular Base/Subbase under an Asphalt Concrete Surface/Base	0.62	0.27	43.8
Subgrade Soil under a Stabilized Subgrade	0.75	0.09	12.7
Subgrade Soil under a Pavement Without a Granular Base	0.52	0.18	34.6
Subgrade Soil Under a Pavement with a Granular Base/Subbase	0.35	0.18	52.2

Field tests are more practical and more desirable because they are rapid to perform, and because they test a large volume of material in its natural state. Field tests typically fall into two categories: material characterization and design simulation. The goal in material characterization is to measure fundamental material properties (e.g., moduli). These material properties are combined with appropriate analytical or numerical models (and often, additional laboratory and field tests) to obtain the design parameters. The design simulation consists of experimentally simulating the design condition in order to backcalculate material parameters that are relevant to that condition. These methods usually measure the response (typically the stiffness) of the pavement system. As an example, seismic methods fall under material characterization (provide linear-elastic modulus); whereas the deflection-based methods fall under design simulation (provide an “effective modulus”).

Both approaches have advantages and disadvantages. In the design simulation, the state of stress applied to a geomaterial is similar to those from vehicular traffic. However, since the state of stress in the pavement depends on the moduli of the layers, it would be difficult to apply measured moduli from one pavement structure to another with different layer thicknesses or underlying layers. The moduli that resemble material characterization can be used universally, but they have to be tied to a pavement design model.

Moduli can also be estimated from soil index properties such as gradation and plasticity or surrogate field tests. Most models exhibit poor predictive power when they are tested on soils that are not used to develop the relationships (Von Quintus and Killingsworth, 1998). Practically speaking, it may never be possible to develop a universal correlation that can be used nationally. However, it may be feasible for each highway agency to develop soil-specific relationships for their most common geomaterials.

2.3 Factors Affecting Modulus of Compacted Geomaterials

There is a consensus on the major factors that could affect the modulus of geomaterials (Puppala, 2008). These factors generally include the stress state, moisture content (including degree of saturation or suction), stress history, density, gradation and Atterberg limits.

State of Stress: Even though simple in concept, the dependency of the modulus on the state of stress brings about the following practical complications in the context of this research:

- The modulus or stiffness of a geomaterial placed in a pavement section is not a unique value and depends on the underlying or overlying layers, or both.

- The state of stress of a geomaterial placed in a pavement section can only be estimated if the moduli of all layers are known. As such, the estimation of the target modulus based on the design modulus has to be carried out iteratively using a numerical structural model.
- The sophistication of the structural model affects the design and target moduli.

Moisture Content: Excellent reviews of the impact of the moisture content on modulus can be found in Richter (2006), Cary and Zapata (2010) and Siekmeier (2011). An increase in moisture content will typically decrease the matric suction, will increase the resilient deformation, and hence will decrease the modulus. Several recent studies have demonstrated that the difference between the moisture content at compaction and testing impacts the modulus more than the moisture content at the time of compaction (Khoury and Zaman, 2004, Pacheco and Nazarian, 2011).

Density: A strong correlation between modulus and density has not been observed in many field studies (Mooney et al., 2010; and Von Quintus et al., 2010). Pacheco and Nazarian (2011) attributed the lack of a strong correlation to the complex interaction between the moisture content, density, and degree of saturation of a given material.

Gradation and Plasticity: The impact of gradation and plasticity on modulus have been extensively qualified (Richter, 2006; Puppala, 2008) and to a lesser extent quantified. In general, as the plasticity of the material or the percent fines increases, the modulus decreases.

Long-term and Short-term Behaviors of Geomaterials: The short-term behavior of compacted geomaterials along a drying path is of interest for quality management. The increase in moisture during construction is usually due to precipitation, which will interrupt the construction and may require re-compaction of the layer. Wetting and drying paths are needed in order to characterize the long-term behavior of in-service pavements. Significant work has been done to predict the long-term changes in the moisture content/suction and modulus of the compacted geomaterials under in-service pavements. However, the amount of work related to short-term behaviors of exposed geomaterials has been limited to a few studies such as Khoury and Zaman (2004) and Pacheco and Nazarian (2011).

The Enhanced Integrated Climatic Model (EICM) is an integral part of the MEPDG, and perhaps the most common algorithm used for predicting the long-term changes in the modulus of compacted geomaterials. Zapata and Houston (2008) incorporated new empirical relationships into the EICM for predicting the change in moisture content with time from climatic information and estimating the soil-water characteristic curve (SWCC) from the soil index properties. Studies that are more recent have focused on the combined effects of suction and mechanical stress as proposed in unsaturated soil mechanics (Gupta et al., 2007; Liang et al., 2008; Sawangsuriya et al., 2009). These studies generally reported more consistent trends between the resilient modulus and suction (as opposed to the degree of saturation or water content).

2.4 Modulus-Based Devices

Table 2.4.1 contains a list of most common portable modulus-based devices available in the market. These devices include the Briaud compaction Device (BCD), Clegg Impact Hammer (CIH), Dynamic Cone Penetrometer (DCP), Electro-Mechanical Stiffness Device (Geogauge), Lightweight Deflectometer (LWD), and Portable Seismic Property Analyzer (PSPA). A detailed compilation of the literature review for each device is included in Appendix B. Based on the analysis of the information in Appendix B, the most common advantages and disadvantages of each device are summarized in Table 2.4.1.

Von Quintus et al. (2009) conducted a utility analysis to objectively evaluate NDT technologies. The same process is followed in this study as reflected in Appendix B. The results of that analysis are summarized in Table 2.4.2. The devices considered in this study are DCP, Geogauge, LWD and PSPA. The Falling Weight Deflectometer (FWD) was not considered since most highway agencies own few of them, and the logistics of the statewide implementation of this device may be problematic. In addition, LWDs work on the same principles at a small fraction of the FWD cost. Plate bearing test was also not

included; many DOTs have moved away from this test because of the time necessary to perform the test and the popularity of the FWD.

The intelligent compaction (IC) technology is also a viable option for process control. Mooney et al. (2010) developed specifications for incorporating IC in earthwork. The evaluation and implementation of IC technology are outside the scope of this project.

Table 2.4.1 - Advantages and Disadvantages of Modulus-Based Devices

Device	Description	Advantages	Disadvantages
Briaud compaction Device (BCD)	BCD measures the bending strain of a plate resting on the ground surface as an indicator of the modulus of geomaterials. The BCD works by applying a small load to a thin plate in contact with the compacted soil of interest and recording the resulting strains**.**	BCD can be used in the laboratory to obtain a target modulus and in the field to verify that the target modulus has been achieved.	Works on geomaterials with moduli up to 22 ksi (150 MPa) which eliminates most unbound base materials.
Clegg Impact Hammer (CIH)	CIH measures the deceleration of a free falling mass or hammer from a set height onto a surface under test that is converted to strength/stiffness of geomaterial.	CIH is simple to operate and correlations with CBR values are available.	Possibility of boundary effects when calibrating with Proctor molds. Not strictly a stiffness/ modulus measuring device.
Dynamic Cone Penetrometer (DCP)	DCP test involves driving a cone shaped probe into a geomaterial and measuring advancement of the device for several intervals of hammer drops. The rate of penetration of the probe is used to obtain layer thicknesses and moduli.	Adapted by selected agencies in QA operations. Does not require extensive support software for evaluating test results. Can test multi-layers.	Takes time to perform a test. Not strictly a stiffness/modulus measuring device as the penetration rate has to go through two levels of empirical correlations to estimate modulus. Not valid in very coarse geomaterials.
Electro-Mechanical Stiffness Device (Geogauge)	Geogauge provides stiffness property of a geomaterial by measuring applied force and resulting displacement induced by a small harmonic oscillator operating over a frequency of 100 to 200 Hz.	Acceptable success rate in identifying areas with different physical conditions or anomalies. Simple training. Provides a reasonable estimate of laboratory-measured moduli with proper calibration.	Intimate contact between Geogauge and soil is difficult to achieve without thorough site preparation. Moduli do not represent stress levels that occur under truck loading. Underlying materials can influence results especially for relatively thin unbound layers.
Portable Falling Weight Deflectometer (PFWD)	PFWD operates in a similar fashion to the FWD with one to three sensors. The FWD analysis method is applicable to PFWD as long as three sensors are used. PFWD with one sensor is often used with a so-called “forward-calculation” to estimate stiffness of the layer.	State of stress is closer to vehicular stresses than any other device. Pavement community is familiar with concept of deflection-based testing.	Unable to consistently identify areas with anomalies. Underlying materials can influence results especially for relatively thin unbound layers. Any error in thickness of the layer being tested can result in large errors and variability in modulus.
Portable Seismic Property Analyzer (PSPA)	PSPA consists of two accelerometers and a source packaged into a hand-portable system. PSPA measures the linear elastic average modulus of a layer based on generating and detecting stress waves.	Measures layer-specific modulus independent of thickness of layer. No back-calculation necessary. High success rate in identifying areas with different physical conditions or anomalies. Results can be calibrated to specific material being tested prior to construction when M-D relationship is measured in laboratory.	Need to calibrate the test results to the material and site conditions under evaluation. User-friendliness may be a concern.. Lowest repeatability, with a high standard deviation due to capability to detect anisotropic conditions.

Table 2.4.2 - Ranking of Parameters Considered in Evaluation of Modulus Measuring Devices

Device		DCP	Geogauge	LWD	PSPA
Applicability to the goals of this project	Ability to harmonize pavement design parameters and field measurements	1	3	3	3
	Ability to make layer specific measurements	5	3	3	3
Suitability of device	Ability to detect construction defects	1	3	3	3
	Repeatability, precision and sensitivity of device	1	3	3	3
Practicality of the device	Applicability of the device to different types of compacted geomaterials	3	3	5	3
	Availability of commercial equipment	5	5	5	5
	Equipment reliability and ruggedness	5	5	5	5
	User-friendliness	5	3	3	3
	Expertise needed for data collection and interpretation	5	3	5	3
	Initial and Operational Costs	1	5	3	3
Overall ranking with 5 being ideal device		**3.2**	**3.6**	**3.8**	**3.4**

2.5 Moisture Measuring Devices

The nuclear density gauge (NDG) is still the most widely used device for this purpose. The field of measuring moisture and density with non-nuclear devices is evolving quite rapidly. Improvements to software and hardware are also being implemented on a number of existing devices. A few devices that estimate the moisture content, density, or both, of the compacted geomaterials are included in Table 2.5.1. The devices that are described in detail in Appendix B include Soil Density Gauge (SDG), Electrical Density Gauge (EDG), M+DI device, and Speedy Moisture Tester (SMT). A device called Road-Bed Water Content Meter (DOT600) has been recently introduced to the market. A recent study sponsored by Minnesota DOT (MnDOT) showed that the DOT600's sensor output period values exhibited a strong correlation with water content (Hansen and Nieber, 2013). A number of less used and known devices are also available (Sebesta et al., 2012). The results of the utility analysis of moisture devices are summarized in Table 2.5.2. The devices considered in this study are SDG, SMT and DOT600. Berney et al (2011) also conducted a comprehensive evaluation of many of moisture measuring devices.

Zapata et al. (2009) contains an excellent review of the suction measurement technologies. The advantages and disadvantages of a number of suction devices are summarized in Table 2.5.3. Even though it is desirable to measure the suction (as opposed to moisture content), none of these devices are currently ready for in situ measurements during QA activities. In addition, based on the survey, highway agencies are not eager to move toward measuring suction directly.

2.6 Structural Design Models

The selection of the appropriate structural model is imperative to harmonizing the design and quality management of compacted geomaterials within a pavement structure. Brown (1996) discusses a spectrum of analytical and numerical models that can be used to estimate the critical stresses, strains, and deformations within a pavement structure. The multi-layer linear elastic model is rather simple since the modulus at a given time is considered as a constant value independent of the state of stress applied to the pavement. The advantage of the layered elastic models is that they can rapidly yield results. Their main limitation is that the results are rather approximate if the loads are large enough for the materials to exhibit nonlinear behavior. In the context of the modulus-based testing, the relevant information is the moduli to be used in the design and as target values.

Alternatively, the model can be a multi-layer nonlinear system. The all-purpose finite element software packages (e.g., ABAQUS) or customized finite element algorithms (e.g., MEPDG's DSC2D) are examples of these models. These programs allow a user to model the behavior of a pavement in the most

comprehensive manner and to select the most sophisticated constitutive model for each layer of pavement.

Table 2.5.1 - Advantages and Disadvantages of Moisture/Density Devices

Device	Description	Advantages	Disadvantages
Electrical Density Gauge (EDG)	EDG uses a radio signal between four spikes to measure capacitance, resistance, and impedance of the soil. These parameters are used to determine the density and water content of an unbound layer.	Does not require a licensed technician. Repeatable.	The necessity to run a series of laboratory and in situ tests for correlation purposes. Poor success rate in identifying areas with anomalies
Moisture + Density Indicator (M+DI)	*M+DI* utilizes time domain reflectometry (TDR) to measure voltage time histories of an electromagnetic step pulse at four soil spikes in the ground. The voltage time histories are analyzed to determine the water content and density of an unbound layer.	Requires no certified operators, safety training, or instrument calibration.	Prior calibration of the device for each specific soil using laboratory compaction molds is required. May not be appropriate for aggregates or earth-rock mixtures that either interfere with penetration of the probes or have numerous and large void spaces. Time required to conduct a test may be of concern.
Soil Density Gauge (SDG)	SDG produces a radio-frequency electromagnetic field using a transmitter and receiver to estimate the in-place density, and moisture content of unbound pavement materials using electrical impedance spectroscopy (EIS).	Requires no certified operators, safety training, or instrument calibration.	The technology is new and limited research has been performed using this device.
Speedy Moisture Tester (SMT)	SMT measures the moisture content of geomaterial by measuring the rise in gas pressure within an airtight vessel containing a mix of soil sample and a calcium carbide reagent.	Portable and requires no external power source. Can measure many materials over a wide moisture content range.	Not suitable for all geomaterials, especially highly plastic clay soils. The reagent used is considered as a hazardous product. Compacted geomaterials have to be excavated before they can be tested.
Road-Bed Water Content Meter (DOT 600)	DOT600 estimates the volumetric water content of soil samples by measuring the dielectric permittivity of the material.	Sample bulk density and compaction force are monitored. The system is completely portable.	The technology is new and limited research has been performed using this device. Prior calibration of the device for each specific soil is needed. Compacted geomaterials have to be excavated before they can be tested.

Table 2.5.2 - Ranking of Parameters Considered in Evaluation of Moisture-Density Devices

Device		**Soil Density Gauge**	**Speedy Moisture Tester**	**DOT 600**
Suitability of Device	Ability to detect construction defects	1	3	2
	Repeatability, precision and sensitivity of device	2	4	3
Practicality of Device	Applicability of the device to different types of compacted geomaterials	3	1	1
	Availability of commercial equipment	5	5	3
	Equipment reliability and ruggedness	5	5	3
	User-friendliness	5	5	5
	Expertise needed for data collection and interpretation	5	5	5
	Initial and operational costs	3	5	--
Overall ranking with 5 being ideal device		**3.60**	**4.10**	**3.10**

Table 2.5.3 - Advantages and Disadvantages of Suction Devices

Device	Description	Advantages	Disadvantages
Standard Tensiometer	Measures matric suction ranging from 0 to 90 kPa	Can be used for low suction levels.	Require daily maintenance; range in suction is limited by air-entry value of ceramic.
Thermister Psychrometers	Measures total suction ranging from 100 to 10,000 kPa	Simple to use; accurate at high suction ranges.	Poor sensitivity in low suction range; frequent re-calibration is required.
Transistor Psychrometers	Measures total suction ranging from 100 to 18,000 kPa	Relatively good accuracy as compared to other psychrometers in low suction ranges.	Accuracy is user-dependent; highly affected by temperature changes.
Thermocouple Psychrometers	Measures total suction ranging from 300 to 7,500 kPa	Can be used in the field if temperature gradients are minimized; relatively fast equilibration time; data can be collected continuously using a data logger.	Affected by temperature fluctuations and gradients; sensitivity deteriorates with time.
Thermal Conductivity Sensors	Measures matric suction ranging from 0 to 1000 kPa	Continuous monitoring of matric suction with a data logger.	High failure rate; long-term problems associated with drift and deterioration with time.

A compromise between the linear and rigorous nonlinear algorithms is an equivalent-linear model, which is based on the static linear elastic layered theory (Abdallah et al., 2005). To implement the algorithm, nonlinear layers are divided into several sub-layers. Several lateral stress points are chosen for each nonlinear sub-layer. The moduli of the stress points are iteratively changed until the assumed and calculated moduli at all points are less than a pre-assigned tolerance.

The implications of selecting different structural models are discussed by Ke et al. (2001) and Meshkani et al. (2002) amongst others. For example, Figure 2.6.1 shows typical moduli of the base and subgrade under several different NDT devices and under a dual-tandem axle. As the thickness of the base changes from 4 in. (100 mm) to 12 in. (300 mm), the moduli of the base and subgrade change moderately to significantly. The variations in modulus that would have been registered by two NDT devices placed on top of the base for different base thicknesses are shown in Figure 2.6.2. The measured modulus for the base layer is significantly influenced by the modulus of the subgrade. This small case study shows the significance and the complications associated with setting the target modulus that is tied to design modulus.

2.7 Modulus-Based Specifications

The existing approaches are summarized in Table 2.7.1. One weakness of most of these methods is relating the design and target moduli. In the MnDOT DCP-based specifications (http://www.dot.state.mn.us/materials/gbmodpi.html), the dynamic penetration index (DPI) is used to judge the quality of the compacted geomaterials. The most recent DCP penetration requirements from MnDOT are summarized in Equation 2.7.1:

$$DPI\ (mm/blow) = (4.76\ GN + 1.68\ MC - 14.4) \tag{2.7.1}$$

where MC is the moisture content at the time of testing and GN is the grading number. The grading number, GN, is obtained from Equation 2.7.2 based on a sieve analysis.

$$GN\ (\%passing) = \frac{\quad . \quad . \quad .}{} \tag{2.7.2}$$

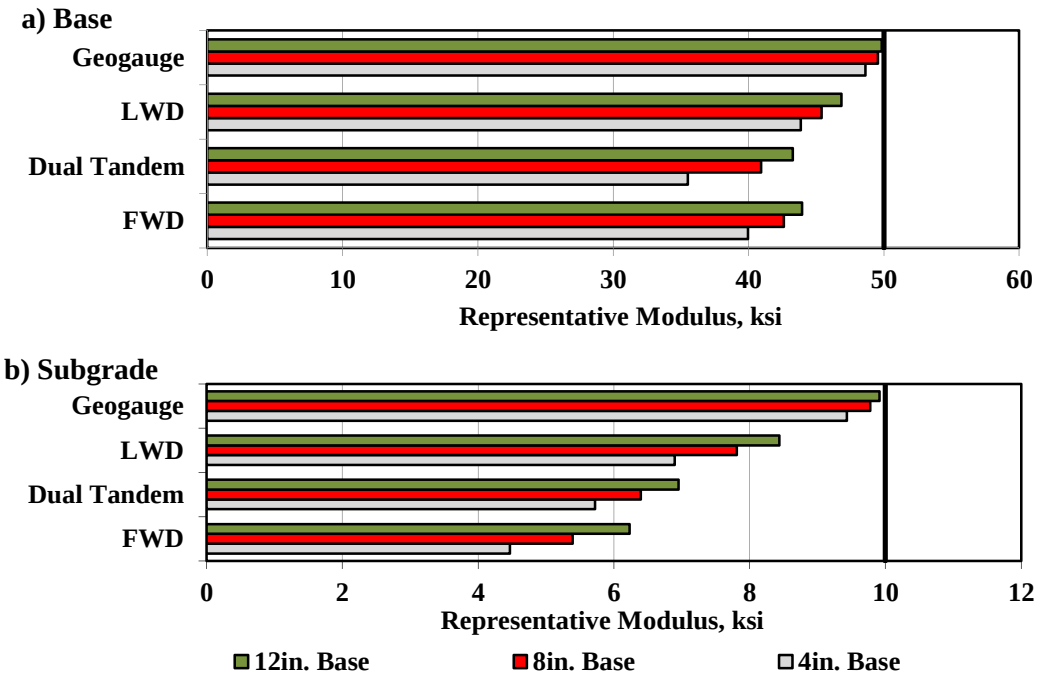

Figure 2.6.1 - Example Comparison of Moduli of Base and Subgrade for Various NDT Devices (Nazarian et al., 2011)

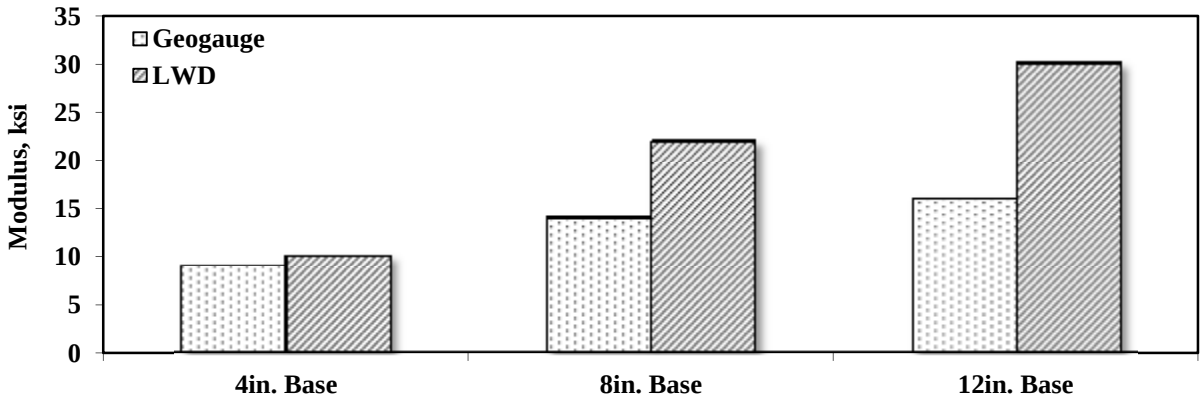

Figure 2.6.2 - Variations in Modulus Registered by NDT Devices for Different Base Thicknesses (Nazarian et al., 2011)

Table 2.7.1 - Current Specifications for Modulus-Based Quality Management

Reference	Tool Used	Principal Constraints
MnDOT (2005)	DCP	Target modulus is not tied to design
MoDOT (2010)		
MnDOT (2009)	LWD	Target modulus is not tied to design
InDOT (2012)		
European Union (EU)		
United Kingdom (UK)		
Celaya et al. (2010)	PSPA	Should be adapted to all NDT devices

MnDOT (http://www.dot.state.mn.us/materials/gblwd.html) has developed specifications for using LWD in quality management of their compacted geomaterials. MnDOT suggests defining the target LWD modulus for each particular base course material and subgrade soil. The grading number (GN) and field moisture content are used to select the LWD target moduli for granular materials, while the plastic limit and field moisture content are used to determine the target moduli for fine-grained soils. Constraints imposed on the LWD testing include the timing when tests should be performed (immediately after compaction). In addition, the LWD tests are not allowed when the water table is less than 2 ft (600 mm) or when the embankment thickness is less than 1 ft (300 mm, when no site preparation is needed) to 1.5 ft (460 mm, when site preparation is needed).

The framework for Missouri DOT (MoDOT) draft specification for the DCP is similar to MnDOT's DCP specification. The method is predominantly used for limestone or dolomitic and crushed stone or sand and gravel bases. The materials under both roadway and shoulders must be compacted to achieve an average DPI of 0.4 in./blow (10 mm/blow) or less within 24 hours after compaction as determined by a standard DCP device with a 40 lb (18 kg) hammer.

Celaya et al. (2010) presented a procedure to close the gap between design and quality management of aggregate layers. Seismic devices, such as the laboratory Free-free Resonant Column (FFRC) and the field Portable Seismic Property Analyzer (PSPA) were recommended. The acceptable design modulus and the target field modulus are determined using conventional and seismic laboratory tests. Finally, field moduli are measured on constructed materials and compared to the established target modulus.

Indiana DOT also developed a test method for "Field Determination of Deflection Using Light Weight Deflectometer" (http://www.in.gov/indot/div/mt/itm/pubs/508_testing.pdf). This test method may be used for granular soils, coarse aggregates and chemical modified soils. This method generally follows the ASTM E2583 standard for measuring deflections with a lightweight deflectometer. Similar to the other LWD specifications, the field modulus is not correlated to the target modulus.

The European Union (EU), especially Austria, Germany, Sweden and the UK have developed specifications for LWD implementation (CEN ICS 93.020). The unbound or geomaterial layer needs to be investigated by performing the following test based on their corresponding specifications: a) compactibility (EN 13286-2), b) grain-size distribution (EN 933-2), c) water content (EN 1097-5), d) water absorption, and e) saturation lines and as built water-content limits (EN 1097-6).

In the UK specifications (Highway Agency, 2009), four foundation classes based on the long-term in-service foundation surface modulus value (a composite value with contributions from all underlying layers) are defined. For construction quality control, the target mean and minimum moduli are specified for the four foundation classes as shown in Table 2.7.2. The moving mean of five consecutive in-situ foundation surface modulus measurements must be equal or exceed the target mean foundation surface modulus. All individual in-situ foundation surface modulus measurements must equal or exceed the target minimum foundation surface modulus. These in-situ foundation surface measurements are based on the standard FWD. A correlation exercise in a demonstration area is needed to harmonize the LWD and FWD values. Twenty-five measurement points are required in this correlation procedure.

2.8 Incorporation of Unsaturated Soil Mechanics in Protocol

A geomaterial that is compacted at or close to its optimum moisture content is usually in an unsaturated state. The estimation of the modulus (or stiffness) of geomaterials at a given moisture content should be based on the principles of unsaturated soil mechanics (Gupta et al., 2007; Sawangsuriya et al., 2009; Siekmeier, 2011). The suction (negative pore pressure) has a significant role in the behavior of unsaturated materials and hence should be considered in the estimation of the moduli (Fredlund and Rahardjo, 1993).

Table 2.7.2 - Target Pavement Foundation Surface Modulus Values (Highways Agency, 2009)

Long-Term In-Service Modulus (MPa)			Class I	Class II	Class III	Class IV
			≥50	≥100	≥200	≥400
Target Mean Modulus (MPa)	Unbound		40	80	…	…
	Bound	Fast Curing	50	100	300	600
		Slow Curing	40	80	150	300
Target Minimum Modulus (MPa)	Unbound		25	50	…	…
	Bound	Fast Curing	25	50	150	300
		Slow Curing	25	50	75	150

Most models for estimating modulus of an unsaturated geomaterial, including those in the MEPDG, are based on its soil-water characteristic curve (SWCC). Several SWCC models are reported in the literature (Lu and Likos, 2004). A compacted geomaterial tends toward an equilibrium state (i.e., minimum energy state in terms of suction equilibrium) even if it placed at its corresponding optimum moisture content. Depending on the soil type, initial moisture content (suction), and environmental conditions, the equilibrium state is reached first under the imposed new construction and moisture boundary conditions. However, the moisture content (suction) will still fluctuate within a specified depth based on the changes in seasonal climatic conditions. The most widely used climatic factor is the Thornthwaite Moisture Index (TMI). The TMI is used in the Enhanced Integrated Climatic Model (EICM) as part of the MEPDG. Zapata et al. (2009) outlined two models for predicting the equilibrium suction for different soils. The suction model for granular base materials is given as:

$$h = \quad + \quad (\quad) \tag{2.8.1}$$

where, h = equilibrium suction and a, b, g = model fitting parameters as a function material gradation. Similarly, the suction model for subgrade materials is given as:

$$h = \quad \overline{\quad} \quad + \tag{2.8.2}$$

where a, b, g, d are functions of material gradation and plasticity index.

Yang et al. (2005) incorporated the effects of suction into the deviator stress model as given below:

$$= \quad (\quad + \quad) \tag{2.8.3}$$

where, s_d = deviatoric stress, c_w = Bishop's effective stress parameter, y_m = matric suction, and k_1, k_2 = model fitting parameters. Their predicted resilient moduli compared well against the laboratory-measured values on two fine-grained soils. However, the model regression coefficients needed to be re-calculated at different water contents for the same soils (Liang et al., 2008).

Gupta et al. (2007) proposed two different models that incorporated the effects of suction on modulus. The implicit equation is as follows:

$$= \quad — \quad — + 1 \quad + \quad Q^k(\quad - \quad) \tag{2.8.4}$$

where, P_a = atmospheric pressure, s_b = bulk stress, t_{oct} = octahedral shear stress, $(u_a - u_w)$ = matric suction, Q = normalized water content, and k_1, k_2, k_3, k_{us} and k = fitting parameters. Their formulation that incorporated the suction effects explicitly is as follows:

$$= \quad \overline{\quad} \quad — + \quad + a \ (\quad - \quad)^b \tag{2.8.5}$$

where k_1, k_2, k_3, k_6, k_7 are fitting parameters, and α_1 and β_1 are determined from clay content or plastic limit of the soil.

Gupta et al. (2007) also proposed a framework for predicting seasonal pore suction resistance factors for use in the MnDOT mechanistic pavement design method. These adjustment factors are needed to account for the increased modulus of the material because of unsaturated soil conditions.

Liang et al. (2008) presented a modified version of the generalized resilient modulus equation given in the MEPDG by incorporating the matric suction into the model:

$$= \qquad \frac{\qquad}{\qquad} \qquad \frac{\qquad}{\qquad} + 1 \tag{2.8.6}$$

where c_w = Bishop parameter, y_m = matric suction, k_1, k_2, k_3 = model parameters. They performed triaxial tests on two fine-grained soils for validation of the proposed model.

Using the general expression for the small-strain shear modulus (G_o) given by Mitchell and Soga (2005) and the expression for the resilient modulus proposed by Oloo and Fredlund (1998), Sawangsuriya et al. (2009) proposed two models for predicting the modulus of compacted subgrades. The first model is based on the two stress-state variable concept of unsaturated soil mechanics and is given as:

$$, \qquad = \qquad (\ )(\qquad - \qquad) \ + \ Q^k(\qquad - \qquad) \tag{2.8.7}$$

where $(G_{o,us})_{hh}$ = unsaturated soil small-strain shear modulus in the horizontal plane, $f(e)$ = void ratio function, $(s_o - u_a)$ = net confining pressure, $(u_a - u_w)$ = matric suction, Q = normalized volumetric water content, A, C, k = fitting parameters, and n = a constant equal to 0.5.

The second model is based on the single-valued effective stress principle given by Bishop (1959) and the modified form of the c coefficient given by Vanapalli and Fredlund (2000), and is listed as:

$$, \qquad = \qquad (\ )[(\qquad - \qquad) + Q^k(\qquad - \qquad)] \tag{2.8.8}$$

where A, n, k are fitting parameters. Equation 2.8.8 has one less unknown parameter as compared to Equation 2.8.7. The experimental data were optimized with the two proposed models using a least-squared optimization algorithm.

Oh and Fernando (2011) evaluated adjustment factors for converting moduli obtained from FWD tests to equivalent laboratory values. Oh and Fernando (2011) used backcalculated FWD moduli of in-service pavement sections. Their laboratory test program included resilient modulus, filter paper tests for soil suction and sample extractions to characterize underlying materials. They proposed the following modified version of the MEPDG resilient modulus model that included a term to account for the effect of soil moisture based on the SWCC of the underlying material.

$$= \qquad \frac{\qquad}{\qquad} \qquad \frac{\qquad}{\qquad} + 1 \tag{2.8.9}$$

where t_{oct} = octahedral shear stress, I = first stress invariant (bulk stress), S = soil suction, q_w = volumetric water content, k_1, k_2, k_3, k_4 are the model parameters.

Siekmeier (2011) proposed a method to estimate moduli and LWD deflection target values (called TVs) for the soils. The following form of the generalized resilient modulus equation was recommended by Siekmeier (2011) for laboratory measurement of the modulus.

$$= \qquad \frac{\qquad}{\qquad^{y}} \qquad \frac{\qquad}{\qquad} + 1 \tag{2.8.10}$$

where s_{eb} = external bulk stress, f_s = pore suction resistance factor, y = matric suction, q_w = volumetric water content, k_1, k_2, k_3 are the model parameters given as follows:

$$= 800 \times \frac{\quad}{\quad} \times \frac{\quad}{(\psi)} \tag{2.8.11a}$$

$$= \psi - 1 \tag{2.8.11b}$$

$$= -8 \tag{2.8.11c}$$

The matric suction of the soil is estimated from the following relationship by Fredlund and Xing (1994):

$$= 1 - \frac{\frac{\psi}{\psi}}{\frac{\quad}{\psi}} \times \frac{\quad}{[\quad (\psi)\ ]} \tag{2.8.12}$$

where, y_r = matric suction at residual volumetric water content, q_{sat} = volumetric water content at saturation and a, n, m are the model fitting parameters.

According to Cary and Zapata (2010), the effects of the environmental factors on the M_R can be evaluated and expressed as the following function:

$$M_R = F_{env} \times M_{Ropt} \tag{2.8.13}$$

where F_{env} is the composite environmental adjustment factor and M_{Ropt} is the resilient modulus at optimum conditions and at any state of stress.

Witczak et al. (2000), as part of the development of the MEPDG, proposed the following equation:

$$\log(\quad) = \frac{\quad}{\quad} = + \frac{\quad}{\quad \times} \tag{2.8.14}$$

where $M_R = MR_{Rep}$ at a degree of saturation S (decimal); $M_{Ropt} = MR_{Rep}$ at the maximum dry density and optimum moisture content; S_{opt}= degree of saturation (in decimal) at the maximum dry density and optimum moisture content; a = minimum of $\log(M_R/M_{Ropt})$ (-0.3123 and -0.5934 for coarse- and fine-grained materials, respectively); b = maximum of $\log(M_R/M_{Ropt})$ (0.3010 and 0.3979 for coarse- and fine-grained materials, respectively); k_m = regression parameter. The MEPDG recommended two separate sets of regression parameters for coarse-grained and fine-grained geomaterials.

Cary and Zapata (2010) proposed a more general form of Equation 2.8.14 by incorporating percent finer than No. 200 sieve (w, in decimals) and plasticity index of the materials (PI, in percent):

$$\log(\quad) = (\quad + \quad \times \quad) + \frac{\quad \times \quad \cdot \quad \times}{\frac{\quad \times \quad \cdot}{\quad \times} \quad \times \quad \cdot \times \frac{\quad}{\quad}} \tag{2.8.15}$$

where a = -0.600, b = -1.87194, d = 0.800, g = 0.080, r = 11.96518, and w = -10.19111.

The Cary and Zapata (2010) equation appears to be empirical and does require the determination of resilient moduli at optimum conditions. On the other hand, equations developed by Yang et al. (2005), Gupta et al. (2007) and Sawangasurya et al. (2009) appear to be lacking when compared to MEPDG requirements. Research that is more recent resulted in the development of modulus equations by Oh and Fernando (2011) and Siekmeier (2011) as functions of soil suctions, moisture levels and stress conditions. These equations are based on the MEPDG guidelines and accounts for unsaturated soil conditions. Only the Cary and Zapata (2010) and Siekmeier (2011) models are considered in this study.

2.9 Summary of Highway Agencies' Survey (February, 2011)

Two criteria for the success of this project are the willingness of the highway agencies to use the new specification and the degree of satisfaction of the DOTs with its robustness. With these criteria in mind,

one of the first steps in this project was to survey the current practices of highway agencies. An on-line survey, as presented in Appendix C, was distributed to the 50 state DOTs. Twenty-seven DOT's that had some experience in this area responded. Salient information from the survey is summarized here.

- Estimated density (22[1]) and moisture content (17) with NDG dominated the state of the practice for quality management of compacted geomaterials. Only two states indicated modulus-based devices as part of their operation.
- The willingness of the DOTs to implement mechanistic-empirical (ME) pavement design methods is important for achieving the goals of this project. Most highway agencies considered using ME pavement design (24).
- The ME pavement design requires the determination of layer moduli. The most common methods for the determination of moduli were the laboratory resilient modulus tests (7) and presumptive values based on soil type (7). Two respondents indicated field tests with FWD or DCP.
- The interest of DOTs in utilizing the nonlinear constitutive models (i.e. more advanced structural models) was moderate. Most DOTs (16) did not consider the stress-sensitivity of the modulus; whereas a few used laboratory resilient modulus test results for quantifying stress dependency (4).
- Twelve DOTs considered the variation of moisture in geomaterials in the design.
- The interest of DOTs in the use of unsaturated soil mechanics concepts in quantifying the variations in modulus with moisture content was low with most not considering them (20). Six DOTs indirectly accounted for them via the MEPDG approach.
- Only three DOTs had implemented a modulus-based specification with a majority of other DOTs (15) expressing interest in implementing it. Table 2.9.1 is a summary of various concerns expressed by the DOTs that were interested in implementing such a specification. The concerns were equally distributed between institutional limitations (14), technical issues (14) and practical implementation (12). Table 2.9.2 summarizes the various reasons stated by respondents that were not interested in implementing a modulus-based specification (7). Several items in Tables 2.9.1 and 2.9.2 are similar.
- DOTs were most familiar with the Geogauge (19), DCP (18), and LWD (13). The highest degree of satisfaction was with the DCP (14 out of 18), and the lowest with the Geogauge (1 out of 19). The degree of satisfaction with the LWD was mixed (6 satisfied out of 13). Only three DOTs were familiar with the PSPA with two being satisfied with its performance.
- NDG was by far the most utilized device (26) for moisture measurement with 20 DOTs being satisfied with its performance. At most, seven DOTs were familiar with other devices such as Electric Density Gauge (7), Purdue MD&I device (4) or Soil Density Gauge (2). None of the DOTs that were familiar with those new devices was satisfied with their performances.

Overall, there was a general interest in implementing a practical modulus-based specification. However, there was no consensus amongst DOTs on the best devices for measuring modulus or moisture content. There was also a lack of enthusiasm for incorporating laboratory resilient modulus and unsaturated soil mechanics principles in the specification.

[1] Numbers in parentheses indicate the number of responses

Table 2.9.1 - Concerns of Respondents Interested in Implementing Modulus-based Specifications

Institutional Limitations	1. New stiffness/modulus-based field test will require additional cost. 2. Lack of field trained personnel.
Technical Issues	1. Stiffness and modulus alone cannot ensure a high quality embankment/subgrade. 2. Devices such as the Geogauge cannot measure lifts less than 250 mm. 3. It is completely new and there is a need to understand more of the basics.
Practical Implementation	1. Contractors do not understand resilient modulus and how to achieve a certain resilient modulus. 2. Soil variability is too complex and therefore gives unpredictable responses. 3. Field equipment and certification for technicians is needed. 4. Difficulty in convincing industry to change established procedures and equipment and adopt performance-based specifications.
Others	1. Tremendous variability in results from the equipment under controlled conditions.

Table 2.9.2 - Reasons Given by Respondents Not Interested in Implementing Modulus-Based Specifications

Institutional Limitations	1. Few engineers, much less contractors, have any understanding of the meaning of modulus. 2. These tests require a higher trained person. 3. Unreliable results. 4. New stiffness/modulus-based field test will require additional cost.
Technical Issues	1. Process/procedure developed using soils/aggregates from other locations, tested by other agencies, can raise questions as to its validity to local conditions. 2. Unreliable results. 3. Stiffness and modulus alone cannot ensure a high quality embankment/ subgrade.
Practical Implementation	1. Would not be acceptable to a contractor. 2. Difficulty in determination of a general moisture adjustment factor would seem to make the process impractical. 3. If sophisticated/time consuming/expensive testing is required, probability of agency adoption is minimal.
Others	1. Lack of resources to research and implement this type of change. 2. Even though modulus-based specifications have not been implemented in the current specifications, very few roadway base failures have been observed.

CHAPTER 3 – FINDINGS FROM LABORATORY STUDY

As indicated in Chapter 1, the research included laboratory, small-scale and field testing programs. This three-prong approach was followed to separate a number of complex and inter-related issues into a number of well-defined hypotheses that, when combined, can provide a practical and scientifically sound specification. The results of the activities associated with laboratory testing are discussed below. The objectives of the laboratory study were the following:

- Establish the impact of moisture content at the time of compaction on modulus,
- Establish the impact of moisture content at the time of testing relative to the moisture content at the time of compaction on modulus, and
- Establish modulus tolerances to accommodate less than 100% relative compaction.

3.1 Geomaterials Used

The index properties of the materials used are summarized in Table 3.1.1 and their gradation curves are shown in Figure 3.1.1. Three fine-grained soils (CL, CH and ML), one sandy material (SC) and two unbound granular base materials (GW and GP) were used. In addition, a sandy material (SM) was primarily used as the support subgrade for most small-scale studies. The optimum moisture contents and maximum dry densities obtained from Proctor tests (AASHTO T 99 or T 180) are also reported in Table 3.1.1. These materials exhibit a variety of behaviors in terms of their interactions with moisture and their use as compacted geomaterials.

Table 3.1.1 - Index Properties of Geomaterials Used in This Study

Material	Gradation %				USCS Class.	Specific Gravity	Atterberg Limits			Moisture/Density*	
	Gravel	Coarse Sand	Fine Sand	Fines			LL	PL	PI	OMC, %	MDD, pcf
El Paso Base	66	19	11	4	GP	2.80	22	13	9	5.7	147
Louisiana Base	51	31	15	3	GW	2.65	0	0	0	8.7	129
Austin Clay	8	12	16	64	CL	2.73	27	13	14	10.0	125
Minnesota Clay	0	1	1	97	CH	2.78	86	33	53	25.9	96
Mississippi Silt	0	22	19	59	ML	2.65	0	0	0	9.4	125
Louisiana Clay	0	0	55	45	SC	2.72	23	11	12	11.4	121
El Paso Subgrade	0	0	73	27	SM	2.65	0	0	0	15.2	112

*As per AASHTO T-99 for CL, CH, ML, SC and SM materials and T-180 for GW and GP materials.

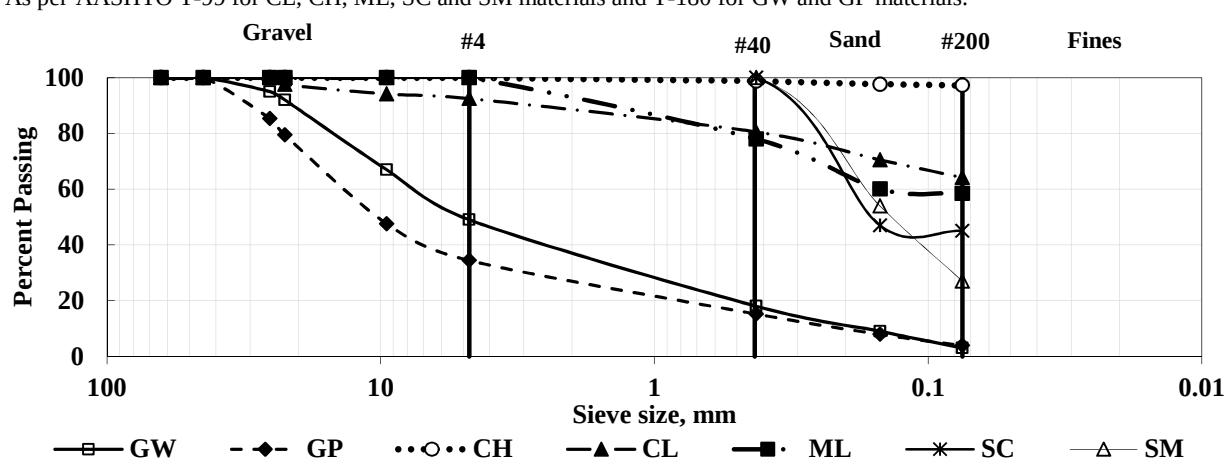

Figure 3.1.1 - Gradation Curves of Geomaterials Used in This Study

3.2 Laboratory Testing

Table 3.2.1 presents the matrix of laboratory tests carried out on each of the geomaterials. Two compaction methods, constant energy and constant density, were used: The constant energy method is simply the traditional Proctor method (AASHTO T 99 or T 180). In that method, soil samples at different moisture contents are subjected to the same number of drops of the compaction hammer, resulting in specimens with variable densities. In the constant density method, which is more representative of field compaction, the goal is to achieve a desired target density (say MDD) for any moisture content. The desired density is achieved through a trial and error process by changing the number of compaction hammer drops. This method is not used in routine laboratory testing, and it is not standardized. The third set of laboratory tests is suction-controlled MR tests conducted on specimens prepared at constant energy. The results and conclusions from these tests are presented in Section 3.6.

Table 3.2.1 - Laboratory Experiments for each Material

Parameter				**Test**		
Compaction Method	**Moisture Content at Compaction[1]**	**Moisture Content at Testing**	**Relative Compaction**	**FFRC[2]**	**Standard MR[3]**	**Suction Controlled MR**
Constant Energy	OMC + 2%, OMC + 1%, OMC %, OMC - 1%, OMC - 2%	OMC + 2%	Variable as per Moisture-Density Curve	ü	ü	ü
		OMC + 1%		ü	ü	ü
		OMC		ü	ü	ü
		OMC -1%		ü	ü	ü
		OMC -2%		ü	ü	ü
Constant Density	OMC + 2%, OMC + 1%, OMC%, OMC -1%, OMC - 2%	OMC + 2%	MDD[4]	ü	ü	
		OMC + 1%		ü	ü	
		OMC		ü	ü	
		OMC -1%		ü	ü	
		OMC -2%		ü	ü	
		OMC - 3%		ü		
	OMC%	OMC + 2%	98% MDD, 96% MDD	ü		
		OMC + 1%		ü		
		OMC		ü	ü	
		OMC -1%		ü		
		OMC -2%		ü		
		OMC - 3%		ü		

[1] Specimens are prepared at all moisture contents listed,
[2] FFRC = Free-free Resonant Column,
[3] MR = Resilient Modulus Tests as per AASHTO T 307-03

3.2.1 Resilient Modulus (MR) and Free-Free Resonant Column (FFRC) Tests

The procedures for conducting MR tests have been under continuous modification. AASHTO alone has adopted several test protocols in the last 20 years (e.g., T 292-91, T 294-92, TP 46-94 and T 307-03). The NCHRP Project 1-28A approach recommended as a part of the MEPDG is gaining popularity as well. These approaches differ in the specimen size, compaction method, loading time, stress sequence, and the types and locations of load cell (e.g., within or outside the confining chamber) and displacement sensors (e.g., mounted on specimen or platen-to-platen measurements).

The AASHTO T 307-03 loading sequences were used for MR tests in this study (see Figure 3.2.1a). The load cell was placed inside the chamber and the displacement measurements were made either in the middle of the specimens with noncontact sensors or with LVDTs within the chamber. Even though similar in concept, different test protocols may yield different modulus parameters. Gupta et al. (2007) indicated that the resilient moduli obtained with internal displacement measurements could be up to three

times greater than those obtained when the displacement measurements were made outside the confining cell. The relationships derived here should be used with caution when they are applied to modulus parameters obtained with other test protocols.

All unbound granular base (GP, GW) specimens were prepared to nominal dimensions of 6 in. (150 mm) by 12 in. (300 mm) as per AASHTO T 180, while the other (CL, CH, ML, SC and SM) materials were compacted to nominal dimensions of 4 in. (100 mm) by 8 in. (200 mm) as per AASHTO T 99. The nominal sizes of the specimens tested in suction control MR were 2.8 in. (70 mm) by 5.6 in. (140 mm) to reduce the time necessary to equilibrate the specimens.

The following constitutive model, as proposed by Ooi et al. (2004), was used to summarize the results from each test:

$$MR = k_1^{'} P_a \left(\frac{q}{P_a} + 1 \right)^{k_2^{'}} \left(\frac{t_{oct}}{P_a} + 1 \right)^{k_3^{'}} \tag{3.2.1}$$

where θ = bulk stress, τ_{oct} = octahedral shear stress, and P_a = atmospheric pressure. Equation 3.2.1 seems to be more appropriate for estimating the nonlinear structural response of geomaterials as compared to the standard MEPDG equation as will be discussed in Chapter 6. Changing the general constitutive model may cause practical complications for those agencies that utilize the MEPDG constitutive model. A process for converting the nonlinear parameters obtained from the MEPDG model to those obtained from Ooi et al. (2004) model is included in Appendix D.

The free-free resonant column (FFRC; Nazarian et al., 2003) tests were also conducted on every specimen prepared for MR tests. The FFRC method estimates the linear-elastic (low-strain) seismic modulus based on the determination of the fundamental resonant frequency of vibration of a specimen. The FFRC modulus can be directly related to the seismic modulus measured by the PSPA in the field without a need for a complex transfer function. The main components of the test setup are shown in Figure 3.2.1b. An accelerometer is securely placed on top of the specimen, and the specimen is impacted with a hammer instrumented with a load cell. As an impulse load is applied to the specimen, seismic energy over a wide range of frequencies propagates within the specimen. The resonant frequency, f_L, wet density of the specimen, ρ, and the length of the specimen, L, are used to determine the modulus, E_{FFRC}, from

$$E_{FFRC} = \rho \, (2 \, f_L \, L)^2 \tag{3.2.2}$$

The results from the MR and FFRC tests on duplicate specimens prepared using constant energy method are shown in Table 3.2.2 . The parameters k'_1 and the representative moduli from duplicate specimens are in most cases similar. Parameters k'_2 and k'_3 show some variations between the duplicate specimens partially because of the slight non-uniqueness associated with fitting a nonlinear curve to the measured data.

The mean values of the stiffness parameters from the MR tests are shown in Table 3.2.2. The representative resilient moduli determined from Eq. 3.2.1 based on the presumptive t_{oct} and q recommended by NCHRP 1-28A are included in the table. Table 3.2.3 contains the same information but for the specimens prepared to constant density. Constant density tests were not carried out on the SM material since it was only used as a foundation layer. Moduli from the specimens compacted to 96% and 98% of MDD are also included in Table 3.2.3.

The representative MR moduli and the FFRC moduli from the same specimens are compared in Figure 3.2.2. These two moduli are reasonably well correlated (R^2 = 0.79). Most outliers are related to the specimens that were compacted much drier or much wetter than their corresponding OMCs.

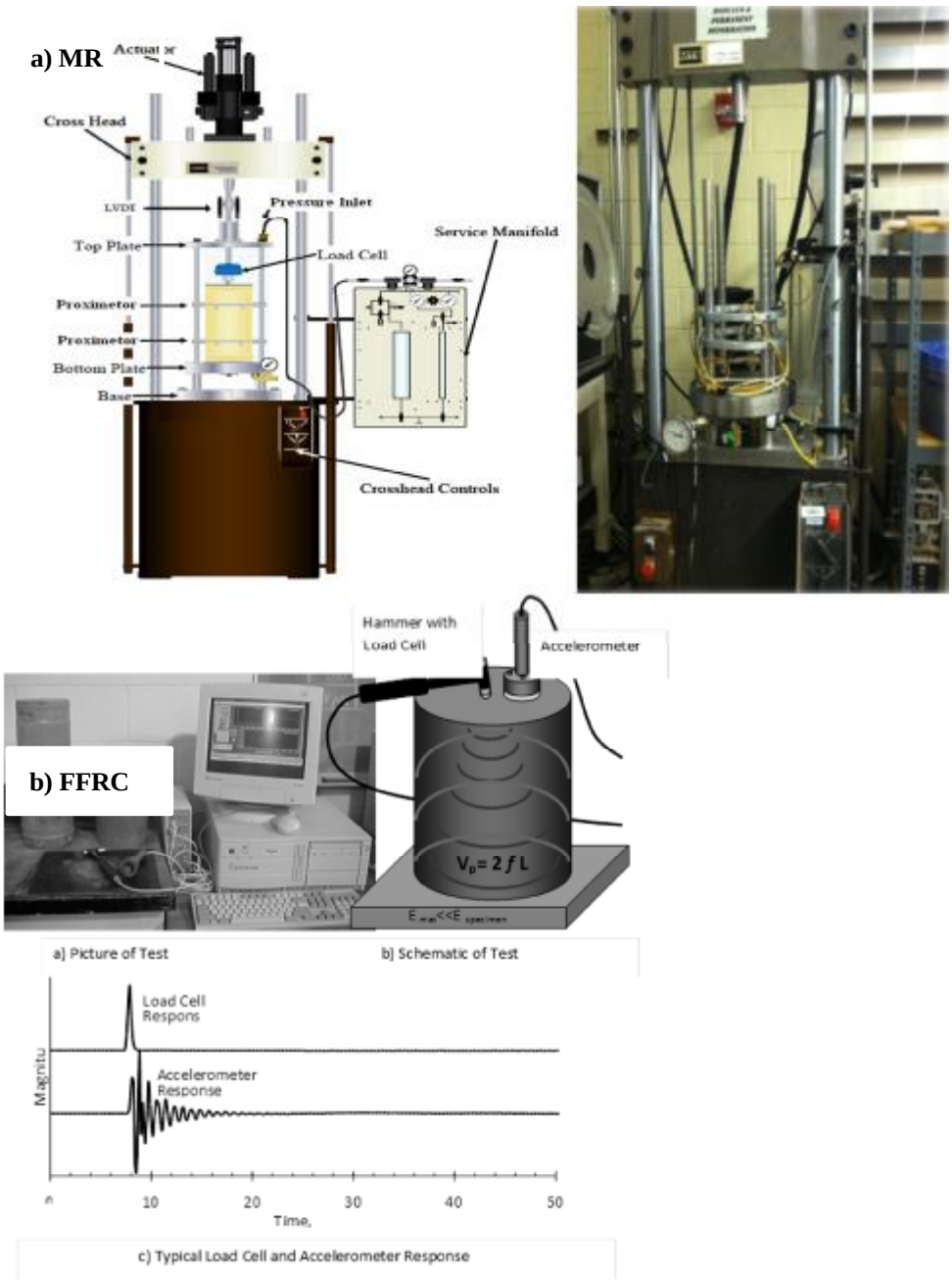

Figure 3.2.1 - Resilient Modulus (MR) and Free-Free Resonant Column (FFRC) Test Setups

Table 3.2.2 - Laboratory Results of MR and FFRC for Constant Energy

Material	Target Moisture Content	Actual Moisture Content, %	Dry Density, pcf	Degree of Saturation, %	FFRC Modulus, ksi	Nonlinear Parameters			Represent-ative MR, ksi*
						k'_1	k'_2	k'_3	
GP	**0.67 OMC**	4.1	145.2	57	44	1370	0.63	-0.19	38.1
	0.83 OMC	5.1	145.7	71	32	415	1.07	-0.29	18.3
	1.00OMC	6.2	147.1	92	13	303	0.95	-0.05	12.7
	1.17 OMC	6.8	146.3	98	7	444	0.66	-0.25	12.4
	1.33 OMC	8.2	144.1	--	4	**Too wet To Test**			
GW	**0.80 OMC**	6.5	125.6	54	24	1087	0.53	-0.10	28.0
	0.90 OMC	7.7	129.6	74	23	952	0.70	-0.10	29.7
	1.00 OMC	8.6	130.9	86	17	769	0.69	-0.14	23.3
	1.10 OMC	9.9	127.9	90	15	681	0.46	-0.10	16.2
	1.20 OMC	10.5	126.4	90	17	709	0.60	-0.10	20.4
CL	**0.80 OMC**	8.2	122.1	56	78	1307	0.43	-0.16	24.3
	0.90 OMC	9.2	124.0	67	81	1670	0.40	-0.20	30.1
	1.00 OMC	10.0	124.5	74	81	1507	0.29	0.00	26.4
	1.10 OMC	11.2	123.8	81	63	1385	0.33	-0.15	24.2
	1.20 OMC	11.8	123.0	84	71	1350	0.29	-0.05	23.5
CH	**0.80 OMC**	20.8	91.6	65	35	828	0.54	-0.22	16.2
	0.90 OMC	23.2	94.3	77	37	785	0.55	-0.59	14.5
	1.00 OMC	26.6	95.9	91	30	940	0.29	-0.42	15.3
	1.10 OMC	29.2	93.9	96	20	670	0.32	-0.90	10.1
	1.20 OMC	31.0	92.5	98	15	606	0.26	-1.37	8.1
ML	**0.80 OMC**	7.1	123.3	55	12	788	0.77	-1.61	13.7
	0.90 OMC	8.4	123.9	66	14	616	0.99	-1.47	12.6
	1.00 OMC	9.3	124.8	76	16	620	1.04	-1.91	12.0
	1.10 OMC	10.3	123.3	80	17	644	0.94	-1.89	11.8
	1.20 OMC	11.8	123.2	91	13	539	1.00	-1.75	10.5
SC	**0.80 OMC**	9.1	118.3	57	88	2158	0.15	-0.50	31.7
	0.90 OMC	10.6	119.9	69	56	1514	0.30	-1.79	19.1
	1.00 OMC	11.3	120.9	76	47	1408	0.34	-2.09	17.3
	1.10 OMC	12.8	120.5	85	22	491	1.08	-3.58	7.2
	1.20 OMC	13.9	118.8	88	11	210	1.70	-4.10	4.0
SM	**0.87 OMC**	13	111.3	71	9	300	1.08	-1.09	7.0
	0.93 OMC	14.1	112.1	79	8	313	1.19	-0.83	8.2
	1.00 OMC	15.1	113.3	87	3	133	2.00	-2.48	4.2
	1.07 OMC	16.1	112.3	90	2	70	2.31	-2.56	2.6
	1.13 OMC	16.9	109.7	88	1	75	2.19	-2.22	2.8

* from Eq. 3.2.1 based on τ_{oct} and θ values of 7.5 psi and 31 psi for base and 3 psi and 12.4 psi for subgrades as recommended by NCHRP Project 1-28A.

Table 3.2.3 - Laboratory Results of MR and FFRC for Constant Density

Material	Target Moisture Content or Density	Actual Moisture Content, %	Dry Density, pcf	Degree of Saturation, %	FFRC Modulus, ksi	Nonlinear Parameters			Represent-ative MR, ksi*
						k'_1	k'_2	k'_3	
GP	**0.67 OMC**	4.6	146.9	68	36	576	0.76	-0.07	19.5
	0.83 OMC	5.3	147.8	81	32	391	0.85	-0.05	14.8
	1.00 OMC	6.2	147.1	92	13	303	0.95	-0.05	12.7
	1.17 OMC	7.0	146.0	100	8	514	0.55	-0.05	13.7
	1.33 OMC	**Too wet to test**							
	98% of MDD**	6.0	144.6	81	19	491	0.60	-0.05	14.0
	96% of MDD**	5.9	141.7	71	22	479	0.80	-0.05	16.3
GW	**0.80 OMC**	6.5	132.0	68	34	1048	0.66	-0.10	31.1
	0.90 OMC	7.5	131.4	77	23	971	0.55	-0.10	25.6
	1.00 OMC	8.6	130.9	86	17	769	0.69	-0.14	23.3
	1.10 OMC	9.5	128.9	89	10	691	0.45	-0.10	16.2
	1.20 OMC	**Too wet to test**							
	98% of MDD**	8.5	128.0	65	17	889	0.61	-0.10	24.9
	96% of MDD**	8.4	124.6	59	32	881	0.70	-0.10	27.5
CL	**0.80 OMC**	8.4	124.0	61	80	1794	0.30	0.00	31.7
	0.90 OMC	9.0	124.4	67	98	1840	0.22	0.00	30.9
	1.00 OMC	10.0	124.5	74	81	1507	0.29	0.00	26.4
	1.10 OMC	11.1	124.3	82	77	1236	0.46	0.00	24.1
	1.20 OMC	12.0	124.5	89	52	1331	0.20	-0.22	21.9
	98% of MDD**	10.0	122.0	69	69	1489	0.29	-0.05	25.9
	96% of MDD**	10.2	118.7	64	58	1212	0.38	-0.05	22.2
CH	**0.80 OMC**	21.1	96.1	73	43	771	0.60	-0.05	16.2
	0.90 OMC	24.3	94.8	81	34	901	0.42	-0.44	15.8
	1.00 OMC	26.6	95.9	91	30	940	0.29	-0.42	15.3
	1.10 OMC	29.3	95.0	98	20	697	0.33	-0.86	10.7
	1.20 OMC	32.1	94.1	106	14	351	0.59	-2.42	4.7
	98% of MDD**	25.3	94.2	83	27	757	0.55	-1.16	12.5
	96% of MDD**	26.1	91.3	81	23	604	0.39	-0.31	10.6
ML	**0.80 OMC**	7.7	124.3	61	15	573	0.96	-1.14	12.2
	0.90 OMC	8.5	123.9	67	18	601	0.94	-1.29	12.3
	1.00 OMC	9.3	124.8	76	16	620	1.04	-1.91	12.0
	1.10 OMC	10.3	124.8	84	18	626	0.86	-1.29	12.2
	1.20 OMC	11.6	124.6	93	16	429	1.14	-1.01	10.5
	98% of MDD**	9.5	122.2	71	16	609	0.90	-1.36	12.0
	96% of MDD**	9.1	120.2	64	15	573	0.94	-1.17	12.0
SC	**0.80 OMC**	9.2	121.2	62	73	1879	0.23	-1.25	25.2
	0.90 OMC	10.5	120.7	70	56	1488	0.38	-1.92	19.3
	1.00 OMC	11.5	120.8	77	48	1145	0.42	-2.21	14.5
	1.10 OMC	12.7	121.3	86	28	533	0.78	-3.36	6.8
	1.20 OMC	13.7	120.9	92	13	233	1.40	-3.90	3.9
	98% of MDD**	11.6	118.6	73	36	1106	0.41	-2.35	13.5
	96% of MDD**	11.4	116.5	68	40	1219	0.40	-2.20	14.9

* from Eq. 3.2.1 based on τ_{oct} and θ values of 7.5 psi and 31 psi for base and 3 psi and 12.4 psi for subgrades as recommended by NCHRP Project 1-28A.

** Target Moisture Content of OMC

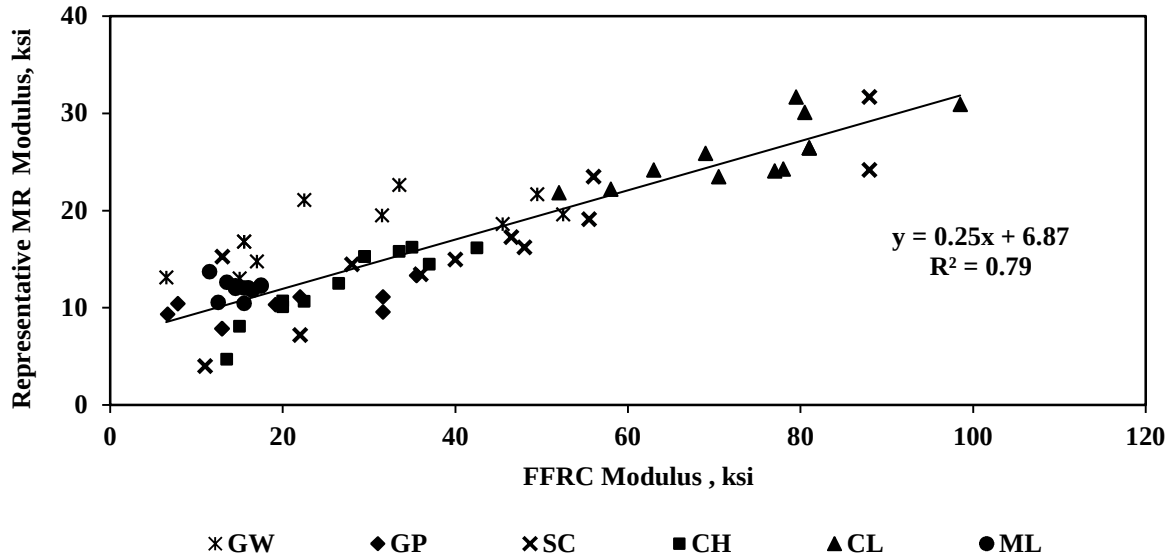

Figure 3.2.2 - Variation in Laboratory Representative MR Modulus with FFRC Modulus
(Representative moduli presented in this graph for all materials are based on τ_{oct} and θ values of 3 psi and 12.4 psi for uniformity)

To establish a better relationship, correlation analyses followed by a regression analysis were carried out between these two moduli and the index properties of the geomaterials. The most favorable relationship is in the form of Equation 3.2.3:

$$MR_{Rep} = 0.24\ E_{FFRC} - 0.32\ MC + 0.03\ DD + 0.11\ Fine \qquad (3.2.3)$$

where MR_{Rep} = predicted representative MR (ksi), E_{FFRC} = FFRC modulus (ksi), MC = moisture content (%), DD = dry density (pcf), and $Fine$ = percent passing sieve #200.

As shown in Figure 3.2.3, the predictive power of Equation 3.2.3 is reasonable (R^2 = 0.94). To check the reasonableness of this model, a set of resilient moduli and seismic moduli from an independent fine-grained soil (SC material) was used. This regression analysis is based on a limited number of materials used in this project (only fine-grained materials), and may need adjustment. This exercise shows that MR_{Rep} and E_{FFRC} are correlated and may be used interchangeably with a reasonable accuracy.

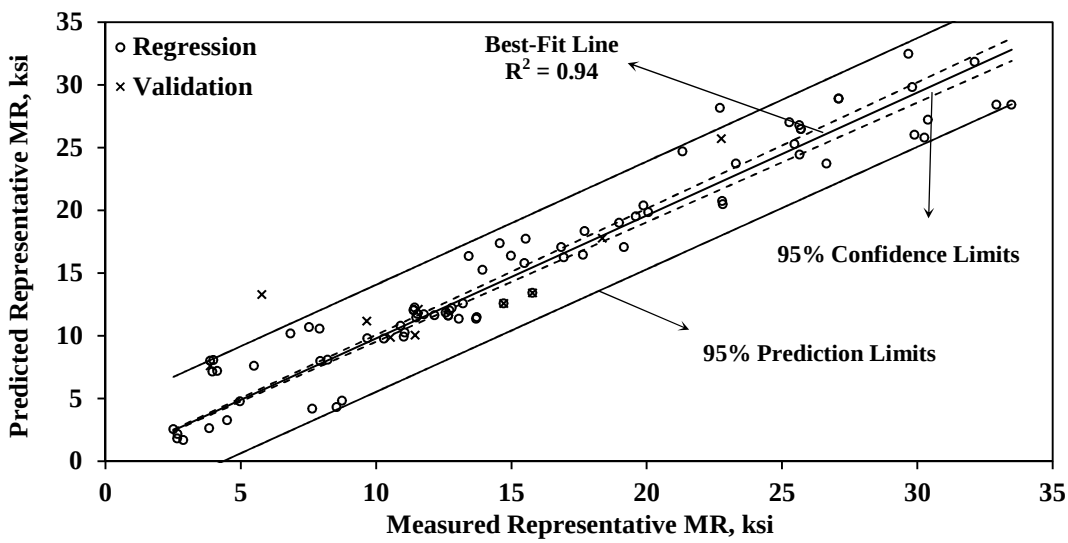

Figure 3.2.3 - Representation of Goodness of Fit of Equation 3.2.3

The relationships between the representative MR moduli from the constant energy and constant density MR tests on specimens prepared at the same nominal moisture contents are demonstrated in Figure 3.2.4a. The results follow the line of equality reasonably well. The same trends are observed for the FFRC moduli as shown in Figure 3.2.4b. These results indicate that the laboratory moduli obtained from specimens prepared with the two compaction methods are similar. As such, in the remainder of the study, the standard constant energy method of compaction was followed.

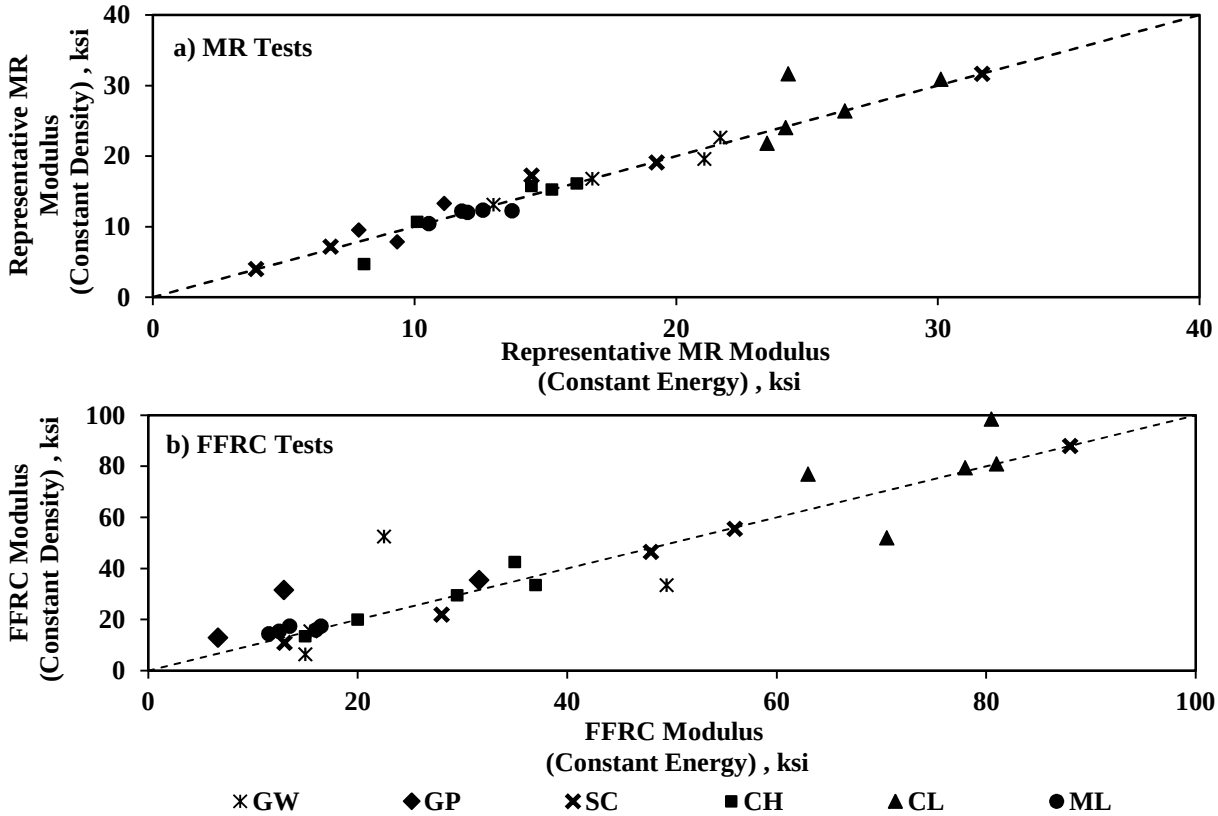

Figure 3.2.4 - Modulus Relationships between Constant Energy and Constant Density Specimens

3.3 Impact of Moisture Content at the Time of Compaction on Modulus

The variations in MR_{Rep} and E_{FFRC} with moisture content from the constant density and constant energy tests are presented in Figure 3.3.1. To ensure the exact moisture content, the amount of water needed to be mixed with geomaterials was added to the mixture. Moisture content at the time of compaction for each specimen was determined by oven-drying three specimens gathered from the materials during compaction. For each material, the modulus decreases as the compaction moisture content increases above the OMC. Likewise, the variations in MR_{Rep} and E_{FFRC} with degree of saturation are presented in Figure 3.3.2. The degree of saturation (x-axis) for each specimen was calculated from its known moisture content and density. The modulus generally decreases as the degree of saturation increases.

The MR test results from all materials tested are superimposed on the MEPDG version (Equation 2.8.14) and Cary and Zapata (2010) version (Equation 2.8.15) in Figure 3.3.3. The same results but from the FFRC moduli are shown in Figure 3.3.4.

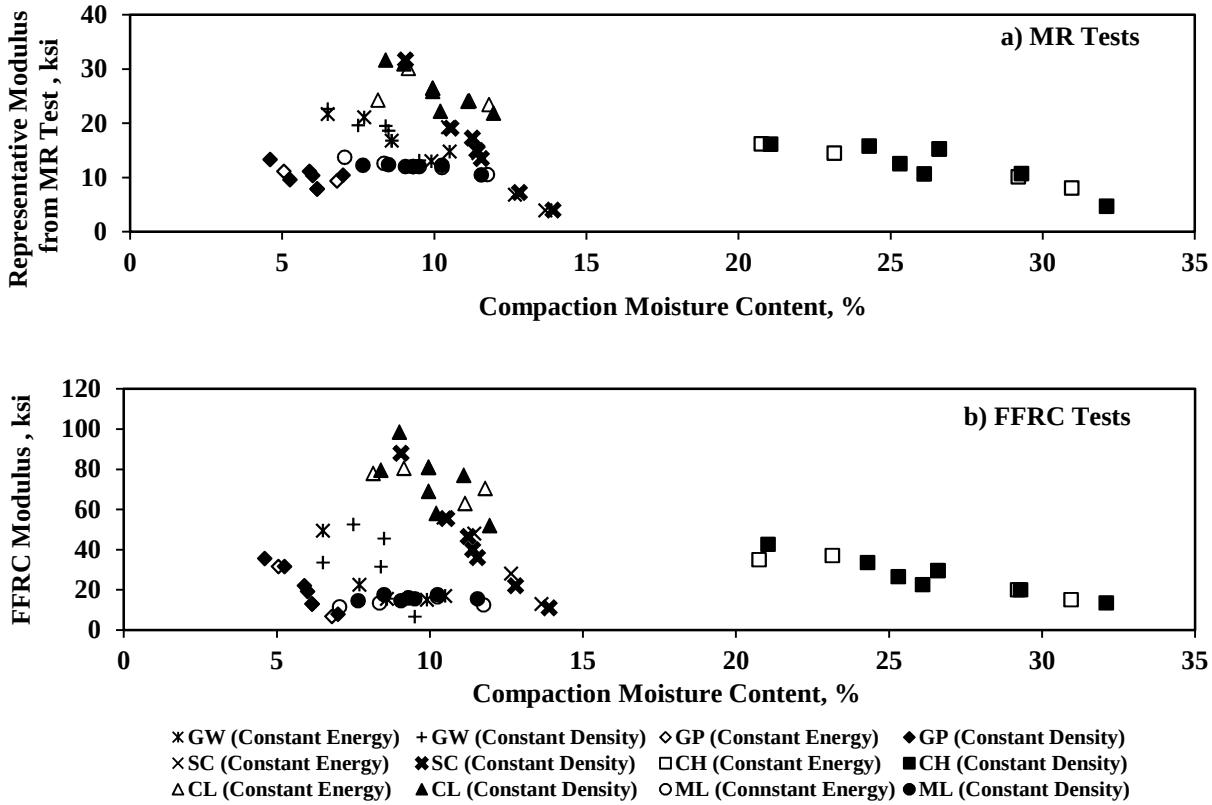

Figure 3.3.1 - Variations in Modulus with Compaction Moisture Content

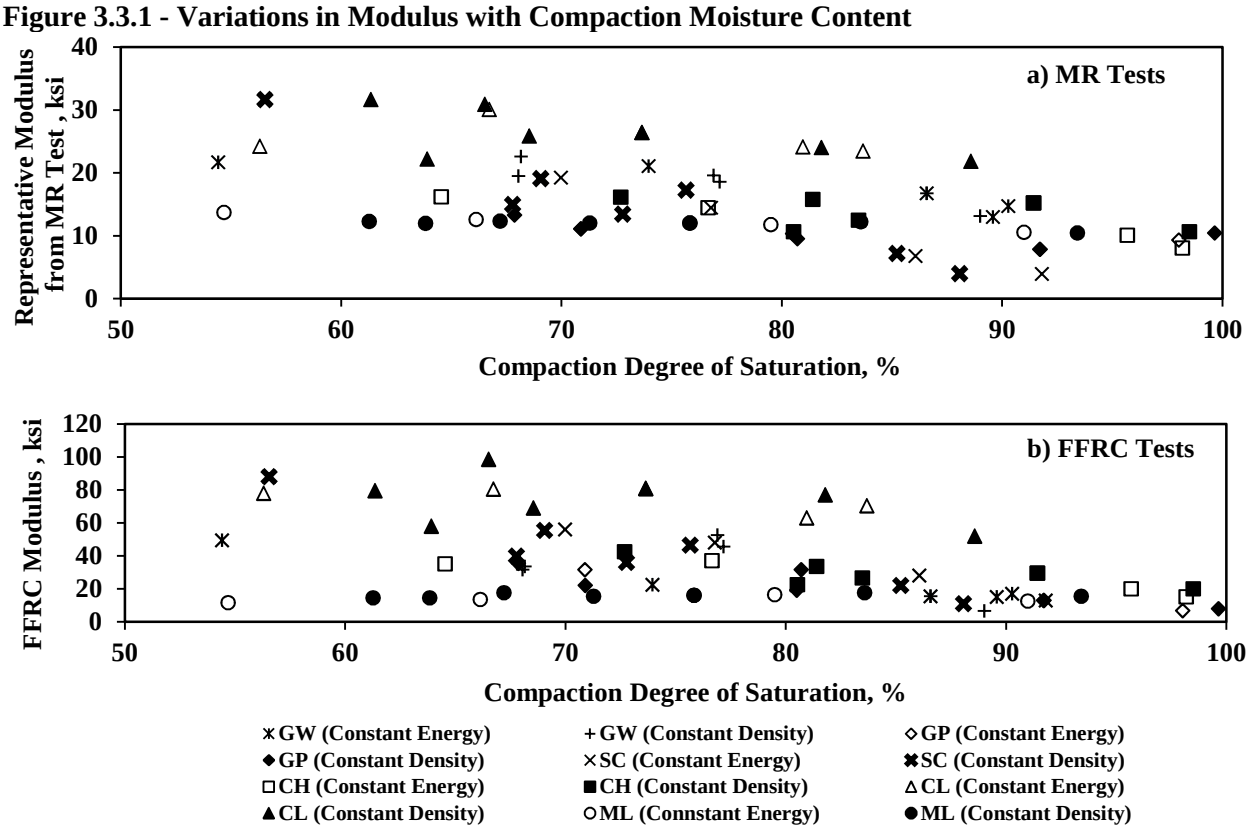

Figure 3.3.2 - Variations in Modulus with Degree of Saturation

The distributions of the estimation error related to Equations 2.8.14 and 2.8.15 are depicted in Figures 3.3.5 and 3.3.6 for measurements made with the MR and FFRC laboratory tests. The Cary and Zapata model seems to agree marginally to significantly better with the experimental results than the MEPDG model. The models also work better for laboratory MR moduli than for the FFRC moduli. Nevertheless, the estimation errors may be considered too significant. The Cary and Zapata curve for ***wPI***=0 predicts the representative MR and FFRC moduli better than either the MEPDG or general Cary and Zapata model with corresponding ***wPI*** of each material (see Figures 3.3.5 and 3.3.6).

An alternative way of developing a relationship between the modulus and moisture content is shown in Figure 3.3.7. Normalized moisture content is used as the independent variable (x-axis) as opposed to the degree of saturation. These results provide a reasonable correlation between the representative MR modulus and moisture content as well as the FFRC modulus and moisture content. These relationships do not seem to be appropriate for the GP and GW bases with less than certain moisture content (i.e. about 15% dry of OMC).

3.4 Impact of Moisture Content at Time of Testing relative to Moisture Content at Time of Compaction on Modulus

The change in the dry density of a compacted layer may be minimal as the time between the compaction and testing increases. However, the modulus of the same layer may change significantly in that period. To study that phenomenon, several specimens were compacted at different moisture contents to a constant density of MDD. Each compacted specimen was covered with a membrane and allowed to mature for 24 hrs. The membrane was then removed to allow the specimen to dry to OMC-3% (or 0.7 OMC). The specimen was tested frequently to measure its FFRC moduli at various testing moisture contents. The testing moisture contents were estimated by measuring the change in the weight of the specimen between consecutive measurements.

Figure 3.4.1 demonstrates the results obtained from that activity. Since moduli measurements performed at variable moisture levels for each specimen, the FFRC moduli were adjusted for specific moisture contents (i.e. OMC+2% to OMC-3%) in Figure 3.4.1 using the exponential modulus-moisture correlations developed for each specific geomaterial.

In general, the greater the differences between the compaction and testing moisture contents are, the greater the modulus will become. In other words, the longer the specimen is allowed to dry and the wetter the specimen is at the time of compaction, the greater the modulus becomes at the time of testing. This was evident when examining the specimens prepared at the wet of OMC and allowed to dry to 0.8 or 0.7 OMC. These specimens were extremely stiff and brittle.

The FFRC moduli presented in Figure 3.4.1 are converted to the form recommended by the MEPDG and Cary and Zapata in Figure 3.4.2. Neither proposed relationship could explain the trends in the data for the unbound aggregate bases. However, the data from the other materials are generally bracketed by the Cary and Zapata and the MEPDG recommendations. The distributions of estimation errors for specimens from fine-grained materials prepared at their corresponding OMCs are depicted in Figure 3.4.3. Once again, the Cary and Zapata model performs better than the MEPDG model. However, the Cary and Zapata model with ***wPI*** = 0 is not appropriate in this case.

To better match the experimental results for the fine-grained materials, a nonlinear estimation process was employed to find the optimum values of constants a, b and k_m in Equation 2.8.14 for this condition. The MEPDG model with a = -0.1119, b = 0.7887 and k_m = 12.372 estimates the experimental moduli with an uncertainty of less than 20% in 87% of cases (see the curve labeled as Modified MEPDG in Figure 3.4.3).

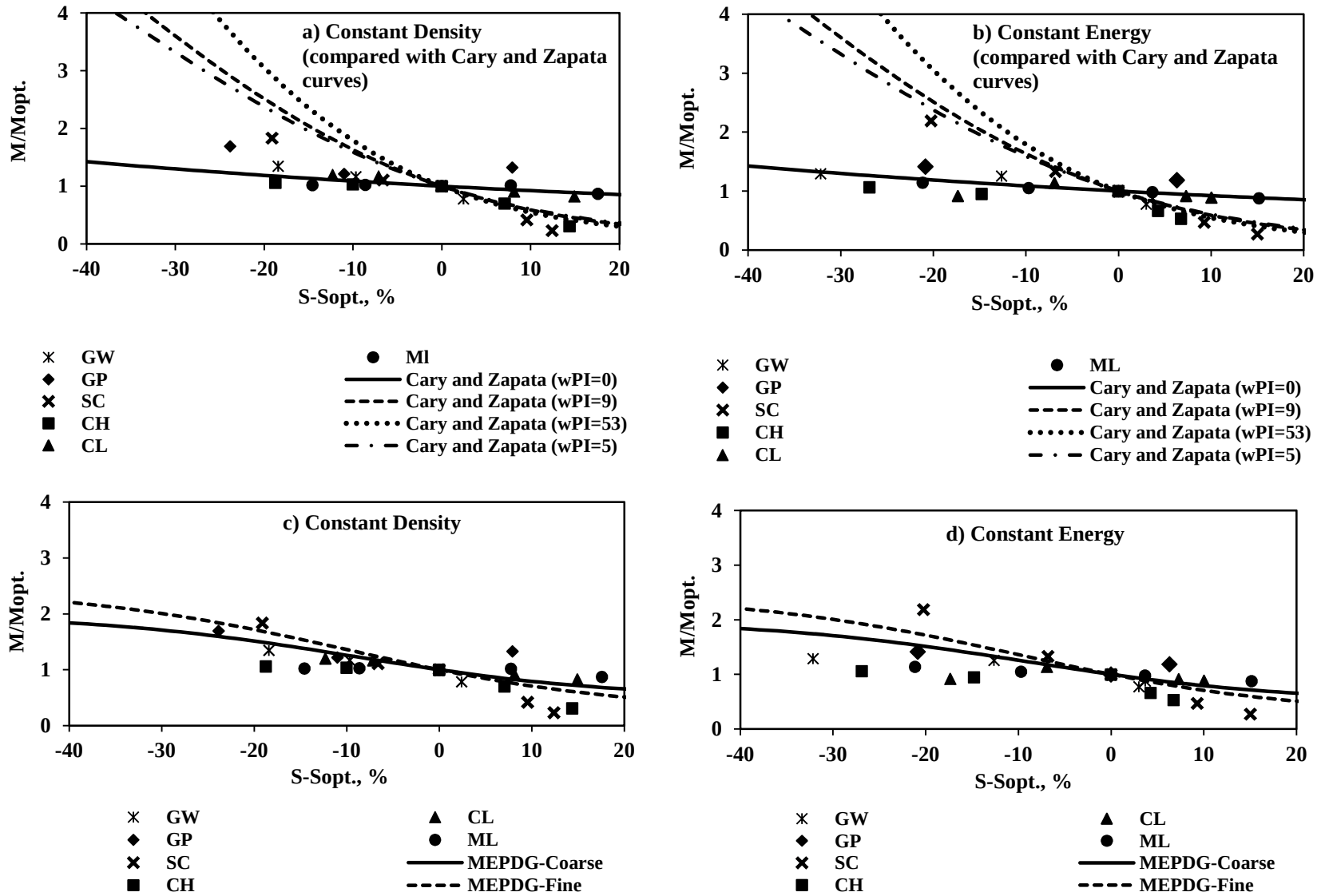

Figure 3.3.3 - Variations of Normalized Representative MR Modulus with Degree of Saturation

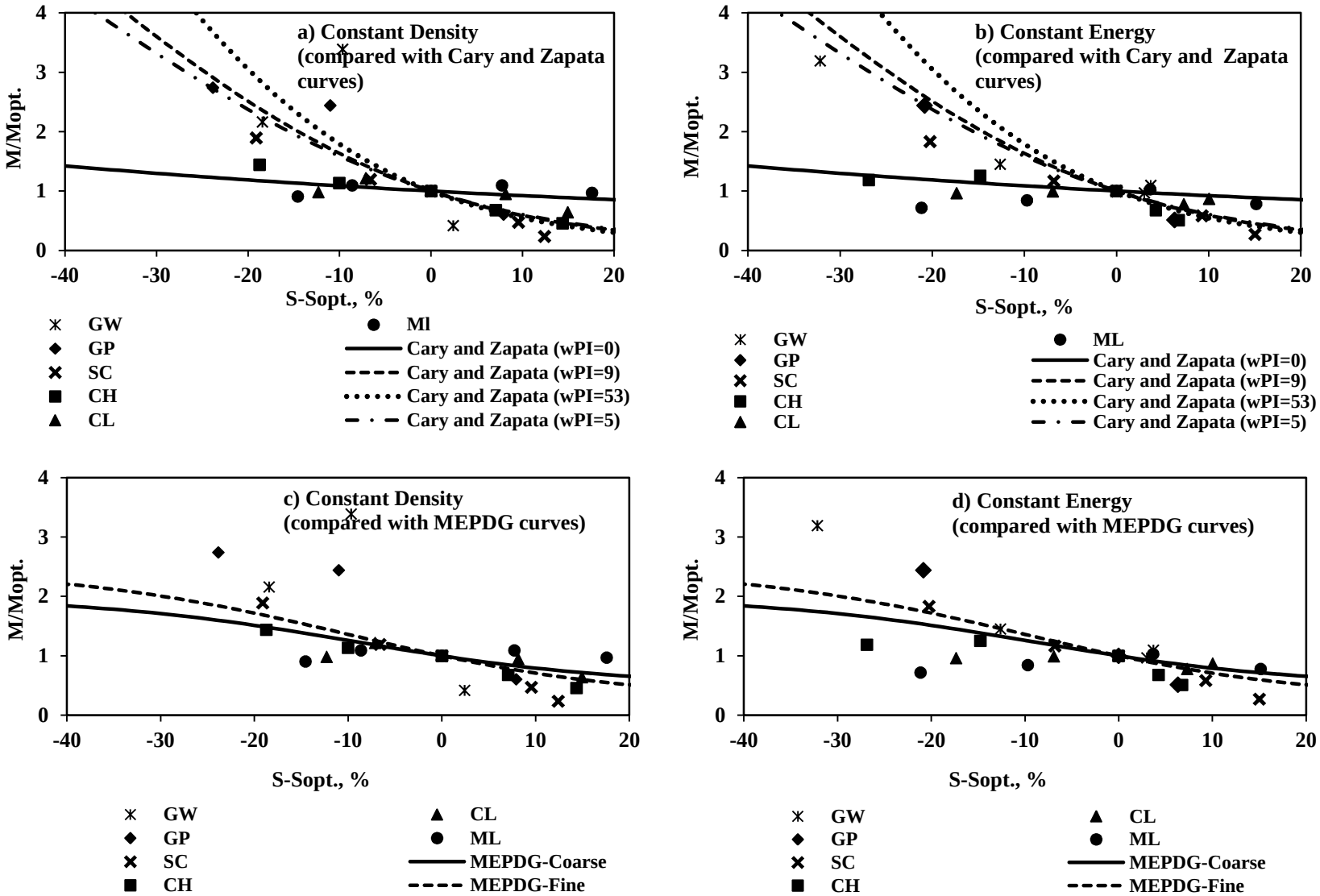

Figure 3.3.4 - Variations of Normalized FFRC Modulus with Degree of Saturation

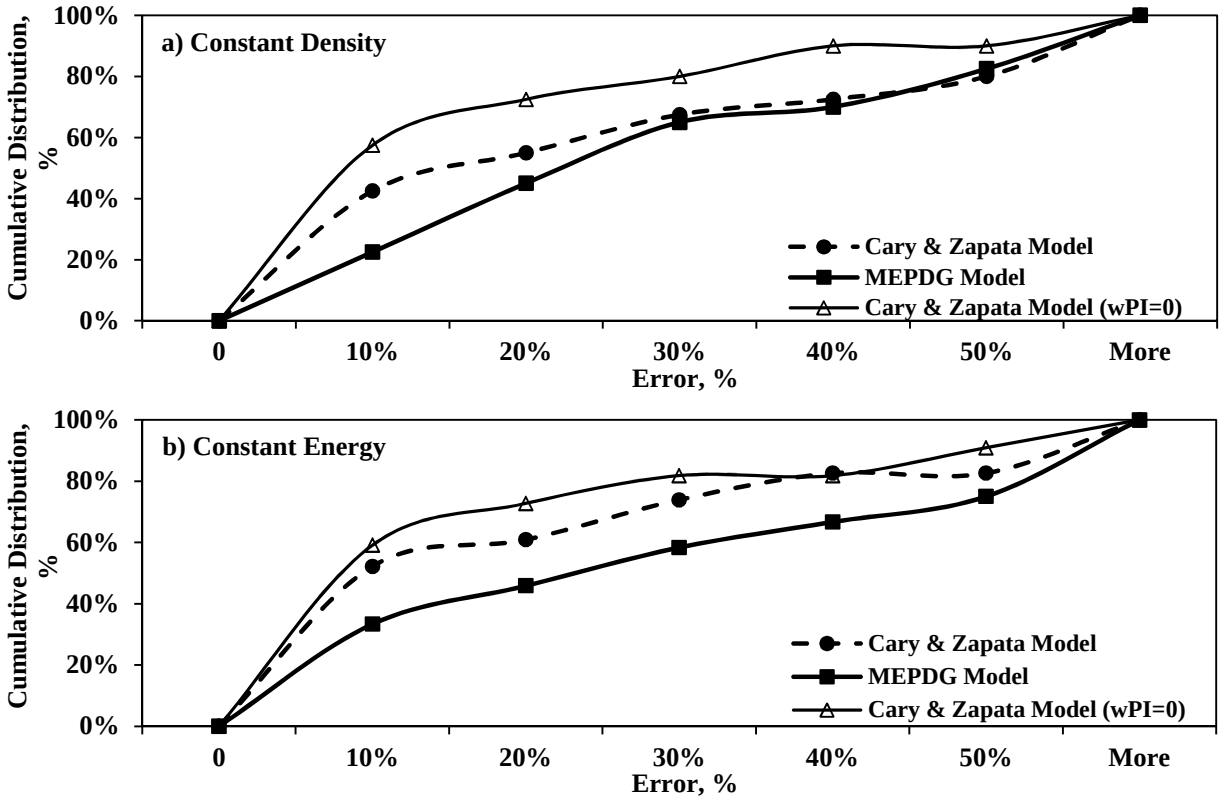

Figure 3.3.5 - Evaluation of Predictive Power of MEPDG and Cary and Zapata Models for MR Moduli

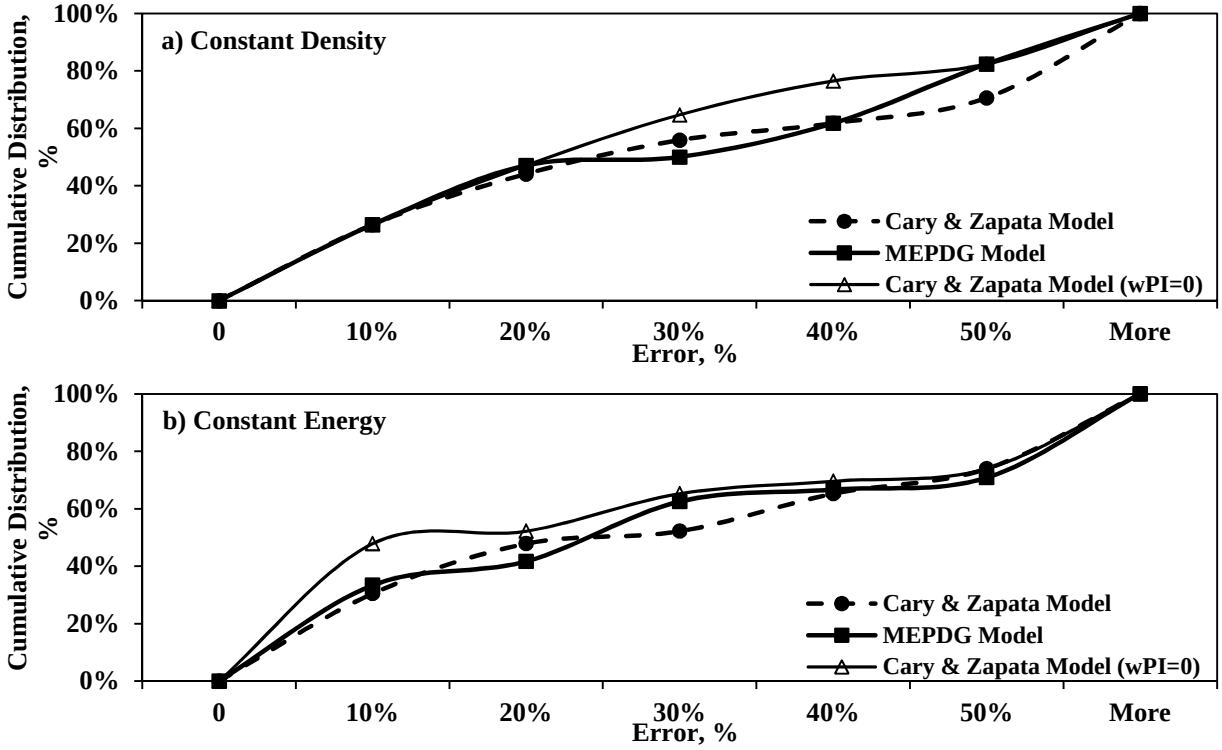

Figure 3.3.6 - Evaluation of Predictive Power of MEPDG and Cary and Zapata Models for FFRC Moduli

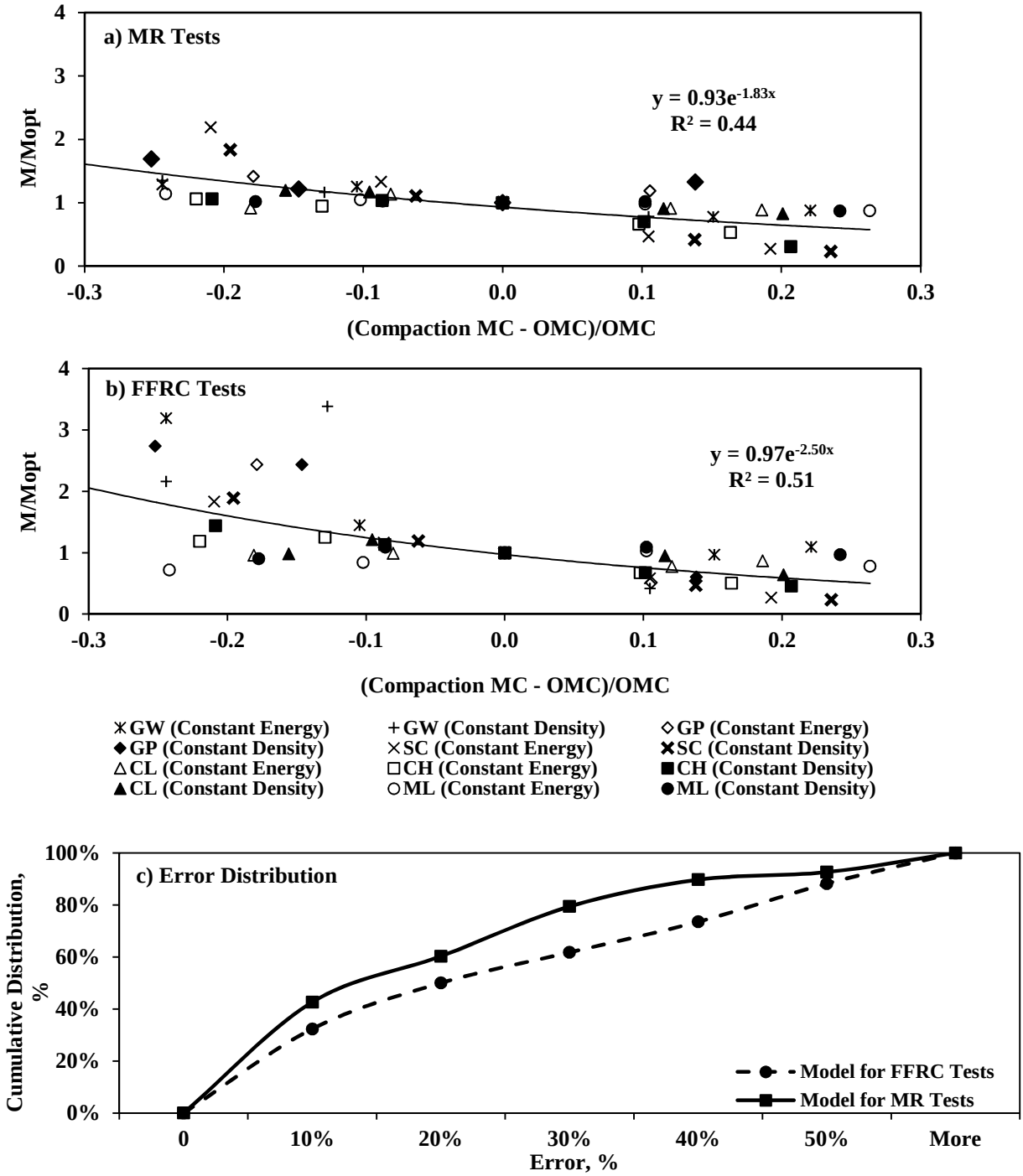

Figure 3.3.7 - Variations in Normalized Modulus with Compaction Moisture Content

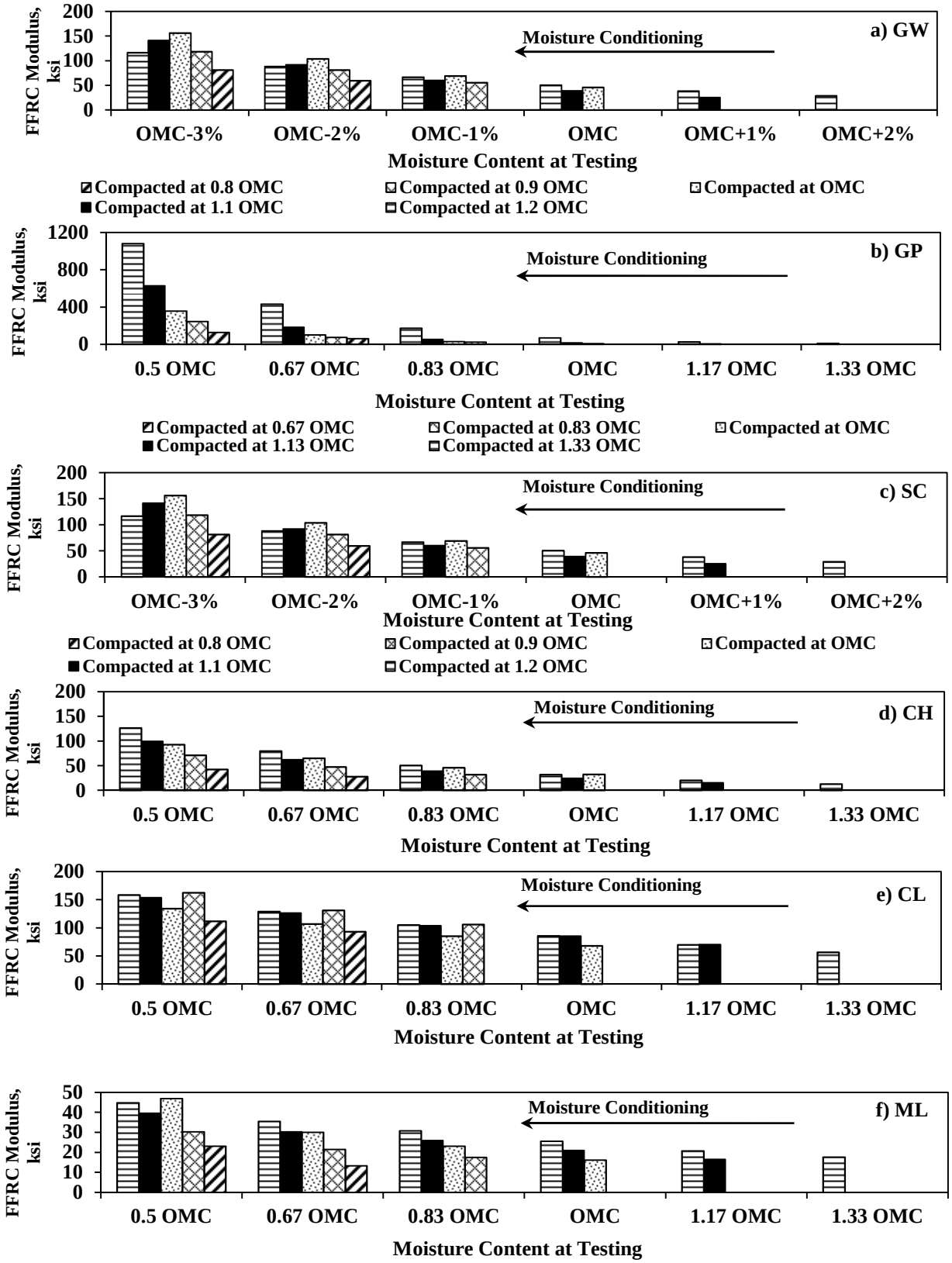

Figure 3.4.1 - Impact of Moisture Content at Time of Testing on Adjusted FFRC Modulus as a Function of Compaction Moisture Content

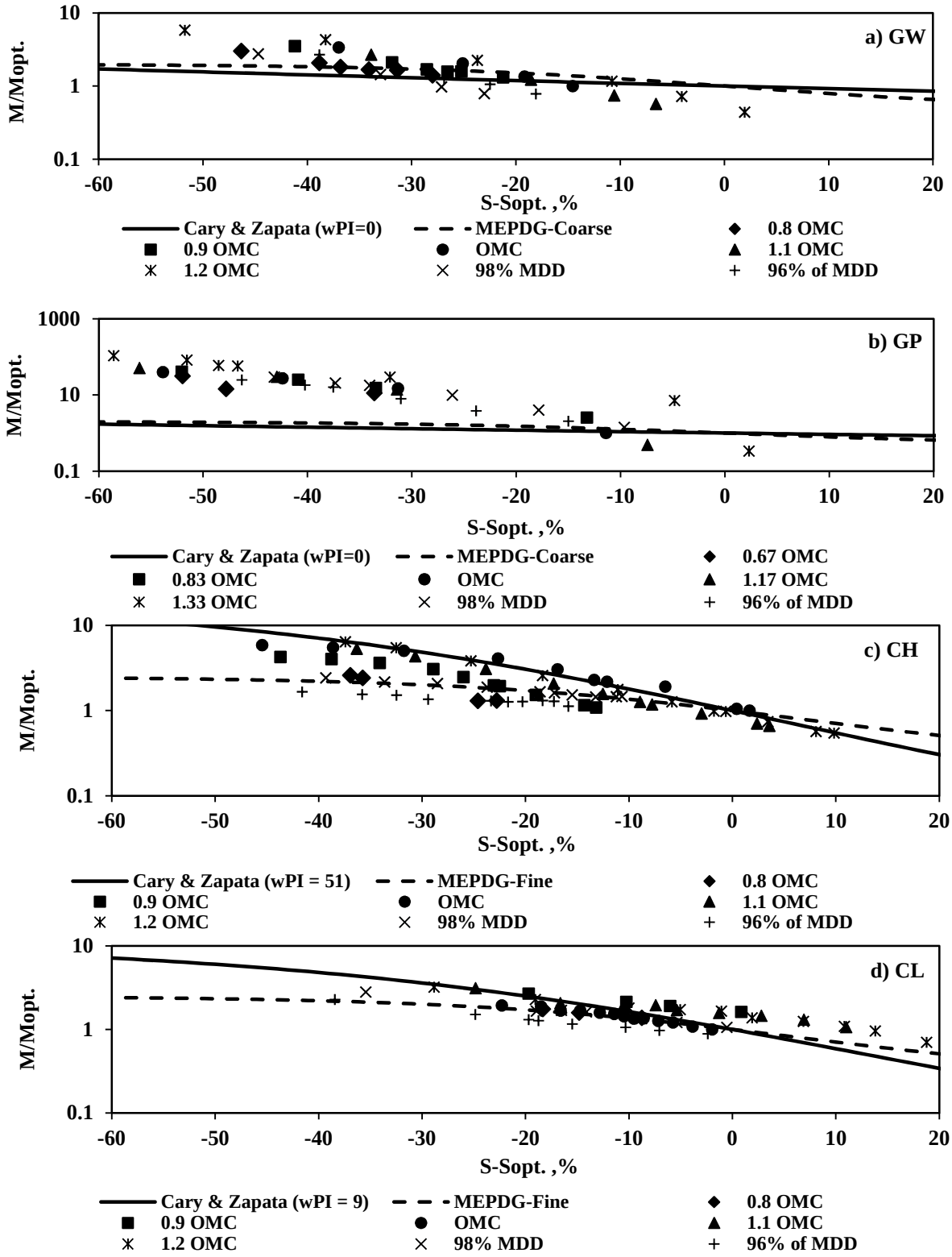

Figure 3.4.2 - Variations of Normalized FFRC Moduli with Degree of Saturation

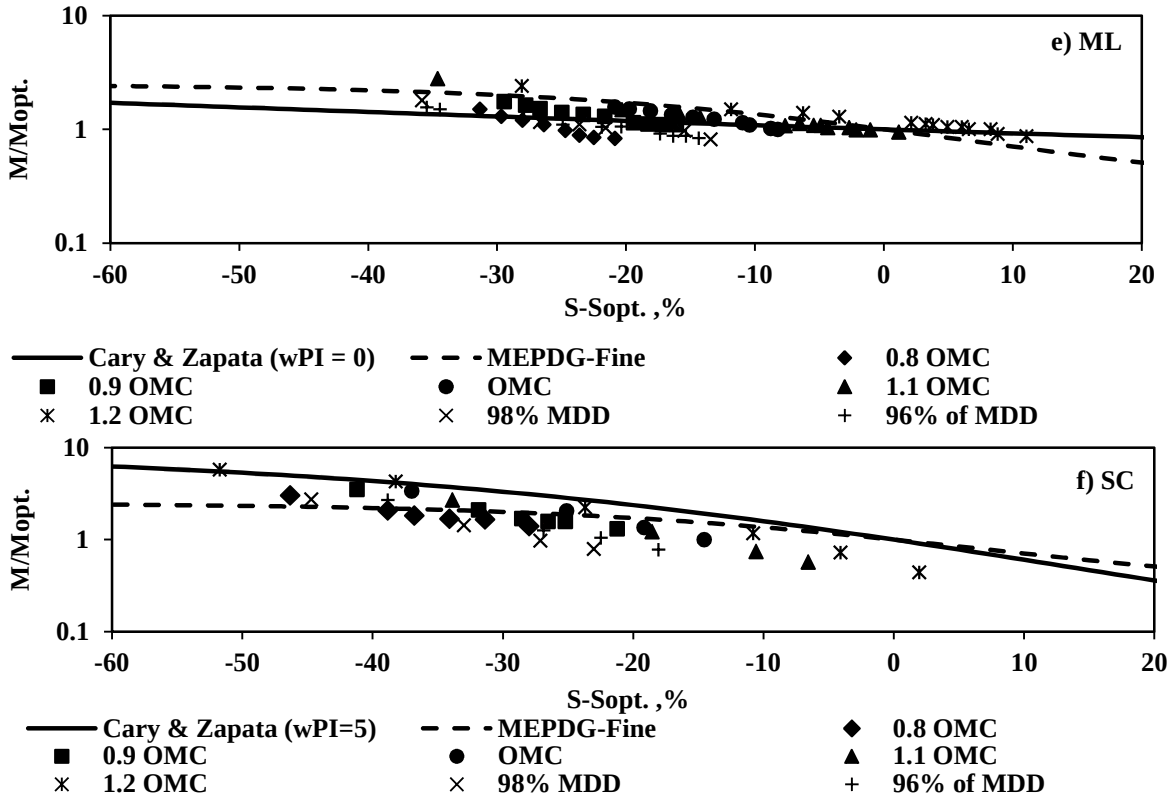

Figure 3.4.2, cont. - Variations of Normalized FFRC Moduli with Degree of Saturation

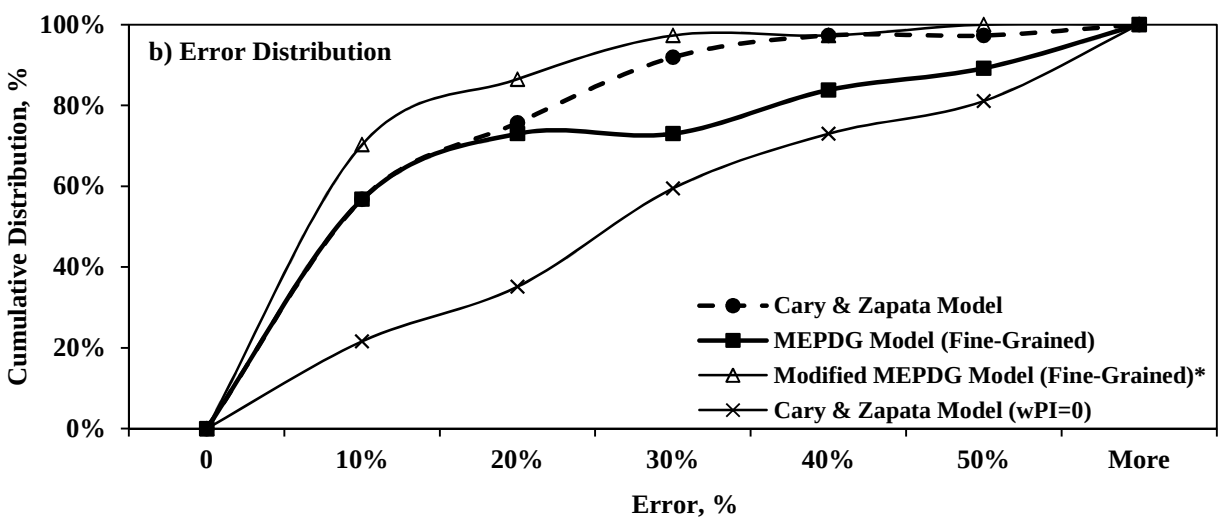

*Regression parameters (a, b and k_m) in MEPDG moisture-modulus model (Equation 2.8.14) were modified to reflect the behavior of fine-grained soils tested in this project.

Figure 3.4.3 - Evaluation of MEPDG and Cary and Zapata Models with Normalized FFRC Moduli during Conditioning Cycles (for Subgrade Materials Compacted at OMC and MDD)

Figure 3.4.4a illustrates a relationship between the ratio of the FFRC modulus at the time of testing and the FFRC modulus after compaction with the difference between compaction and testing moisture contents for each material. The alternative to MEPDG and Cary and Zapata relationships based on moisture content as an

independent variable is in the form of Equations. 3.4.1 through 3.4.3 for the two base and four subgrade materials used in this project:

$$Modulus_{Testing} / Modulus_{Compaction} = EXP[0.18(MC_{Compaction}-MC_{Testing})] \text{ (Subgrade Materials)} \quad (3.4.1)$$

$$Modulus_{Testing} / Modulus_{Compaction} = EXP[1.19(MC_{Compaction}-MC_{Testing})] \text{ (GP Base Materials)} \quad (3.4.2)$$

$$Modulus_{Testing} / Modulus_{Compaction} = EXP[0.66(MC_{Compaction}-MC_{Testing})] \text{ (GW Base Materials)} \quad (3.4.3)$$

The distributions of estimation errors from these equations are shown in Figure 3.4.4b. The model for the subgrades performs better than that for the bases. However, both models require further refinement with more materials.

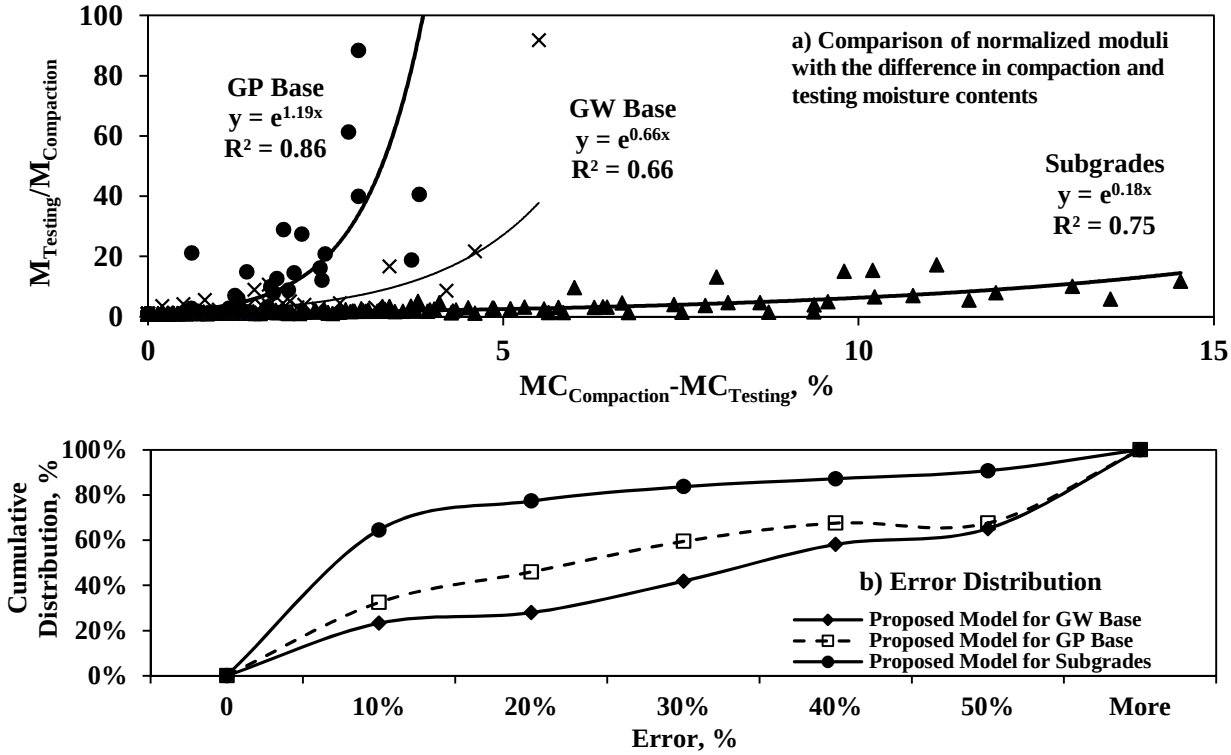

Figure 3.4.4 - Impact of Differences between Compaction and Testing Moisture Contents on FFRC Modulus

3.5 Tolerances to Accommodate Relative Compactions less than 100%

To study the impact of dry density on modulus, several specimens were prepared at nominal relative compactions of 96%, 98%, and 100% of MDD from each material. All specimens were compacted at the OMC. The representative MR and FFRC moduli for these specimens after compaction are presented in Figure 3.5.1. The representative MR moduli of the GP and GW base materials increase as the relative density decreases. The representative MR and FFRC moduli of the ML material do not seem to be impacted much by the variations in moisture content, as expected.

The moduli presented in Figure 3.5.1 are demonstrated in a normalized fashion in Figure 3.5.2. The normalized moduli can be used to adjust the target modulus during acceptance testing. Comparing Figures 3.4.1 and 3.5.2, the variation in the moisture content influences the modulus significantly more than the variations in density. It seems that an allowance of 10% to 30% can be incorporated in the target modulus for the densities less than the MDD.

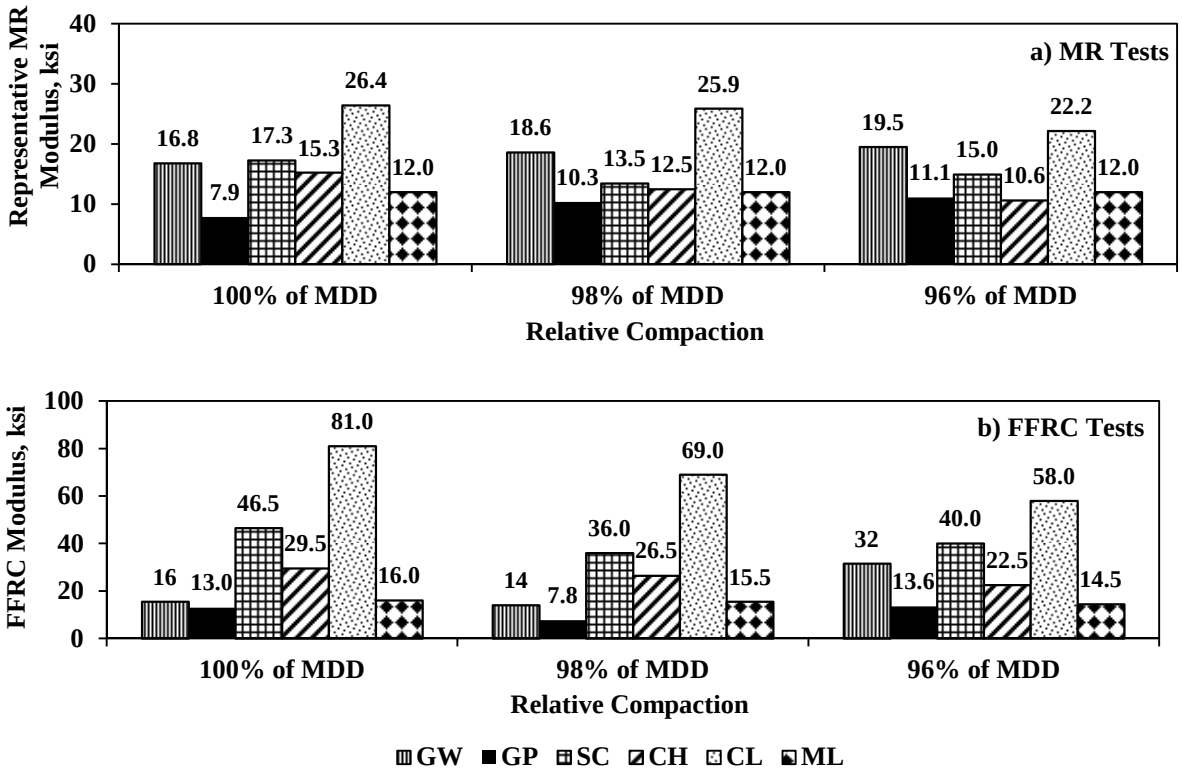

Figure 3.5.1 - Impact of Relative Density on Modulus (all specimens prepared at OMC)

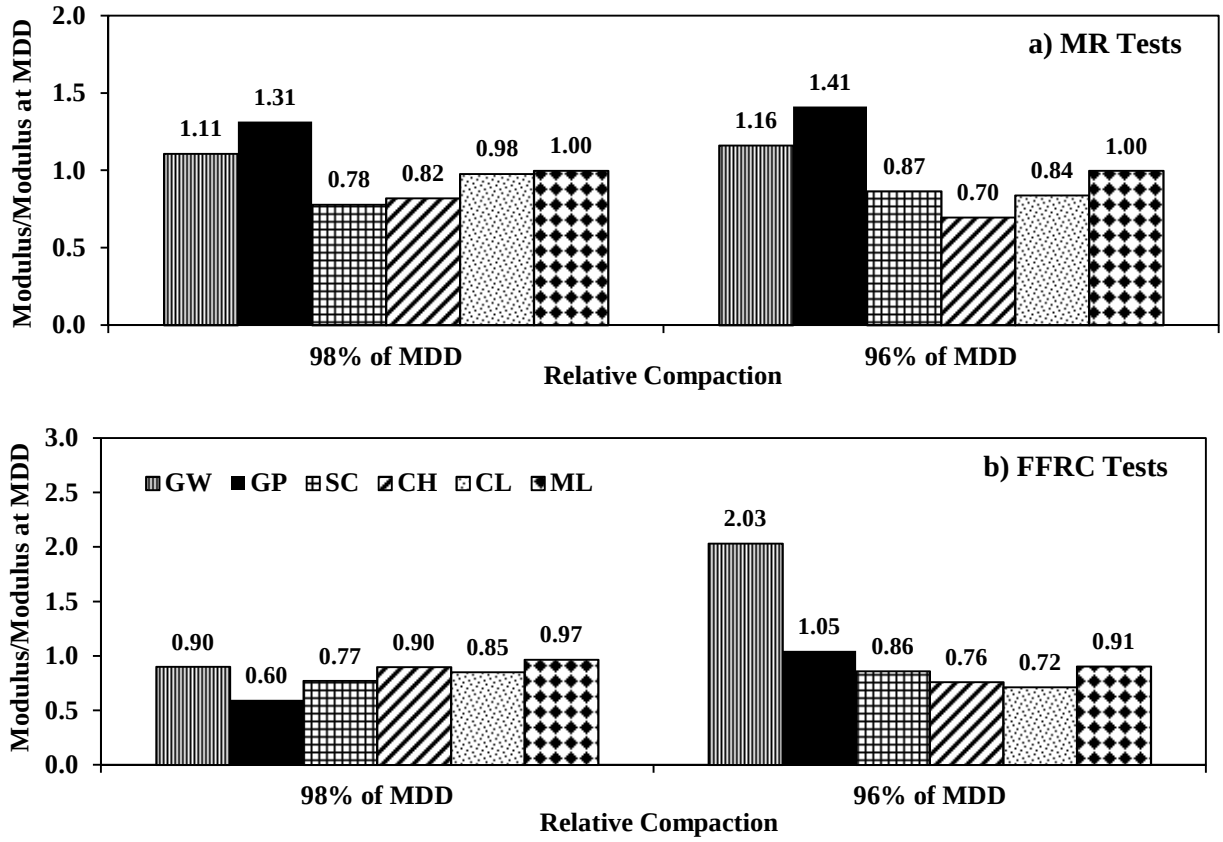

Figure 3.5.2 - Impact of Relative Density on Normalized Modulus (all specimens prepared at OMC)

The variations of moduli at different densities are superimposed on the MEPDG and Cary and Zapata curves in Figure 3.5.3. The Cary and Zapata curve with *wPI*=0 describes the experimental results better than the other two models as depicted in Figure 3.5.3c.

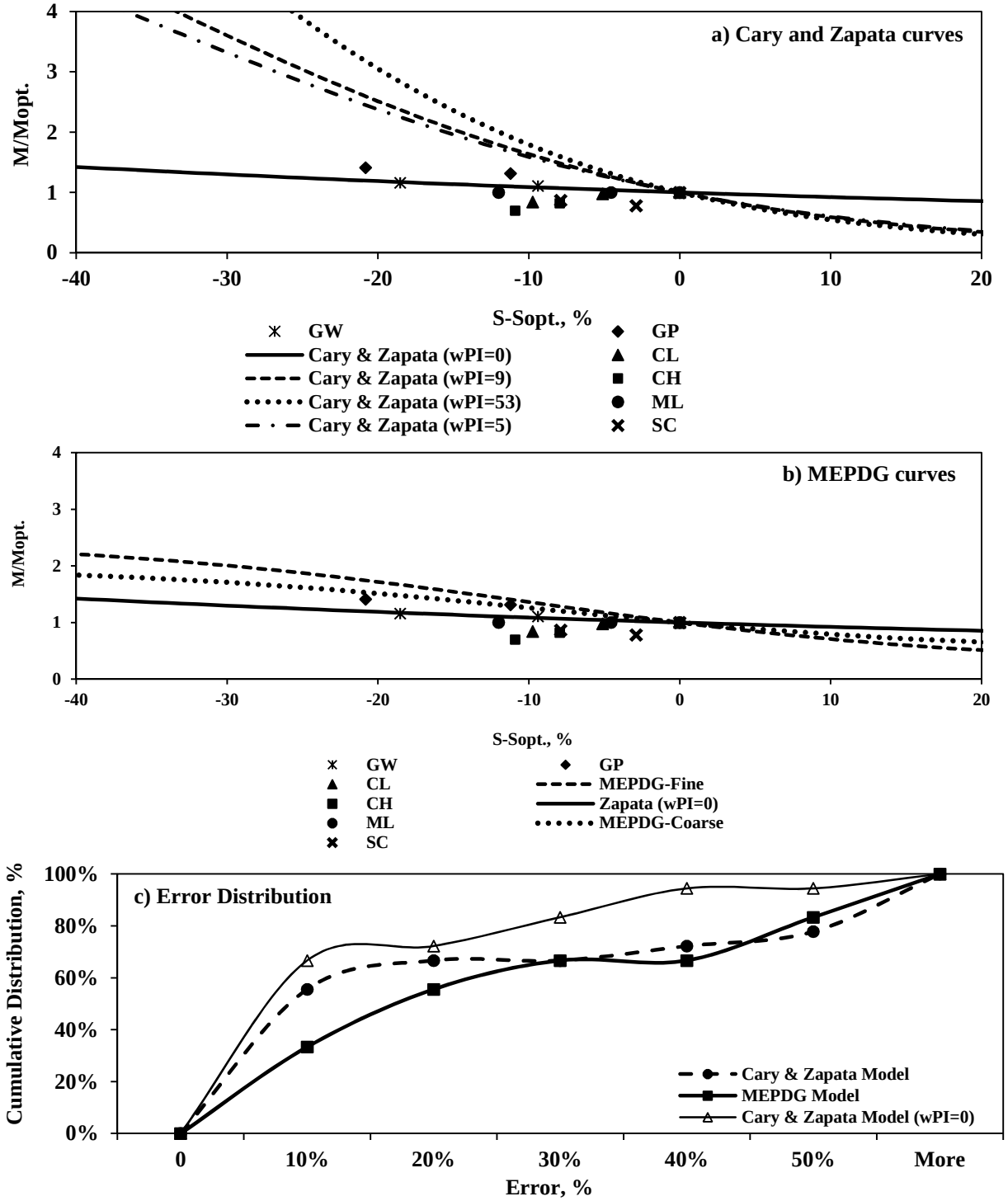

Figure 3.5.3 - Variations of Normalized Laboratory MR Modulus at Different Densities (MDD, 98%MDD, and 96%MDD) with Degree of Saturation

3.6 Suction-Controlled Resilient Modulus Tests

Two approaches were followed to perform resilient modulus tests under compaction moisture-related matric suction conditions. The first approach was to induce controlled soil suction conditions by axis translation technique. In the second approach, the resilient modulus tests were performed in accordance with the AASHTO T 307-03 standard method in order to compare the results of measured resilient moduli with the first approach. The soil suction during the resilient modulus testing was monitored via changes to the prior and after testing moisture contents, which in turn indirectly explains the changes in soil suction during the repeated loading (AASHTO T 307-03 procedure). Figure 3.6.1 shows comparisons between the resilient moduli measured from suction-controlled testing (first approach) and AASHTO T 307-03 (second approach) for the same net confining and deviatoric stresses. The AASHTO T 307-03 method appears to be sufficient for resilient modulus testing of these materials. Suction-controlled MR testing, which requires substantial time for each test specimen to reach suction equilibrium condition at each compaction moisture condition, is not needed. This is mainly due to the nondestructive nature of MR testing where the suction does not appreciably change during the repeated loading testing steps and hence suction controlled MR testing is not needed. Hence, the remaining specimens were compacted with known initial moisture contents and tested as per AASHTO T 307-03 procedure. The initial soil suction value was established based on the soil water characteristic curve data and the initial compaction moisture content.

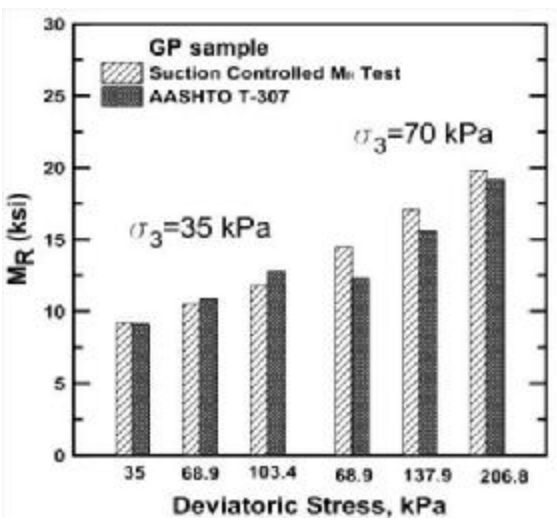

Figure 3.6.1 - Comparison of MR Results from First and Second Approaches

The regression coefficients k_1, k_2 and k_3 as per AASHTO T 307-03 procedure for three (CH, ML, and SC) geomaterials are shown in Table 3.6.1. The soil suction values were measured before and after resilient modulus testing using filter paper method. The matric suctions before and after MR tests are similar, indicating that no major change in soil suction occurred during the testing process. It is likely that soil suction may vary moderately in the specimen. However, global suction changes can only be identified if significant moisture flow takes place during testing. Any moisture changes would have yielded different suction values when samples were tested with filter paper method. In addition, no excess pore pressure development was observed as the applied deviatoric loads are small as compared to the ultimate loads at which soil specimens fail. Since soil suction measured is similar and there is no moisture migration during M_R testing, it is reasonable to assume that the soil suction remained the same during testing. There is no practical way of directly measuring soil suction as the current instrumentation with a tensiometer can only reliably measure very low suctions. Fredlund thermal conductivity (FTC) sensors are not appropriate because they are too large to fit within the samples.

From Table 3.6.1, the variations in resilient modulus with matric suction are nonlinear for all soils tested. In general, M_R increases with increase in matric suction. In this study, the samples were compacted at different

densities, which indicate some changes in the matric suction values. For example, GP sample compacted at OMC exhibits lower matric suction than the sample compacted at OMC+1 due to different compaction densities.

Two types of predictive models were evaluated. The first one focused on the MEPDG models to estimate the SWCCs based on soil properties. The second one used the moisture-based resilient modulus models recently developed in the literature. The following sections present these results.

Figure 3.6.2 presents a comparison of the estimated SWCC curves from the MEPDG Level 2 and Level 3 algorithms with the data measured in this study using a Tempe cell and the filter paper method. The Level 2 prediction is used when the direct measurements of optimum gravimetric water content ( ), maximum dry unit weight ( ), specific gravity of solid ( ), , , and *PI* are provided. The Level 3 prediction is available in the case where values of , , and *PI* are directly measured. The parameters such as optimum volumetric water content ( ), initial degree of saturation ( ), saturated volumetric water content ( ) and SWCC model parameters (, , , and h) are computed. The SWCC is generated based on the Fredlund and Xing (1994) equation (see Equation 2.8.12). The Level 2 and Level 3 estimates are similar to the measured results for the CL, ML, and CH soils. The Level 2 estimates are more reasonable as compared to the Level 3 estimates for the GP base material.

As indicated in Chapter 2, the Cary and Zapata (2010) model and the Siekmeier (2011) model that accounts for soil suction information were used to estimate the MR results. Figure 3.6.3 compares these two models and their predictive powers. The Cary and Zapata model shows good agreement with the measured resilient moduli. Parameters of the Cary and Zapata model are summarized in Table 3.6.2.

The Siekmeier model is reported to be appropriate for fine-grained material (Siekmeier, 2011). The initial parts of the analysis showed that the model parameters from the Siekmeier model provided results that were different from the measured results. After revising the model parameters, the predictions are close to measured results as can be seen in Figure 3.6.3. Revised model parameters, k_1, k_2, and k_3, obtained by analyzing the results received from MR testing on different moisture content soil specimens with the statistical multiple regression analysis are presented in Table 3.6.3.

The resilient moduli results obtained from the suction controlled testing are close to those from AASHTO T 307-03 method for the same stress state conditions. The closeness of these results indicates that the T 307-03 method is sufficient for resilient modulus testing of the soils. Considering that time periods of several weeks are needed to reach equilibrium soil suction conditions for cohesive soils prior to MR testing, it is recommended that the traditional T 307-03 method be used for testing soils. Soil suction information of these soil samples can be provided to address the moisture variation during this MR testing and then to evaluate soil suction details from the SWCC studies.

Table 3.6.1 - Laboratory Results of MR Tests including Suction-Controlled MR Test on GP Material

Material	Moisture Content	Dry Density, (pcf)	Nonlinear Parameters				Representative MR, (ksi)	Suction**, (kPa)
			k_1	k_2	k_3	R^2		
GP	OMC-2%	142	389	1.04	-0.20	0.99	17.3	100
	OMC-1%	145	288	0.98	-0.01	0.96	13.9	50
	OMC	147	234	1.03	-0.01	0.94	12.8	10
	OMC+1%	145	191	1.10	0.00	0.97	11.2	20
	OMC+2%	138	-	-	-	-	-	< 5
	OMC (Suction Controlled)	147	263	1.00	0.00	0.95	13.5	50
CL	OMC-2%	122	349	0.92	-0.34	0.90	13.6	160
	OMC-1%	124	340	0.88	-0.39	0.98	11.6	120
	OMC	125	269	0.80	-0.12	0.97	9.6	30
	OMC+1%	124	251	0.71	-0.27	0.99	7.4	25
	OMC+2%	122	209	0.79	-0.32	0.97	7.1	20
CH	OMC-20%OMC	93	623	0.40	-2.80	0.96	7.0	310
	OMC-10%OMC	94.4	370	0.40	-2.60	0.98	4.5	290
	OMC	95.5	303	0.26	-1.50	0.97	3.9	180
	OMC+10%OMC	94.4	180	0.30	-1.10	0.88	2.6	105
	OMC+20%OMC	92	164	0.20	-1.00	0.87	2.2	50
ML	OMC-20%OMC	123.4	415	0.88	-0.72	0.96	9.2	26
	OMC-10%OMC	124.3	293	1.00	-0.50	0.94	7.1	26
	OMC	124.6	252	1.10	-0.45	0.99	6.5	25
	OMC+10%OMC	124.3	213	1.03	0.00	0.83	5.8	24
	OMC+20%OMC	123.4	122	1.10	0.00	0.83	3.7	23
SC	OMC-20%OMC	118.7	790	0.43	-2.44	0.96	10.0	120
	OMC-10%OMC	120.7	491	0.77	-2.02	0.97	8.0	118
	OMC	121.4	461	0.80	-1.97	0.96	7.5	115
	OMC+10%OMC	120.7	260	1.27	-2.76	0.94	4.6	110
	OMC+20%OMC	118.7	153	1.60	-2.30	0.96	3.6	90

**The suction estimated from Soil Water Characteristic Curve (SWCC)

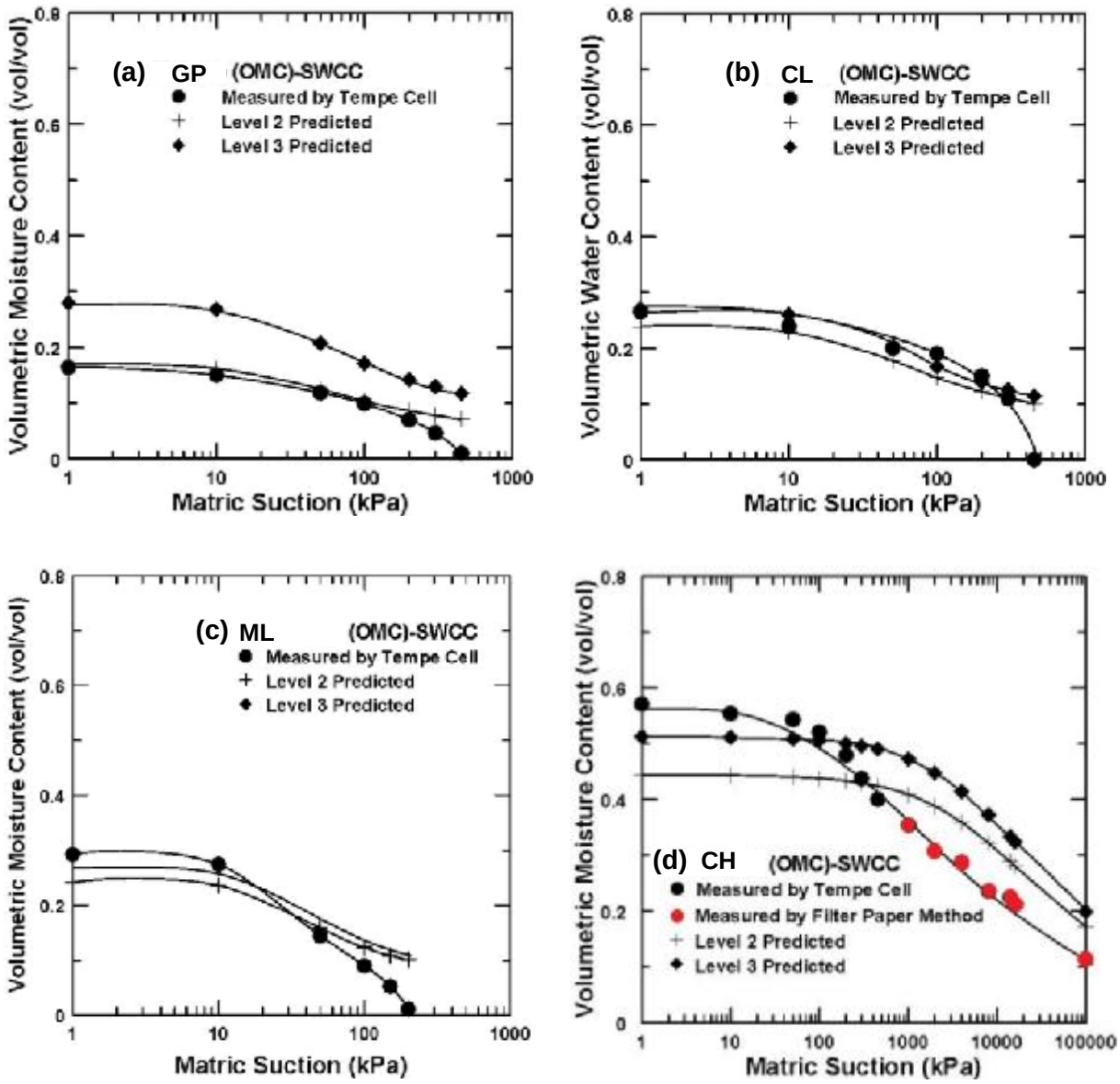

Figure 3.6.2- Predicted vs. Measured SWCCs

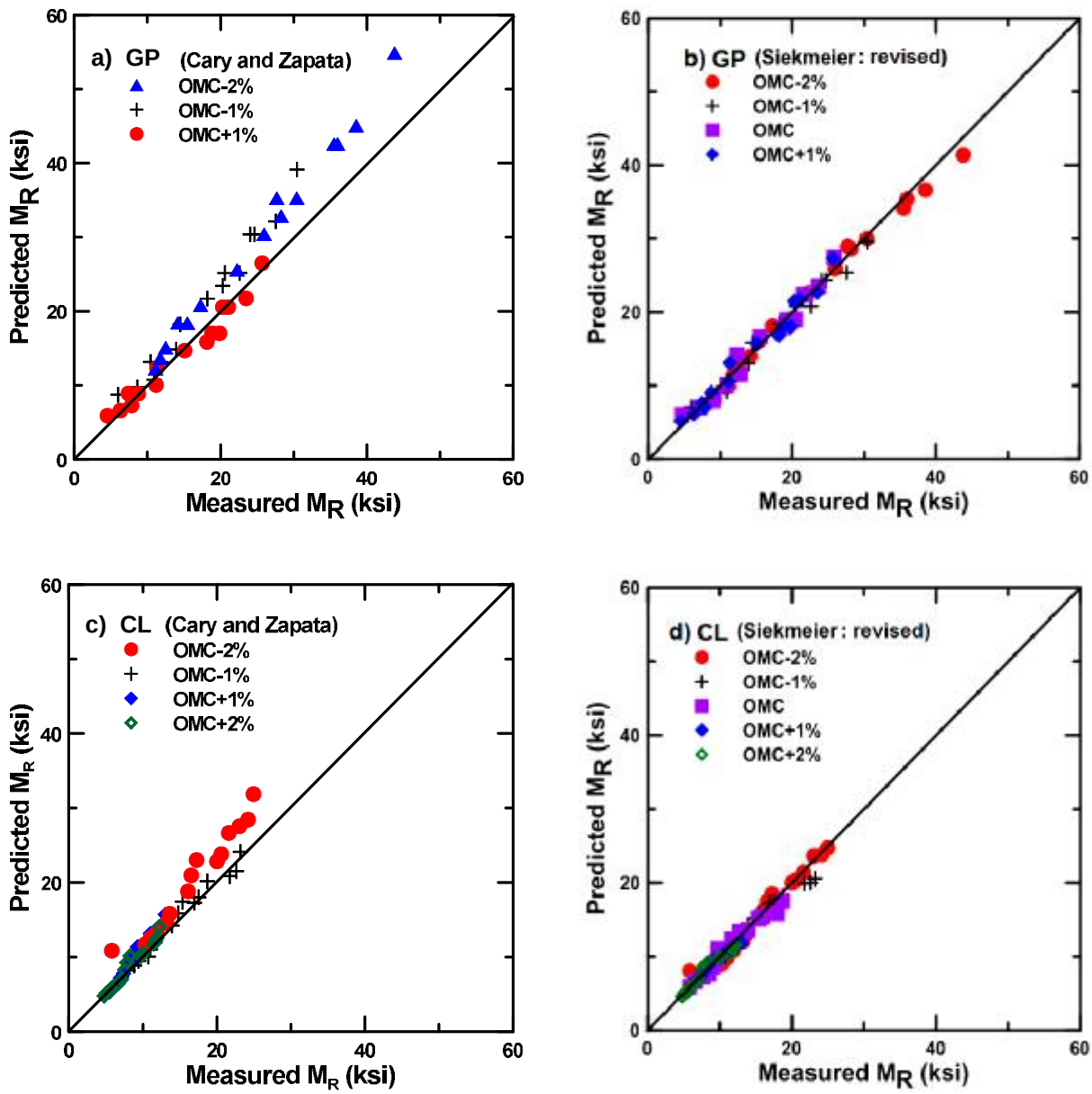

Figure 3.6.3 - Comparison of Cary and Zapata (2010) and Revised Siekmeier (2011) Models

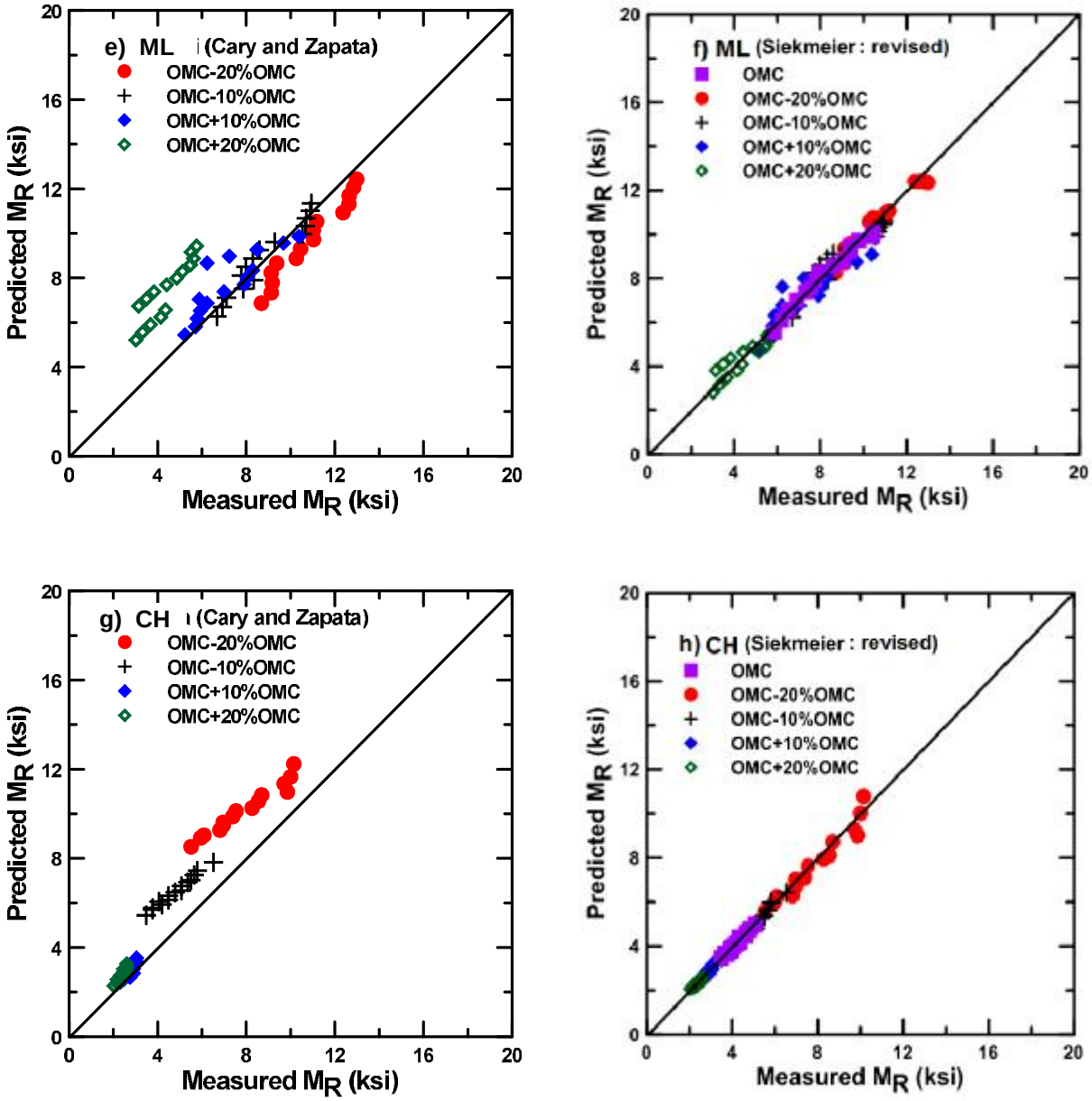

Figure 3.6.3, cont. - Comparison of Cary and Zapata (2010) and Revised Siekmeier (2011) Models

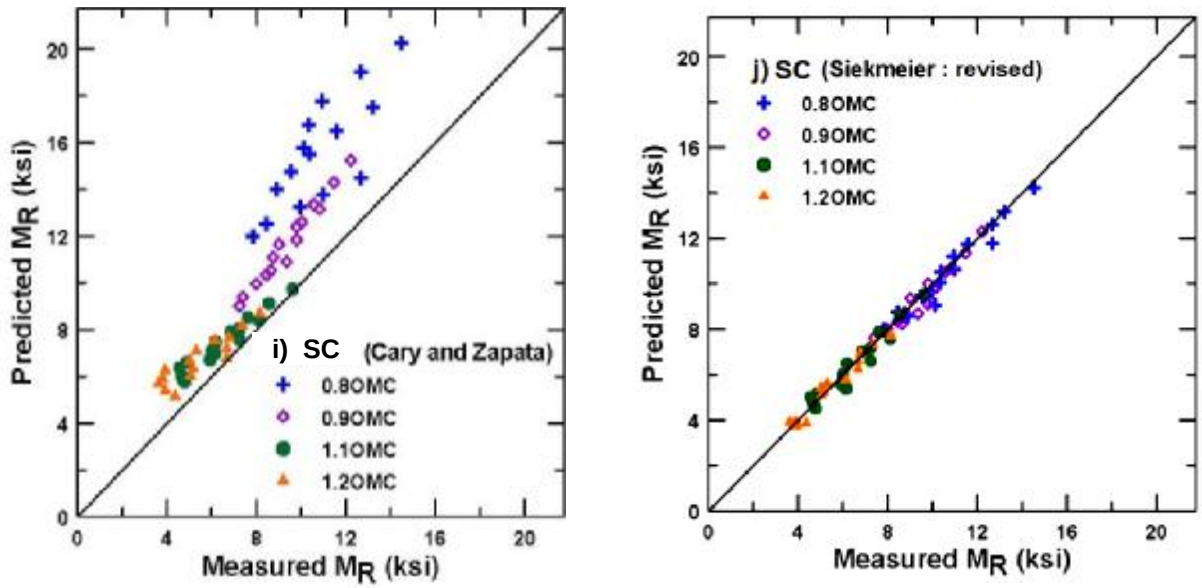

Figure 3.6.3, cont. - Comparison of Cary and Zapata (2010) and Revised Siekmeier (2011) Models

Table 3.6.2 - Model Parameters for Cary and Zapata (2010) Model

Material	Water Content, w (%)		Plasticity index, PI	Degree of saturation, S	Optimum Degree of Saturation, S_{opt}	Representative MR at OMC, MR_{opt} (ksi)	Model Parameters						Predicted MR (ksi)
GP	OMC – 2%	4.0	9	0.49	0.89	12.8	-0.6	-1.87194	0.8	0.08	11.96518	-10.19111	20.8
	OMC – 1%	5.0	9	0.71	0.89	12.8	-0.6	-1.87194	0.8	0.08	11.96518	-10.19111	14.8
	OMC + 1%	7.0	9	0.92	0.89	12.8	-0.6	-1.87194	0.8	0.08	11.96518	-10.19111	10.0
	OMC + 2%	8.0	9	0.97	0.89	12.8	-0.6	-1.87194	0.8	0.08	11.96518	-10.19111	-
CL	OMC – 2%	8.0	14	0.55	0.75	9.6	-0.6	-1.87194	0.8	0.08	11.96518	-10.19111	15.8
	OMC – 1%	9.0	14	0.66	0.75	9.6	-0.6	-1.87194	0.8	0.08	11.96518	-10.19111	12.0
	OMC + 1%	11.0	14	0.80	0.75	9.6	-0.6	-1.87194	0.8	0.08	11.96518	-10.19111	7.8
	OMC + 2%	12.0	14	0.83	0.75	9.6	-0.6	-1.87194	0.8	0.08	11.96518	-10.19111	7.0
CH	OMC– 20% OMC	21.0	53	0.67	0.89	3.9	-0.6	-1.87194	0.8	0.08	11.96518	-10.19111	9.6
	OMC – 10% OMC	23.5	53	0.79	0.89	3.9	-0.6	-1.87194	0.8	0.08	11.96518	-10.19111	6.1
	OMC + 10% OMC	28.5	53	0.96	0.89	3.9	-0.6	-1.87194	0.8	0.08	11.96518	-10.19111	2.8
	OMC + 20% OMC	31.0	53	0.97	0.89	3.9	-0.6	-1.87194	0.8	0.08	11.96518	-10.19111	2.6
ML	OMC – 20% OMC	7.4	0	0.61	0.81	6.5	-0.6	-1.87194	0.8	0.08	11.96518	-10.19111	7..8
	OMC – 10% OMC	8.4	0	0.72	0.81	6.5	-0.6	-1.87194	0.8	0.08	11.96518	-10.19111	7.1
	OMC + 10% OMC	10.4	0	0.89	0.81	6.5	-0.6	-1.87194	0.8	0.08	11.96518	-10.19111	6.2
	OMC + 20% OMC	11.4	0	0.94	0.81	6.5	-0.6	-1.87194	0.8	0.08	11.96518	-10.19111	5.9
SC	OMC – 20% OMC	9.1	12	0.58	0.78	7.5	-0.6	-1.87194	0.8	0.08	11.96518	-10.19111	13.3
	OMC – 10% OMC	10.3	12	0.69	0.78	7.5	-0.6	-1.87194	0.8	0.08	11.96518	-10.19111	10.0
	OMC + 10% OMC	12.5	12	0.84	0.78	7.5	-0.6	-1.87194	0.8	0.08	11.96518	-10.19111	6.4
	OMC + 20% OMC	13.7	12	0.87	0.78	7.5	-0.6	-1.87194	0.8	0.08	11.96518	-10.19111	5.7

Table 3.6.3 – Revised Model Parameters for Siekmeier (2011) Model

Material	Moisture Content	Dry Density, (pcf)	Model Parameters (Regression Analysis)				Predicted MR, (ksi)
			k_1	k_2	k_3	R^2	
GP	OMC-2%	142	741	0.75	-0.13	0.99	18.1
	OMC-1%	145	537	0.69	0.00	0.97	13.0
	OMC	147	468	0.73	-0.01	0.96	11.5
	OMC+1%	145	398	0.79	-0.03	0.98	10.5
	OMC+2%	138	-	-	-	-	-
CL	OMC-2%	122	602	0.68	-0.34	0.92	12.9
	OMC-1%	124	589	0.59	-0.32	0.97	11.7
	OMC	125	447	0.54	-0.06	0.97	9.4
	OMC+1%	124	389	0.47	-0.20	0.98	9.4
	OMC+2%	122	355	0.53	-0.25	0.96	6.9
CH	OMC-20%OMC	93	800	0.238	-2.81	0.96	7.1
	OMC-10%OMC	94.4	466	0.245	-2.60	0.97	4.3
	OMC	95.5	349	0.163	-1.53	0.97	3.9
	OMC+10%OMC	94.4	218	0.166	-1.13	0.86	2.6
	OMC+20%OMC	92	186	0.104	-1.02	0.85	2.2
ML	OMC-20%OMC	123.4	766	0.46	-0.72	0.96	9.1
	OMC-10%OMC	124.3	586	0.53	-0.50	0.92	7.2
	OMC	124.6	536	0.58	-0.46	0.98	6.6
	OMC+10%OMC	124.3	437	0.54	0.00	0.80	5.8
	OMC+20%OMC	123.4	263	0.58	0.00	0.81	3.5
SC	OMC-20%OMC	118.7	1034	0.24	-2.43	0.95	9.6
	OMC-10%OMC	120.7	790	0.45	-2.01	0.95	8.0
	OMC	121.4	749	0.48	-1.96	0.96	7.7
	OMC+10%OMC	120.7	556	0.76	-2.76	0.93	5.0
	OMC+20%OMC	118.7	407	0.95	-2.31	0.96	3.9

CHAPTER 4 - FINDINGS FROM SMALL-SCALE TESTING STUDY

The objectives of the small-scale study were to:

1. Establish relationships among the density, moisture content, and the parameters measured with the modulus-based devices,
2. Relate field and laboratory moduli under controlled conditions,
3. Evaluate how well the moisture-modulus relationships developed from laboratory specimens represent the field values under similar moisture content and density, and
4. Establish the repeatability and reproducibility of the selected modulus and moisture devices.

The first three items are discussed below after some introductory information. The fourth objective is addressed in Chapter 5.

4.1 Testing Program for Small-Scale Study

The experimental plan of the small-scale study tests was summarized earlier in Table 1.5.2. The compaction method for the small-scale experiments was limited to constant density to better simulate actual construction practices. Four unique specimens were prepared for each geomaterial. Three of the specimens were compacted to MDD but at different moisture contents (OMC, 0.7 OMC and 1.3 OMC for the base materials, and OMC, 1.2 OMC and 0.8 OMC for the fine-grained geomaterials). The fourth specimen was compacted at OMC but at a density equal to 96% of MDD. All specimens were placed over a similar subgrade.

4.2 Construction of Specimens

Figure 4.2.1 shows a schematic of the general setup of the small-scale study detailing the location of the sensors. The soil profile in each specimen consisted of 6 in. (150 mm) of one of the six geomaterials selected for this project (called geomaterial layer hereafter) and 16 in. (400 mm) of a local silty sand material (SM material in Table 3.1.1, called subgrade hereafter). The focus of this study was the geomaterial layer. A 3-in. (75-mm) thick layer of pea gravel was placed at the bottom of the specimen to facilitate the saturation of the subgrade under capillary conditions. The specimens were prepared in a 36 in. (900 mm) diameter PVC pipe that was placed on a hard floor (4 ft, 1.2 m of concrete) to minimize the movement of the bottom of the specimen. The size of the specimens was determined through finite element modeling by Amiri et al. (2009) to ensure that the interaction between the horizontal and vertical boundaries and model pavement is minimal. A diameter of 36 in. (900 mm) was deemed adequate since the stresses and strains at the boundaries were typically less than 3% of the stresses applied to the specimen. A geophone was used to monitor the movement of the floor to ensure that the specimen did not move excessively.

A concrete mixer was used to prepare the subgrade and geomaterial materials to the desired moisture contents. An amount of dry geomaterial necessary to achieve a desired density for a 2 in. (50 mm) lift was placed in the mixer. A precise amount of water was added to the soil with a water sprayer to ensure precise moisture content. The moist material was transferred into the PVC container and was compacted to desired density with a hand compactor. This process was repeated until the subgrade and geomaterial layers were completed.

Sensors were embedded within the geomaterials at predetermined depths during the construction of the specimen (Figure 4.2.1). Nine geophones were embedded within the specimen to measure the displacements at different locations with different modulus-based devices. These displacements were used to calibrate the analytical models as described in Chapter 6. Two sets of resistivity probes were placed in the subgrade to monitor the progression of water within the specimen during the saturation process. The upper resistivity probes were used to determine the appropriate time to test the specimens under subgrade-saturated condition. A third set of resistivity probes was placed in the geomaterial layer to monitor the change in its moisture content during the dry back. Two sets of Decagon moisture sensors were also placed in the geomaterial layer as shown in Figure 4.2.1.

As will be discussed in Chapter 5, additional small-scale specimens were prepared with different materials to investigate the variability and accuracy of different moisture devices (i.e. Soil Density Gauge, Speedy Moisture Tester, and DOT600 roadbed water content meter) selected in this study.

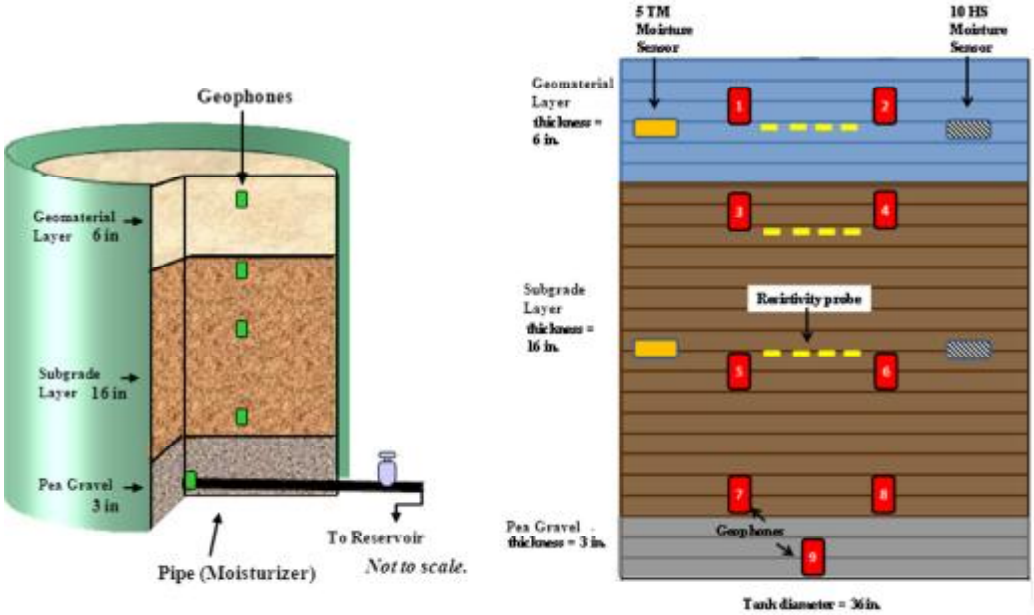

Figure 4.2.1 - Profile of Small-Scale Specimen

4.3 Impact of Compaction and Testing Moisture Contents at Constant Density

The average moduli measured with the ultrasonic surface wave (PSPA), electro-mechanical stiffness (Geogauge), DCP, and LWD (Dynatest and Zorn) technologies are superimposed on the Cary and Zapata and MEPDG versions of Equation 2.8.13 in Figures 4.3.1 through 4.3.5, respectively. Visually, the MEPDG relationship for the fine-grained soils is the most appropriate relationship for wet materials (when S-S_{opt} is greater than 5%). For very dry materials, (when S-S_{opt} is less than -20%), the Cary and Zapata relationship for *wPI*=0 describes the moisture-modulus relationship reasonably well, except for the ultrasonic surface wave technology (PSPA). This exception can be explained by the fact that the PSPA is essentially measuring the modulus of the geomaterial layer while the moduli measured with the other devices are impacted by the properties of the subgrade layer.

The distributions of estimation errors are quantified in Figures 4.3.1c through 4.3.5c. The Cary and Zapata model with *wPI*=0 estimates the experimental results with less uncertainty for all devices. A few outliers are observed in most graphs. These points typically correspond to the measurements carried out on small-scale specimens that were placed at wet of OMC and allowed to dry to less than the OMC. This pattern points out the importance of moisture process control during field compaction.

An alternative way of considering the impact of the variation in moisture content on modulus is shown in Figures 4.3.6 and 4.3.7. The difference between the moisture contents at the time of testing and compaction divided by the optimum moisture content is used as a normalized moisture content. The moduli are reasonably well correlated to the normalized moisture content, with similar scatter in the data as in Figures 4.3.1 through 4.3.5.

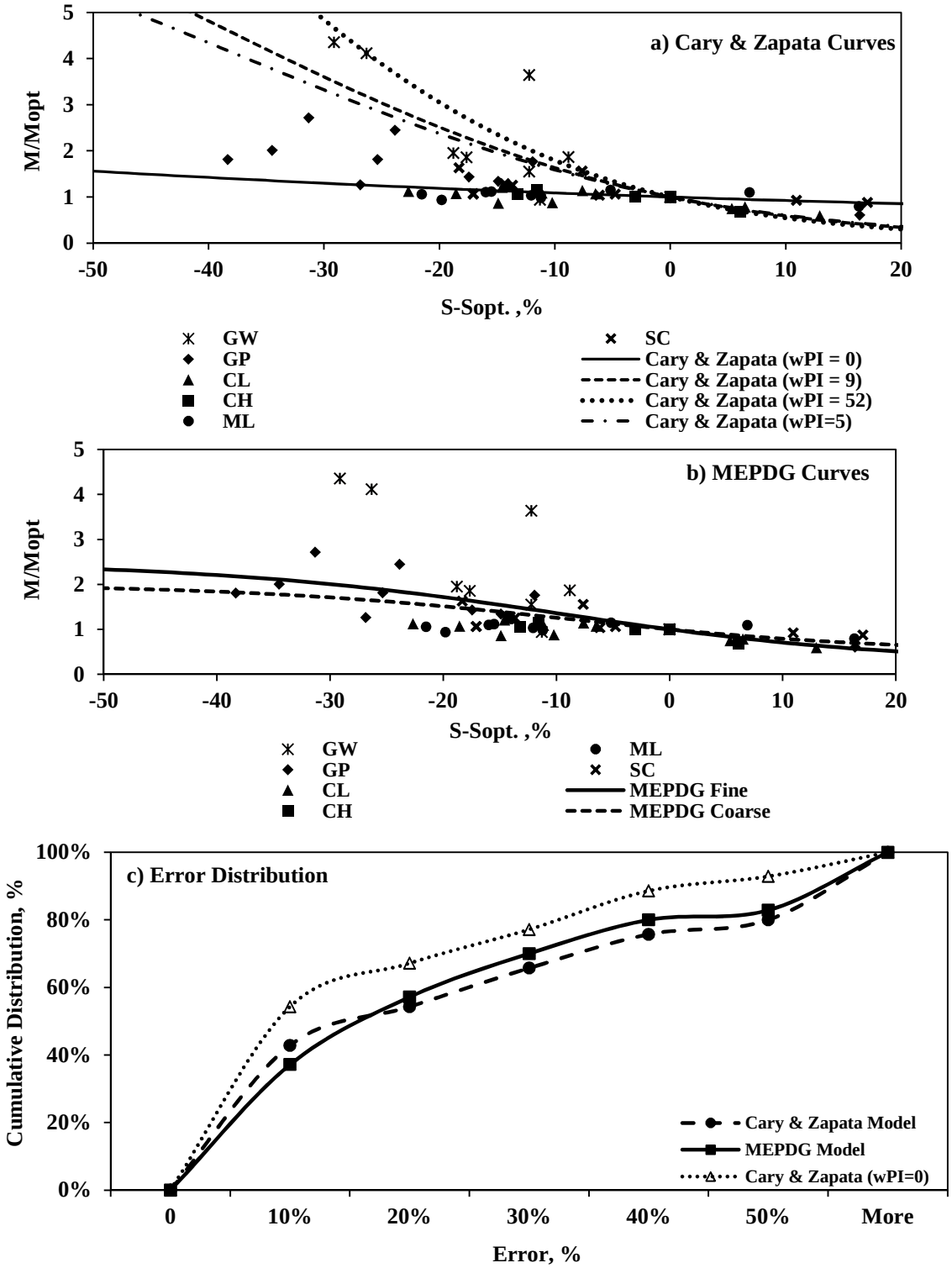

Figure 4.3.1 - Variations of Normalized Field Moduli from PSPA with Degree of Saturation

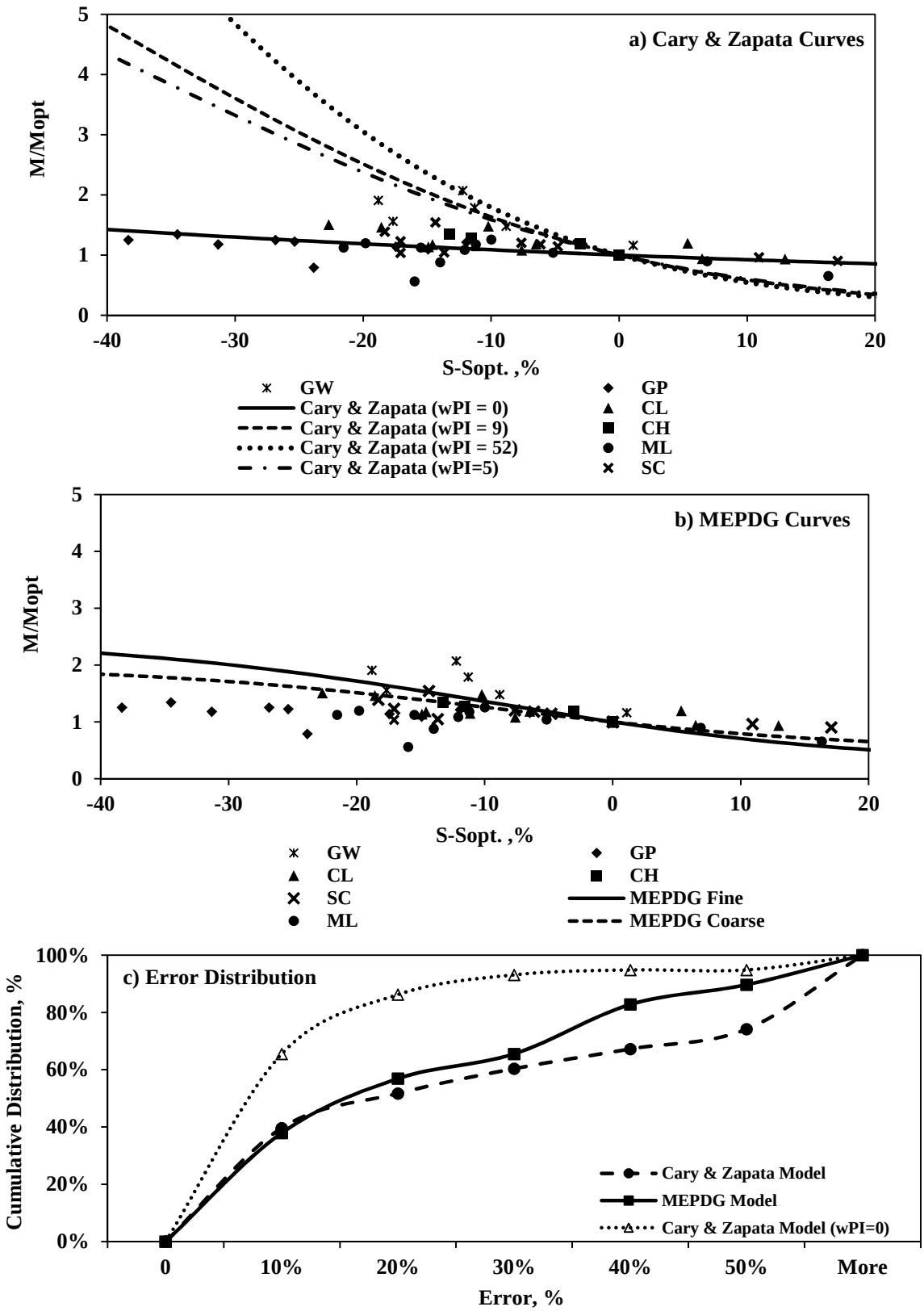

Figure 4.3.2 - Variations of Normalized Field Moduli from Geogauge with Degree of Saturation

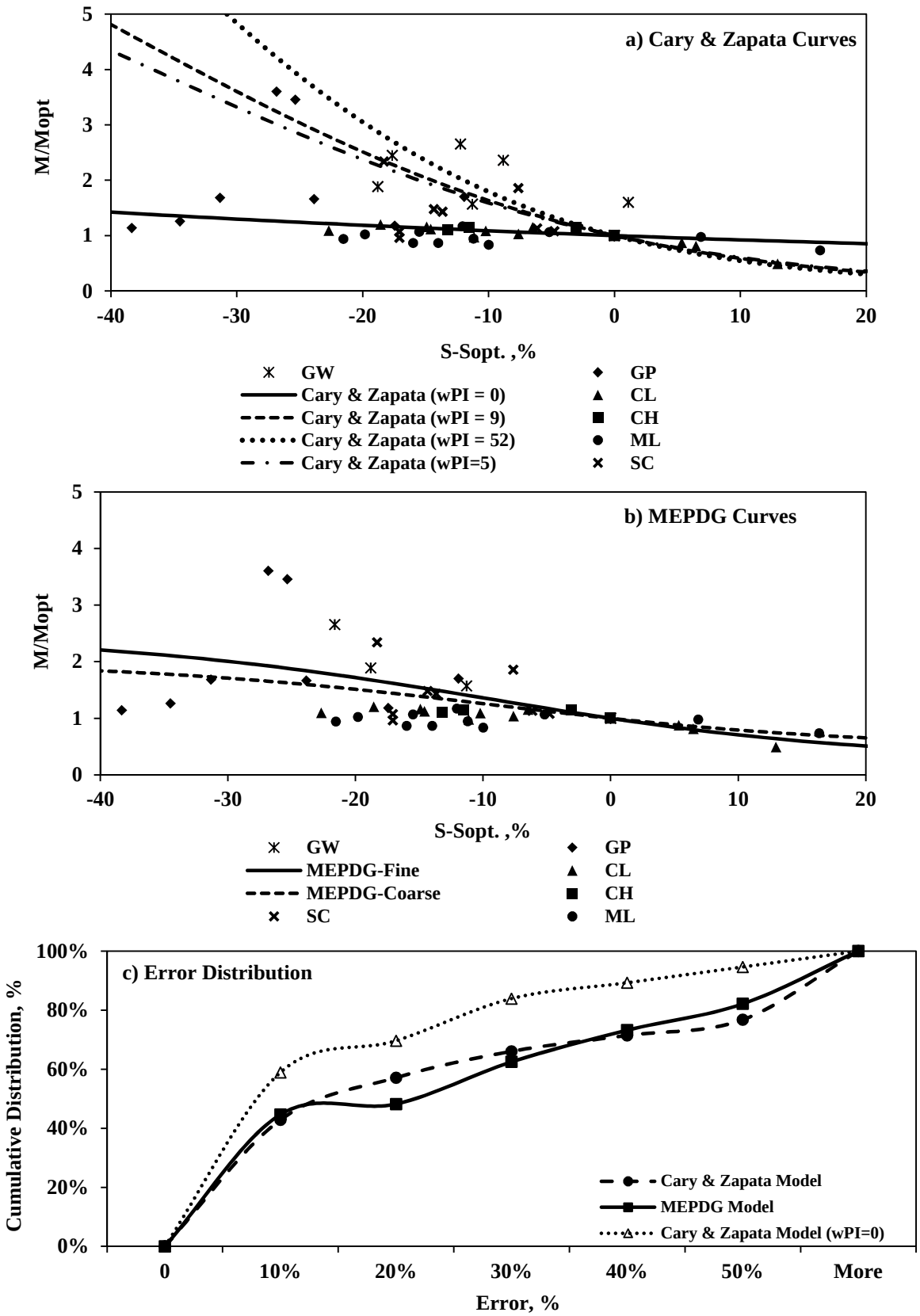

Figure 4.3.3 - Variations of Normalized Field Moduli from LWD Zorn with Degree of Saturation

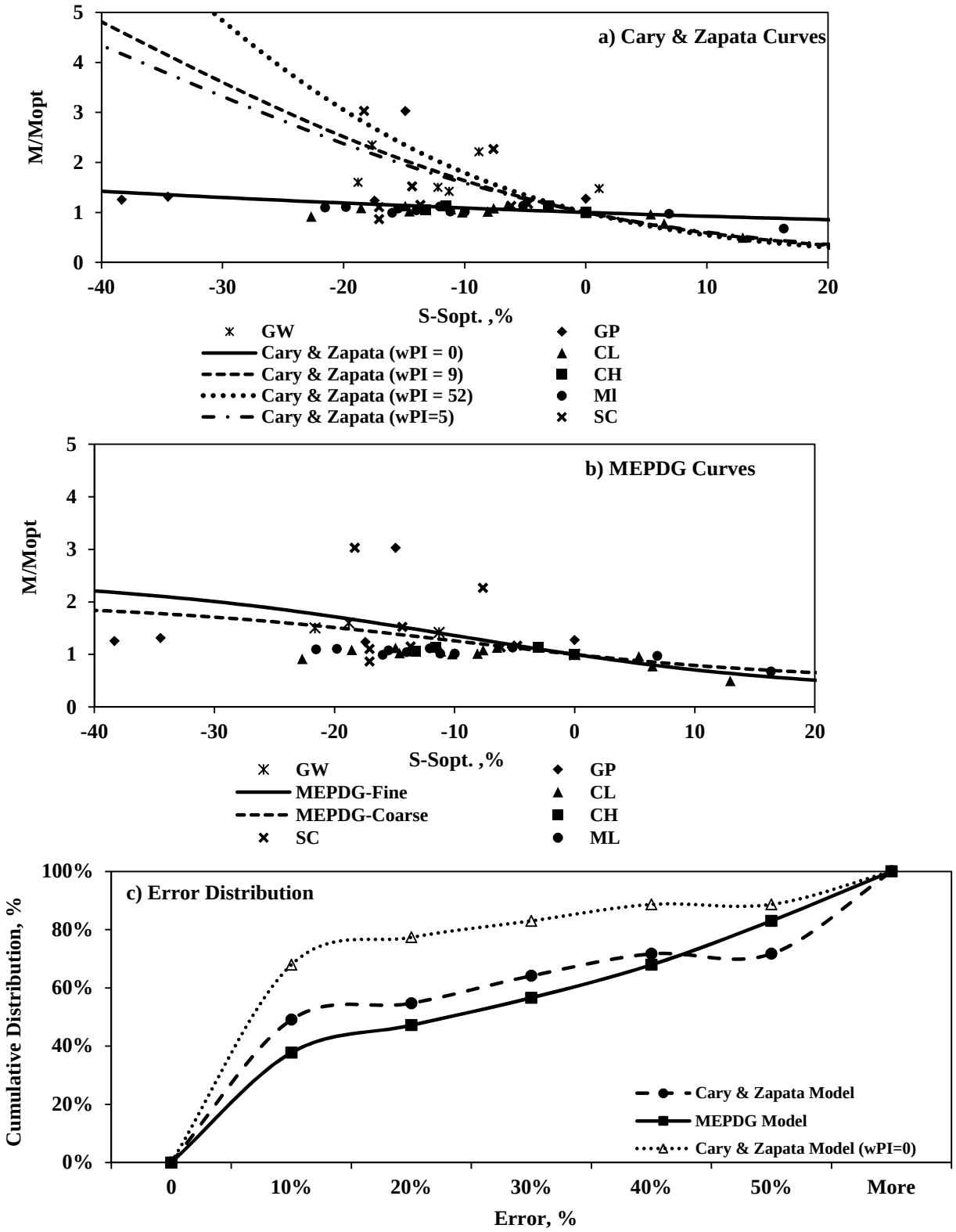

Figure 4.3.4 - Variations of Normalized Field Moduli from LWD Dynatest with Degree of Saturation

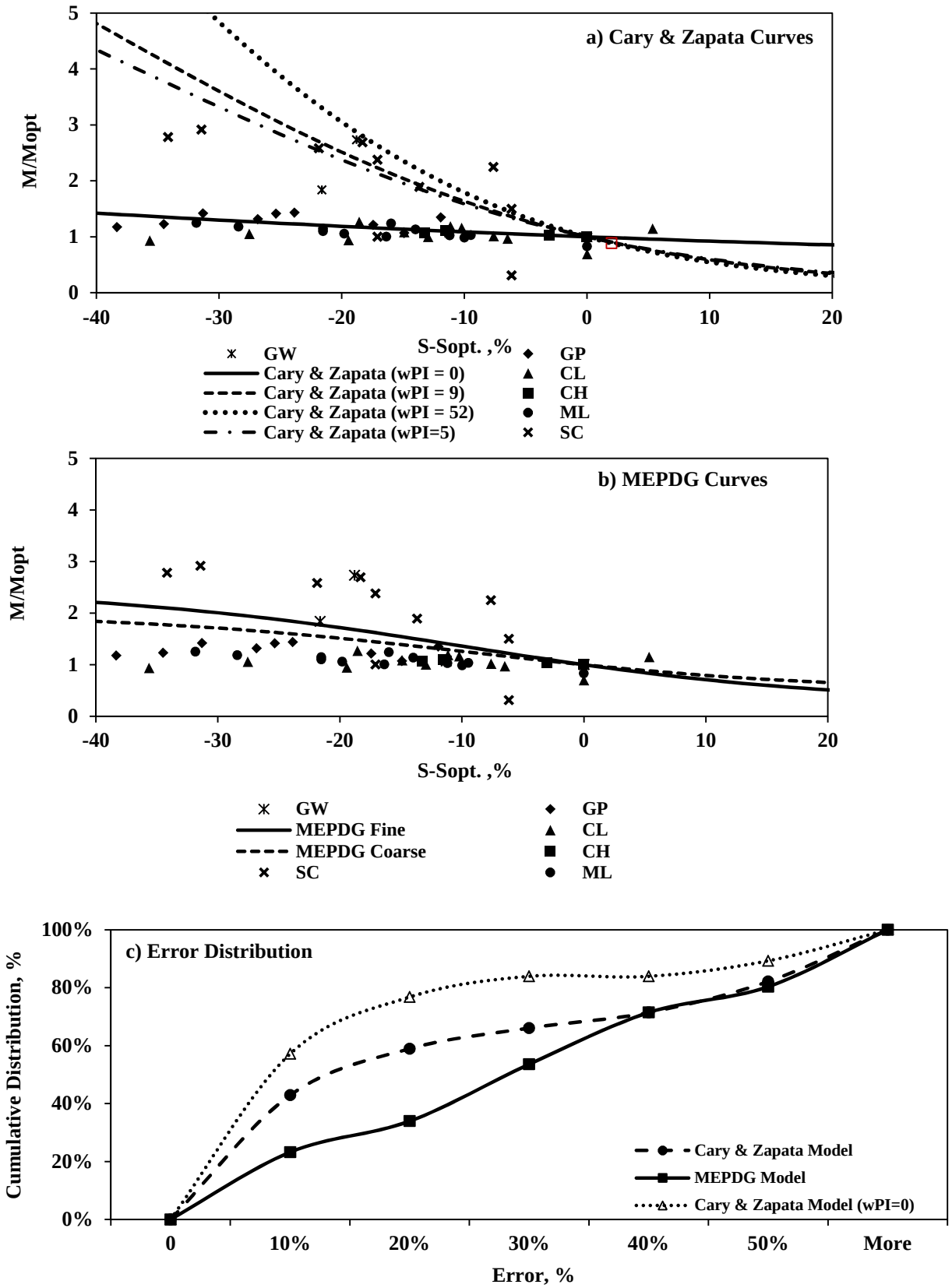

Figure 4.3.5 - Variations of Normalized Field Moduli from DCP with Degree of Saturation

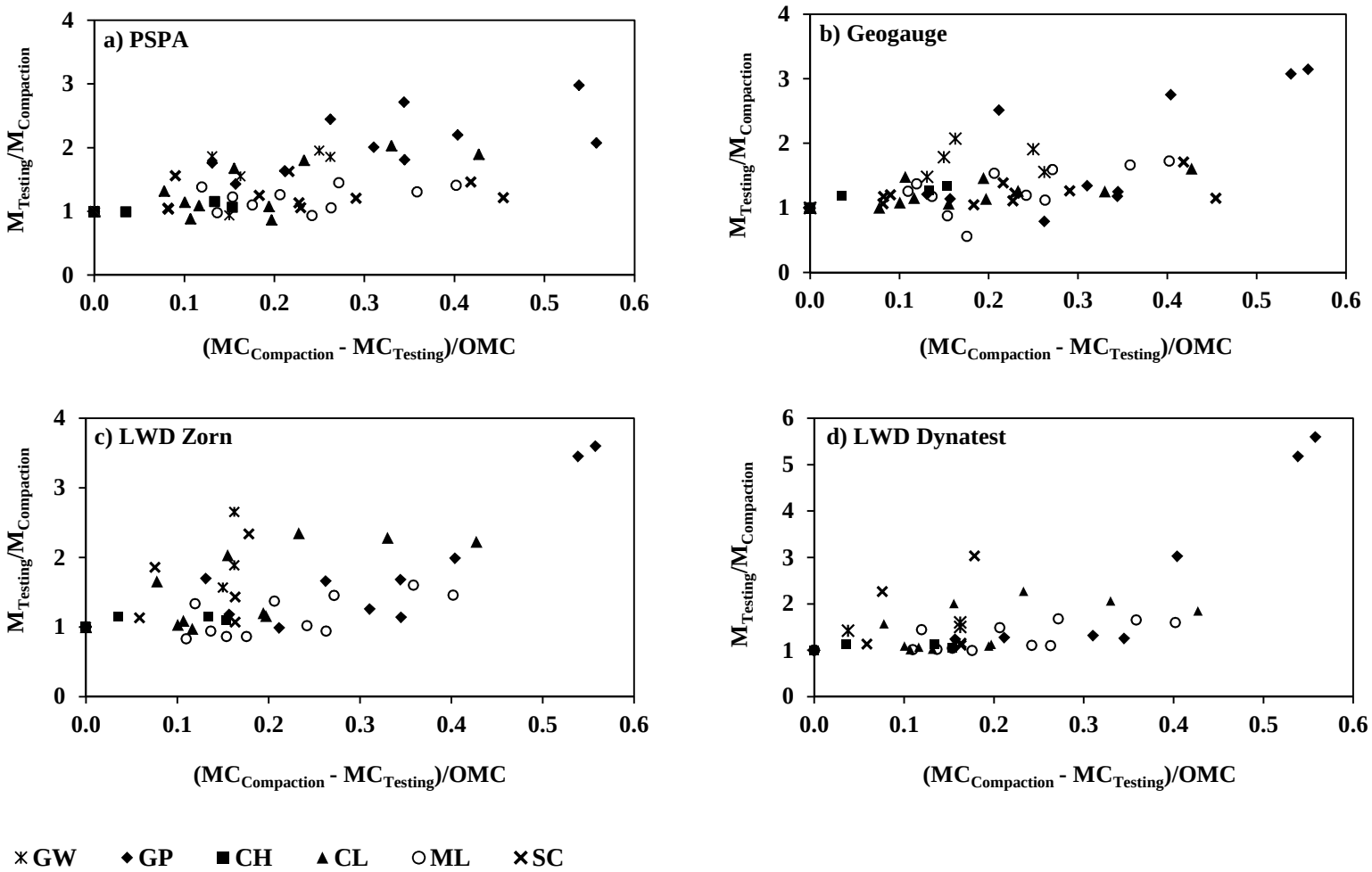

Figure 4.3.6 - Variations in Modulus with Moisture Content from Modulus-Based Devices

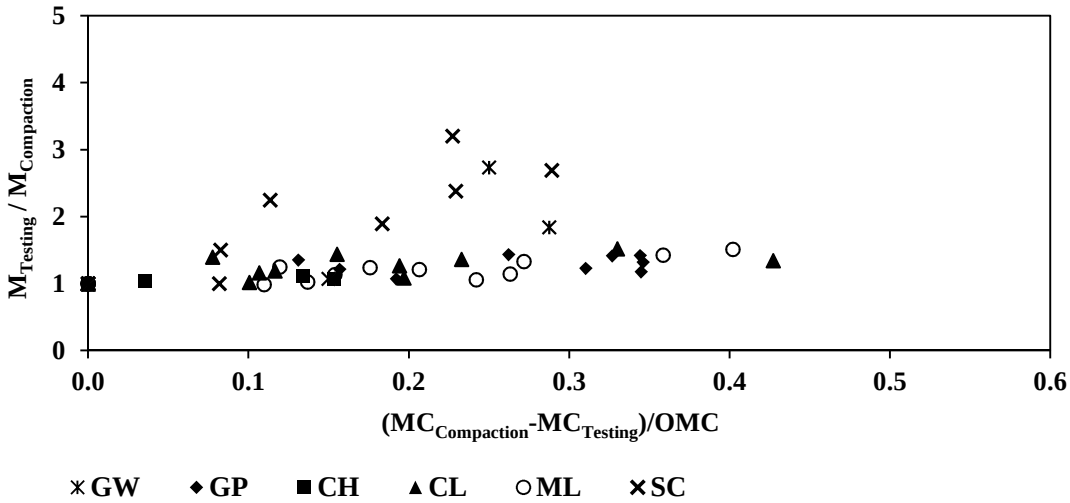

Figure 4.3.7 - Variations in Modulus with Moisture Content from DCP Device

4.4 Impact of Density

Figures 4.4.1 and 4.4.2 present the variations in modulus from all devices for specimens prepared at the OMC with densities of MDD and 96% MDD. A clear pattern cannot be observed from the presented data. In many instances, the moduli at relative compactions of 100% and 96% are similar. The GP base material exhibits more sensitivity to relative compaction in the laboratory than in the small-scale tests, while the reverse trend is evident for the SC material. Similar to the laboratory FFRC data, the GW base material seems to be impacted more with density changes, especially for the PSPA and Dynatest LWD. Also the same as laboratory results, the silty and somehow clayey materials are not sensitive to density changes during small-scale tests. Overall, the variation in moisture content impacts modulus more significantly than the change in density.

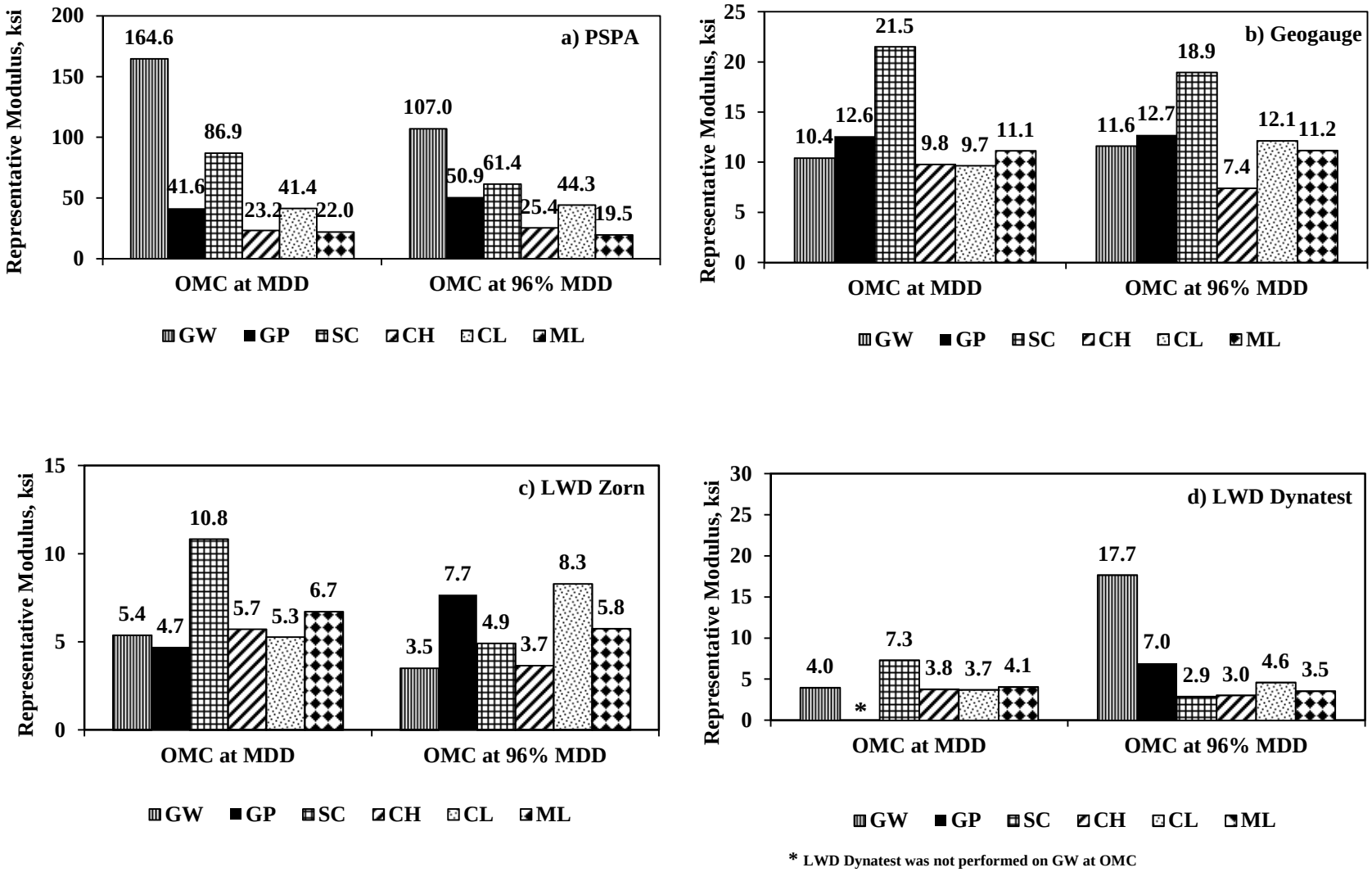

Figure 4.4.1 - Impact of Density on Moduli Measured with Field Devices

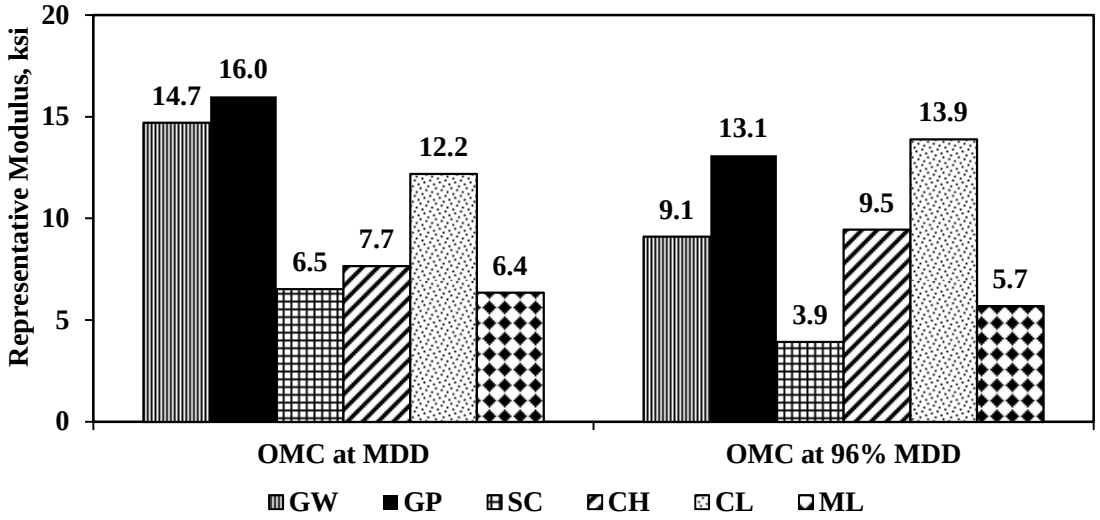

Figure 4.4.2 - Impact of Density on Modulus Measured with DCP

CHAPTER 5 - IN DEPTH EVALUATION OF SELECTED TECHNOLOGIES

5.1 Introduction

Technologies and corresponding devices that can be used to measure the modulus of a compacted geomaterial were described in Chapter 2. Moisture measuring technologies and devices are also briefly described in Chapter 2. Analyses of their suitability for this project are provided in this chapter.

5.2 Modulus-based Technologies

Device-related uncertainties can be classified into three categories: accuracy, repeatability (precision), and reproducibility. The Gauge R&R method can be used to quantify the repeatability and reproducibility. Gauge is defined as any device used for any kind of measurement. R&R is defined as the combination of the device variability (repeatability) and operator variability (reproducibility). The parameters estimated from a Gauge R&R study are *EV* (repeatability or equipment variability), *AV* (reproducibility or the operator variability), and *SV* (specimen variability).

Different methods can be used to perform Gauge R&R analysis including Average and Range (X-bar/R) and Analysis of Variance (ANOVA). The X-bar/R method considers specimen-to-specimen variability, repeatability and reproducibility without considering the device-operator interaction. The Gauge R&R study utilizing two-way crossed ANOVA method is more sophisticated than the X-bar/R method since it also considers the interaction between the device and the operator. This method provides similar parameters as X-bar/R method, but it also indicates whether a device is capable of discriminating between different specimens.

The equations used in the X-bar/R and ANOVA methods are presented in Table 5.2.1 where m replicate measurements are performed by p operators on n specimens. Parameter y_{ijk}, which refers to a measurement made with device i by operator j on specimen k, can be expressed by the following equation:

$$y_{ijk} = x_i + u_j + w_{ij} + \varepsilon_{ijk} \tag{5.2.1}$$

where x_i is the actual value of the desired parameter, u_j represents the operator variation, w_{ij} represents the interaction between the specimen and operator; and ε_{ijk} represents the repeatability error. The Gauge R&R is obtained from

$$\& = \quad = \sqrt{\quad + \quad} = \sqrt{\quad + \quad} \tag{5.2.2}$$

The total variation (TV) of the measurement system is calculated by combining the gauge R&R with the specimen variation (SV,):

$$= \quad = \sqrt{\quad + \quad + \quad} = \sqrt{\quad + \quad + \quad} \tag{5.2.3}$$

Measured subgrade moduli from 20 independent small-scale specimens prepared before placing the geomaterial layer were used first to assess the repeatability and reproducibility of the devices. Tests were carried out at three different locations three times per location in each specimen to investigate the repeatability of these devices. To study the reproducibility of these devices, the same measurements were repeated with two operators. Even though it is more desirable to utilize three operators, due to budgetary constraints a third operator was not considered.

Since the PSPA and Geogauge tests are truly nondestructive, they were carried out before the LWD tests. The PSPA and Geogauge were repositioned in a slightly different location in between measurements. An LWD test at each location consisted of two seating drops, followed by three measurement drops. The

repositioning of the two LWDs between tests was deemed too damaging to the specimens. As such, instead of averaging the three LWD measurements, each of the three measurement drops was considered as an independent measurement.

Despite tremendous care to maintain all specimens almost identical, the standard deviation of moisture contents for all lifts of all 20 specimens was 0.5%. The average and standard deviation of moduli from all devices are presented in Figure 5.2.1. The average moduli among the four devices are quite different and vary from 22.3 ksi for PSPA to 2.7 ksi for Dynatest LWD (see Table 5.2.2a). These variations occur because different devices measure different types of modulus as discussed in Chapter 2. The PSPA measures the small-strain linear-elastic modulus of the specimen, whereas the Geogauge measures the system response at small strains to estimate modulus. The two deflection devices estimate the high-strain modulus of the material by measuring the combined recoverable and permanent surface deformation of the material due to the heavier loads they apply to the material. The differences between the moduli of the Dynatest and Zorn LWDs can be attributed to the differences in the locations where displacements are measured. The Dynatest LWD measures the displacement of the soil, whereas the Zorn LWD estimates the displacement of the load plate.

Table 5.2.1 - Equations Used to Calculate Variability Parameters

a) X-bar/R Method according to AIAG[a] Guidelines

Equipment Variation (EV)	Operator Variation (AV)	Combined Device Variability *(Gauge R&R)*	Specimen Variation (SV)	Total Variation (TV)
$\frac{6}{}$	$\sqrt{\frac{6}{*} - (\frac{}{})}$	$\frac{}{+}$	$\frac{6}{*}$	$\frac{}{+ \quad +}$

[a]Automotive Industry Action Group, = average range of measurements, d_2 = bias correction factor obtained from statistical tables, = range of operator averages, d_2^* = correction factor for estimating variances obtained from statistical tables, $n_{specimens}$= number of specimens, $n_{measurements}$ = number of measurement repetitions

b) ANOVA Method according to ASTM E 2782

Source of Variation	Degree of Freedom	Sum of Squares, SS	Mean Sum of Squares, MSS	Estimate of Variance Component	Expected Value of Variance Estimate**
Specimens	*n-1*	$(\;_{..} - \;_{...})$	$\frac{}{-1}$	$\frac{-}{}$	
Operators	*p-1*	$(\;_{..} - \;_{...})$	$\frac{}{-1}$	$\frac{-}{}$	
Interaction	*(n-1)(p-1)*	$= \quad - \quad - \quad -$	$\frac{}{(-1)(-1)}$	$\frac{-}{}$	
Error	*np(m-1)*	$(\quad - \quad)$	$\frac{}{(-1)}$		

var(y_{ijk})=$\upsilon^2 + \theta^2 + \alpha^2 + \sigma^2$, SSO = Sum of Squares of Objects, SSA = Sum of Squares of Operators, SSI = Sum of Squares of Interactions, SSE = Sum of Squares of Errors, SST = Sum of Squares of Total, MSSO = Mean Sum of Squares of Objects, MSSI = Mean Sum of Squares of Interactions, MSSA = Mean Sum of Squares of Operators, MSSE = Mean Sum of Squares of Errors. $_{..}$ represents the average of the measurements from the ith object (the "dot" symbol shows averaging over the second and third indices, j and k).

$= \quad = \quad ; \quad = \quad = \;^2 + \;^2; \quad = \;^2; \quad _{\&} = \quad + \quad ; \quad = \sqrt{\quad + \quad +}$

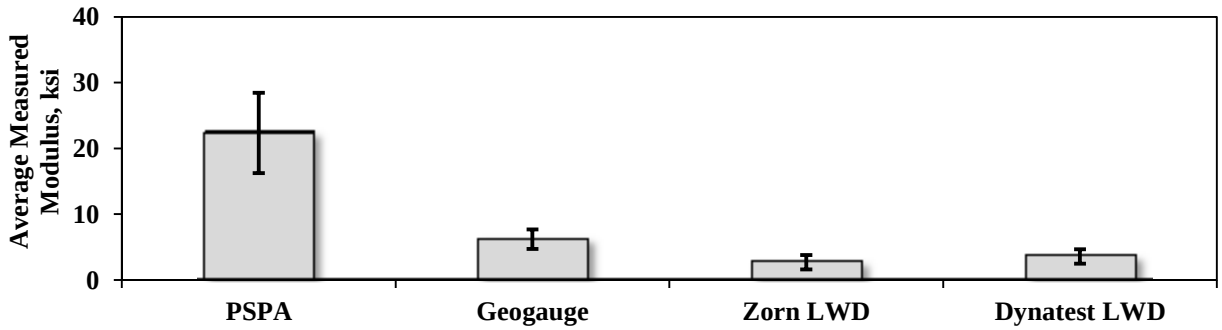

Figure 5.2.1 - Mean and Standard Deviation of Modulus Measurements with each Device

The standard deviations of measured moduli varied by 29±5% of their corresponding means as reflected in Table 5.2.2a. Given the rigid control in the preparation of the specimens, these values seem high. However, in light of the variation in laboratory modulus with moisture content shown in Tables 3.2.2 and 3.2.3 (i.e., a change in representative MR of more than three times with a change in moisture content from OMC-1% to OMC+1%), these values may be considered reasonable.

From Table 5.2.2, the two LWDs are more repeatable than the PSPA and Geogauge partly because the LWDs were not resituated between tests. According to X-bar/R method, where the interaction between the operator and device is ignored, all four devices are reproducible with less than 5% variation. The more accurate ANOVA analyses indicate that the reproducibility of the two LWDs diminishes somewhat when that interaction is considered.

Table 5.2.2 - Results from Gauge R&R Analyses of Modulus-Based Devices

a) ANOVA Method

Measurement Device	Mean of Modulus Measurements, ksi	Equipment Variation, Repeatability, ksi**	Operator Variation, Reproducibility, ksi	Combined Device Variation, Gauge R&R , ksi	Specimen Variation, SV, ksi	Total Variation, TV, ksi	COV* of Total Variation , %
Zorn LWD	2.67	0.08 (3%)	0.33 (12%)	0.34 (13%)	0.65 (24%)	0.73	28
Dynatest LWD	3.60	0.27 (8%)	0.24 (7%)	0.36 (10%)	1.18 (34%)	1.23	34
PSPA	22.33	3.22 (14%)	1.09 (5%)	3.40 (15%)	5.36 (24%)	6.35	29
Geogauge	6.21	0.71 (11%)	0.44 (7%)	0.84 (14%)	1.28 (21%)	1.52	24

Confidence level = 95%, No. of specimens = 20, No. of operators =2, No. of measurement repetitions = 9, *COV = Coefficient of Variation; **Numbers in parenthesis is the variation divided by mean

b) X-bar/R Method

Measurement Device	Range of Modulus Measurements, ksi	Equipment Variation, Repeatability, ksi**	Operator Variation, Reproducibility, ksi	Combined Device Variation, Gauge R&R, ksi	Specimen Variation, SV, ksi	Total Variation, TV, ksi	Total Variation divided by Range, %
Zorn LWD	2.54	0.07 (3%)	0.05 (2%)	0.09 (3%)	0.59 (22%)	0.60 (22%)	24
Dynatest LWD	5.43	0.15 (4%)	0.03 (1%)	0.15 (4%)	1.32 (38%)	1.33 (38%)	24
PSPA	29.87	2.90 (13%)	1.10 (5%)	3.10 (14%)	5.66 (25%)	6.45 (29%)	22
Geogauge	9.01	0.63 (10%)	0.29 (5%)	0.69 (11%)	1.60 (26%)	1.75 (28%)	19

The contributions of the specimen changes to variability are similar among the devices with an average of about 24% from the ANOVA analyses, except for the Dynatest LWD that is about 34%. These variabilities can be due to non-uniform changes in properties between the time of construction and testing and the alteration of properties due to higher loads applied to the specimens with the two LWDs.

Wheeler (*2009)* proved that the contribution of repeatability, reproducibility and specimen variations could be more accurately estimated from the following relationships:

Repeatability Proportion = ———— = —— (5.2.4)

Reproducibility Proportion= ———— = —— (5.2.5)

Combined R&R Proportion= ——— = ——— & (5.2.6)

Specimen Variation Proportion= —— = —— (5.2.7)

These values are reported in Table 5.2.3. Since the coefficients of variation estimated from the total variations and average moduli of all devices are similar, the values in Table 5.2.3 can be used to understand better the characteristics of the devices. The two LWDs are more repeatable than the PSPA and Geogauge, since less than 5% of their total variability is associated with their repeatability. This is anticipated because the LWDs were not resituated between tests. The greater repeatability proportions from the ANOVA analyses for the Zorn LWD, PSPA and Geogauge as compared to the X-bar/R analyses demonstrate that the operator-device-specimen interactions are important for these devices, with the greatest importance for the Zorn LWD and Geogauge.

Table 5.2.3 - Contribution of each Variability Component to Total Variability of Device

a) ANOVA Method

Measurement Device	Equipment Variation (Repeatability) Proportion, %	Operator Variation (Reproducibility) Proportion, %	Combined R&R Proportion, %	Specimen Variation Proportion, %
Zorn LWD	1.2	20.4	21.6	78.4
Dynatest LWD	4.8	3.8	8.6	91.4
PSPA	25.7	2.9	28.7	71.3
Geogauge	21.8	8.4	30.2	69.8

b) X-bar/R Method

Zorn LWD	1.3	0.1	1.3	98.7
Dynatest LWD	1.4	0.7	2.1	97.9
PSPA	20.2	2.9	23.1	76.9
Geogauge	13.0	2.7	15.7	84.3

The contributions of the reproducibility to the total variability are rather small for all devices in the X-bar/R analyses. These values are significantly greater for the Dynatest LWD and somewhat greater for the Geogauge measurements from the ANOVA analyses, indicating that the operator-device-specimen interaction is critical for the reproducibility of those devices. This translates to a practical recommendation that the operator should pay more attention during the placement of these two devices than the other two.

Based on the combined R&R values, the Zorn LWD yields the least uncertain values when the operator-device-specimen interaction is considered. The high uncertainty associated with the Dynatest LWD was not anticipated since the operation of that device is very similar to the Zorn LWD. The only plausible

explanation at this time is that the first set of tests by the first Dynatest LWD operator might have altered the properties of the specimens.

For a fair and equitable quality management system, statistics-based methods should be used to optimize the sampling plan and testing frequency for a transparent level of reliability. The variability of measurements and the tolerable errors are the most important parameters in defining the required sample size. The tolerable error is defined as the error limits that both the contractor and owner will accept during the construction process. The following equation can be used to estimate the sample size, *n*:

$$= \frac{\quad}{\quad} \tag{5.2.8}$$

where α = Type I (contractor's) risk, β = Type II (owner's) risk, Z_α = the $(1-\alpha)^{th}$ percentile of the standard normal distribution, Z_β = the $(1-\beta)^{th}$ percentile of the standard normal distribution, σ = standard deviation, and e = tolerable error. Typically, σ approximates the variability of material properties tested by different devices.

The overall patterns of sample size based on different a, b, s, and e are presented in Figure 5.2.2. The tolerable error, e, is assumed to be equal to 1.5 times s_t (i.e. total variation) and s is assumed to be equal to s_{Gauge} (combined device variation). AASHTO categorizes projects into four groups (critical, major, minor and contractual) with corresponding a and b values shown in Figure 5.2.2. Using α=5.0% and β=0.5% (critical project), the sample sizes necessary are three for the Zorn LWD, five for the Dynatest LWD, six for the PSPA and seven for the Geogauge. Given the limitation in assessing the repeatability of the two LWDs, a sample size of five to seven for all devices may be reasonable.

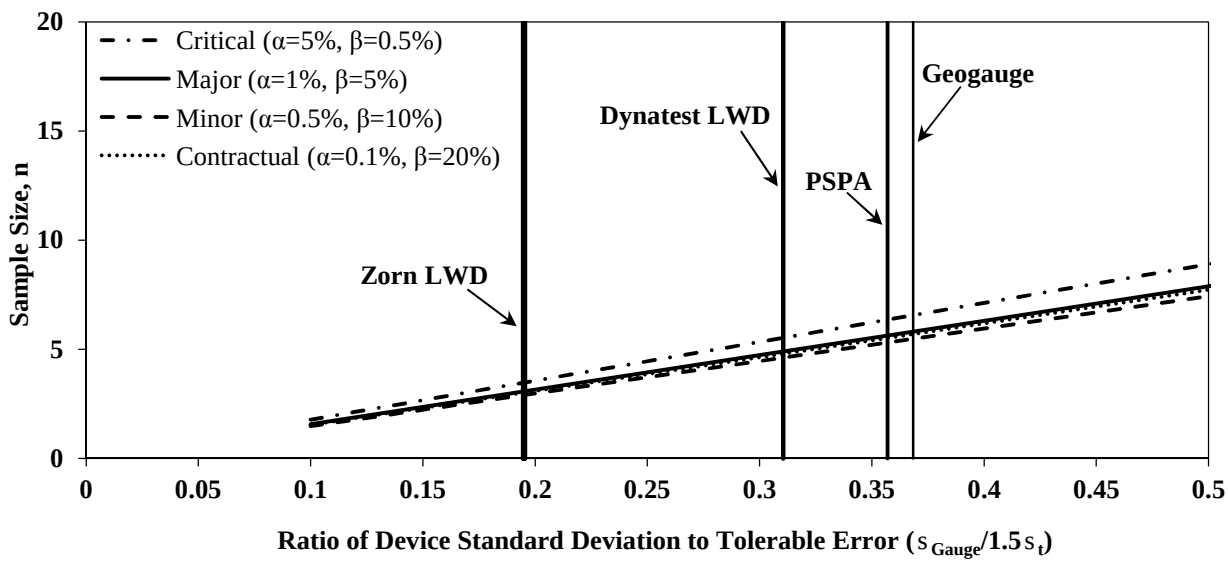

Figure 5.2.2 - Suggested Sample Sizes for Different Type I and II Risk Levels

To investigate the variability of each modulus-based device on composite pavement layers, the testing patterns described above were also implemented on top of the twenty small-scale specimens after their corresponding geomaterial layers were compacted. To establish the characteristics of each device, the process recommended by Burati et al. (2003) was followed by defining each triplicate measurement as a "lot." The variance of each specimen at each testing moisture content was calculated from

$$= \frac{\sum[(\quad)\times\quad]}{} \tag{5.2.9}$$

where SD = standard deviation of each lot, N = the total number of measurements, n = the number of test replicates, and M = the number of lots. The coefficient of variation, COV, of each lot (which contains three measurements) was calculated from Equation 5.2.10:

$$= \frac{\sqrt{\ }}{\bar{\ }} \qquad (5.2.10)$$

where V = variance as calculated from Equation 5.2.9, and $\bar{\ }$ is the mean modulus of samples within a lot.

Figure 5.2.3 shows the distribution of COVs for different devices. On average (at 50% cumulative distribution), the COV of the PSPA is 15%, and the COVs of the Geogauge and the two LWDs are about 7%. For a confidence level of 80%, these COVs were less than 22% for the PSPA and 15% for the Geogauge and the two LWDs. The factors that contribute to the higher variability of the PSPA are that the device directly measures the modulus of the geomaterial layer, and that the cracking of the materials affects the PSPA measurements more than the other devices.

Figure 5.2.4 contains the distributions of the COVs for the PSPA and Geogauge by material type. The variability in PSPA measurements is more material dependent as compared to the Geogauge. The Geogauge measurements are less variable for fine-grained soils as compared to the base materials. As reflected in Figure 5.2.5, the uncertainties in the measurements with the Dynatest LWD seem to be more material dependent than the Zorn LWD.

The sensitivity of each device to changes in moisture content was also studied by comparing the average moduli from tests performed after the geomaterial layers were placed in the small-scale specimens. The average moduli measured with the four devices are summarized in Figure 5.2.6 for the GP materials as an example (the results from all materials are presented in Appendix E). Each data point is the average of six replicate tests at three different locations by two operators (total of 36 measurements at each moisture content) for PSPA and Geogauge and average of three replicates at three locations with two operators (total of 18 measurements at each moisture content) for the LWDs. The x-axes in the figures represent the nominal moisture content at the time of testing and different datasets correspond to the moisture contents at the time of compaction. The PSPA moduli are more sensitive to change in moisture content than the other devices because the PSPA measures the modulus of the geomaterial layer alone while the other devices provide a composite modulus of the base and subgrade.

5.3 Moisture Measuring Technologies

The moisture measuring technologies and devices considered in this study were electrical impedance spectroscopy (Soil Density Gauge (SDG)), pressure rise (Speedy Moisture Tester (SMT)) and dielectric permittivity (Decagon 5TM and 10HS moisture sensors, and DOT600 water content meter).

Soil samples were retrieved to measure the oven-dry moisture content of the in-place material after each measurement. The volumetric moisture contents from the two Decagon devices are compared with the volumetric moisture contents calculated from oven dried gravimetric moisture contents in Figure 5.3.1. The pattern observed for the two sensors is similar for moisture contents in excess of 25%. Based on these results, these two devices were not further evaluated in this research.

The X-bar/R and ANOVA analyses discussed in Section 5.2 were also applied to the SDG data collected concurrently with the modulus data. These results are summarized in Table 5.3.1. The repeatability of the device is about 10% while the reproducibility is about 1%. As shown in Table 5.3.2, 86% of the total variation in measurements can be attributed to the repeatability of the device. Such comprehensive data were not available for the SMT and DOT600 because those two devices require loose materials for testing. To evaluate thoroughly the three moisture devices, additional small-scale specimens were prepared at five nominal moisture contents (OMC, 1.1 OMC and 1.2 OMC, 0.9 OMC and 0.8 OMC) from each geomaterial (30 new specimens). Each small-scale specimen contained 2 ft. (0.6 m) of uniformly compacted geomaterials compacted at MDD following the procedure discussed in Chapter 4.

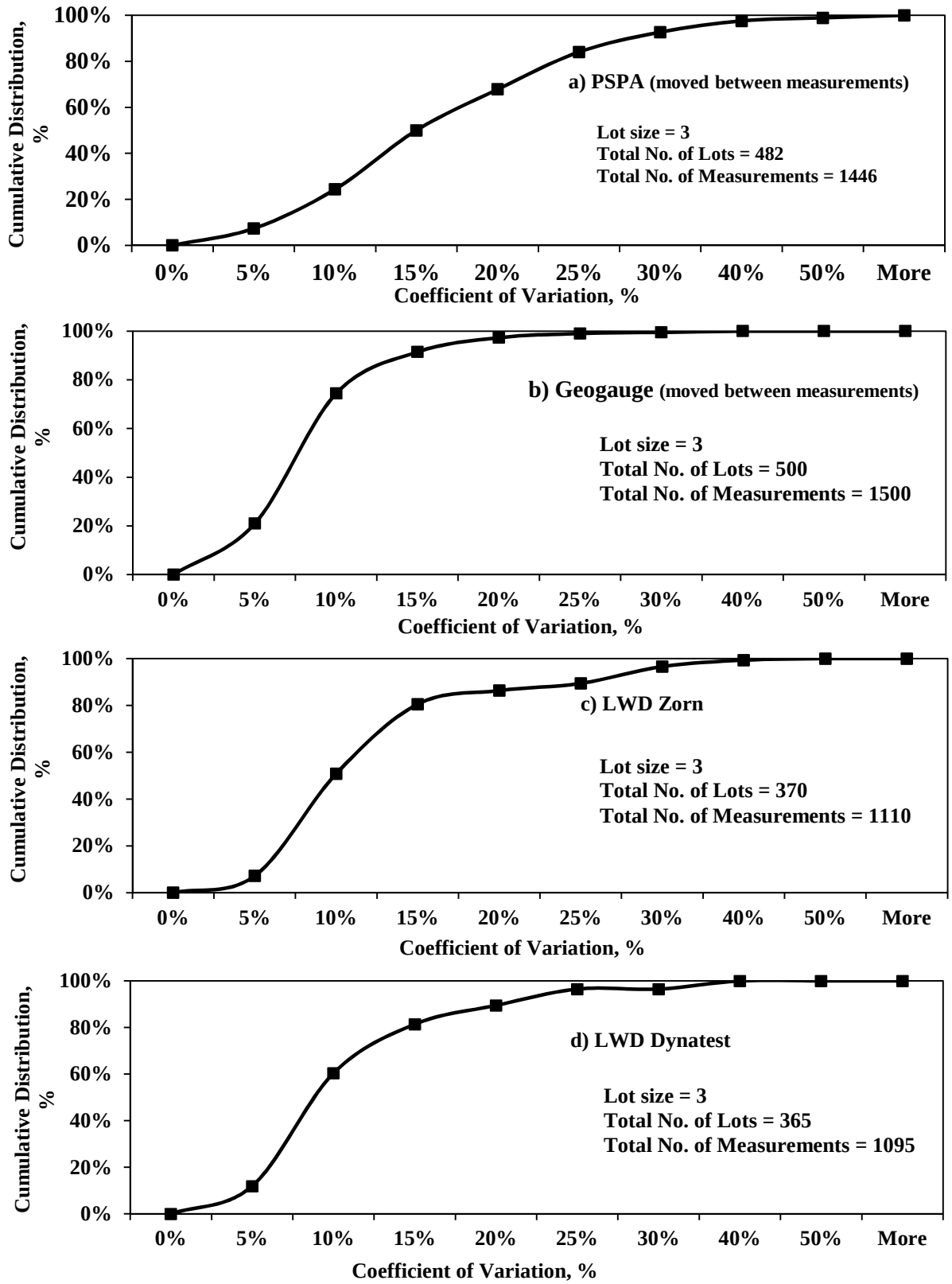

Figure 5.2.3 - Distributions of Coefficients of Variation for Modulus-based Devices for Two-Layer Small-Scale Specimens

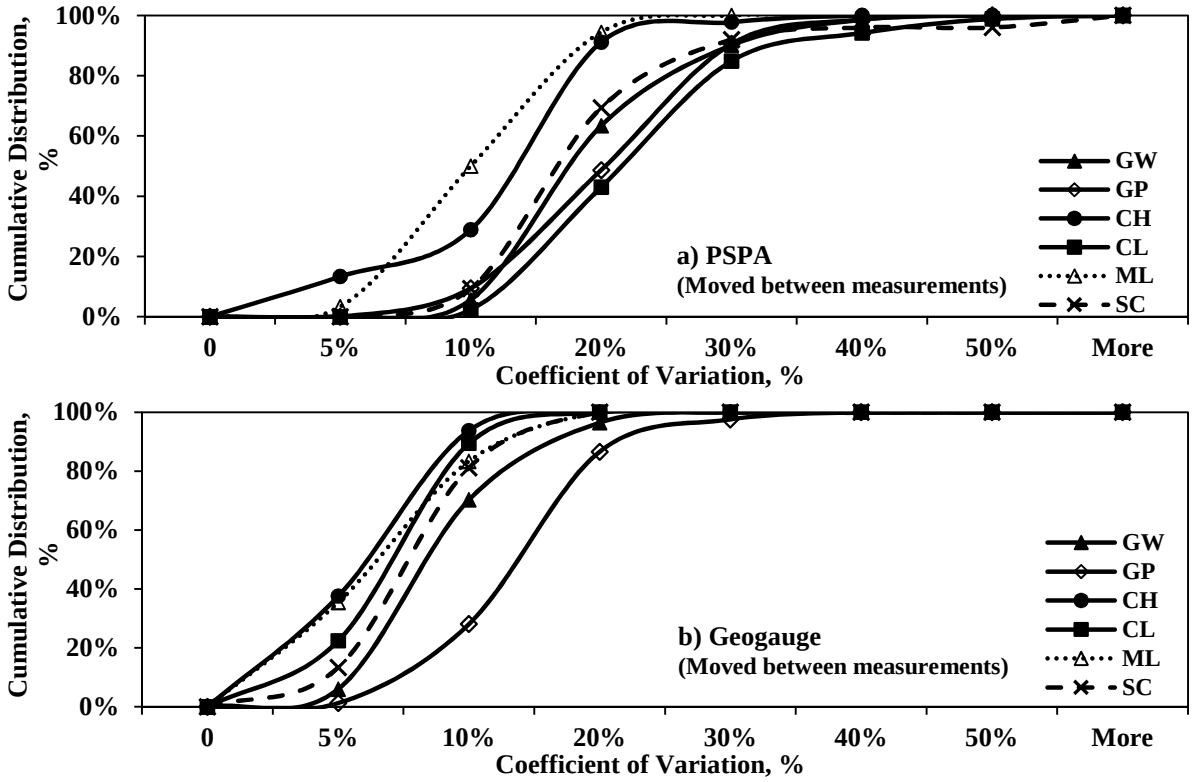

Figure 5.2.4 - Distributions of Coefficients of Variation for Modulus-based Devices on Different Materials for Two-Layer Small-Scale Specimens (PSPA and Geogauge)

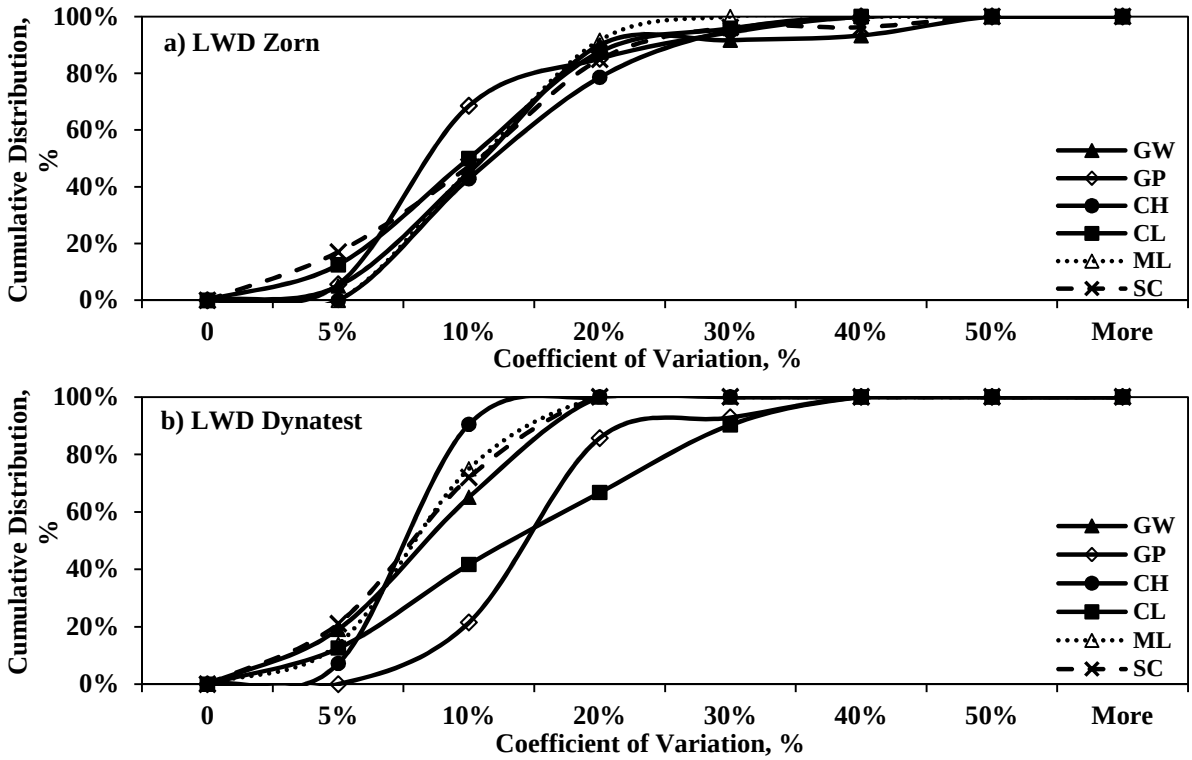

Figure 5.2.5 - Distributions of Coefficients of Variation for Modulus-based Devices on Different Materials for Two-Layer Small-Scale Specimens (Zorn and Dynatest LWDs)

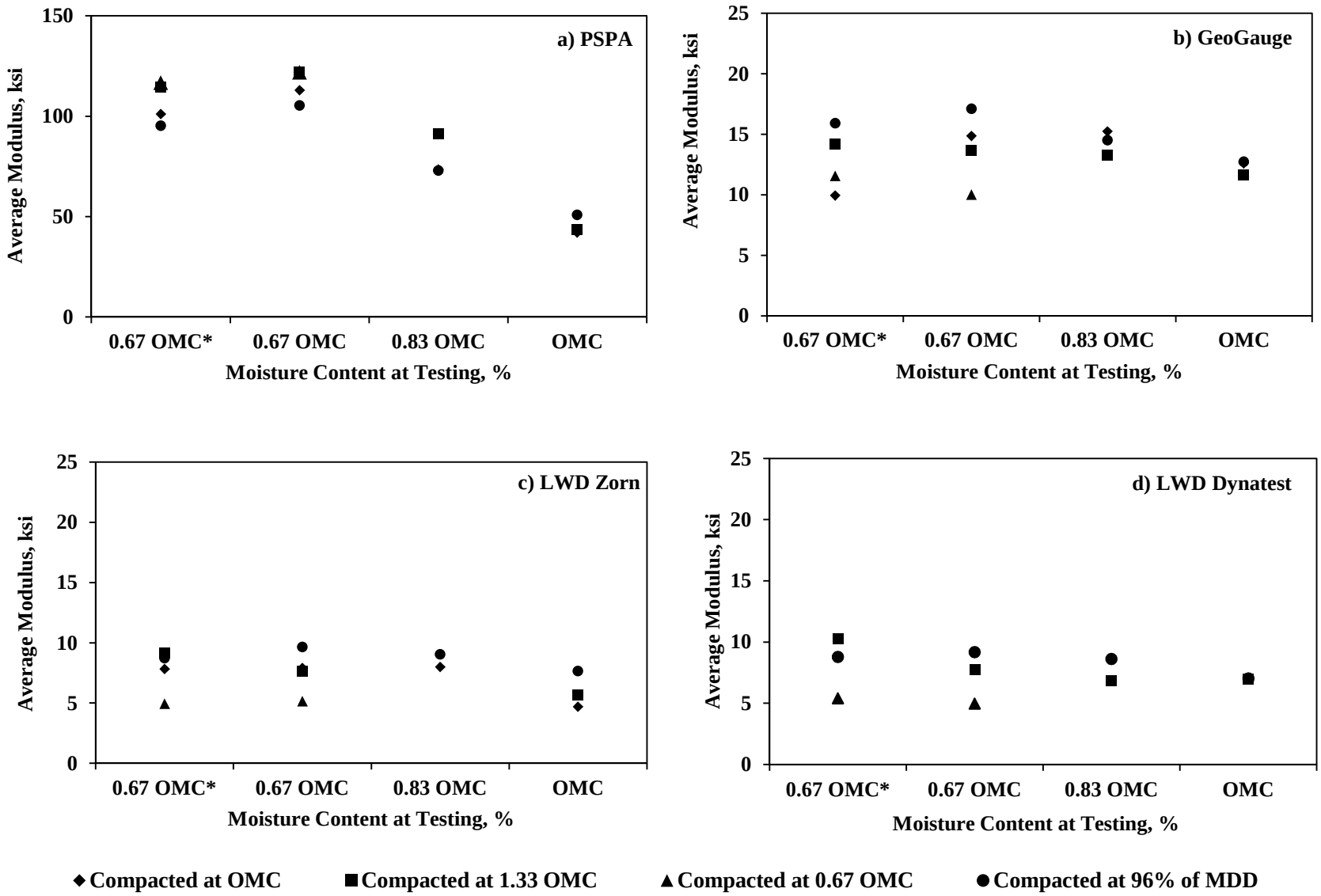

- Note: 0.67 OMC* = Subgrade saturated when Geomaterial dried to 0.67 OMC

Figure 5.2.6 - Average Moduli from Different Modulus-based Devices at Various Moisture Contents (GP Materials)

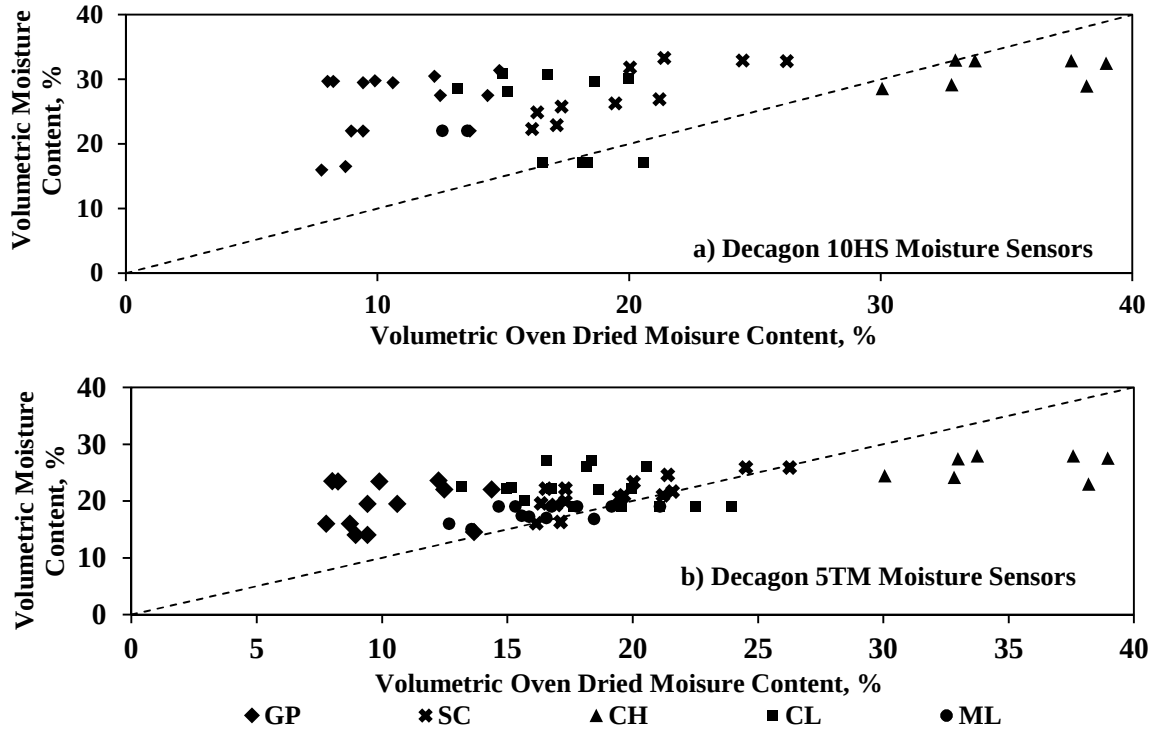

Figure 5.3.1- Results from Decagon 10HS and 5TM Moisture Sensors

Table 5.3.1- Results from Gage R&R Analyses of SDG on SM Subgrade

a) ANOVA Method

Mean of Moisture Measurements, %	Equipment Variation, Repeatability, %**	Operator Variation, Reproducibility, %	Combined Device Variation, Gauge R&R, %	Specimen Variation, SV, %	Total Variation, TV, %	COV* of Total Variation, %
16.04	1.49 (9%)	0.10 (1%)	1.49 (9%)	0.61 (4%)	1.61	10

Confidence level = 95%, No. of specimens = 16, No. of operators =2, No. of measurement repetitions = 9, *COV = Coefficient of Variation;
**Numbers in parenthesis is the variation divided by mean

b) X-bar/R Method

Range of Moisture Measurements, %	Equipment Variation, Repeatability, %**	Operator Variation, Reproducibility, %	Combined Device Variation, Gauge R&R, %	Specimen Variation, SV, %	Total Variation, TV, %	Total Variation divided by Range, %
8.90	1.54 (10%)	0.09 (1%)	1.54 (10%)	0.73 (5%)	1.70 (11%)	19

**Numbers in parenthesis is the variation divided by mean

Table 5.3.2 - Contribution of each Variability Parameter to Total Variability of SDG Moisture Device

Method	Equipment Variation (Repeatability) Proportion, %	Operator Variation (Reproducibility) Proportion, %	Combined R&R Proportion, %	Specimen Variation Proportion, %
ANOVA	85.6	0.4	86.0	14.0
X-bar/R	82.1	0.3	82.3	17.7

Moisture evaluations involved using SDG, DOT600 and SMT during and after construction of the specimens. The results from this activity are summarized in Table 5.3.3 for the ANOVA method. The combined device variability (repeatability and reproducibility) of all three devices are material dependent. The SDG is the least material dependent device with a combined variability of 7% or less. The repeatabilities of the SMT (less than 12%) and SDG (less than 2%) are acceptable, with the SDG being more repeatable. All three devices exhibit acceptable reproducibility (less than 11%). Since the oven-dried moisture contents of the specimens were measured concurrently with the tests carried out with the three devices, further analyses were performed to evaluate the linearity and bias of the devices. The linearity can be used to assess whether a device has the same accuracy when estimating different moisture contents of different materials. The bias provides a means of evaluating the accuracy of a given device. The reference values in this study were the oven-dry moisture contents of the specimens. In general the lower the bias value is, the more accurate the device will be.

Table 5.3.3 - Results from Gage R&R Analyses Using ANOVA Method on Additional Specimens

a) Speedy Moisture Tester (SMT)

Geomaterial	Mean of Moisture Content Measurements, %	Equipment Variation, Repeatability, %**	Operator Variation, Reproducibility, %	Combined Device Variation, Gauge R&R , %	Specimen Variation, SV, %	Total Variation, TV, %	COV* of Total Variation, %
GP	6.2	0.76 (12%)	0.69 (11%)	1.03 (17%)	1.57 (25%)	1.87	30%
CH	27.0	1.21 (4%)	0.00 (0%)	1.21 (4%)	3.63(13%)	3.83	14%
SM	15.4	0.71 (5%)	0.86 (6%)	1.12 (7%)	2.45 (16%)	2.70	18%
ML	8.9	0.28 (3%)	0.00 (0%)	0.28 (3%)	1.38 (16%)	1.41	16%
SC	10.7	0.31 (3%)	0.32 (3%)	0.44 (4%)	1.65 (15%)	1.71	16%

b) Soil Density Gauge (SDG)

Geomaterial	Mean of Moisture Content Measurements, %	Equipment Variation, Repeatability, %**	Operator Variation, Reproducibility, %	Combined Device Variation, Gauge R&R , %	Specimen Variation, SV, %	Total Variation, TV, %	COV* of Total Variation, %
GP	5.2	0.12 (2%)	0.26 (5%)	0.29(6%)	0.40 (8%)	0.49	9%
CH	21.4	0.15 (1%)	0.28 (1%)	0.31(1%)	0.31(1%)	0.44	2%
SM	16.2	0.30 (2%)	0.98 (6%)	1.03(6%)	1.62(10%)	1.92	12%
ML	13.2	0.13 (1%)	0.92 (7%)	0.93(7%)	1.53(12%)	1.79	14%
SC	8.8	0.05 (1%)	0.23 (3%)	0.23(3%)	0.14(2%)	0.27	3%

c) DOT600

Geomaterial	Mean of Moisture Content Measurements, %	Equipment Variation, Repeatability, %**	Operator Variation, Reproducibility, %	Combined Device Variation, Gauge R&R , %	Specimen Variation, SV, %	Total Variation, TV, %	COV* of Total Variation, %
GP	12.1	1.35 (11%)	0.65 (5%)	1.50 (12%)	2.22 (18%)	5.68	47%
CH	18.5	0.59 (3%)	0.11 (1%)	0.60 (3%)	0.38 (2%)	0.71	4%
SM	16.5	1.47 (9%)	0.62 (4%)	1.59 (10%)	1.30 (8%)	2.06	12%
ML	14.0	0.29 (2%)	0.00 (0%)	0.29 (2%)	0.07 (1%)	0.30	2%
SC	9.4	1.67 (18%)	0.49 (5%)	1.74 (19%)	0.00 (0%)	1.74	19%

Confidence level = 95%, No. of specimens = 30, No. of operators =2, No. of measurement repetitions = 6, *COV = Coefficient of Variation, **Numbers in parenthesis is the variation divided by mean

Table 5.3.4 contains the average of six oven-dry moisture contents (as reference) and the average bias (which is defined as the absolute difference between the reference and the device moisture contents) of all six samples at the same target moisture contents. Biases were calculated for each material separately to evaluate the influence of the material type on the accuracy of the devices. In general, the biases of the three devices increase as the soil becomes wetter and more plastic.

Table 5.3.4 - Values of Average Bias for Different Reference Moisture Contents from SDG, DOT600 and SMT Measurements

Geomaterial (USCS Class)	Soil Density Gauge (SDG)		Speedy Moisture Tester (SMT)		DOT 600	
	Reference Moisture Content*, %	Absolute Average Bias**, %	Reference Moisture Content, %	Absolute Average Bias, %	Reference Moisture Content, %	Absolute Average Bias, %
GP	4.2	0.6	4.2	0.6	4.2	5.7
	4.6	0.3	5.0	0.7	5.0	5.0
	6.7	1.2	6.2	0.5	6.2	5.8
	6.9	1.3	7.2	1.0	7.2	6.3
	7.7	2.0	8.1	0.6	8.1	7.1
CH	21.3	0.2	23.0	1.3	20.1	1.0
	21.7	0.6	25.5	1.3	23.2	3.9
	24.5	3.0	28.4	1.3	26.2	7.0
	27.6	6.3	30.8	1.5	29.5	10.2
	30.3	8.3	33.5	2.3	32.6	12.4
SM	11.0	3.1	12.6	0.9	12.2	2.7
	13.6	2.1	14.4	0.8	14.2	1.4
	15.0	1.1	16.9	1.4	16.3	1.0
	15.6	0.8	18.3	1.4	18.2	1.3
	17.5	1.6	20.7	2.2	20.4	2.7
ML	7.5	4.2	7.6	0.4	7.5	6.4
	7.6	4.2	8.6	0.6	8.5	5.4
	8.8	4.1	9.5	0.7	9.5	4.6
	10.3	4.3	10.5	0.7	10.5	3.4
	11.0	4.0	11.5	0.9	11.4	2.7
SC	8.4	0.3	9.4	0.8	9.1	2.4
	10.3	1.6	10.6	1.0	10.3	2.2
	11.2	2.4	11.7	1.0	11.4	2.6
	11.6	2.6	12.7	0.8	12.5	3.2
	12.7	3.7	13.9	1.1	13.6	3.5
Overall Average	**--**	**2.5**	**--**	**1.0**	**--**	**4.4**

*Average of Oven Dry Moisture Content
**Absolute Difference of Reference and Device Moisture Content

Figure 5.3.2 represents the variations of the bias of moisture measurements with the reference moisture content. Each data point represents the bias (the difference between measurement and reference moisture content), and the red symbol shows the average bias at each reference moisture content for each material. On the basis of the results in Table 5.3.4, the SMT seems to be the most accurate device. The latest test protocol and calibration procedure recommended by the manufacture of each device were followed to obtain the data presented in this section. Observing the trends for individual materials in Figure 5.3.2, the biases for the SDG and DOT600 for each individual material are linearly related to the reference moisture content. These two devices estimate the moisture contents from elaborate material models that may require further refinement. It may be possible to improve the accuracy of these two devices with a more rigorous material-specific calibration process, or by relating the raw data measured by each device to the moisture content.

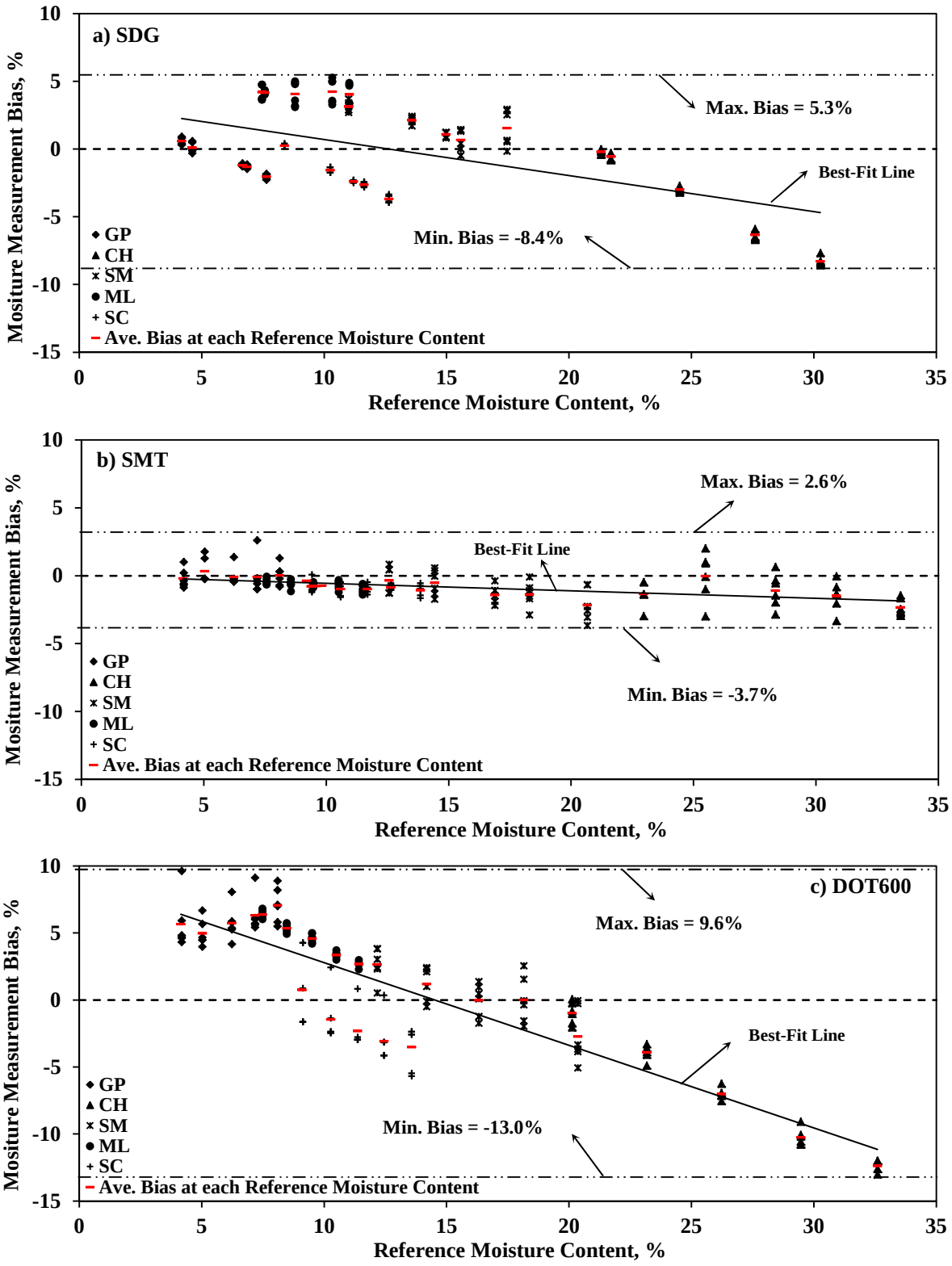

Figure 5.3.2 - Moisture Measurements and Bias for Moisture Devices

5.4 Establishing Characteristics of Modulus Devices

Several studies have documented differences in the responses among different LWDs even with similar plate diameters. For example, Vennapusa (2009) reported that LWDs that use accelerometers to measure the deflection of the load plate (e.g., Zorn LWD) reported larger deflections compared to the LWDs that measure deflections of the ground surface (e.g., Dynatest LWD). As a result, they reported that the moduli estimated by a Dynatest LWD are on average 1.7 times greater than moduli estimated from Zorn LWD, when both devices were equipped with 8-in.-diameter (nominal) plates. Another issue still being debated is the depth of influence of the devices (especially LWDs) that measure the system response. Most information provided in the literature estimate the depth of influence using the Boussinesq theory where the dynamic nature of the loading, layering of the geomaterials, and the plate-soil interaction are not considered. Furthermore, most studies focus on the distribution of the vertical stress but not the distribution of strains.

To address these issues, an axisymmetric dynamic nonlinear Finite Element (FE) model was developed using LS-DYNA tool to model the LWD testing on top of a pavement system. The FE modeling of the LWD testing considered a two-dimensional surface-to-surface contact model to assess the soil-plate interaction with the layered soil. About 100,000 elements were used in the FE analysis. The model used 0.2in. × 0.2 in. square elements in the region directly under the LWD with a mesh transition occurring at 20 in. away from the plate to 0.4 in. × 0.2 in. rectangular elements to optimize the computational speed. The LWD plate was modeled using quad elements and impact force was applied at the top of the plate. The soil was modeled as 80 in. wide and 80 in. depth. The steel plate was modeled using a linear elastic model rather than rigid. The LWD impact was modeled using a 1500 lb force with pulse duration of 17 msec. Both Zorn and Dynatest LWDs were modeled, as shown in Figure 5.4.1. Although soil was divided in two layers (parts) to account for future study of two-layered systems, a single material is considered in this part of the study.

Geomaterials were modeled using the nonlinear constitutive material model introduced in Equation 3.2.1. To determine the impact of LWD testing on soil response in terms of influence depth, a parametric study was carried on a single layer system. For this study, three cases within the typical range of k' values for fine-grained materials, presented in Table 5.4.1, were selected.

Table 5.4.1 – Pavement Sections Properties for One Layer System

k'_1	400, 1500, 3000
k'_2	0.01, 1.50, 3.00
k'_3	0, -2.0, -4.0
Poisson's ratio, ν	0.35

Pressure and displacement contours were generated for every 1 msec time intervals. Time histories of responses were measured underneath the center of the plate and along the soil surface. With this information, profiles of vertical deflection and stress were calculated during the plate impact.

Figure 5.4.2 shows the distribution of the vertical stress profiles at the soil surface with respect to the radial distance from the center of the loading plate for different geomaterials impacted with both a Zorn LWD and a Dynatest LWD. Figure 5.4.2a shows the pressure distribution for three geomaterials with variable k'_1 (with constant $k'_2 = 1.50$ and $k'_3 = 0$) indicating that only the hardening term of the nonlinear constitutive model (k'_2) is present. Figure 5.4.2b shows the stress profile for three geomaterials with $k'_1 = 400$, $k'_3 = 0$, and variable k'_2. Finally, Figure 5.4.2c shows the stress under the plate for three geomaterials with $k'_1 = 400$, $k'_2 = 1.50$, and varying k'_3. These figures show that the pressure exerted by both LWD loading plates concentrates at the outer edge of the plate while having a lower pressure zone along the central part of the plate. Greater stresses are developed under the Zorn's loading plate despite both plates being subjected to the same load of 1500 lb. The surface vertical stresses are not sensitive to different k'_1

and k'_3 values when k'_2 is constant, but they are sensitive to changes in k'_2 values when k'_1 and k'_3 remain constant.

A parameter called Stress Recovery Ratio (SRR) was used to estimate how much of the load imparted by the LWD was transferred to the soil. This parameter is defined as:

$$= \quad \frac{}{} \times 100\% \ , \tag{5.4.1}$$

where σ_u is the stress under the plate assuming uniform stress distribution (30 psi) and σ_{ave} is the average stress applied to the soil. Alternatively, the Load Recovery Ratio (LRR) can be calculated by integrating the surface stress, σ, and the area under the plate, defined as:

$$= \quad \frac{\int \int \quad ( )(\quad)}{} \times 100\% \ , \tag{5.4.2}$$

where P_u is the applied load (1500 lb), *d( )* is the first derivative, *r* and *q* are the polar coordinates of the loaded element.

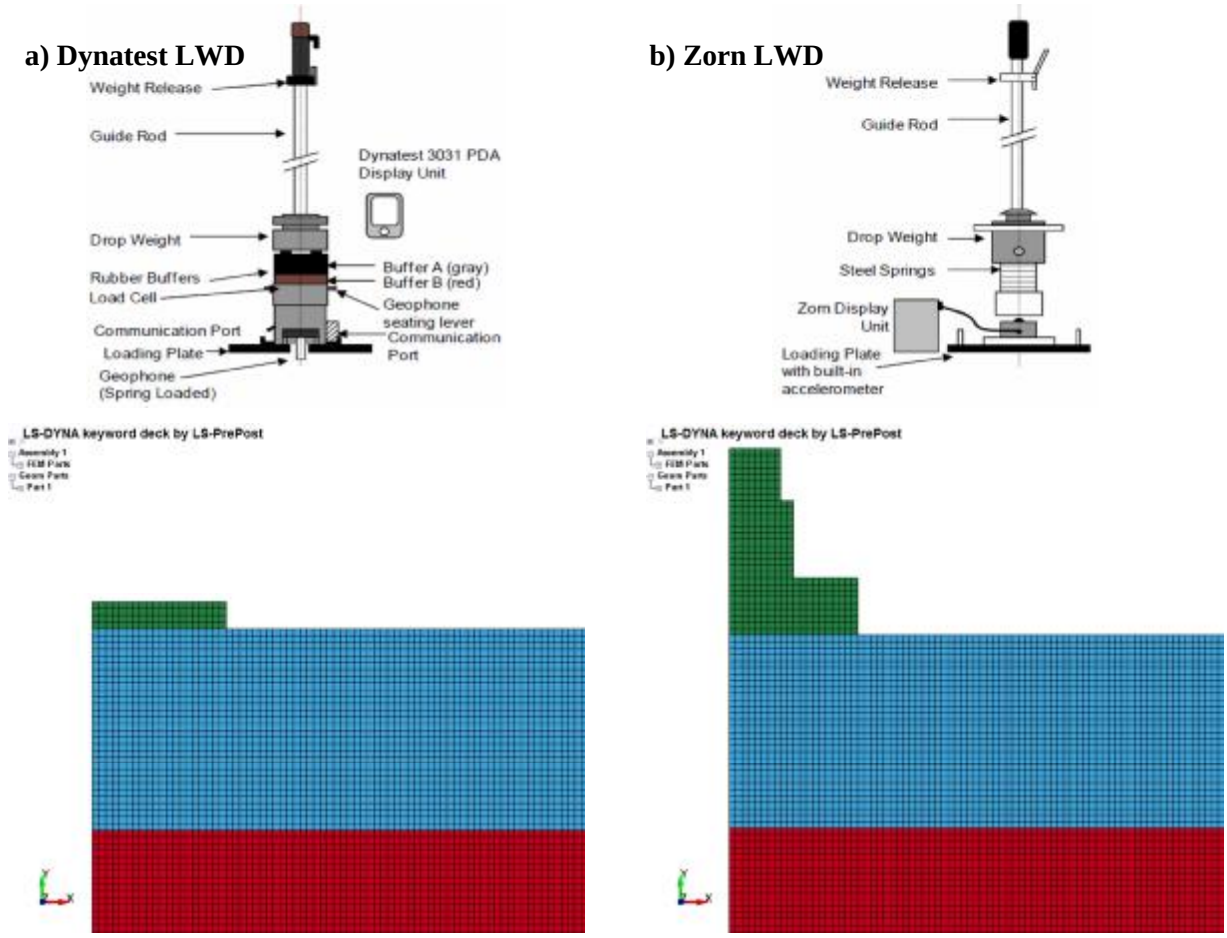

Figure 5.4.1 – Schematics of LWD and Finite Element Models for (a) Dynatest LWD and (b) Zorn LWD

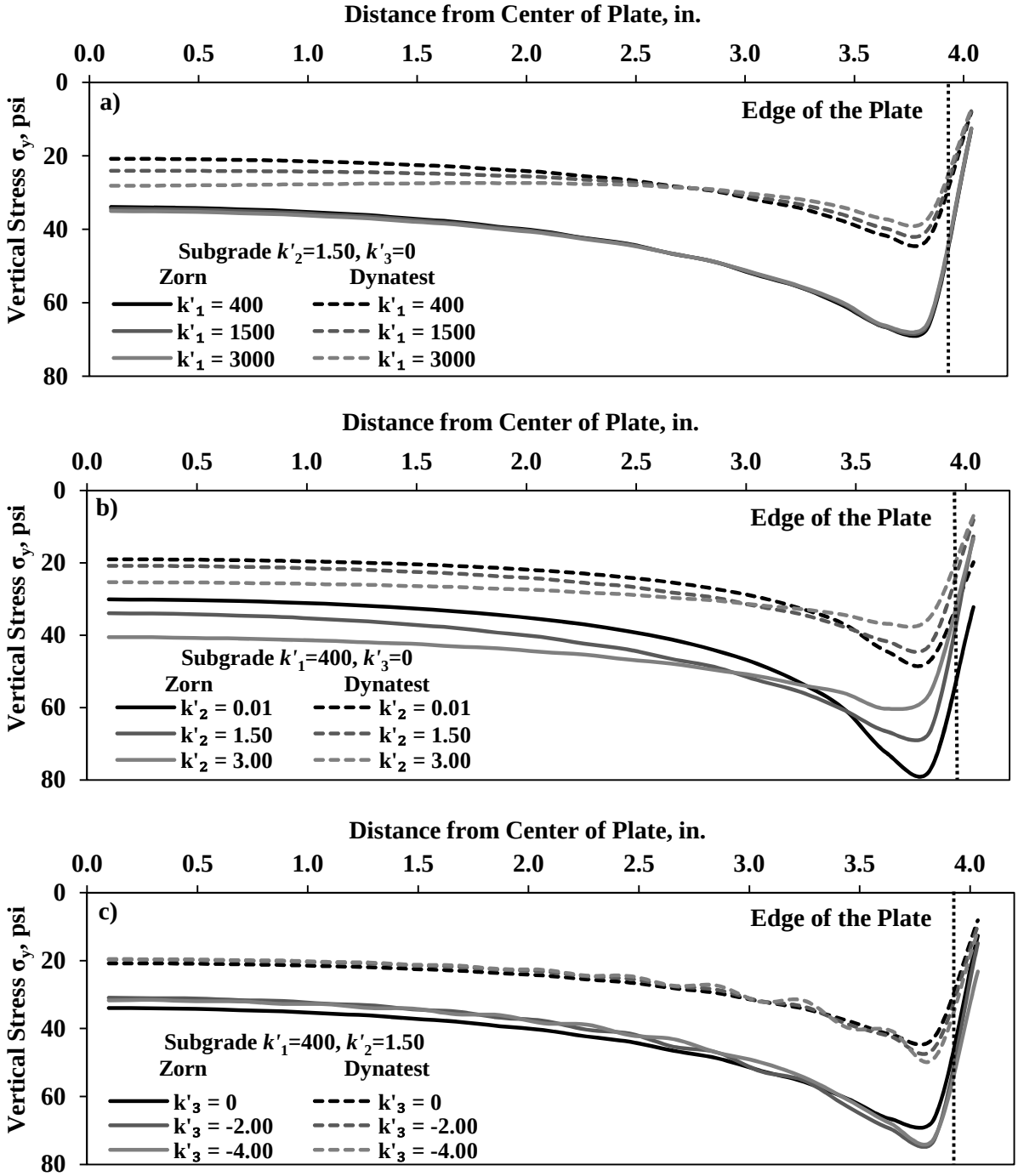

Figure 5.4.2 – Stress Profiles under Zorn and Dynatest LWD Plates, for (a) subgrade with varying k'_1, k'_2=1.50 and k'_3 = 0, (b) Subgrade with Varying k'_2, k'_1=400 and k'_3=0, and (c) Subgrade with Varying k'_3, k'_1=400 and k'_2=1.50.

Figure 5.4.3 shows that the SRR values for the Zorn LWD plate to be 1.5 to 1.6 times larger than those under Dynatest LWD plate. The LRR values, shown in Figure 5.4.4, result in similar trend. This

difference in magnitude is also evident in the stress profiles, where the peak stresses occurring at the edge of the Zorn LWD plate are 1.6 to 1.9 times larger than Dynatest LWD. This range decreases to 1.2 to 1.6 when the stresses occurring at the center of the plate are considered. Both the stress and SRR values suggest the pavement response to be most sensitive to the k'_2 parameter, related to a more granular material.

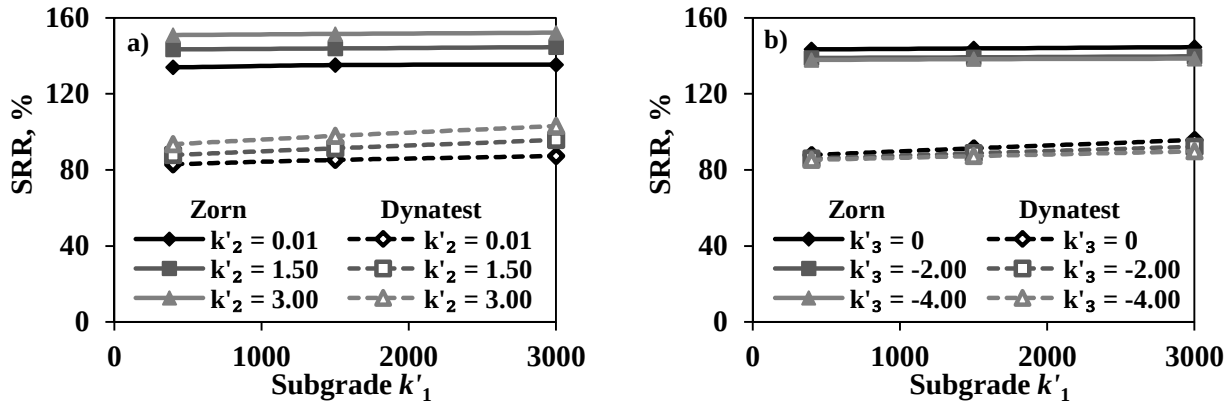

Figure 5.4.3 – Stress Recovery Ratio (SRR) for Zorn and Dynatest LWD Plates, for (a) Subgrade with Varying k'_1 and k'_2, and k'_3 = 0, (b) Subgrade with Varying k'_1 and k'_3, and k'_2=1.50

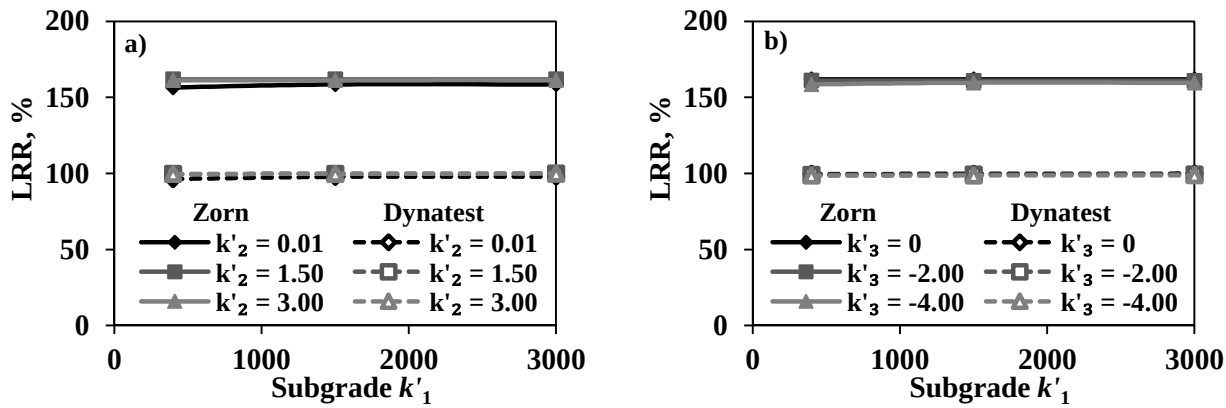

Figure 5.4.4 – Load Recovery Ratio (LRR) in terms of the Loading under Zorn and Dynatest LWD Plates, for (a) Subgrade with Varying k'_1, k'_2=1.50 and k'_3 = 0, and (b) Subgrade with Varying k'_2, k'_1=400, and k'_3=0

To explain these differences, it would be beneficial to study the propagation of the vertical stresses through the LWD loading plates. As reflected in Figure 5.4.1, even though the loading plate radiuses are nominally 4 in., the areas subjected to impact on top of these plates have different diameters. The Dynatest LWD loading impact occurs within a 2.75-in.-radius on top of the plate while the Zorn LWD impact occurs within an area with a 0.50-in.-radius. Figure 5.4.5 shows the distribution of the vertical stress through the plate and the soil under each LWD. Fringe levels, shown in *Pa*, were limited to a magnitude of 500 kPa (approximately 72 psi) in compression, cropping higher compression values that actually occur within the darker shaded areas. Particularly for the case of the Zorn LWD shown in Figure 5.4.5b, the vertical stress propagates towards the outer boundary of the plate, creating high stress concentration at the edge of the plate. The concentration of the load at the edges results in significantly greater than average vertical stresses in the soil.

Similarly, Figure 5.4.6 shows the surface deflection profiles under the plates for both devices. The deformations within the plates are minimal. Unlike stress, maximum surface deflection occurs at the center of the plate. The differences in the magnitude of the surface deflection under the two LWDs for the same geomaterial are noticeable. These differences have an effect on the measured surface moduli.

a) Dynatest LWD **b) Zorn LWD**

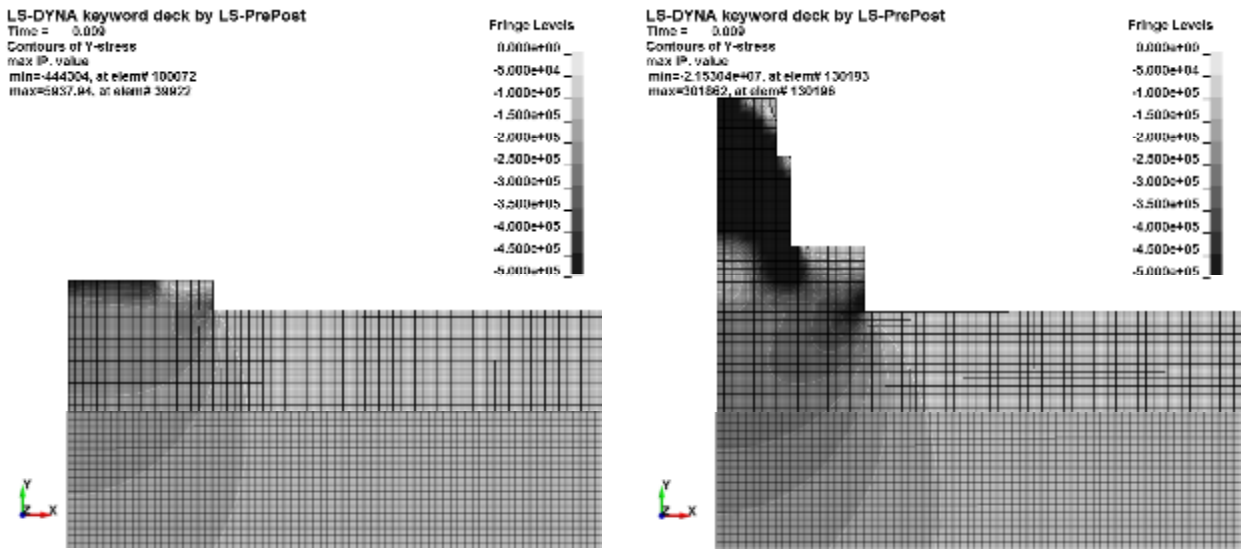

Figure 5.4.5 – Distributions of Vertical Stresses through Geomaterial Subjected to (a) Dynatest LWD and (b) Zorn LWD (fringe levels in Pa)

a) Dynatest LWD **b) Zorn LWD**

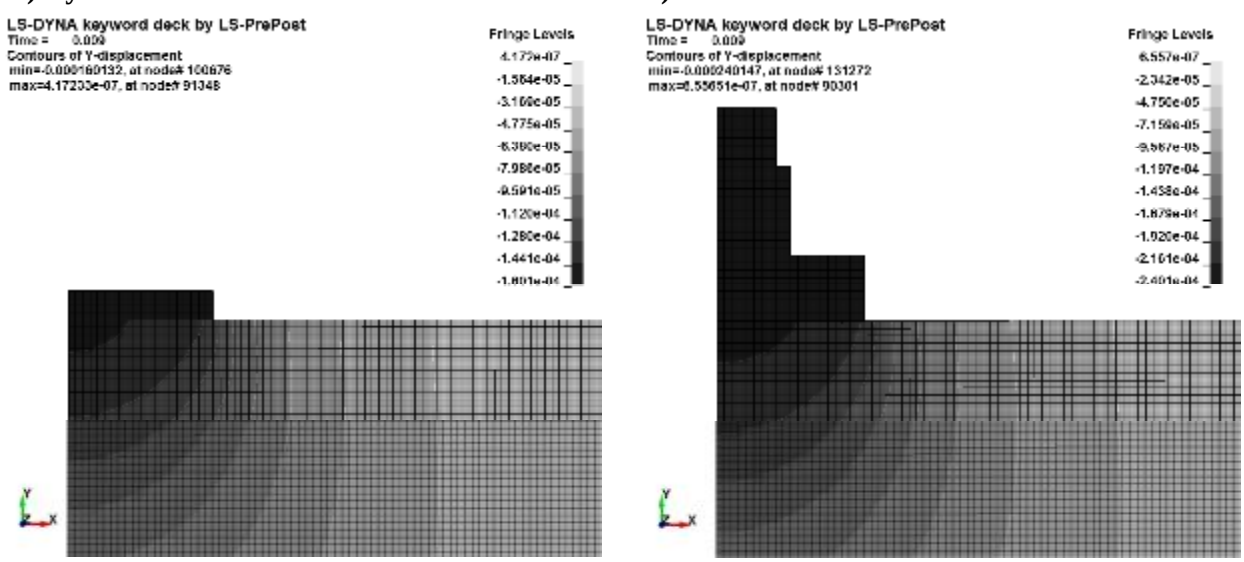

Figure 5.4.6 – Distributions of Vertical Deformation of Geomaterial Subjected to (a) Dynatest LWD and (b) Zorn LWD (fringe levels in m)

Figure 5.4.7 shows surface deflection for different soils with different nonlinear k' parameters. The deflections are mostly uniform close to the center of plate and decrease towards the edge. Surface deflections are sensitive to all three nonlinear k' parameters, particularly to k'_1 parameter. Moreover, the deflections under the Zorn LWD are 1.4 to 1.7 times greater than Dynatest LWD.

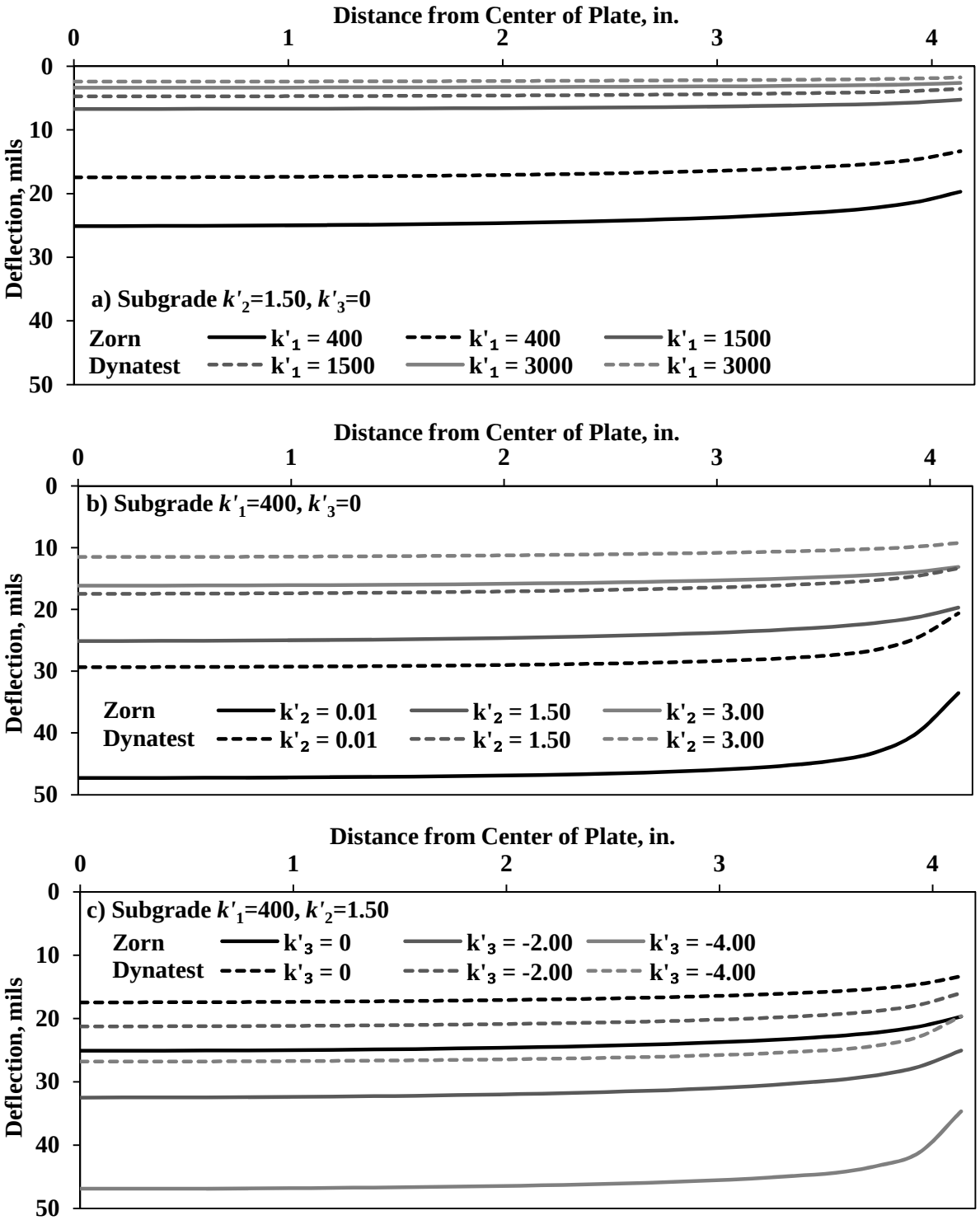

Figure 5.4.7 – Distribution of Surface Deflections under Zorn and Dynatest LWD Plates, for (a) Subgrade with Varying k'_1, k'_2=1.50 and k'_3 = 0, and (b) Subgrade with Varying k'_2, k'_1=400, and k'_3=0, and (c) Subgrade with Varying k'_3, k'_1=400 and k'_2=1.50

Using the soil surface deflections at the center of the plate, the surface modulus (E_{LWD}) is determined by the Boussinesq solution from (Terzaghi and Peck, 1967):

$$E_{LWD} = [(1 - n^2)a\ \sigma_0 / (\ d_{LWD})]\ f \qquad (5.4.3)$$

where v is Poisson's ratio, σ_0 is the uniformly distributed applied stress under the plate, a is the radius of the plate, d_0 is measured deflection. Parameter f is the shape factor to account for stress distribution. It is assumed as π/2 for a rigid plate that creates an inverse parabolic distribution shape (clay, subgrade and lime stabilized subgrade materials), 2 for flexible plates that creates a uniform distribution shape suitable (granular base underlain by clay subgrade), and 8/3 also for flexible plates that creates a parabolic shape (cohesionless sand). In this study, a value of π/2 was assumed for the shape factor, suiting the inverse parabolic distribution of the soil response.

Figure 5.4.10 shows the surface modulus as obtained from the finite element analysis for cases with variable nonlinear k' parameters. Unlike the Dynatest LWD, the surface modulus for the Zorn LWD is obtained from the sensor located on top of the plate.

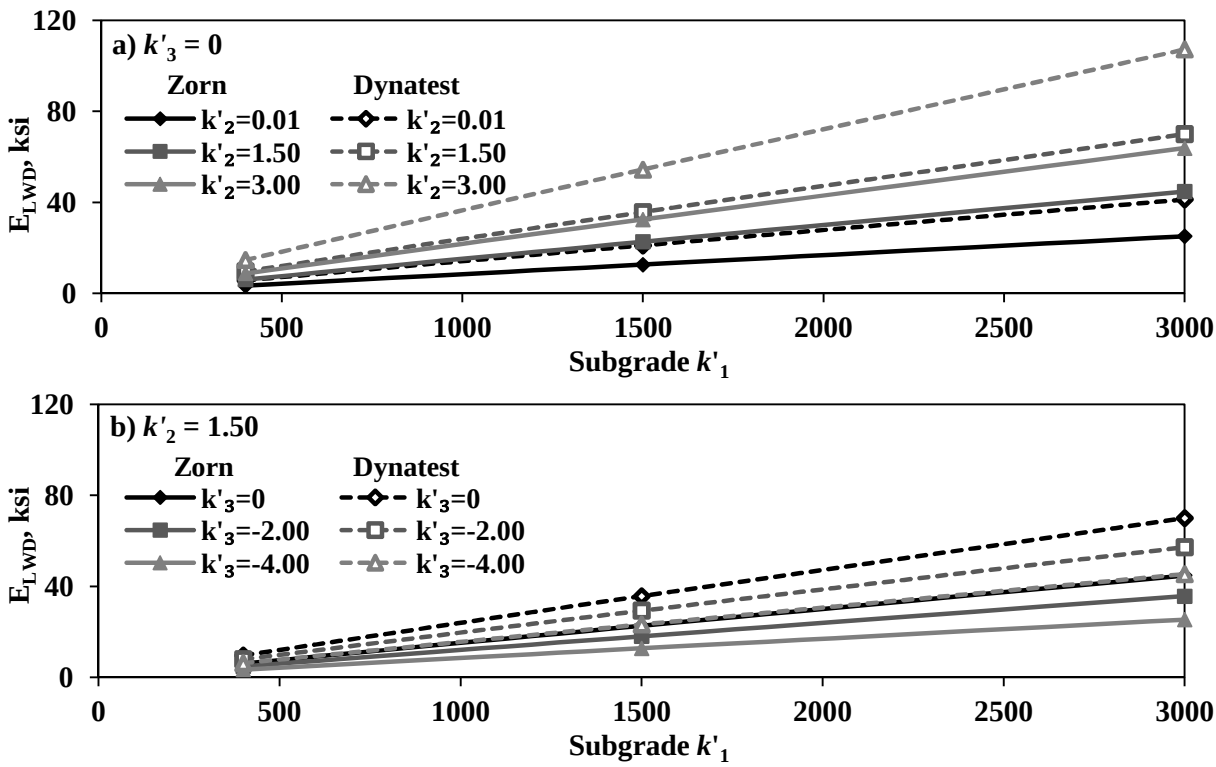

Figure 5.4.8 – Surface Modulus E_{LWD} for Zorn and Dynatest LWD Plates for (a) Subgrade material with Varying k'_1 and k'_2, and k'_3 = 0, and (b) Subgrade with Varying k'_1 and k'_3, and k'_2 = 1.50

The calculated surface moduli (for all the cases) are collectively shown in Figure 5.4.9 for both devices. Since deflections under Zorn LWD are larger than Dynatest LWD, the resulting moduli were lower for Zorn LWD than Dynatest device. Using the soil responses for all considered cases, a relationship was established relating surface modulus (E_{LWD}) obtained between Zorn and Dynatest LWDs as:

$$E_{\text{LWD Dynatest}} = 1.65 E_{\text{LWD Zorn}} \quad (R^2 = 0.99) \qquad (5.4.4)$$

These results are in agreement with the findings from Vennapusa (2009).

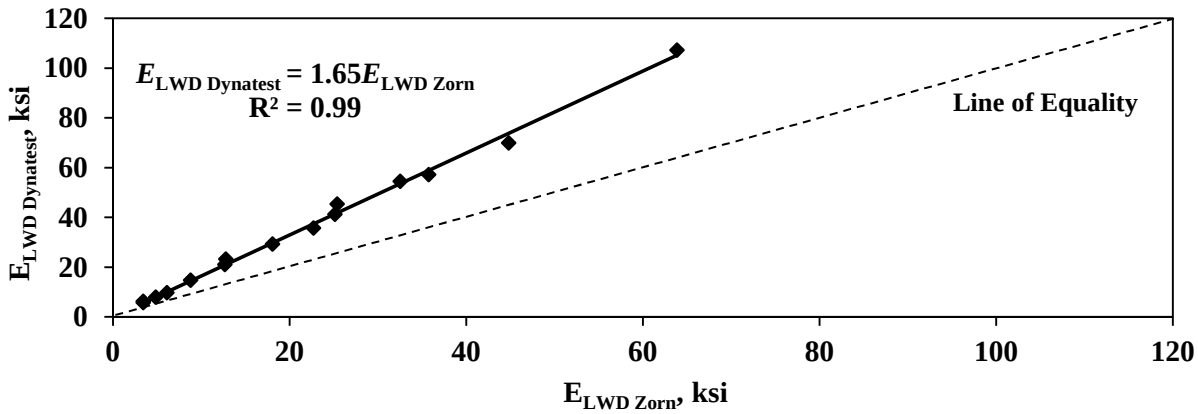

Figure 5.4.9 – Relationship of E_{LWD} for Zorn and Dynatest Devices for all Considered Cases

Depth of influence of LWD impact was also studied using the selected parameters as shown in Table 5.4.1. The vertical stress profiles with respect to depth for a geomaterial with k'_1=400, k'_3=0 and variable k'_2 is shown in Figure 5.4.10a. From this figure, it is particularly evident that stresses vary within 5 in. from the surface. The deflection profiles with respect to depth for the same soil types are shown in Figure 5.4.10b. The nonlinear parameters clearly have an effect on the soil deformation. In this study, influence depth was established at a 10% of the surface response.

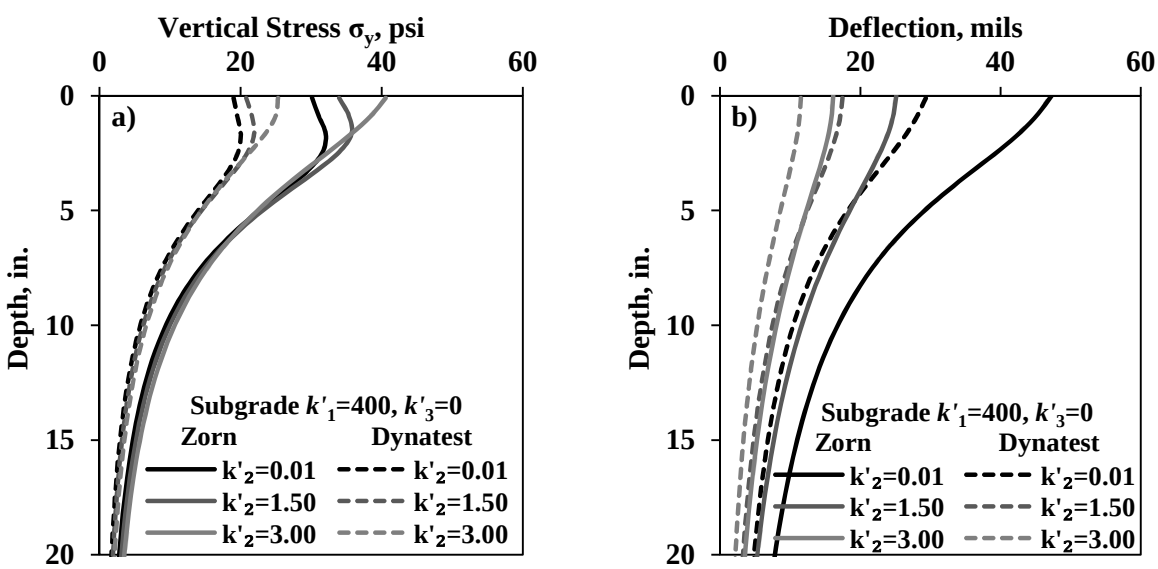

Figure 5.4.10 – Depth Profiles for (a) Vertical Stress and (b) Deflection under Zorn and Dynatest LWD Plates for Soil with k'_1=400, k'_3=0, and Varying k'_3.

Figure 5.4.11 shows the depth of influence of both devices in terms of stress at 10% of the surface stress. This figure shows influence depth varies between 16 in. and 19 in. Moreover, it can be seen that influence depth decreases with stiffer materials, i.e. higher k'_1, and with more granular materials, i.e. higher k'_2, as shown in Figure 5.4.11a. However, k'_3 did not have a significant impact on influence depth, as shown in Figure 5.4.11b, meaning that influence depth is not sensitive to more clayey materials. Variation of influence depth seems to be more sensitive when Dynatest LWD is used. This may be because of the stress propagation due to the different contact stress profiles occurring at the soil-plate interface.

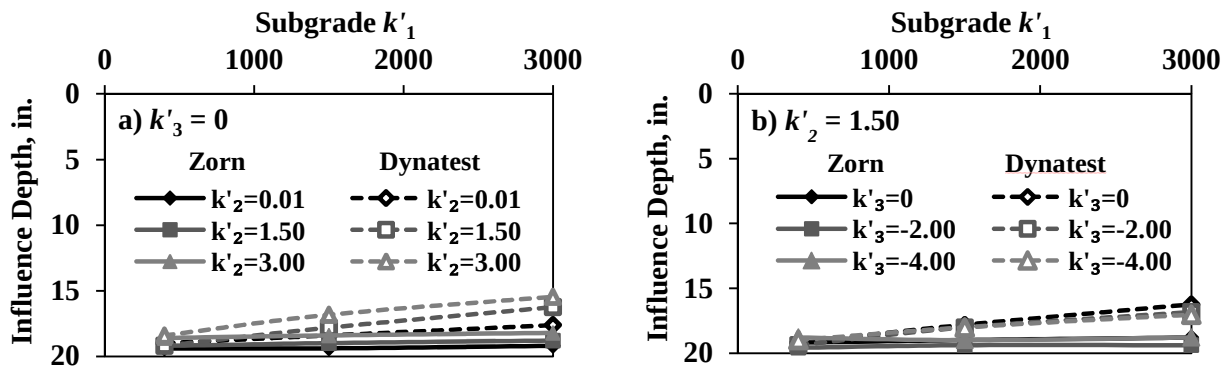

Figure 5.4.11 – Influence Depth based on Vertical Stress at 10% of Surface Stress for (a) Varying k'_1 and k'_2, and k'_3=0, and (b) Varying k'_1 and k'_3, and k'_2=1.50, for both Zorn and Dynatest LWD.

Likewise, the depth of influence was determined in terms of 10% of surface deflection. Figure 5.4.12 shows how depth of influence varies with different nonlinear parameters, changing between 24 in. and 32 in. Influence depth decreases with lower k'_2, i.e. when material is less granular, as shown in Figure 5.4.12a. Moreover, it decreases with higher k'_3, i.e. more clayey material, as shown in Figure 5.4.12b. Yet, both figures indicate influence depth is not sensitive to parameter k'_1 which is the parameter related to stiffness. Generally, the Zorn LWD has a slightly greater deflection based on depth of influence.

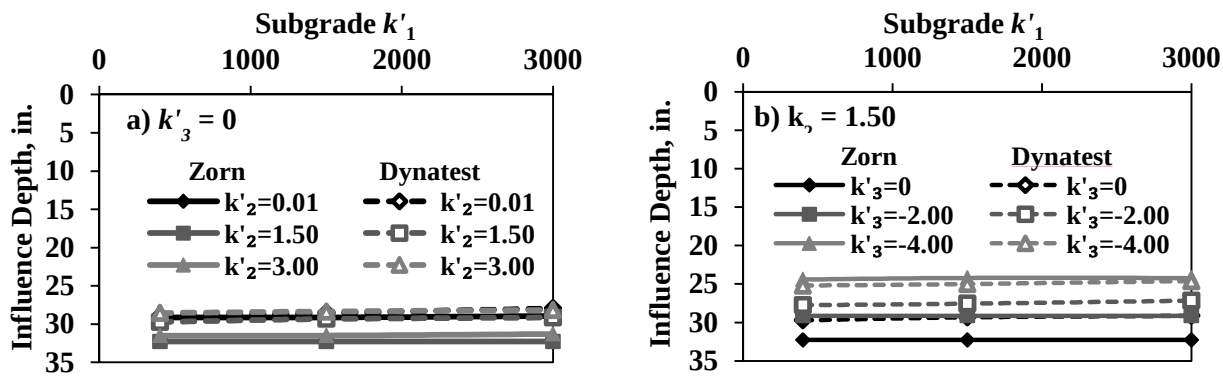

Figure 5.4.12 – Influence Depth based on Deflection at 10% of Surface Deflection for (a) Varying k'_1 and k'_2, and fixed k'_3=0, and (b) Varying k'_1 and k'_3, and fixed k'_2=1.50, for both Zorn and Dynatest LWD.

Both deflection and stress dependent depths of influence indicate that it is material and device dependent. Zorn LWD seemed to be less sensitive to material properties as compared to Dynatest LWD.

CHAPTER 6 – ESTABLISHING TARGET MODULI

6.1 Introduction

One of the goals of this project is to establish the target values based on the structural design parameters. The main design parameter of each pavement layer is its laboratory modulus (especially its resilient modulus). Setting the target modulus for devices like the DCP or PSPA is straightforward because they provide layer-specific moduli. Since devices like the PLT, LWD and Geogauge measure the surface responses to provide effective moduli of the pavement system, the establishment of their target moduli requires the use of a numerical algorithm. The processes proposed for estimating the target moduli for different devices are discussed in the next sections. Laboratory and field moduli differ even at the same moisture content and density as discussed in Chapter 2. This matter has to be considered when the target moduli are being established.

6.2 Structural Models

As discussed in Chapter 2, a direct estimation of field moduli in general (and target field moduli in particular) from laboratory moduli for technologies that measure the response of the system (e.g., LWD and Geogauge) is not technically prudent. These moduli have to be related through an appropriate and calibrated structural model. A response algorithm was developed and calibrated with experimental results from the small-scale specimens. The developed algorithm can simulate the testing of the small-scale specimens or actual pavement sections in two ways:

1. Using a layered elastic system with representative moduli of layers as per MEPDG
2. Using a layered nonlinear system where the resilient modulus parameters k_1 through k_3 of the layers are input as per MEPDG Level 1 analysis.

The response algorithm used for Item 1 is based on a multi-layered elastic analysis system similar to JULEA used in the MEPDG software. A multi-layered equivalent-linear model, as discussed in Chapter 2, is used for nonlinear analyses. The equivalent linear model utilizes the multilayer linear elastic layered theory. However, an iterative process is employed to consider the nonlinear behavior of the pavement materials. The nonlinear layers are divided into several sublayers (1 in. thick in this study). One stress point is chosen for each nonlinear sublayer. An initial modulus is assigned to each stress point. The relevant stresses are calculated for all stress points to determine the corresponding bulk and octahedral stresses. These stresses are used to calculate a new modulus using the Ooi et al. (2004) nonlinear model introduced in Equation 3.2.1 and repeated in Equation 6.2.1:

$$MR = k_1^{'} P_a \left(\frac{q}{P_a} + 1 \right)^{k_2^{'}} \left(\frac{t_{oct}}{P_a} + 1 \right)^{k_3^{'}} \tag{6.2.1}$$

where q = bulk stress, t_{oct} = octahedral shear stress and P_a = atmospheric pressure. The assumed and the newly calculated moduli at each stress point are compared. If the difference between them at any stress point is greater than a pre-assigned tolerance (1% in this study), the process is repeated using updated assumed moduli. The above procedure is repeated until the modulus differences are within the assigned tolerance for all stress points. In a linear-elastic layered solution, the lateral variation of modulus within a layer cannot be considered. To compensate to a certain extent for this disadvantage, a set of stress points at different radial distances are also considered. The results from this algorithm were compared with a rigorous nonlinear finite element program. The differences in the estimated deflections were at most 7%.

To simulate the modulus devices, the pavement system is loaded by one or more circular load(s) with uniform stress distribution over the loaded area(s). The algorithm can simulate the following technologies and devices:

- Plate Load Test (PLT) with different plate diameters and different stress levels

- Light Weight Deflectometer (LWD) with specific load and plate diameter, and
- Electro-mechanical stiffness (e.g., Geogauge)

The input parameters for this response algorithm include:

- thickness of each layer,
- Poisson's ratio of each layer,
- unit weight of each layer, and
- the values of k'_1, k'_2 and k'_3 of each layer obtained from resilient modulus tests

The detailed output of this response algorithm contains the following information for each selected modulus-based device within the pavement structure:

- components of stress tensor in the middle of each sublayer and other user-defined locations
- components of strain tensor in the middle of each sublayer and other user-defined locations
- vertical displacements in the middle of each sublayer and other user-defined locations
- moduli of all sublayers as well as a representative modulus for each main layer
- target modulus value for a given modulus-based device

6.3 Evaluation of Numerical Models

The deflections from the embedded geophones during the LWD tests in the small-scale specimens that were calculated from the laboratory MR parameters of the GP material are compared to the experimental deflections in Figure 6.3.1 for the linear and nonlinear analyses. Laboratory values of k'_1, k'_2, k'_3 and representative MR moduli in Table 3.2.2 were used in the analyses. The experimental deflections for the GP base material are about 0.92 and 0.56 times the numerical ones for the linear and nonlinear analyses, respectively. The patterns observed for other materials, as shown in Appendix F, are similar to the ones shown in Figure 6.3.1.

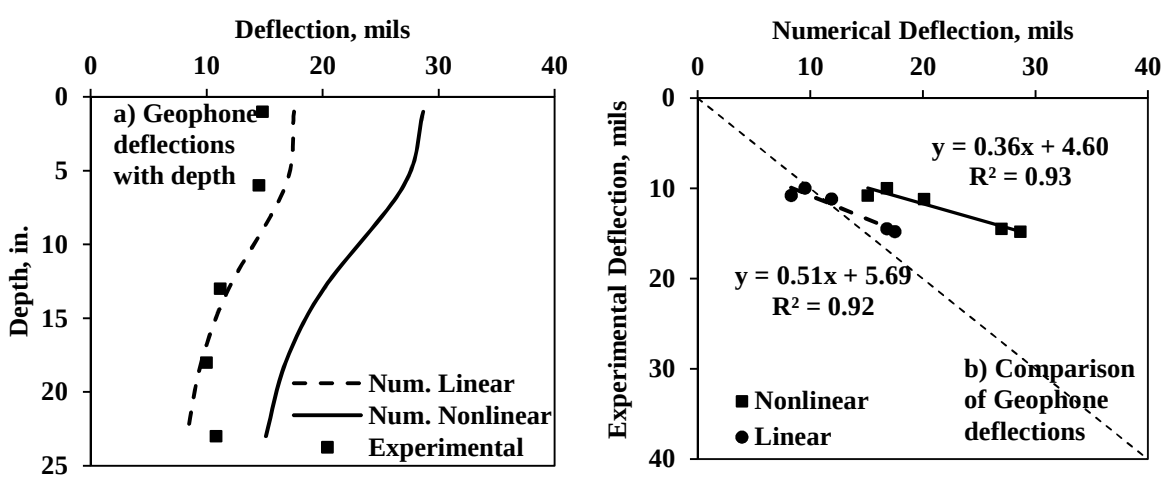

Figure 6.3.1 - Comparison of Experimental and Numerical Deflections during LWD Tests (GP Material Compacted and Tested at OMC%)

The observed differences between the measured and numerical results can be due to the differences in the laboratory and field moduli of the materials. Seismic methods can describe such differences because the FFRC laboratory moduli and the PSPA field moduli are theoretically related without any need for adjustment for the testing boundary conditions. For example, the FFRC moduli of the GP base and subgrade were measured as 13 ksi and 7 ksi, respectively; whereas the PSPA moduli for the compacted layers at the same moisture contents and densities were 42 ksi and 21 ksi, for the base and subgrade,

respectively. Since the moduli from the small-scale tests are greater than the laboratory values, the patterns observed, especially for the nonlinear analyses, are reasonable. Even though the linear-elastic deflections within the specimens for some materials are closer to the experimental ones, the linear-elastic analyses result in some complications as discussed later.

Figure 6.3.2 presents the relationships between the FFRC and PSPA moduli for the GP material. Strong relationships exist between the PSPA moduli from the small-scale study and the FFRC laboratory moduli for all moisture contents. At lesser FFRC moduli, which typically correspond to the results when the testing moisture contents are close to the compaction moisture contents, the PSPA moduli are greater than the FFRC moduli. This indicates that shortly after compaction, the field moduli are greater than the corresponding laboratory moduli. As the FFRC moduli increase (i.e. the compacted materials are allowed to dry more), the PSPA moduli progressively become less than the corresponding laboratory moduli. In that case, the laboratory results overpredict the corresponding field moduli.

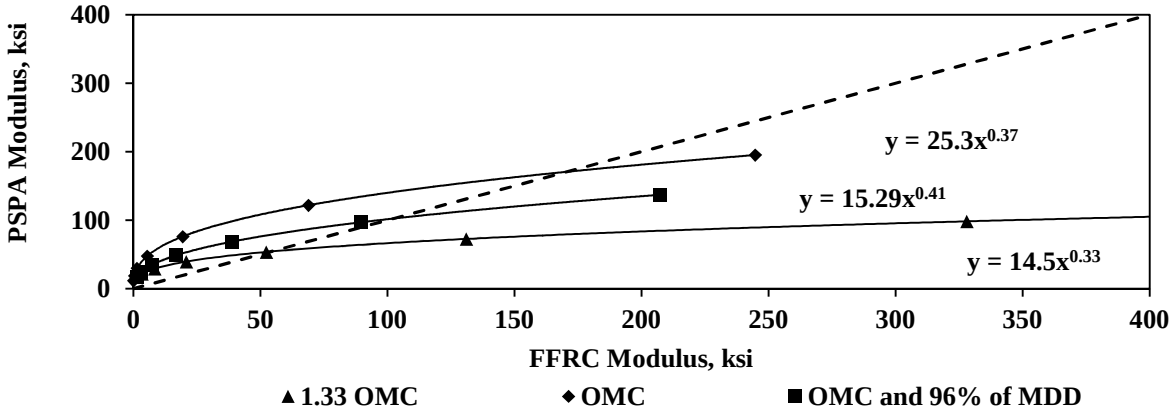

Figure 6.3.2 - Relationships between PSPA Moduli and FFRC Moduli for GP Materials at Corresponding Compaction Moisture Contents

To generalize the relationship for all moisture conditions, the moduli from the PSPA and FFRC tests are normalized with respect to their corresponding moduli at optimum moisture contents. As shown in Figure 6.3.3, a single relationship exists that can relate the two parameters. One can conveniently adjust the laboratory-measured resilient modulus at optimum moisture content for the differences in the compaction methods between the field and the laboratory, the differences in the placement moisture content from the OMC, and the differences in density relative to MDD.

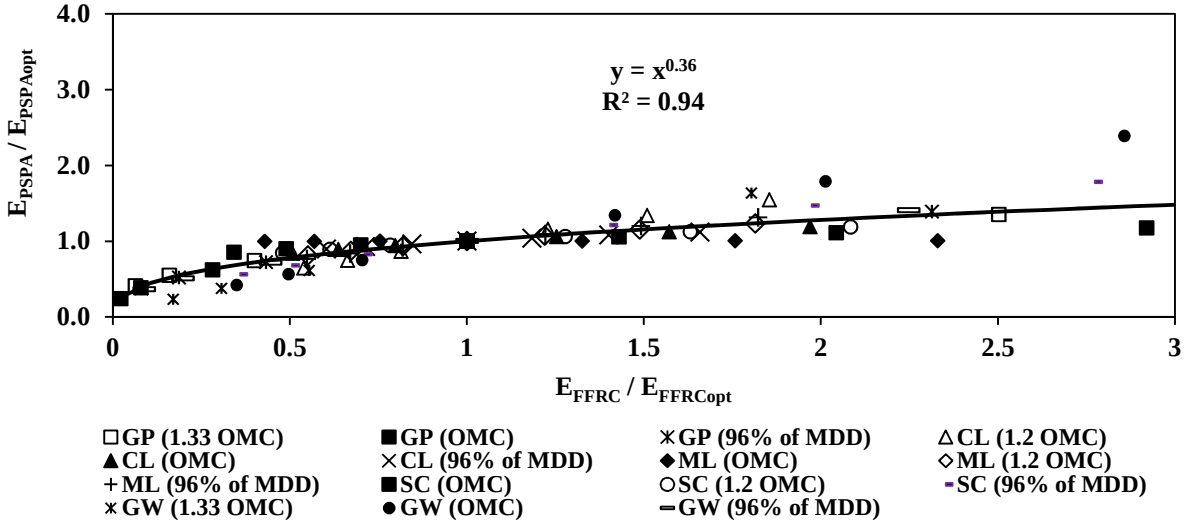

Figure 6.3.3 - Normalized Relationship between Moduli from Laboratory and Field for all Materials

6.4 Calibrating Numerical Models

If one assumes that the laboratory and field compaction efforts would yield identical final moduli, the seismic modulus measured with the PSPA, E_{PSPA_ideal}, should be equal to:

$$\_ \quad = \quad \_ \quad /((1+\ )(1-2\ )/(1-\ )) \tag{6.4.1}$$

where E_{FFRC_Lab} = laboratory measured modulus with the FFRC device and υ = Poisson's ratio of the geomaterial. The laboratory and field seismic moduli under the same moisture content and density differ due to the differences in compaction methods (see Figure 6.3.3). To account for such differences, stiffness parameter k'_1 from the laboratory MR testing is adjusted as per Equation 6.2.1:

$$k'^{*}_1 = (E_{PSPA\text{-}Field} / E_{PSPA\_ideal})\, k'_1 = C.k'_1 \tag{6.4.2}$$

where k'^{*}_1 is the adjusted k'_1 and $E_{PSPA\text{-}Field}$ is the PSPA modulus from the field accounting for the difference in compaction method and the difference in moisture content at the time of compaction and testing. Parameter k'^{*}_1 is then replaced with parameter k'_1 in the response algorithm, to accommodate the differences between the laboratory and the field stiffness.

To evaluate the appropriateness of this process, a small-scale specimen was prepared with only the SM subgrade (i.e., the specimen consisted of 22 in. of the same material). Numerical results from the nonlinear analysis (as per MEPDG Level 1) and linear analysis (as per MEPDG Level 2) from a PLT test with an 8 in. diameter plate and a contact stress to 30 psi are compared with the numerical results in Figure 6.4.1 without adjusting the parameter k'_1. The numerical deflections are about 2.5 times greater than the experimental deflections. Figure 6.4.2 depicts the same results but with the adjusted k'_1 parameter k'^{*}_1. The differences between the numerical and experimental deflections are about 5%.

To evaluate further the appropriateness of the nonlinear model, the experimental results from the PLT tests for several different contact stresses are compared with the corresponding nonlinear numerical results in Figure 6.4.3. The adjustment process described above seems to be reasonable for all contact stresses.

Based on the initial success with a uniform layer, the process was repeated for the small-scale specimens with the other geomaterials placed at OMC and MDD. As shown in Figure 6.4.4, the numerical PLT deflections with the unadjusted k'_1 parameter are about 2.5 times greater than the experimental deflections, whereas the numerical deflections after adjusting k'_1 are on average 15% different from the experimental ones. In addition, less scatter in the data is present after k'_1 is adjusted.

This process was further applied to all geomaterials at different moisture contents to assess the closeness of the numerical and experimental deflections. The results are summarized in Figure 6.4.5. The differences between the experimental and numerical results before adjusting k'_1 are more than 100% for about 80% of the cases. After adjusting k'_1, 84% of the experimental results are estimated with an error of less than 40%. The theoretical and experimental results differ significantly typically when the differences between the compaction and testing moisture contents are substantial or the small-scale specimens are cracked.

As reflected in Figure 6.4.6, the numerical deflections with k'_1 are overall 43% greater than experimental ones when the same process was applied to the Zorn LWD results, whereas the numerical deflections are 36% less than the experimental ones when k'^{*}_1 was used in the analyses. These differences can be partially due to the dynamic nature of the LWD loading or due to the LWD plate-soil interaction that were ignored in the numerical analyses.

Figure 6.4.7 illustrates a comparison between the surface deflections reported by the Zorn LWD and corresponding deflections from a geophone buried in the small-scale specimens very near the surface during the LWD tests of all materials (except CH due to excessive cracking). Surface deflections from the Dynatest LWD are 12% and from the Zorn LWD device are 32% greater than the geophone

deflections. The differences observed in Figure 6.4.6 and 6.4.7 could be explained by the results of FE analyses as discussed in Section 5.4.

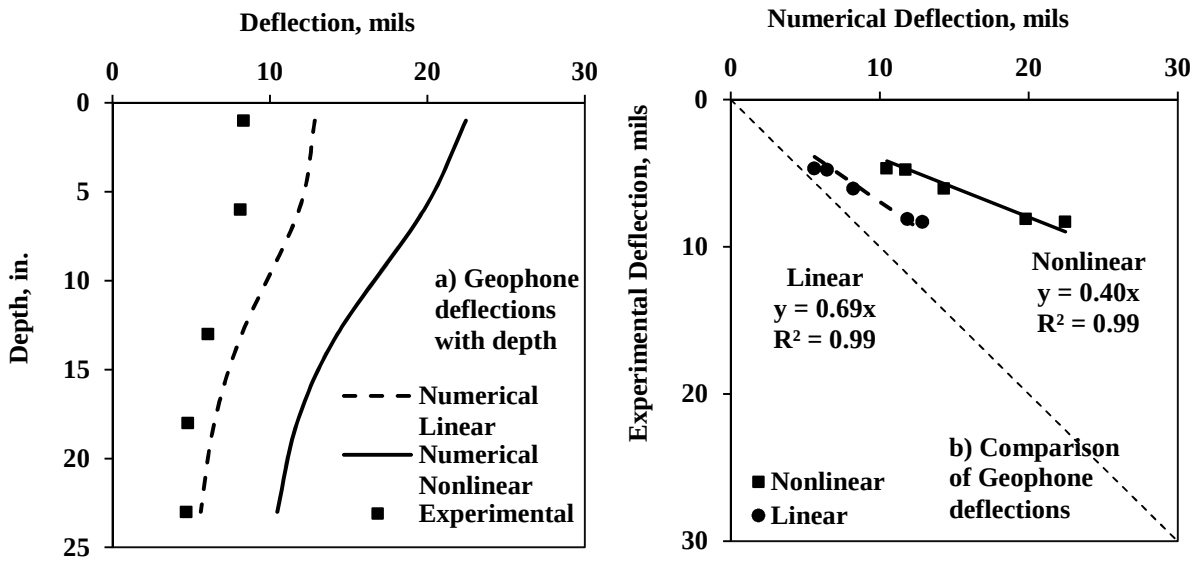

Figure 6.4.1 - Comparison of Experimental and Numerical Results from PLT Tests with 8 in. Plate and 30 psi Nominal Contact Pressure without Adjustment (SM Subgrade Material Compacted and Tested at OMC)

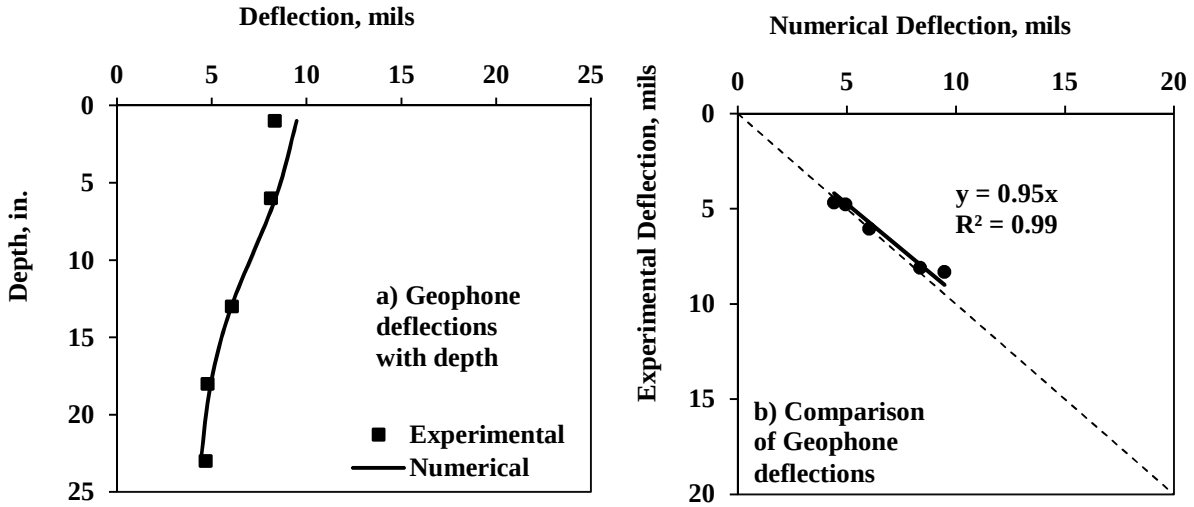

Figure 6.4.2 - Comparison of Experimental and Numerical Results from PLT Tests with 8 in. Plate and 30 psi Nominal Contact Pressure with Adjustment (SM Subgrade Material Compacted and Tested at OMC)

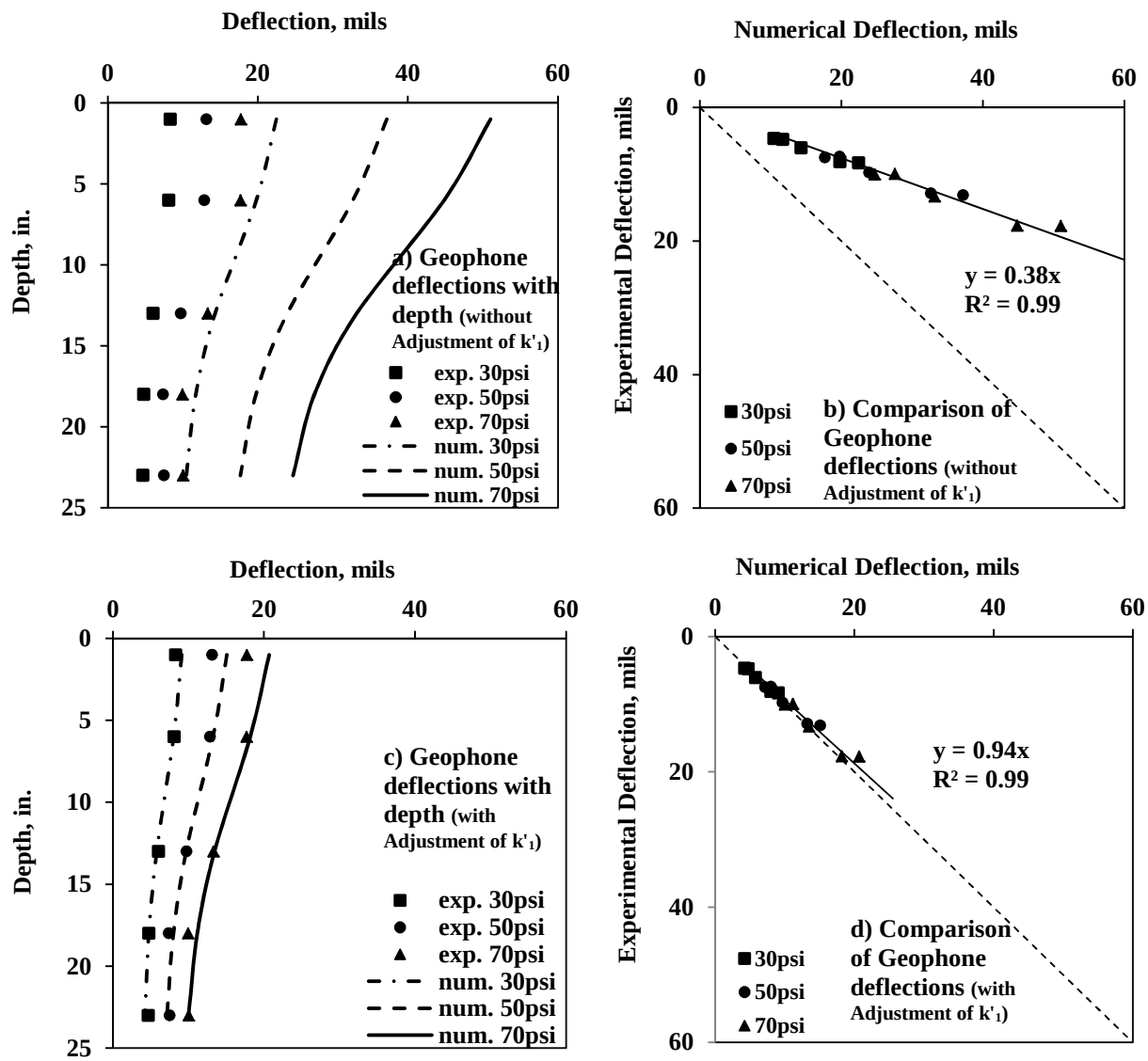

Figure 6.4.3 - Comparisons of Experimental and Numerical Results from PLT Tests with 8 in. Plate and Various Nominal Contact Pressure with and without Adjustments of k'_1 Parameter (SM Subgrade Materials Compacted and Tested at OMC%)

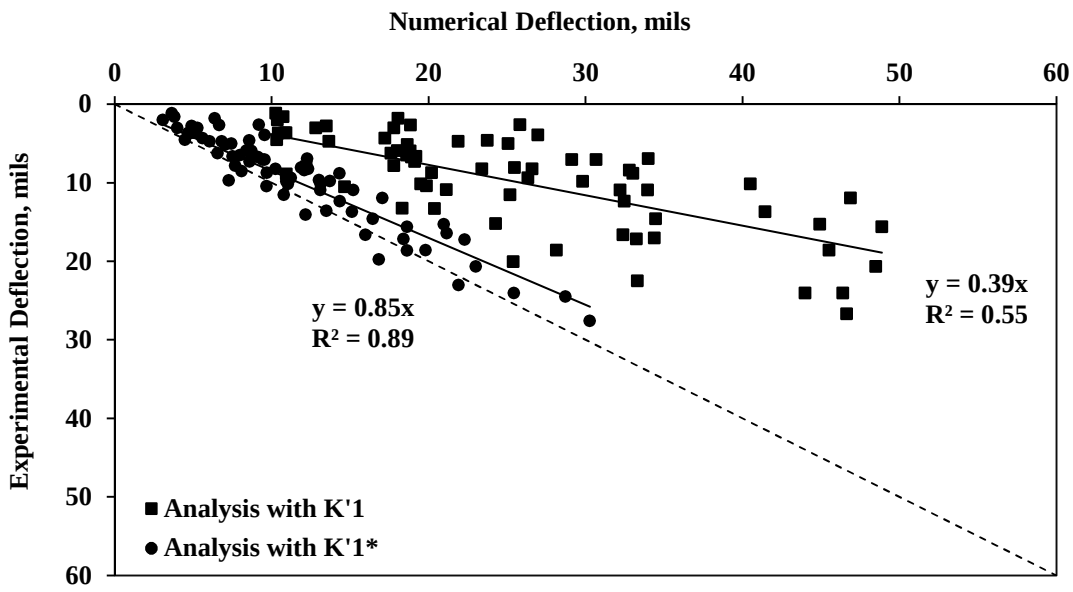

Figure 6.4.4 - Improvements in Estimating Numerical PLT Deflections (with 8 in. plate tested at OMC) due to Adjustment of k'_1 Parameter (GW and GP Base, CL, CH, ML and SC Subgrades)

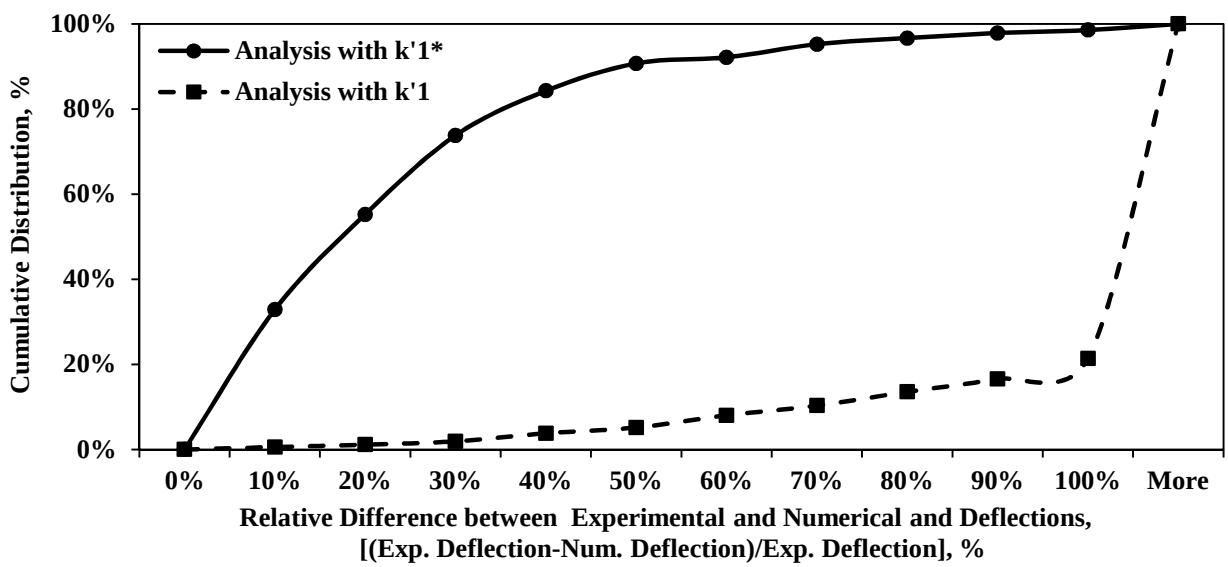

Figure 6.4.5 - Distributions of Errors in Estimating PLT Deflections due to Adjustment of k'_1 Parameter (GW and GP Base, CL, CH, ML and SC Subgrades)

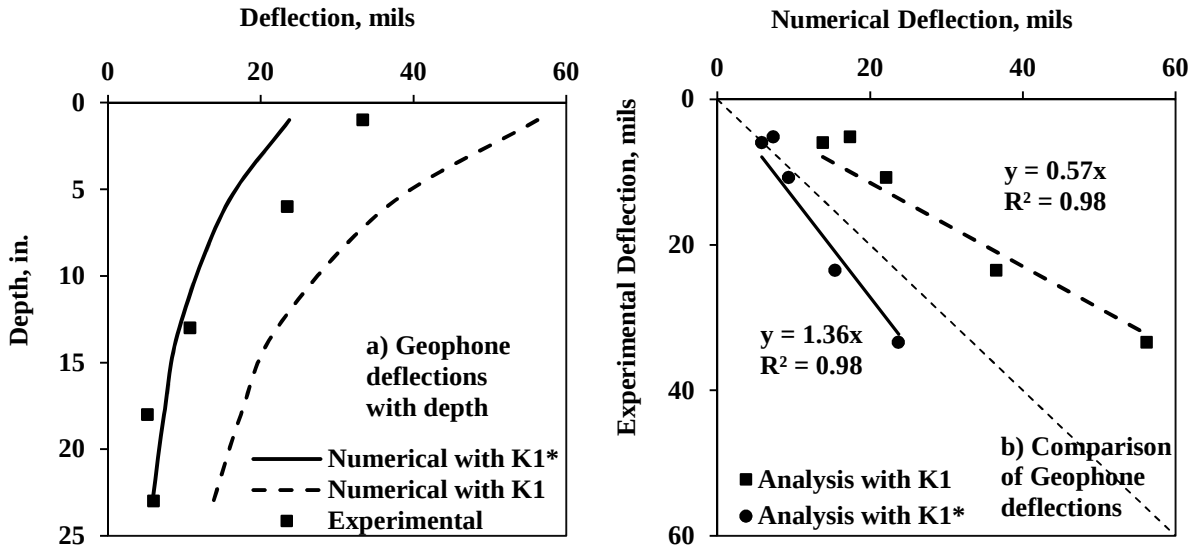

Figure 6.4.6 - Comparisons of Experimental and Numerical Results from Zorn LWD Tests with and without Adjustments of k'_1 Parameter (SM Subgrade Materials compacted and Tested at OMC%)

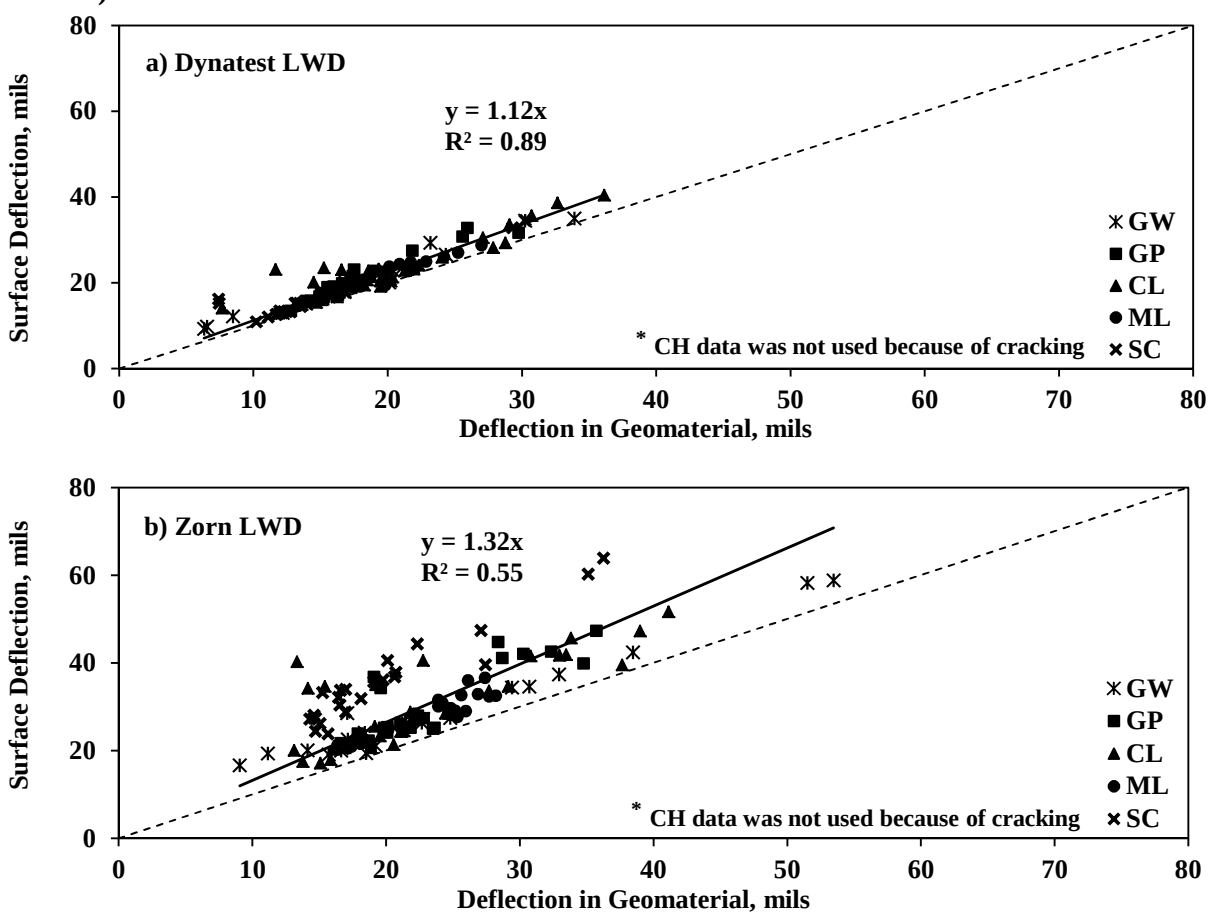

Figure 6.4.7 - Relationship between Surface Deflections and Deflections within Geomaterials during LWD Tests (GW and GP Bases, CL, CH, ML and SC Subgrades)

Figure 6.4.8 shows the results of FE analyses (as described earlier in Section 5.4) for LWD sensor deflections (at the surface) with respect to the deflection at 1 in. depth from the soil surface. The surface deflection is 35% greater than the deflection at 1 in. depth for the Zorn LWD, similar to 32% difference in the experimental results (see Figure 6.4.7). For the Dynatest LWD, the FE analyses indicate a 28% difference, which is greater than the 12% difference obtained from the experimental data..

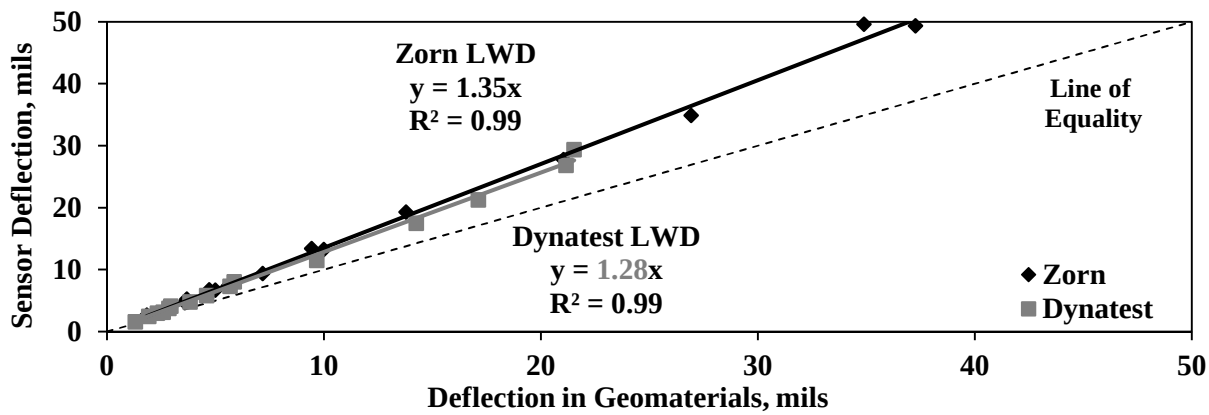

Figure 6.4.8 – Relationship between Surface Deflection and Deflection within Geomaterials as Obtained from FE Modeling

6.5 Selecting Target Modulus for Light Weight Deflectometer (LWD)

LWD measures the surface deflection under a given load. To avoid back-calculation, the measured deflection is translated to an *effective modulus*, E_{eff}, assuming that the geomaterial is a single elastic layer. The following equation is used to estimate the LWD modulus, E_{LWD}:

$$E_{LWD} = [(1 - n^2)\, F / (p\, a\, d_{LWD})]\, f \qquad (6.5.1)$$

where n = Poisson's ratio of geomaterial, a = radius of load plate, F = LWD load, d_{LWD} = LWD surface deflection, and f = shape factor which is a function of the plate rigidity and soil type (Vennapusa and White, 2009).

An analytical study was carried out to propose a convenient method for estimating the LWD target modulus. A database of 1000 random combinations of k' parameters were generated using a discrete uniform distribution with equal probability of outcomes and Latin Hypercube sampling method. As recommended by the MEPDG, the representative laboratory MR modulus from each set of k' parameters were estimated using θ = 12.4 psi and t_{oct} = 3 psi in Equation 6.2.1 (Section 6.2). The ranges of k' parameters were constrained to $50 < k'_1 < 3000$, $0 < k'_2 < 3$, and $-4 < k'_3 < 0$. The representative laboratory MR modulus was limited to 50 ksi to ensure that the database was realistic.

The nonlinear response algorithm was utilized to determine the target surface deflection for an LWD with a nominal load of 1200 lbs applied to an 8-in.-diameter plate for each of the 1000 cases. The target field moduli were estimated using Equation 6.5.1 assuming a Poisson's ratio of 0.40.

As depicted in Figure 6.5.1, the field target moduli are systematically under-predicted by about 11% relative to their corresponding representative laboratory MR moduli. The random errors that manifest as scatter about the best-fit line were of concern.

Observing the strong correlation between the representative laboratory MR and target LWD field moduli, it was hypothesized that another combination of θ and t_{oct} might reduce the errors of estimate between the two moduli in Figure 6.5.1. A nonlinear optimization algorithm using the Levenberg-Marquardt (1978) method was used to find the optimum values of θ and τ_{oct} that should be used for the specified LWD. As shown in

Figure 6.5.2, the optimal target LWD field moduli are obtained when θ and t_{oct} are selected as 10.5 psi (instead of 12.4 psi) and 3.2 psi (instead of 3 psi), respectively. These values minimized the systematic differences between the two moduli but still the errors of estimate were considered as unacceptable.

Additional correlation analyses were carried out to understand the source of variability in the estimated target LWD field moduli. These analyses indicated that the major source of variability observed in Figures 6.5.1 and 6.5.2 was the nonlinear parameter k'_2. Evidence of this observation is included in Figure 6.5.3 where a subset of the database with $0 < k'_2 < 1$ was optimized separately. The estimated target LWD field modulus is almost perfectly correlated to the representative laboratory MR modulus provided θ and t_{oct} of 15.0 psi and 4.2 psi are used.

To establish a methodology for estimating the target field LWD modulus from the nonlinear parameters k'_1 through k'_3 from laboratory MR tests, thirty new databases were developed following the procedure described above. A constant value of k'_2 (ranging between 0 and 3 in increments of 0.1) was selected for each database. Each database contained 1000 cases with randomized parameters k'_1 and k'_3. The optimization algorithm discussed above was then applied to each database to obtain the most appropriate θ and t_{oct} to be used in Equation 6.2.1.

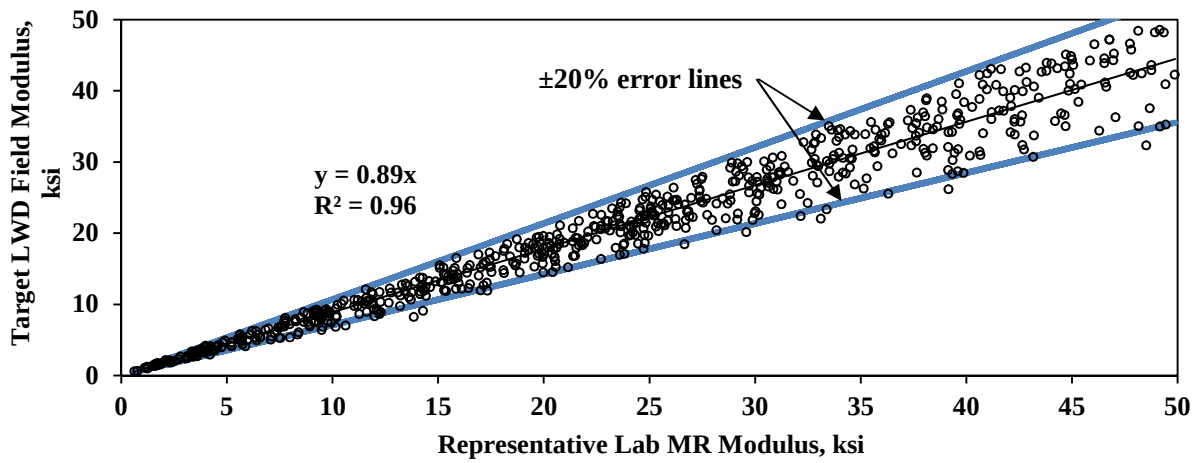

Figure 6.5.1 - Comparison of Representative Laboratory MR Modulus with corresponding Target LWD Field Modulus for Random Values of *k'* Parameters

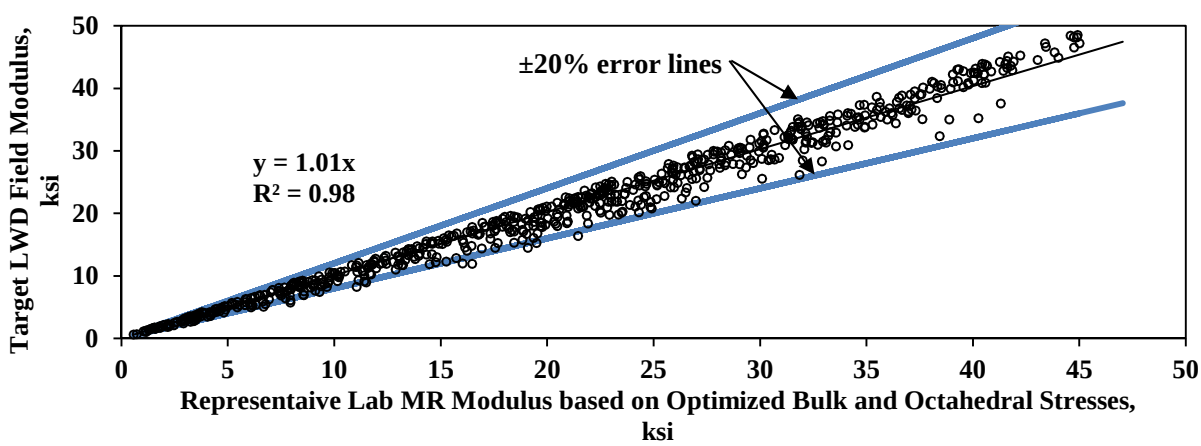

Figure 6.5.2 - Comparison of Representative Laboratory MR Modulus with corresponding Target LWD Field Modulus for Random Values of *k'* Parameters with Optimized Octahedral and Bulk Stresses in Equation 6.2.1

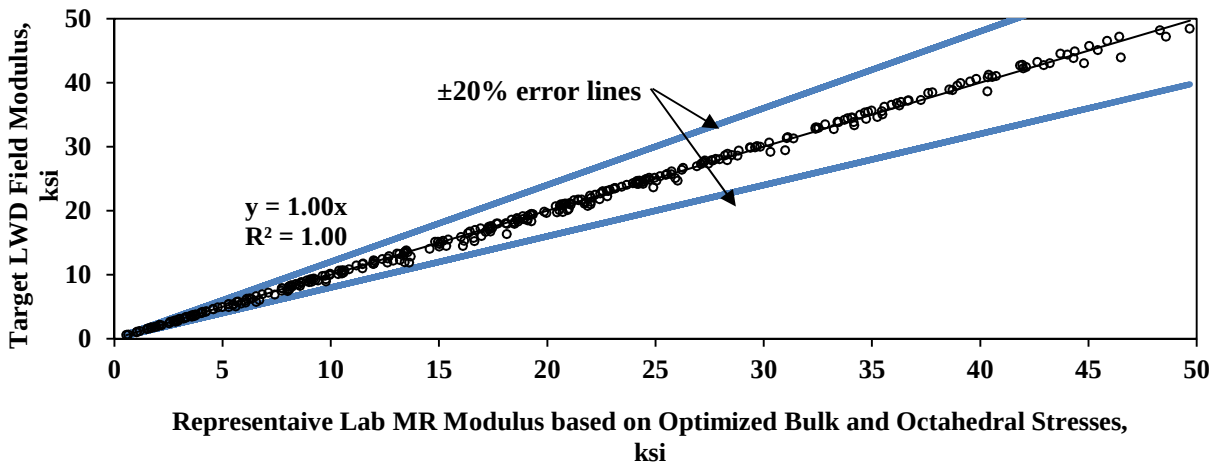

Figure 6.5.3 - Comparison of Representative Laboratory MR Modulus with corresponding Target LWD Field Modulus for Random Values of *k'* Parameters with Optimized Octahedral and Bulk Stresses in Equation 6.2.1 ($0<k'_2<1$)

The variations in the parameters θ and t_{oct} with parameter k'_2 are shown in Figure 6.5.4. These relationships demonstrate that as the k'_2 increases (i.e., the geomaterial becomes more granular and exhibits more stress hardening behavior), smaller bulk stress q and octahedral stress t_{oct} values should be considered in estimating the target modulus from Equation 6.2.1. In practical terms, the target LWD field modulus can be obtained through the following steps:

1. Obtain parameters k'_1 through k'_3 for a given material.
2. Estimate the most appropriate θ and t_{oct} from the following equations:

$$q = -4.27 \ln (k'_2) + 12.77 \quad (6.5.2)$$

$$t_{oct} = 1 / (0.22 + 0.052\, k'^{1.5}_2) \quad (6.5.3)$$

3. Input k'_1 through k'_3 parameters and estimated θ and t_{oct} in Equation 6.2.1.

The process discussed above is based on an applied load of 1200 lbs and a Poisson's ratio of 0.40 for a plate diameter of 8 in. Further analyses were carried out to develop relationships that are more general. The impact of the changes in Poisson's ratio on the developed relationships was minimal as long as the same Poisson's ratio was used in the numerical model and Equation 6.5.1.

The variations of optimal θ and t_{oct} with applied LWD loads of 1500 lbs and 1800 lbs are superimposed on the results from the 1200 lbs load in Figure 6.5.5. The patterns for different applied loads are quite similar. To demonstrate the impact of material nonlinearity on the results, the optimal θ and t_{oct} axes in Figure 6.5.5 can be normalized with respect to the applied surface stress by the LWD (i.e., the applied load divided by the plate area). The normalized results are shown in Figure 6.5.6. For a given k'_2, the normalized stresses for different loading conditions slightly deviate from one another. This deviation becomes more pronounced as k'_2 increases (i.e., the material exhibits more stress hardening). However, in almost all cases the differences are rather small. For practical implementation, general relationships between the stresses and k'_2 can be described in the following forms:

$$\theta = \sigma\ [-0.193 \ln(k\ \ ) + 0.513] \quad (6.5.4)$$

$$\tau\ \ = \sigma\ \frac{\quad}{\quad} \quad (6.5.5)$$

where s_0 = surface stress applied by the LWD.

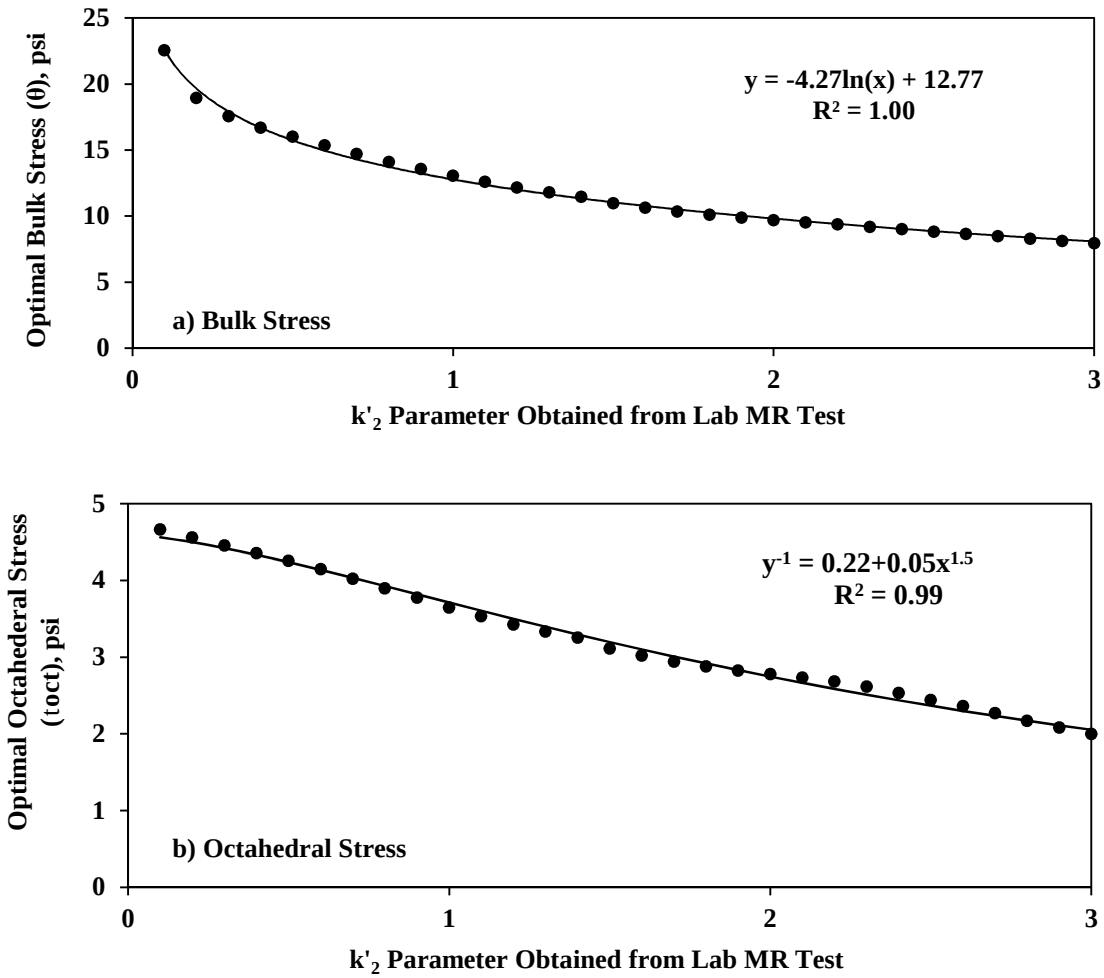

Figure 6.5.4 - Variations of Bulk and Octahedral Stresses with Laboratory MR Parameter k'_2 due a 1200 lb Load Applied by an LWD

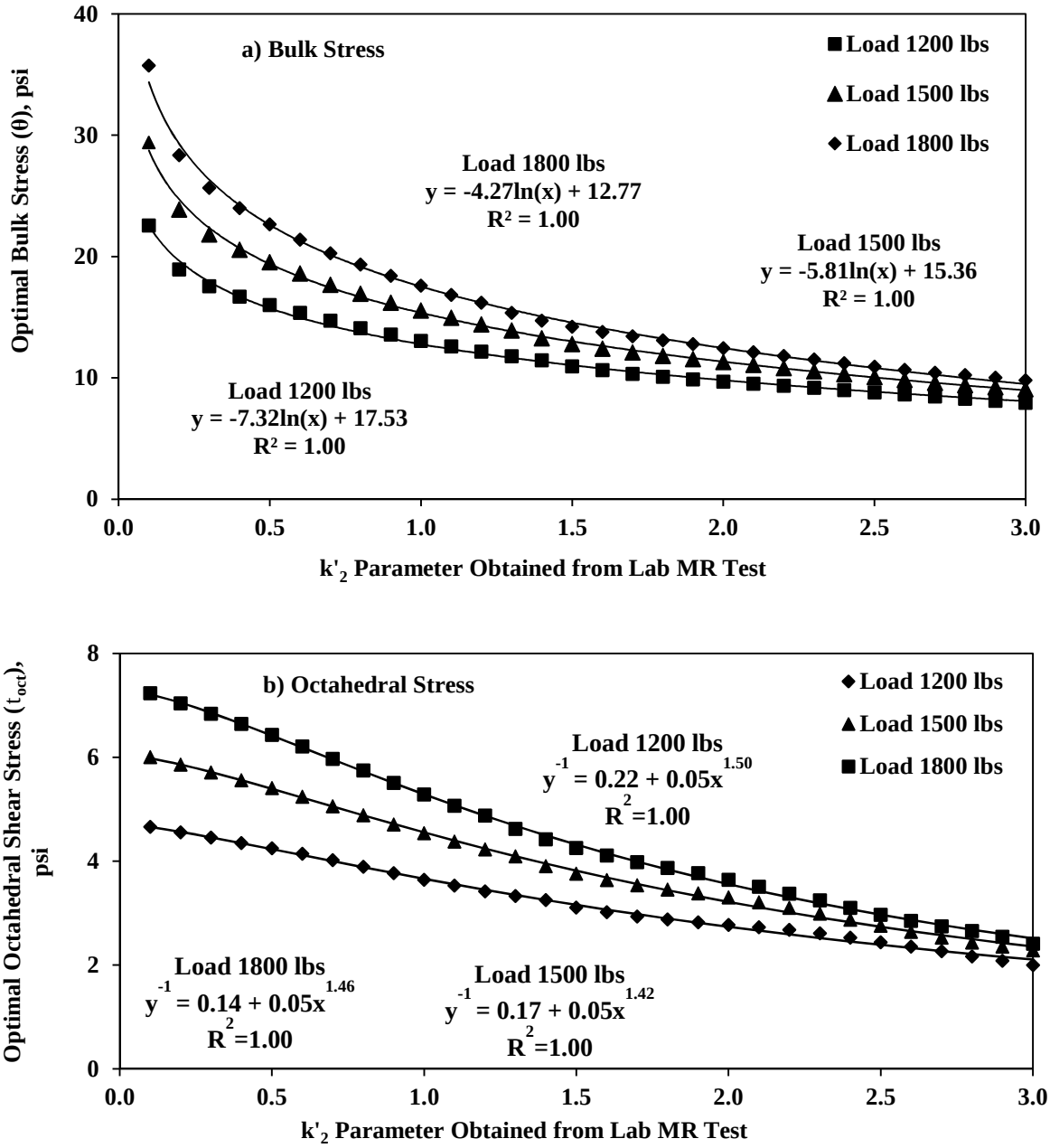

Figure 6.5.5 - Variations of Bulk and Octahedral Shear Stresses with Laboratory MR Parameter *k'₂* due to Different Loading Condition Applied by an LWD

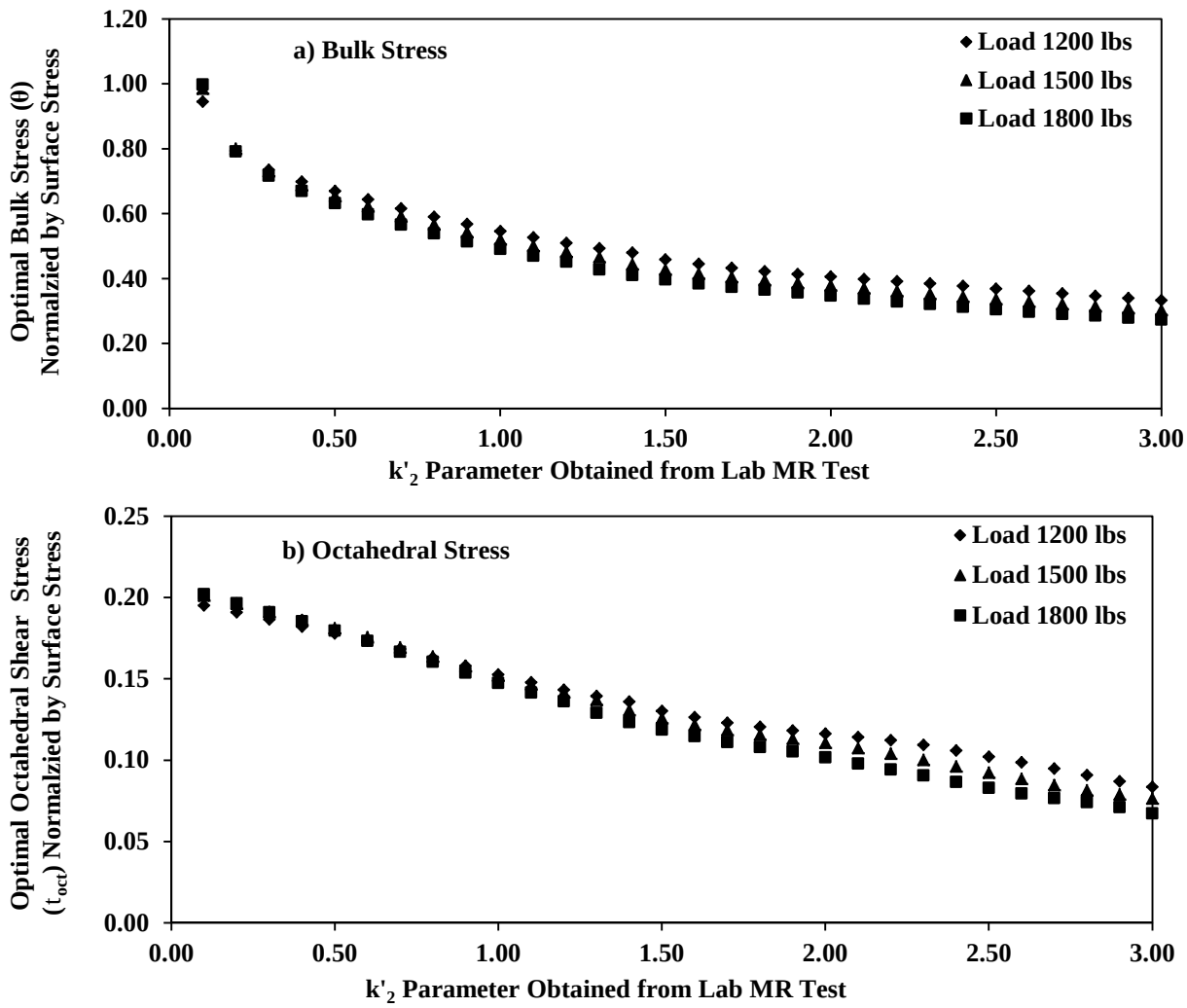

Figure 6.5.6 - Relationship between k'_2 Parameter and Normalized Bulk and Octahedral Shear Stresses due to Different Loading Conditions Applied by LWD

To evaluate the predictive power of the proposed model, another dataset of 500 uniformly distributed random cases was generated. Equations 6.5.4 and 6.5.5 were used to estimate the bulk and octahedral shear stresses based on k'_2, surface stresses, and the target field moduli from Equation 6.5.1. The estimated field target moduli using both the MEPDG representative stress values (θ = 12.4 psi and t_{oct} = 3 psi) and based on predicted values of θ and t_{oct} from Equations 6.5.4 and 6.5.5 are compared in Figure 6.5.7. The new model improves the estimation of the field target modulus significantly.

Equations 6.5.4 and 6.5.5 were developed based on 8 in. plate diameter. The same process was repeated with 4 in. and 12 in. plate diameters to develop a more general relationship. The results of such analyses are summarized in the form of:

$$q = s_0\,[(0.001D^2 - 0.012D - 0.169)\ln(k'_2) + (0.04D + 0.2)] \quad (6.5.6)$$

$$t = s_0 \exp[(-0.01D - 1.47) + (k'_2)(-0.006D^2 + 0.066D - 1.269)] \quad (6.5.7)$$

where D = plate diameter (in.) and s_0 = surface stress (psi). In order to further validate the general proposed model, another 500 uniformly distributed random combinations of k' parameters, plate diameter and load magnitude were generated to validate the predictive power of Equations 6.5.6 and 6.5.7. As shown in Figure 6.5.8, the proposed relationships seem to produce reasonable results.

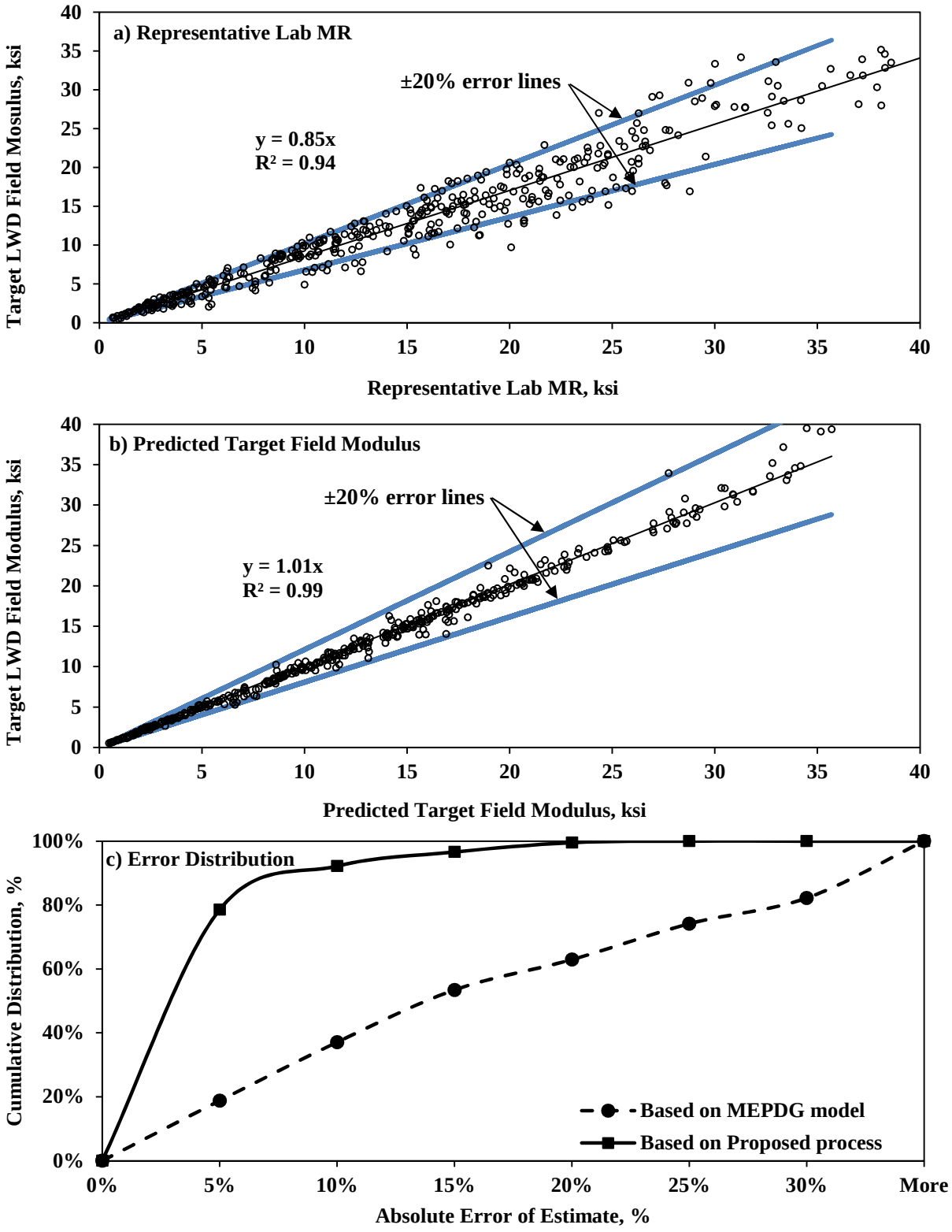

Figure 6.5.7 - Evaluation of Predictive Power of Proposed Process

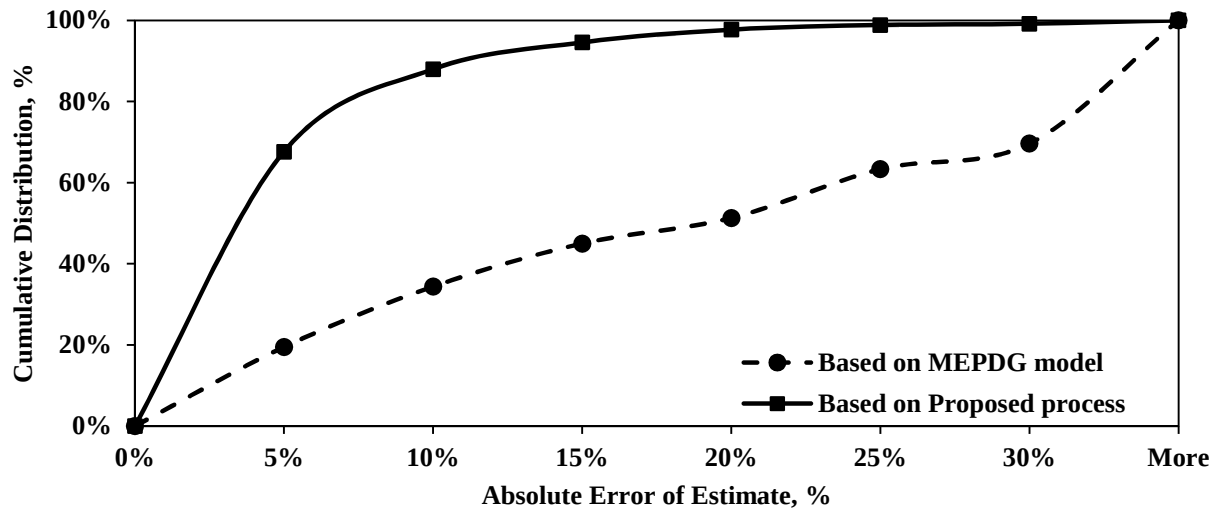

Figure 6.5.8 - Evaluation of Predictive Power of Generalized Proposed Process

In many cases, the compacted geomaterials may consist of more than one layer. An attempt was made to develop simplified models to predict the target modulus for a two-layer pavement system consisting of a base and a subgrade layer. A database of 5000 random combinations of base and subgrade layers with different nonlinear laboratory MR parameters (k'_1, k'_2, and k'_3), random base thickness, and random Poisson's ratios for base and subgrade layers was generated. The response algorithm was then utilized to determine the surface deflection and the target field LWD modulus (using Equation 6.5.1) of the layered system. Given the nature of the problem, the magnitude of applied load, base thickness, and Poisson's ratios for both layers were also assumed as random variables. The minimum and maximum ranges of the variables are summarized in Table 6.5.1.

Table 6.5.1 - Minimum and Maximum Values of Variables used in Numerical Analysis of Two-Layer Pavement Systems

Parameter	k_{1Base}	k_{2Base}	k_{3Base}	$k_{1Subgrade}$	$k_{2Subgrade}$	$k_{3Subgrade}$	Poisson's Ratio	Base Thickness	Applied Load
Minimum	50	0.0	-4.0	50	0.0	-4.0	0.30	6	600
Maximum	3000	3.0	0.0	3000	3.0	0.0	0.45	12	2400

Significant efforts aiming at developing straightforward statistical models similar to those for one-layer cases were not successful. As such, an attempt was made to train an artificial neural network (ANN) for this purpose. The neural network architecture for the developed model is depicted in Figure 6.5.9. The summary of neural network properties is included in Table 6.5.2. The number of input parameters is ten consisting of six k' parameters corresponding to the base and subgrade laboratory MR nonlinear parameters, two Poisson's ratios, base thickness, and applied load. The only output parameter is the target LWD field modulus. In this study, 70% of the data were used for training, 15% for validation and 15% for testing the appropriateness of models. A back-propagation algorithm (McClelland and Rumelhart, 1986) with a Levenberg-Marquardt nonlinear optimization was used in training. In the ANN field, this algorithm is suitable for training small- and medium-sized databases.

The performance of the ANN model in terms of absolute errors of estimation between the calculated and predicted moduli is shown in Figure 6.5.10. In 85% of the testing cases not used in training, the error of estimate is less than 10%. This shows that the ANN model can predict the values of field target modulus from the input parameters well.

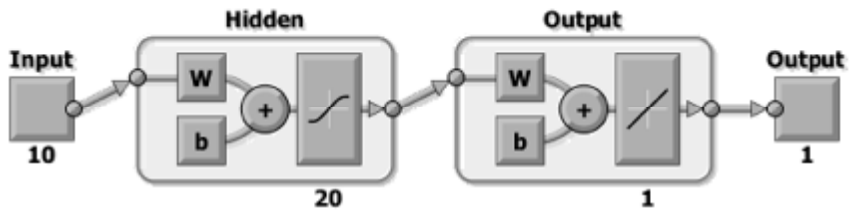

Figure 6.5.9 - ANN Architecture Used

Table 6.5.2 - Summary of Neural Network Properties

Number of input parameters	10
Number of hidden layers	1
Number of neurons in hidden layer	20
Inputs pre-processing function	Sigmoid function
Outputs post-processing function	Linear function
Neural network type	Feed-forward
Network training algorithm	Levenberg-Marquardt backpropagation
Number of epochs (maximum number of training iterations before training is stopped)	83
Training ratio	70%
Validation ratio	15%
Testing ratio	15%

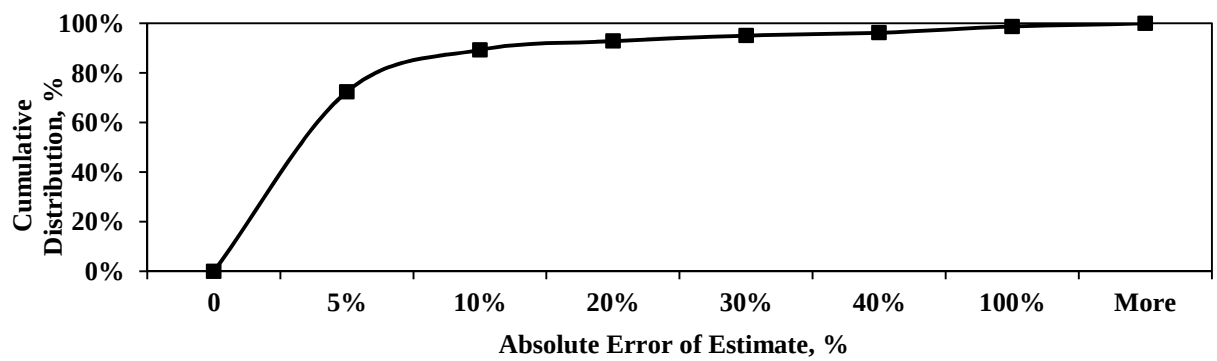

Figure 6.5.10 - Histogram of Absolute Errors for Predicted Target Moduli from ANN Model

6.6 Establishing Target Modulus for Geogauge

The Geogauge modulus, E_{Geo}, is calculated from the following equation:

$$E_{Geo} = P\,(1 - \upsilon^2) / (1.77\,R\delta) \qquad (6.6.1)$$

where: P = Geogauge weight (22 lb), υ = Poisson's ratio, R = outside radius of the ring foot (2.25 in.), δ = surface deflection (mils), and E = modulus (ksi). The multi-layered response algorithm, as discussed earlier in this chapter, was used to establish the Geogauge target modulus.

The moduli estimated from the numerical analyses for a one-layer pavement system are compared in Figure 6.6.1 with those obtained using the representative laboratory MR moduli with the recommended values of q and t_{oct}. These two moduli are poorly correlated. A correlation analysis revealed that the target Geogauge

modulus is strongly related to the laboratory k'_1 parameter, and marginally related to k'_2 parameter. The variation in the target Geogauge modulus with k'_1 is shown in Figure 6.6.2.

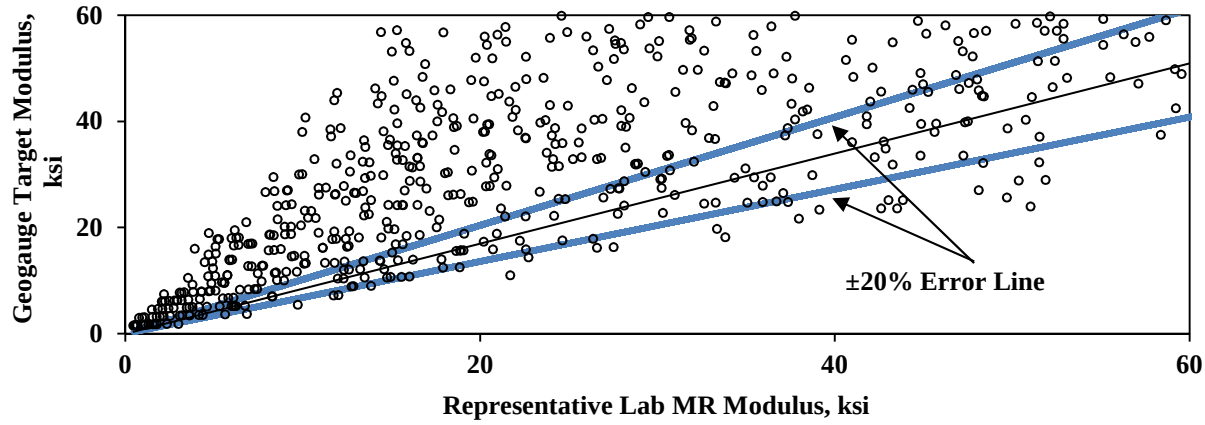

Figure 6.6.1 - Correlation between Geogauge Target Modulus and Representative Laboratory MR Modulus for a One-Layer System

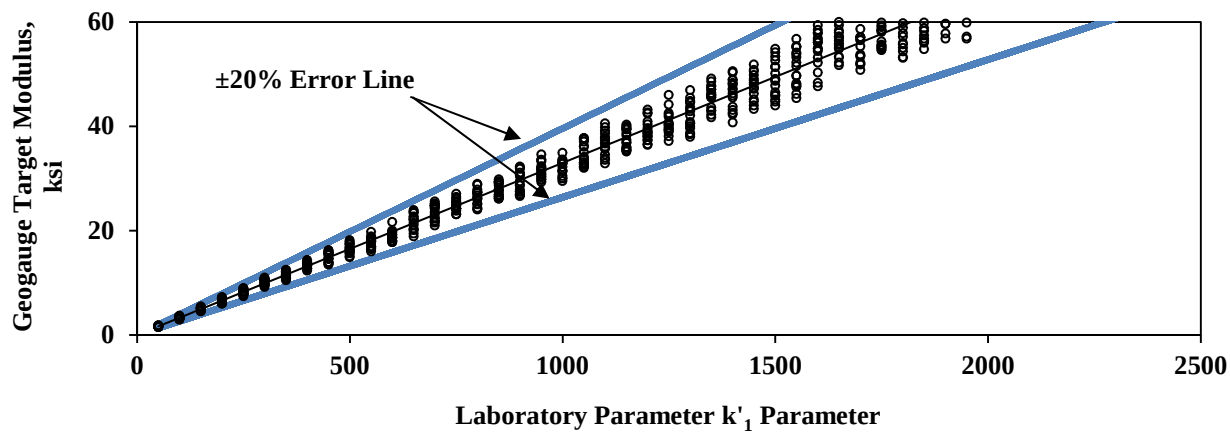

Figure 6.6.2 - Correlation between Geogauge Target Modulus and Parameter k'_1 for a One-Layer System

The proposed relationship for estimating the target Geogauge modulus, $E_{T\text{-}Geo}$ (ksi), for a uniform material is in the form of

$$E_{T\text{-}Geo} = k'_1 (0.002k'_2 + 0.03) \qquad (6.6.2)$$

The distribution of estimation errors for target moduli estimated from Equation 6.6.2 is shown in Figure 6.6.3. As compared to representative laboratory modulus, this equation more accurately estimates the target moduli.

The process was then expanded to a two-layer pavement system. The optimal relationship proposed to estimate the Geogauge target modulus for a two-layer pavement system is in the form of Equation 6.6.3:

$$E_{T\text{-}Geo} = [(0.0093h_1\text{-}0.163)\, k'_{1\text{-}SG} - (0.0991h_1\text{-}1.642]\, (k'_{1\text{-}Base})^{[(-0.0028h1\ +0.1339)\ k'1\text{-}SG\ +\ (0.0454h1\text{-}0.4121)]} \qquad (6.6.3)$$

where h_1 = thickness of top layer (in.).

Figure 6.6.4 shows the predictive power of the proposed equation. The estimated moduli are within 30% of the calculated ones as shown in Figure 6.6.5. An ANN model was also developed as discussed for the LWD. As shown in Figure 6.6.5, the estimation error of the ANN model is less than 10% with 85% confidence level.

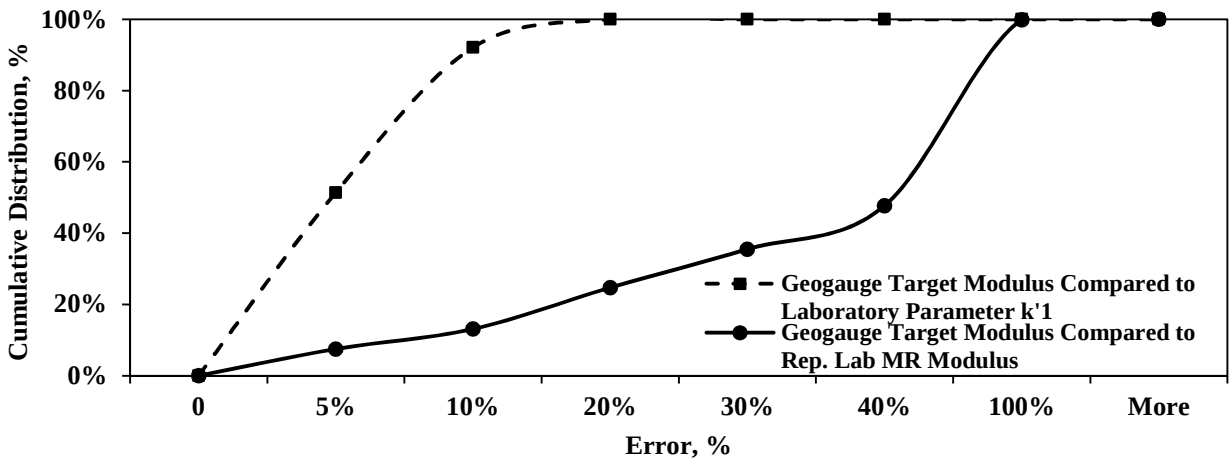

Figure 6.6.3 - Distributions of Estimation Error of Geogauge Target Modulus (for a One-Layer Pavement System)

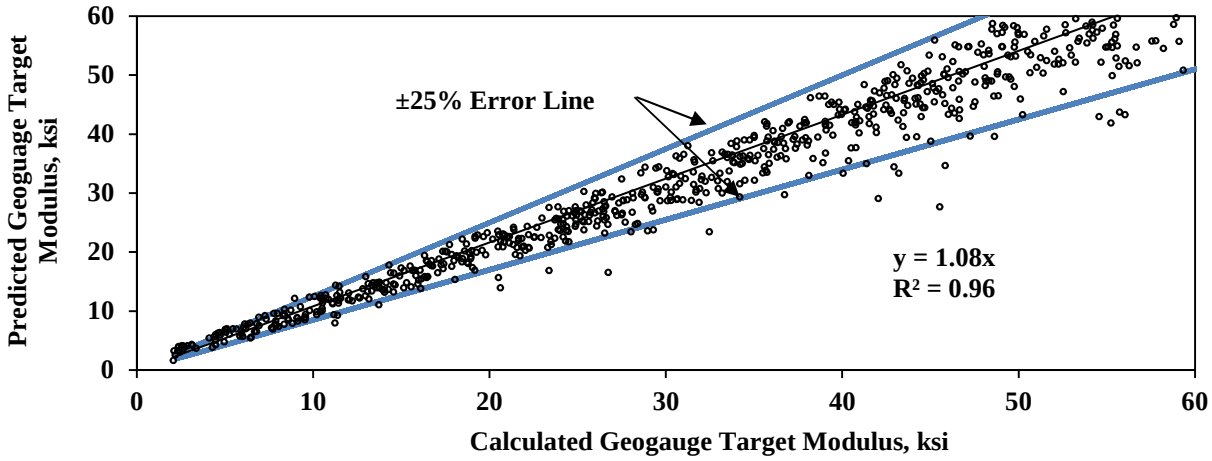

Figure 6.6.4 - Evaluation of Predictive Power of Equation 6.6.3 for a Two-Layer Pavement System

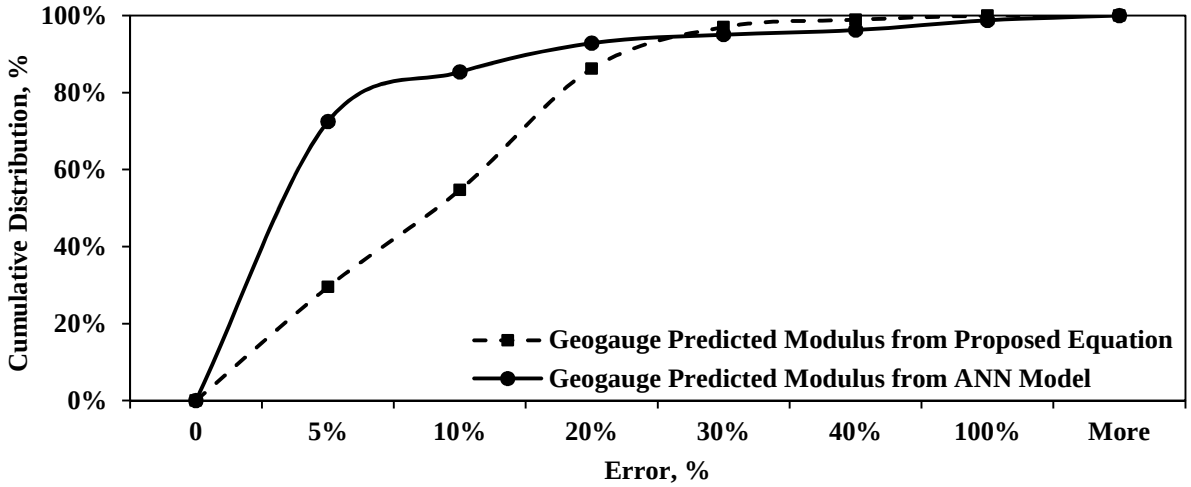

Figure 6.6.5 - Distributions of Estimation Error of Geogauge Target Modulus for a Two-Layer Pavement System

6.7 Case Studies

The target moduli for all materials used in the small-scale tests are shown in Figure 6.7.1. As the compaction moisture content decreases, the target modulus increases. Since the thickness of the base is considered as 6 in., the LWD target moduli are mostly impacted by the modulus parameters of the subgrade layer. As reflected in Figure 6.7.2, the change in the target modulus is proportional to the power of 0.41 of the representative MR modulus (replacing q = 12.4 psi and t_{oct} = 3 psi in Eq. 3.2.1) of the base.

Geogauge measures the deflection of the system (similar to LWD) but at small strains. Figure 6.7.3 shows the target moduli for the Geogauge for all small-scale tests. As anticipated, for each material and moisture condition, the Geogauge target modulus is normally greater than the LWD one. The trends in Figure 6.7.3 are similar to those for LWD. The relationship between the actual base modulus and target modulus is shown in Figure 6.7.4. The Geogauge target moduli are 1.74 times greater than the LWD target moduli as shown in Figure 6.7.5. This occurs because of significant differences in the states of stress and the loading pattern.

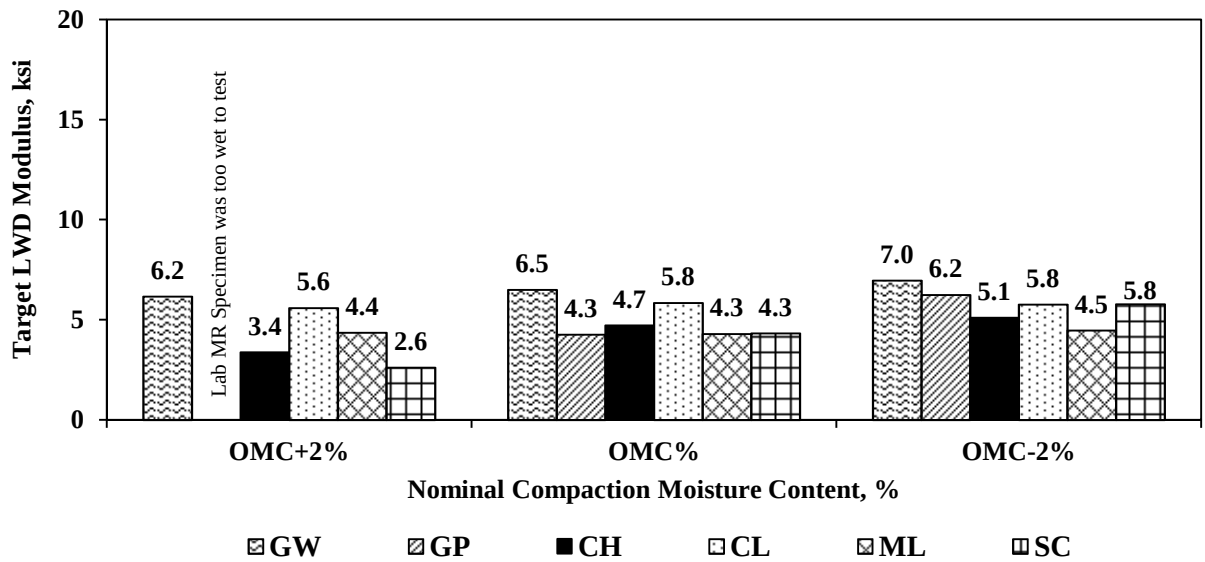

Figure 6.7.1 - Estimated Target Moduli for LWD based on Laboratory MR Test Results (6 in. Top Layer)

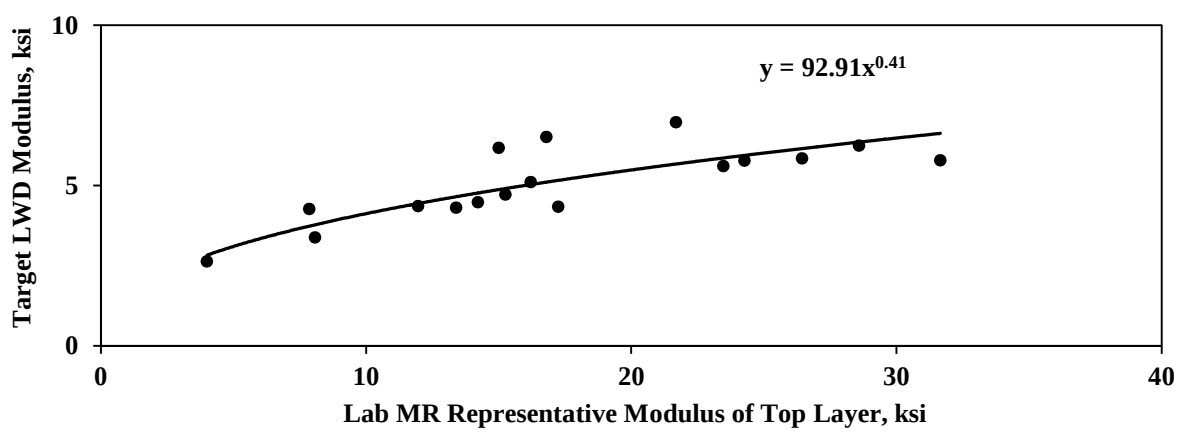

Figure 6.7.2 - Relationship between Base Representative Laboratory Modulus and Field Target Modulus for LWD (6 in. Top Layer)

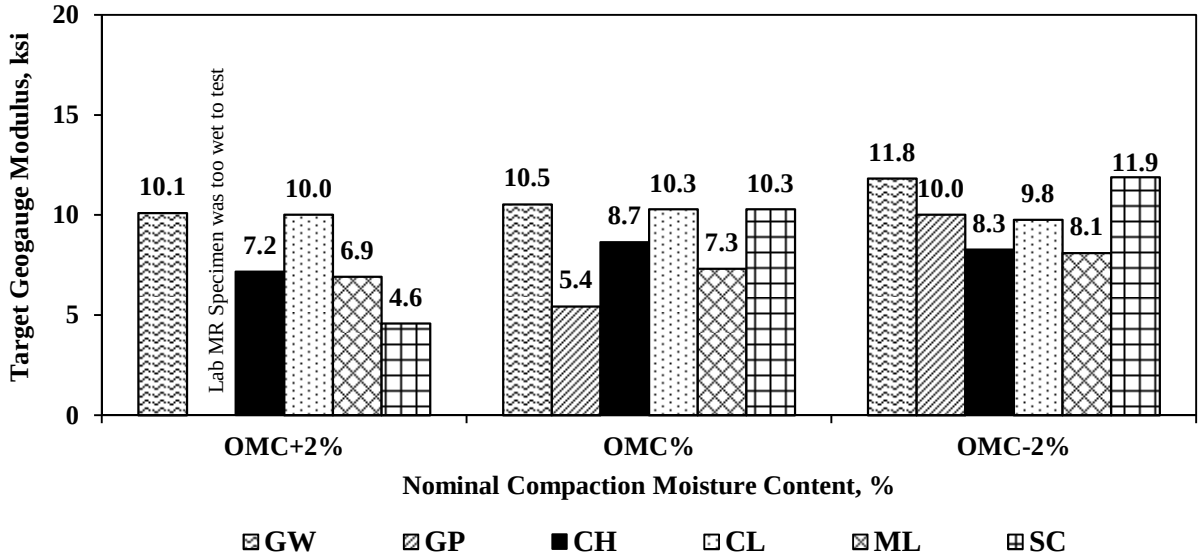

Figure 6.7.3 - Estimated Target Moduli for Geogauge based on Laboratory MR Test Results

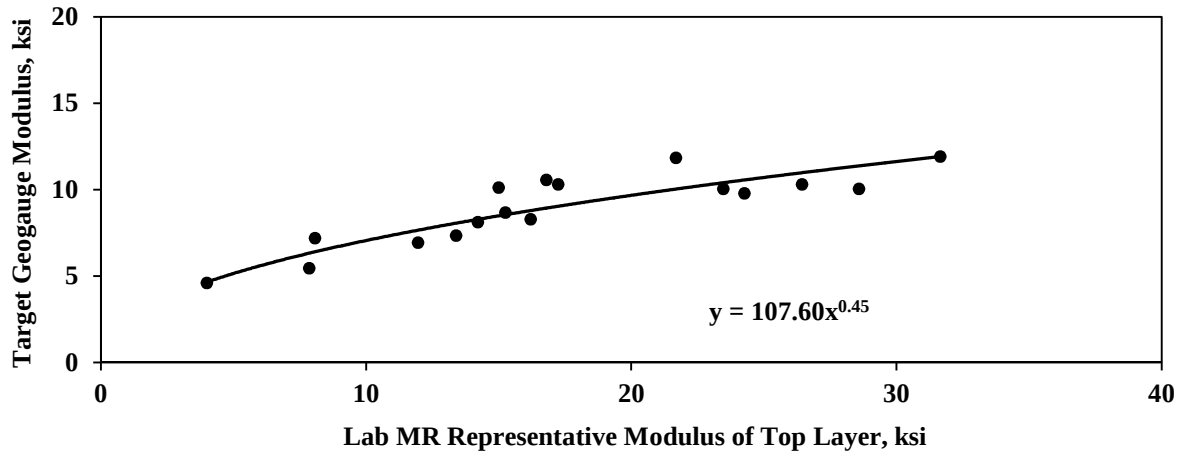

Figure 6.7.4 - Relationship between Base Modulus and Field Target Modulus for Geogauge

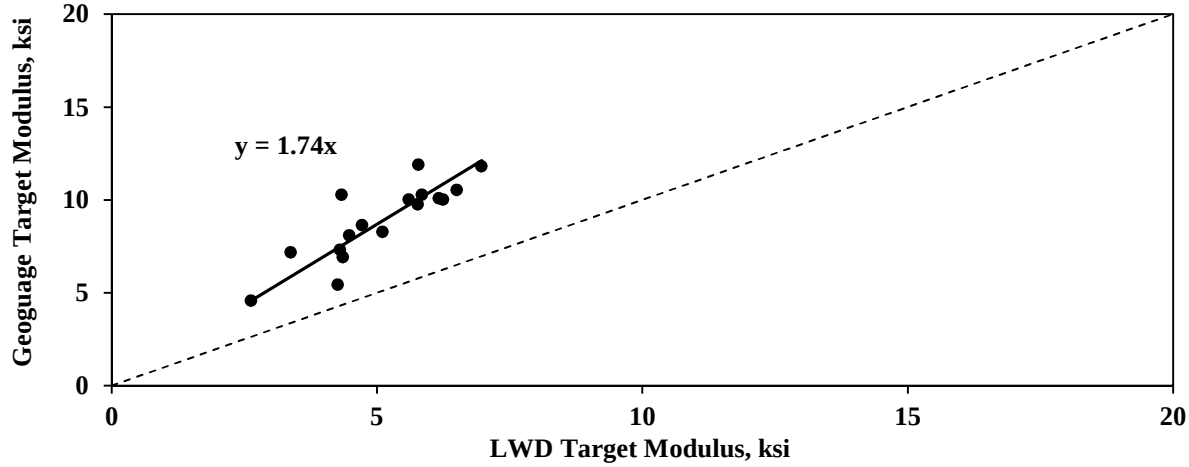

Figure 6.7.5 - Comparison of LWD and Geogauge Target Moduli

Dynamic Cone Penetrometer (DCP) measures the rate of penetration, which is related to the strength of a layer. The rate of penetration is then converted to modulus through established empirical relationships. Since the DCP provides a layer-specific modulus, the target moduli can be simply related to the modulus parameters measured in the laboratory. To that end, the representative laboratory MR moduli provided in Table 3.2.2 (Chapter 3) were used. Figure 6.7.6 is a comparison of the DCP target moduli and moduli estimated from the measurements made during the small-scale testing. Once again, the trends are appropriate but the target moduli based on laboratory results seems to require a transfer function. Fortunately, a number of studies have proposed such transfer functions.

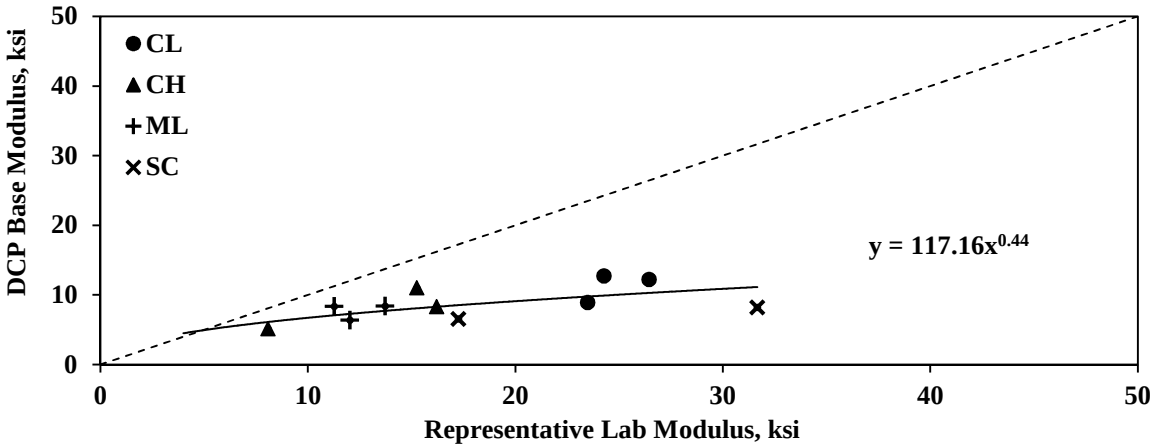

Figure 6.7.6 - Comparison of Target and Field Moduli for DCP (Subgrade Materials)

The same study was repeated but with 12 in.-thick layers of different geomaterials. Target LWD moduli are illustrated in Figure 6.7.7. The LWD target moduli for fine-grained soils (CL, CH, ML and SC) are on average 73% and for coarse-grained materials (GW and GP) 55% greater than those for a 6-in.-thick layers. The variation in the target LWD modulus with representative laboratory modulus of the top, as shown in Figure 6.7.8, yield a power of 0.61 (as compared to the power of 0.41 for 6 in base layer).

The laboratory representative moduli of the top layers were also compared to the Geogauge target moduli for a 12 in. thick top layer in Figure 6.7.9. In this case, the target Geogauge modulus is proportional to the laboratory representative MR with a power of 0.62 (as compared to the power of 0.45 for a 6 in. top layer).

These trends indicate that the thicker the top layer is, the more sensitive the LWD and Geogauge results will be to the stiffness of the top layer. These case studies also show that the depths of penetration of these devices are greater than 12 in.

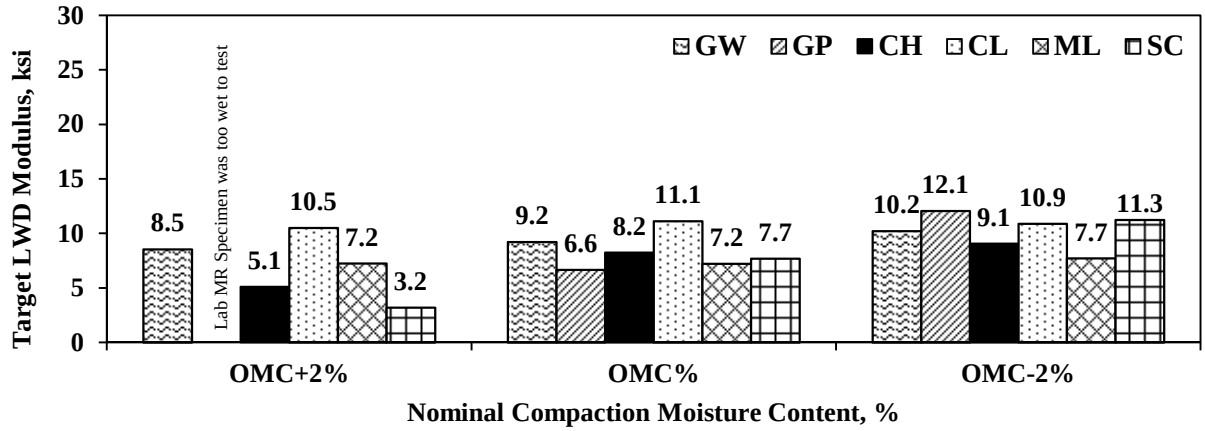

Figure 6.7.7 - Relationship between Base Representative Laboratory Modulus and Field Target Modulus for LWD (12 in. Top Layer)

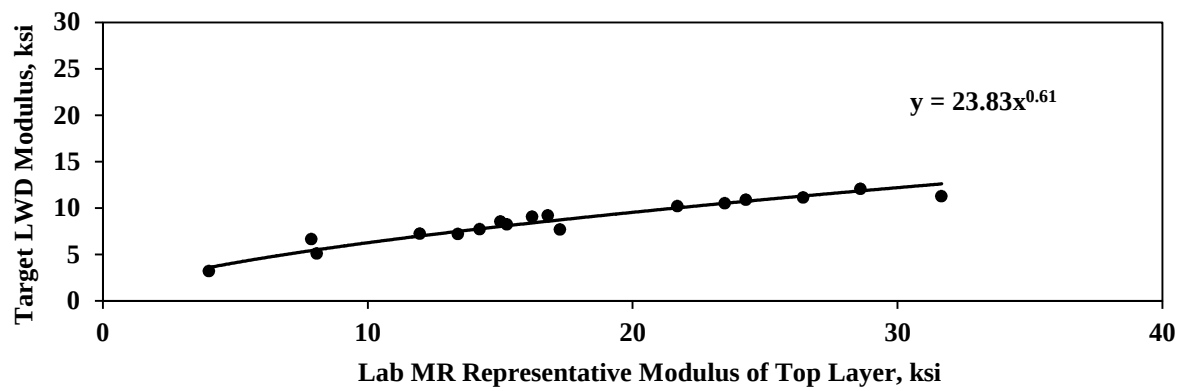

Figure 6.7.8 - Relationship between Base Representative Laboratory Modulus and Field Target Modulus for LWD (12 in. Top Layer)

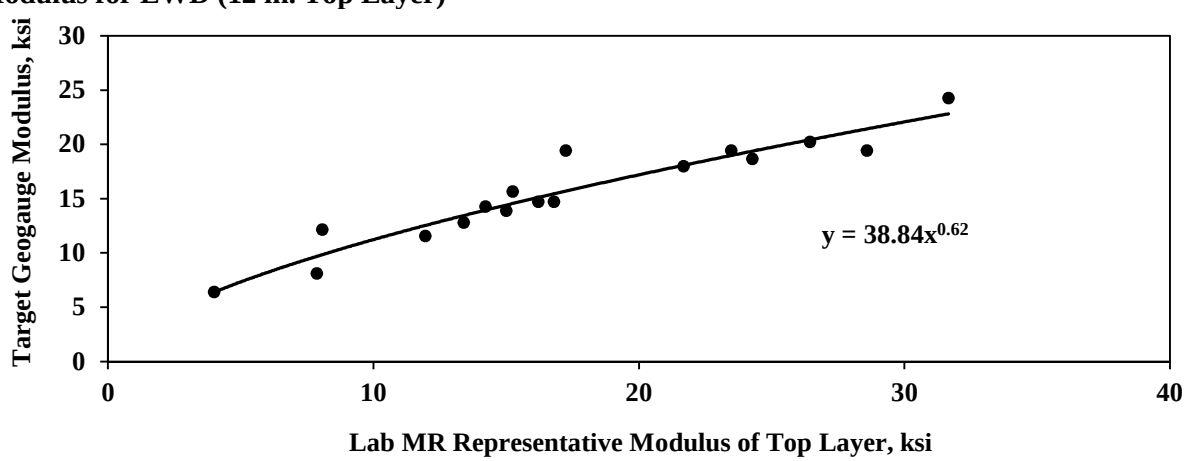

Figure 6.7.9 - Relationship between Base Representative Laboratory Modulus and Field Target Modulus for Geogauge (12 in. Top Layer)

CHAPTER 7 - FINDINGS FROM FIELD EVALUATION

7.1 Introduction

The processes and relationships developed in Chapters 3 through 6 were applied to a site. Field evaluations were carried out at several test sections constructed at the Louisiana Transportation Research Center (LTRC) in Port Allen, Louisiana. Those results are presented in this chapter.

7.2 Field Testing Layouts

Figure 7.2.1 illustrates the testing section in LTRC site. Seven test sections (four sections for subgrade and three for base layer) were constructed. Test sections were built with full-scale construction equipment to simulate normal highway construction as per the Louisiana Department of Transportation and Development (LADOTD) specifications.

Figure 7.2.1 – Location of Field Evaluation Site

A detailed description of each test section is included in Appendix G. Figure 7.2.2 summarizes the location of test sections at the LTRC site. Before placing the subgrade layer, the top layer of embankment soil was removed and the embankment layer was prepared to the proper grade. The subgrade was placed at different moisture contents (dry of OMC, OMC, wet of OMC, and saturated) with a 12 in. thickness. The base layer (8 in. thick) was placed after the reworking and compacting the subgrade layer nominally to OMC for all three sections. The base layer was prepared and compacted at three different moisture levels (dry of OMC, OMC, and wet of OMC). The site was divided into two zones (Zone A and Zone B) and several subsections as illustrated in Figure 7.2.3. Test spots were defined on a numeric basis as illustrated in Figure 7.2.3.

A detailed explanation of test protocols for this site is included in Appendix G. The following tests were performed on compacted layers (subgrade and base):

- ***Geogauge,*** triplicate testing at each station.
- ***Soil Density Gauge (SDG),*** triplicate testing at each station.
- ***PSPA,*** three times at each station (the device was slightly moved and rotated between readings)
- ***Zorn and Dynatest LWDs,*** according to ASTM specifications (three seating drops followed by three reading drops).
- ***Nuclear Density Gauge (NDG),*** once at each subsection (for the OMC section) and three times at each subsection (for the dry and wet of OMC sections).

- ***Oven Moisture Content,*** random soil samples were extracted at different spots from the compacted layer to determine the laboratory oven-dry moisture content.

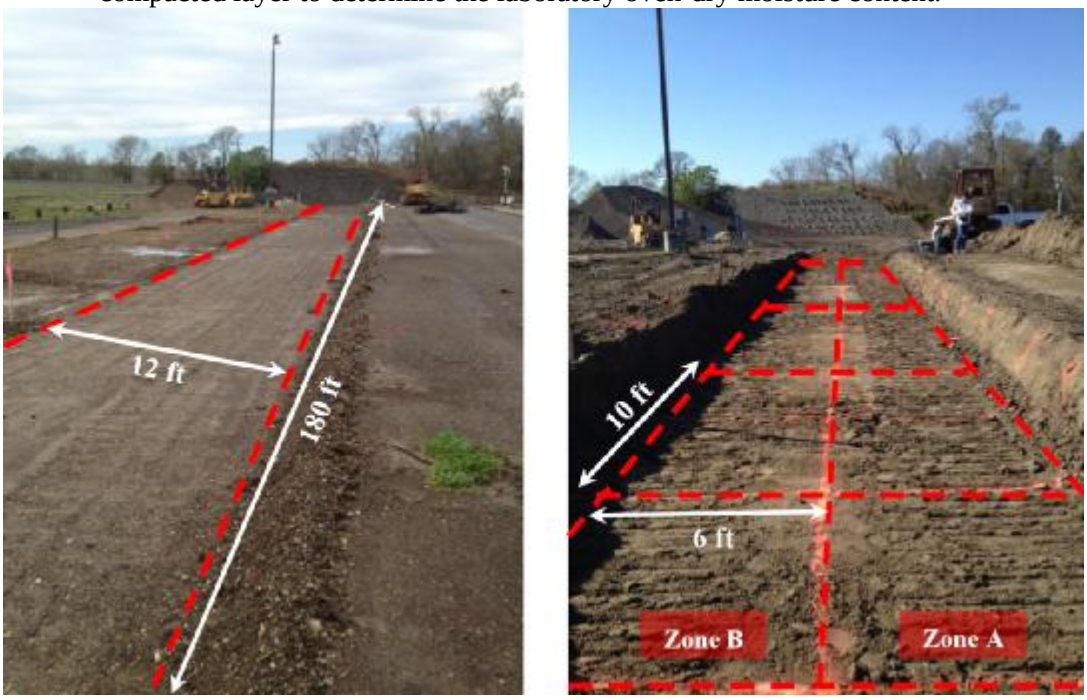

Figure 7.2.2 – Illustration of Field Evaluation Section

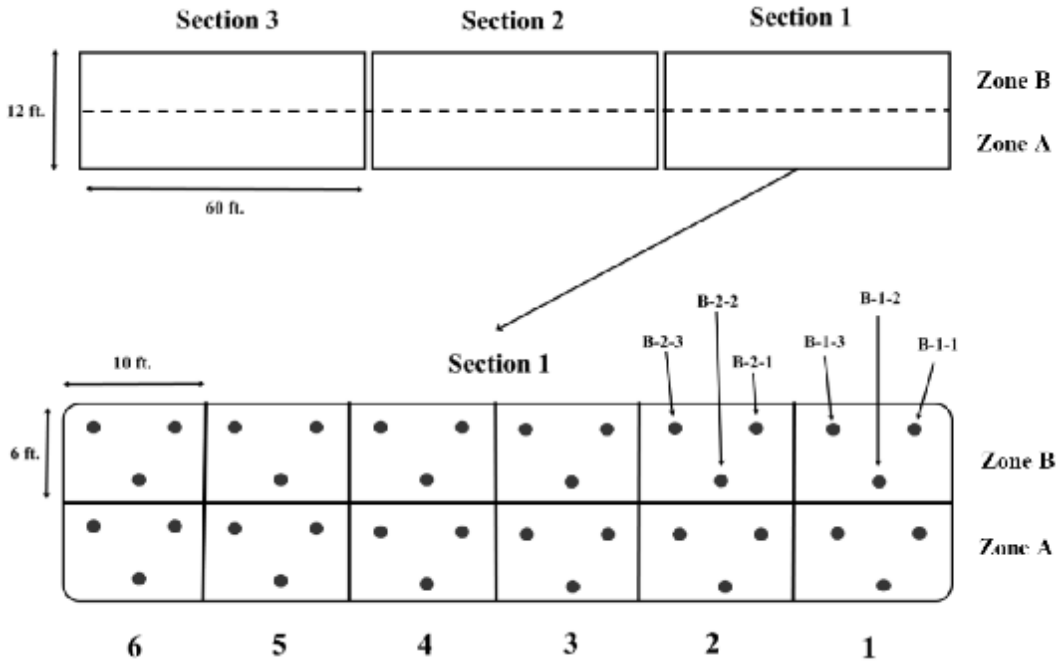

Figure 7.2.3 - Schematic of Test Stations on LTRC Section

7.3 Laboratory Results

The index properties of the geomaterials are summarized in Table 7.3.1 and the gradation curves are depicted in Figure 7.3.1. The optimum moisture contents and maximum dry unit weights obtained from the standard Proctor tests for the embankment and subgrade and modified Proctor tests for the base are

reported in Table 7.3.1 as well. The base material is the same as the GW base used in the laboratory studies in Chapter 3 (see Table 3.2.2).

Table 7.3.1 - Index Properties of LTRC Geomaterials

Geomaterial	Gradation %				USCS Class.	Specific Gravity	Atterberg Limits			Moisture/Density	
	Gravel	Coarse Sand	Fine Sand	Fines			LL	PL	PI	OMC*, %	MDUW**, pcf
Embankment and Subgrade	0	21	8	71	CL	2.74	37	18	19	13.8	113.3
Base	51	31	15	3	GW	2.65	Non-Plastic			8.7	129.0

*OMC = Optimum Moisture Content, **MDUW = Maximum Dry Unit Weight

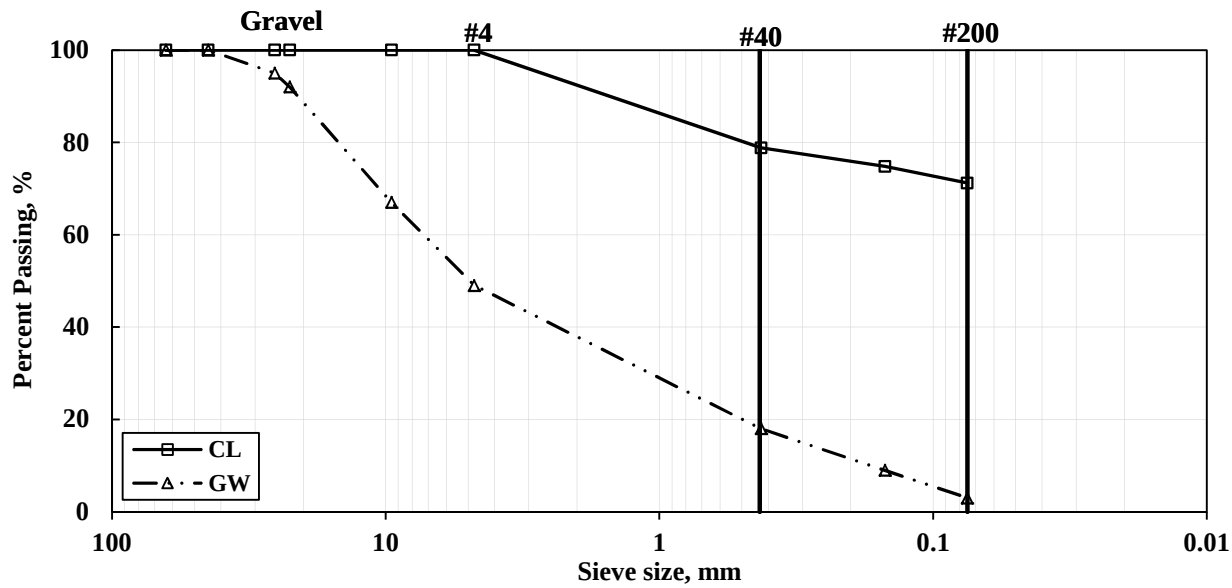

Figure 7.3.1 – Gradation Curves of LTRC Field Evaluation Geomaterials

The MR and FFRC tests were performed on laboratory specimens prepared at the OMC, dry of OMC, and wet of OMC. The results of these tests are summarized in Table 7.3.2. Figure 7.3.2 depicts the variations of the FFRC moduli and representative MR values with moisture content. Figure 7.3.3 summarizes the relationship between the laboratory representative MR and FFRC moduli for each material. For the subgrade (CL soil), the laboratory representative MR is on average 40% of the FFRC modulus while for the GW base, the laboratory representative MR is 16% greater than the FFRC moduli. As shown in Figure 7.3.3, these trends are comparable to those from laboratory studies.

7.4 Evaluation of Moisture-Density Technologies

Detailed results for devices based on the nuclear density (NDG) and the electrical impedance spectroscopy (SDG) technologies are included in Appendix G. Figure 7.4.1a compares the oven-dry field moisture contents of the base and subgrade layers with their corresponding laboratory OMCs. Figure 7.4.1b compares the NDG field dry densities with laboratory Maximum Dry Density (MDD) for both base and subgrade geomaterials. All test sections except for the saturated subgrade section pass the 95% MDD criterion for dry density.

Table 7.3.2 – Laboratory Results of MR and FFRC Tests of LTRC Geomaterials

Geomaterial	Target Moisture Content	Actual Moisture Content, %	Dry Density, pcf	FFRC Modulus, ksi	Nonlinear Parameters			Representative MR, ksi*
					k'_1	k'_2	k'_3	
Subgrade (CL)	0.8 OMC	10.9	111.5	46	1026	0.28	-0.05	18
	0.9 OMC	12.6	113.3	43	1231	0.19	-0.26	19
	1.0 OMC	14.4	113.4	39	672	0.23	-0.05	11
	1.1 OMC	15.2	112.5	21	908	0.44	-1.48	13
	1.2 OMC	16.7	112.8	7	98	1.53	-2.78	2
	1.4 OMC	19.0	110.7	2	76	0.97	-3.00	1
Base (GW)	0.8 OMC	6.5	125.6	24	1087	0.53	-0.10	28
	0.9 OMC	7.7	129.6	23	952	0.70	-0.10	30
	1.0 OMC	8.5	131.0	18	897	0.50	-0.10	22
	1.1 OMC	9.9	126.4	16	618	0.52	-0.10	16
	1.2 OMC	10.4	126.1	15	480	0.61	-0.10	14

* from Eq. 3.2.1 based on τ_{oct} and θ values of 7.5 psi and 31 psi for base and 3 psi and 12.4 psi for subgrades as recommended by NCHRP Project 1-28A.

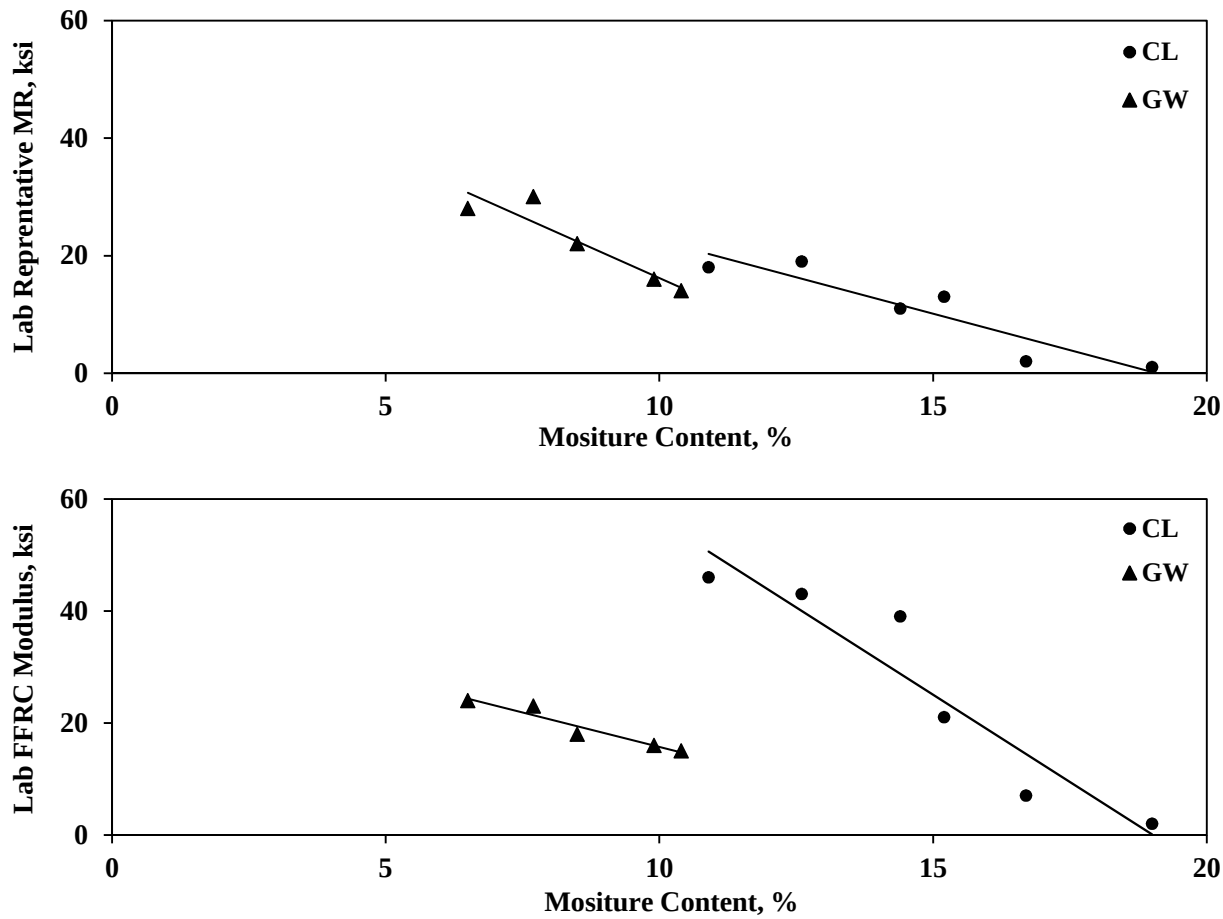

Figure 7.3.2 – Variation of Laboratory Representative MR and FFRC Moduli with Moisture Content

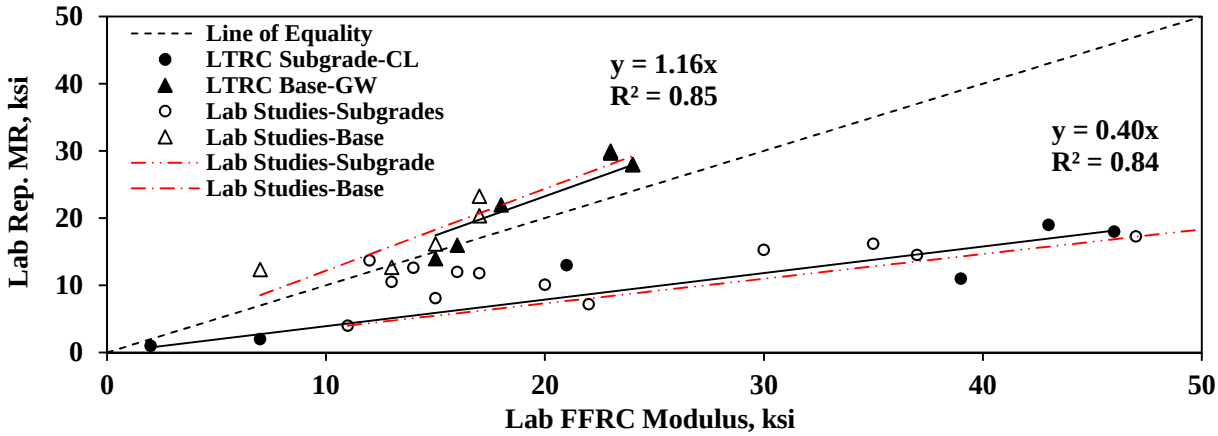

Figure 7.3.3 – Correlation of Laboratory Representative MR with Laboratory FFRC Modulus

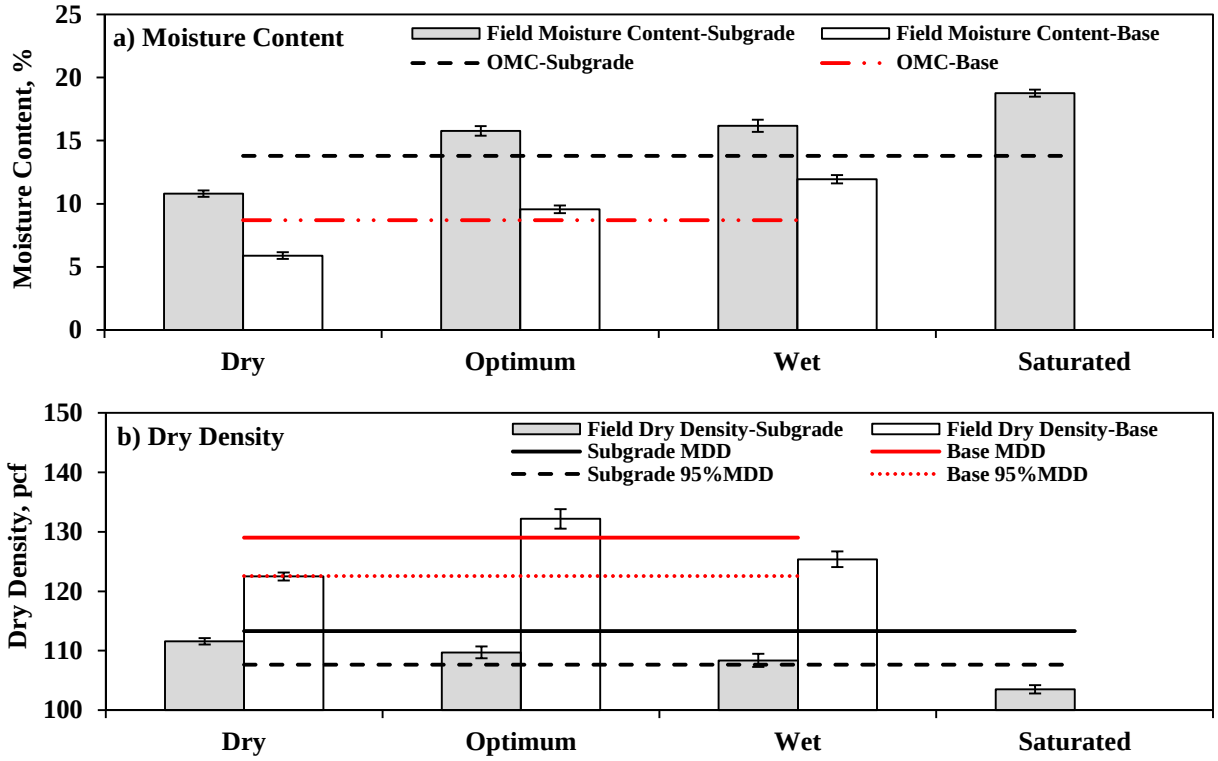

Figure 7.4.1 – Comparison of Field NDG and Laboratory Results

Figure 7.4.2a illustrates the comparison of the calibrated SDG and the oven-dry moisture contents for different materials tested. The SDG-estimated moisture contents are in most cases within 30% of the oven moisture contents but they are not very sensitive to the changes in the soil moisture contents. As reflected in Figure 7.4.2b, the NDG moisture contents exhibit better agreement with the oven-dry moisture contents. The cumulative distributions of the misestimating errors for the base and subgrade are shown in Figure 7.4.2c from the SDG and NDG. The maximum absolute error of estimate for the SDG readings is 47% with an average of 11%. The NDG readings exhibit less than 13% absolute error (with an average of 5%).

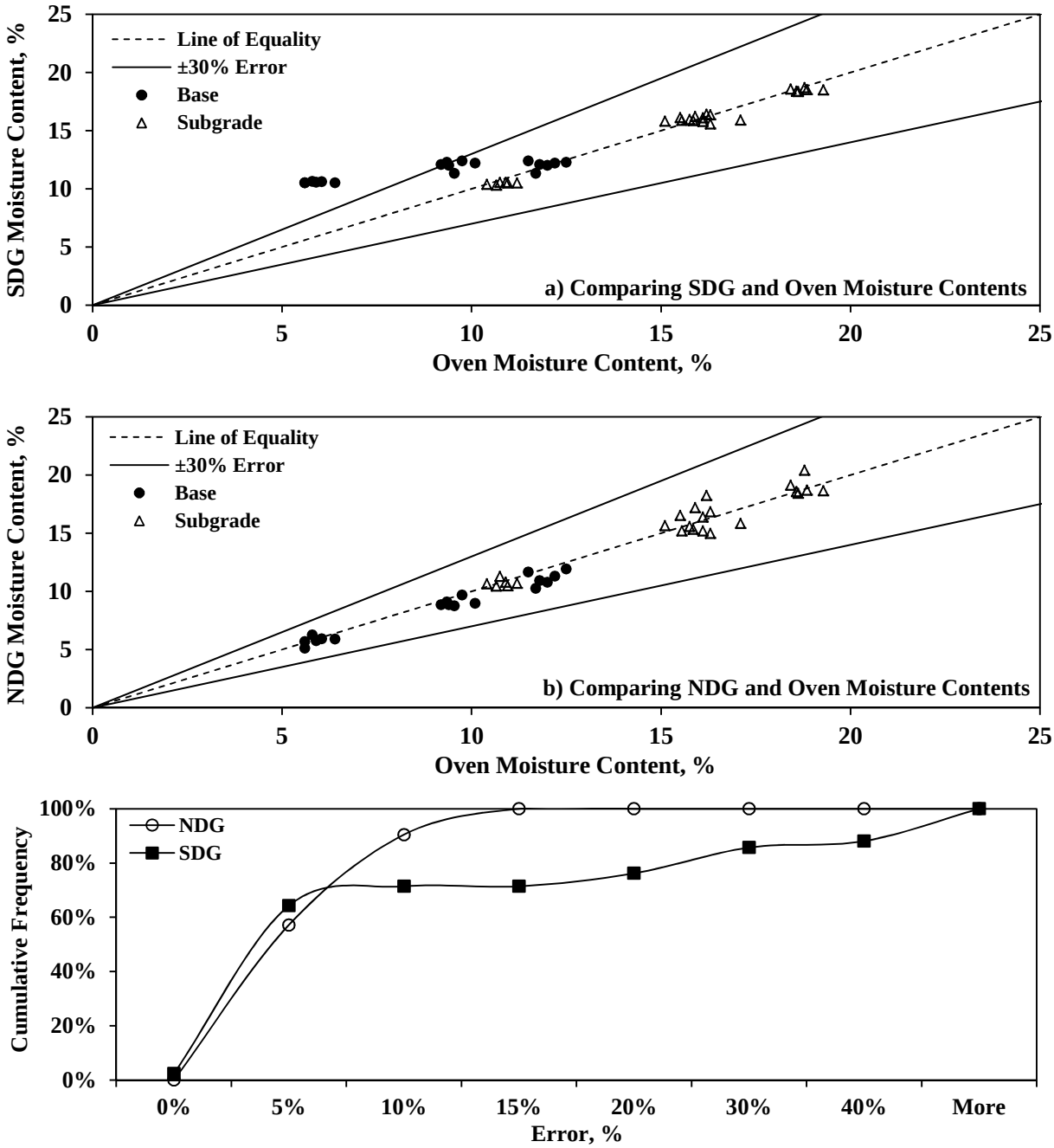

Figure 7.4.2 – Evaluation of Moisture-Density Devices at LTRC Site

7.5 Evaluation of Modulus-Based Technologies

Detailed results for modulus-based-technology devices at LTRC testing facility are included in Appendix G. Figure 7.5.1 compares the average field subgrade moduli measured with the ultrasonic surface wave (PSPA), electro-mechanical stiffness (Geogauge), LWD (Zorn and Dynatest), and DCP technologies at four nominal moisture levels (saturated, optimum, dry of optimum, and wet of optimum). Most devices, except for Geogauge due to high variability of the device, exhibit lower modulus with increased moisture content. The DCP and Zorn LWD indicate a slightly higher modulus for the wet section as compared to the optimum section. Figure 7.5.1a also includes the laboratory representative MR moduli (from Table

7.3.1). The trend of the laboratory representative MR at different moisture levels follows the field trends except for the section placed at the optimum moisture content. One interesting observation is the differences between the moduli from the Zorn and Dynatest LWDs as discussed in Chapter 5 (due to functional differences between these two devices, they reflect different modulus estimations in the field). Figure 7.5.1b compares the field PSPA moduli with the laboratory FFRC moduli at various moisture levels. The PSPA results for the saturated section are not included because the material was too soft to be within the operational constraints of the device. There is a reasonable correlation between field PSPA and laboratory FFRC moduli. The PSPA moduli at the optimum section is again slightly less than the wet section. Comparing Figure 7.5.1a and 7.5.1b reveals that the PSPA and DCP exhibits the same trends between the dry, optimum, and wet sections since both these devices are layer specific.

Figure 7.5.1b also includes the estimated field PSPA moduli from the laboratory-field correlation that was discussed in Section 6.4. The estimated field PSPA modulus using a Poisson's ratio of 0.35 is close to the measured field moduli except for the wet section.

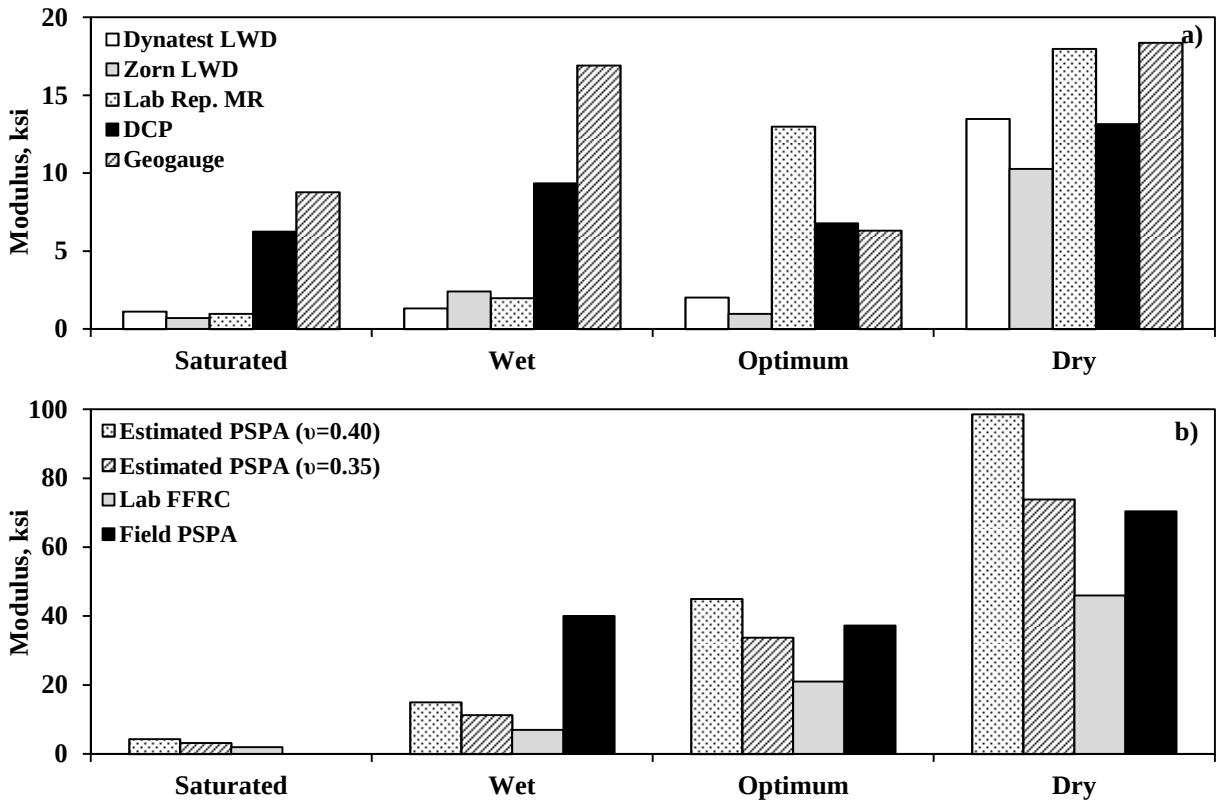

Figure 7.5.1 – Variation of Field and Laboratory Moduli of Subgrade Layer at LTRC Site

Base materials were prepared and compacted at three moisture levels (dry of optimum, optimum, and wet of optimum). Figure 7.5.2a compares the field moduli with the laboratory representative MR values. The representative laboratory MR values follow the expected trend based on moisture content. However, the variations of the field moduli from different device are not quite similar to the laboratory trend. The Geogauge device exhibits high variability in measured moduli. Once again, the Zorn and Dynatest LWDs measured different moduli.

Figure 7.5.2b compares the measured field base PSPA moduli with the laboratory FFRC moduli. The field PSPA moduli increase when the field moisture content declines especially between the wet and optimum sections. The same trend is observed from the laboratory FFRC moduli. The estimated PSPA moduli using laboratory-field correlations from FFRC modulus and Poisson's ratio are also included in

Figure 7.5.2b. The estimated PSPA moduli utilizing a Poisson's ratio of 0.40 better represents the measured field moduli.

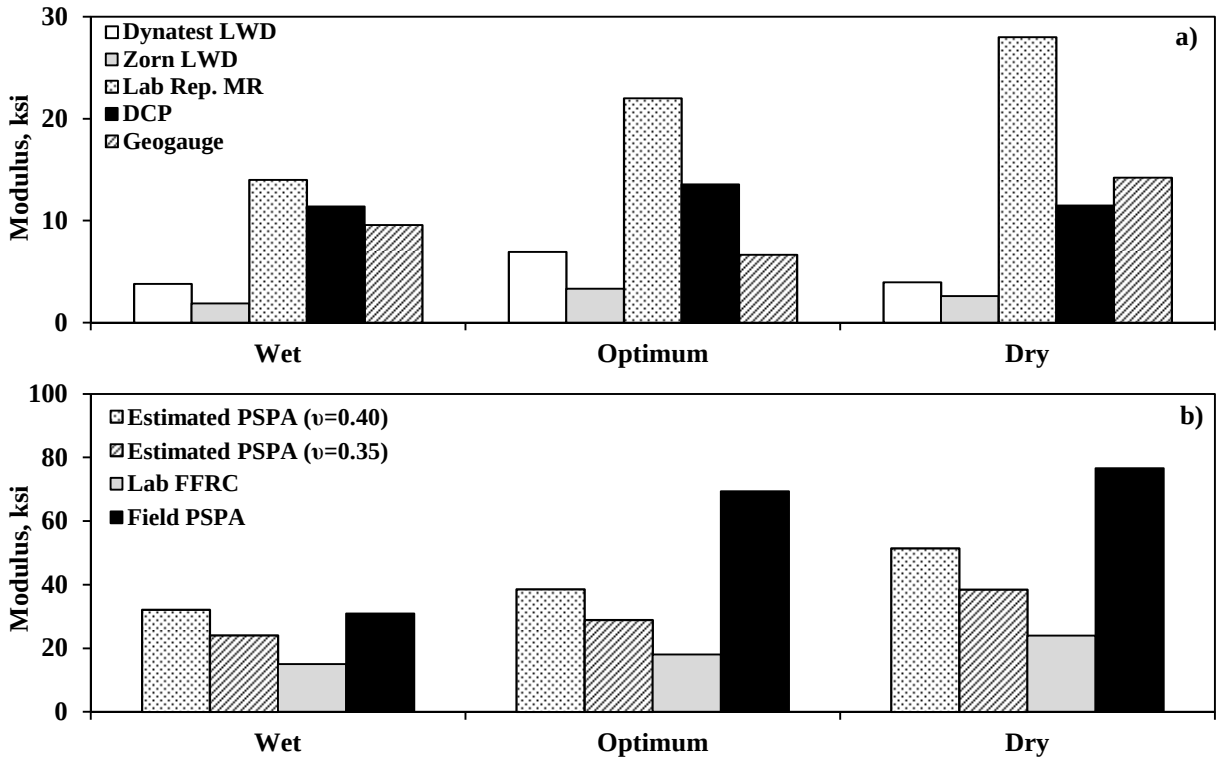

Figure 7.5.2 – Variation of Field and Laboratory Moduli of Base Layer at LTRC Site

7.6 Modulus-Moisture Correlations

The relationships between the laboratory MR or FFRC moduli and moisture content were evaluated in Chapter 3 and compared with the moduli measured during the small-scale studies in Chapter 4. Field data obtained at the LTRC site were employed in this section to validate the aforementioned models.

As recommended by the MEPDG (2004) and Cary and Zapata (2010), the normalized field moduli (M/M_{opt}) are plotted against the normalized in-situ degree of saturation ($S\text{-}S_{opt}$) in Figure 7.6.1. The results from the PSPA (Figure 7.6.1a) and DCP (Figure 7.6.1e) are in agreement with the MEPDG model for fine-grained soils as long as the soil is compacted dry of OMC and with the Cary and Zapata model (with *wPI*=0) when the subgrade is placed wet of OMC. The Geogauge demonstrates high variability (Figure 7.6.1b).The results of the two LWDs follow the MEPDG or Cary and Zapata model when the subgrade is placed close to or wetter than OMC, while the moduli do not closely follow the models dry of OMC.

The variations of the normalized field moduli (M/M_{opt}) with normalized moisture content [(MC-OMC)/OMC] are presented in Figure 7.6.2. The PSPA (Figure 7.6.2a) and DCP (Figure 7.6.2e) yield relationships that follow the proposed relationships developed in Chapter 3 reasonably well. The results from the two LWDs follow the proposed trends for subgrades placed close to or wet of the OMC. For the data collected at sections placed dry of OMC, the field LWD data show a dramatic increase as compared to the laboratory-developed models. Considering the depth of influence of the LWD (which penetrates the underlying layer) and compared with the data from the PSPA and DCP (which are both layer specific), the sudden increase in the LWD moduli at the dry section could be due to a stiffer embankment layer. Again, the Geogauge data shows high variability.

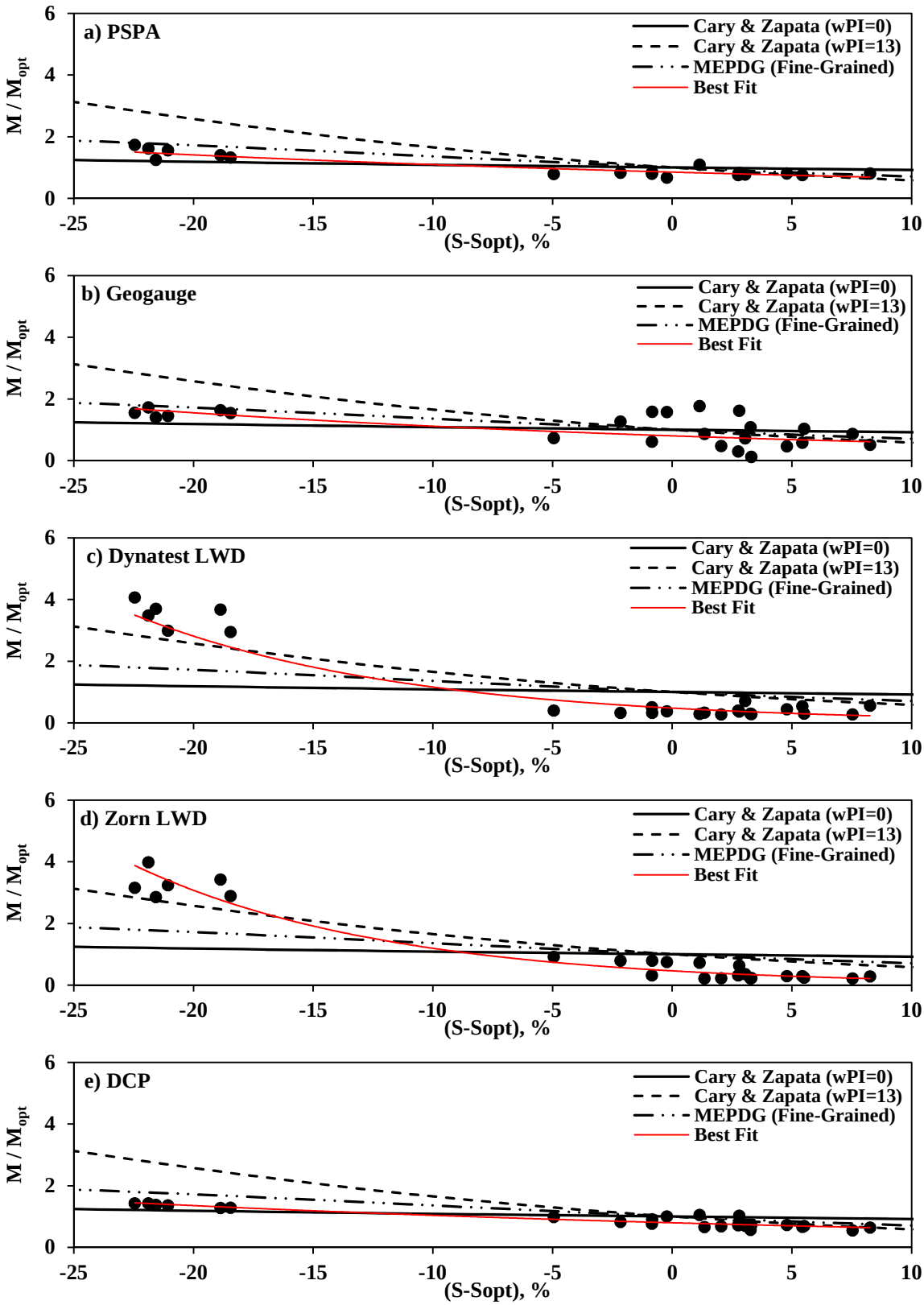

Figure 7.6.1 – Variations in Normalized Field Modulus with Normalized Degree of Saturation of Subgrade Layer at LTRC Site

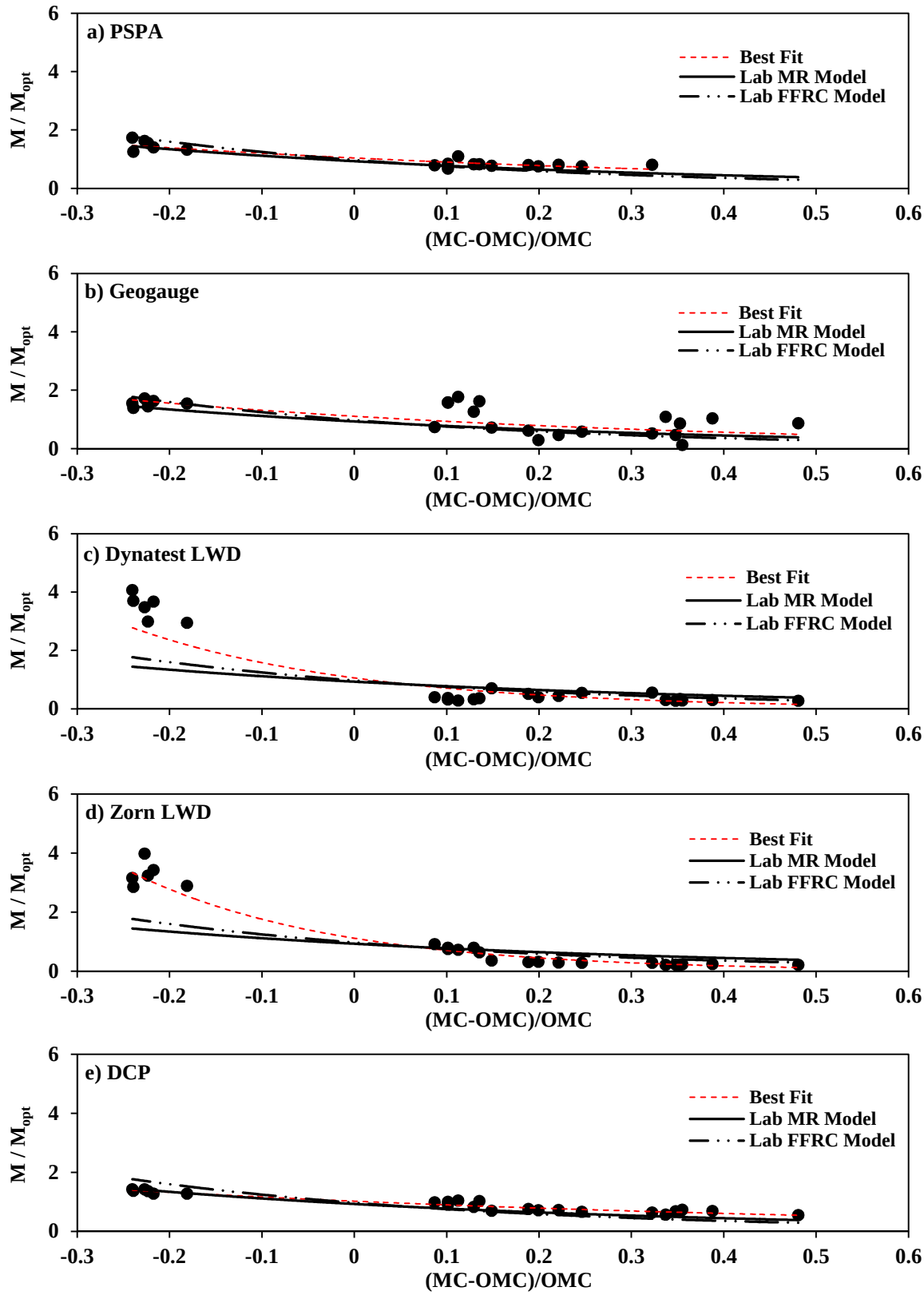

Figure 7.6.2 – Variations in Field Modulus with Normalized Moisture Content of Subgrade Layer at LTRC

The moisture-modulus relationships from the base materials for all devices are included in Appendix G. These relationships are not as promising as those are for the subgrade. Among all technologies, only the ultrasonic surface wave (PSPA) technology moduli exhibited a reasonable correlation with the field moisture contents as shown in Figure 7.6.3. The variation in the normalized PSPA modulus with normalized degree of saturation exhibits some scatter especially for the section placed wet of the OMC. However, the trends have reasonable agreement with the relationships developed from the laboratory and small-scale tests in the previous chapters.

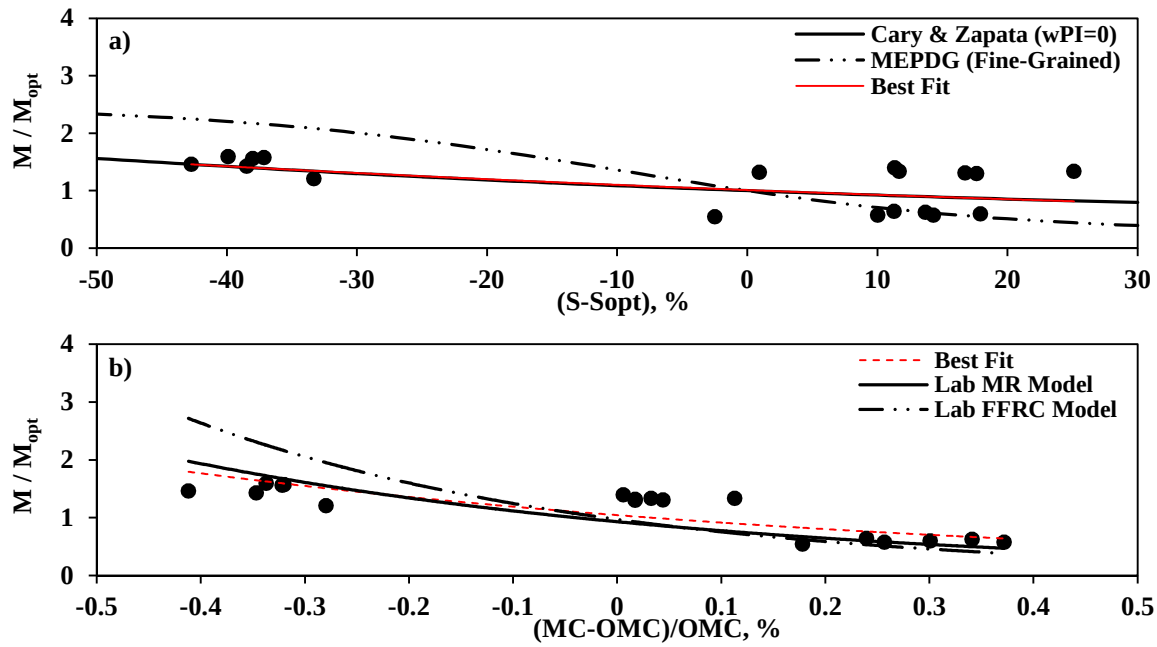

Figure 7.6.3 – Correlation of PSPA Moduli with Degree of Saturation and Moisture Content of Base Materials at LTRC

7.7 Variability of Modulus/Stiffness-Based Technologies

The coefficient of variation (COV) of triplicate measurements at each test spot was calculated and compared with their corresponding modulus at various test sections. Furthermore, the standard deviation of such measurements was estimated and compared with the field moduli for each technology and associated device. Detailed results are included in Appendix G. Figure 7.7.1 summarizes the distribution of the COVs from different technologies tested on subgrade and base sections. The Zorn LWD and DCP exhibit the lowest COVs for the subgrade layer (see Figure 7.7.1a). For the base layer, the DCP again has the lowest variability followed by the electro-mechanical stiffness (Geogauge) and ultrasonic surface wave (PSPA) technologies (see Figure 7.7.1b). Most technologies (except for the DCP) exhibit greater variability on base materials as compared to the subgrade soils. To investigate further the variability of each technology, the COVs corresponding to an 80% confidence level are compared in Table 7.7.1. The ultrasonic surface wave (PSPA) technology has the same range of COV for both base and subgrade layer. The electro-mechanical stiffness (Geogauge) technology exhibits reasonable variation on base materials while reflecting a relatively high uncertainty on subgrade soils. The two LWDs demonstrate high variability on the base material while they show lower COVs on the subgrade layer. The DCP exhibits the lowest uncertainty level among all technologies for both the subgrade and base materials.

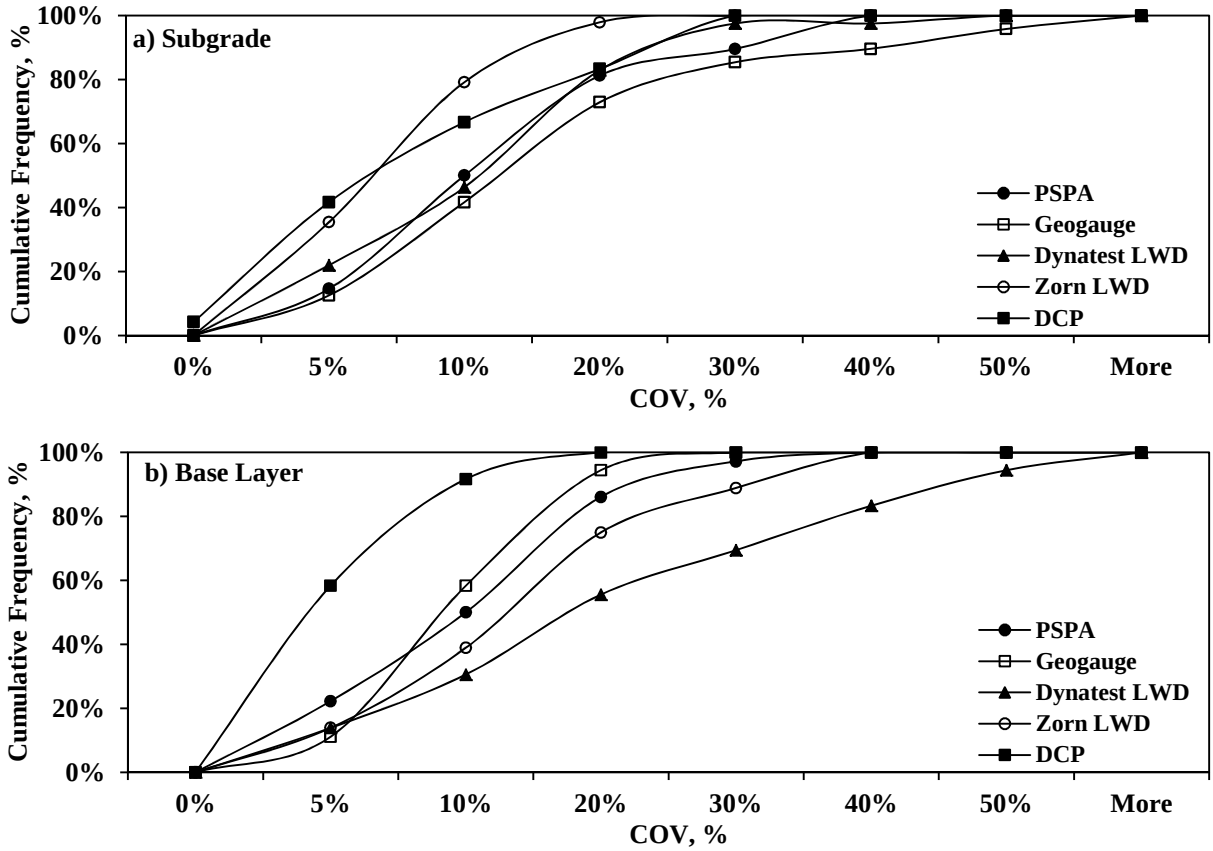

Figure 7.7.1 – Distributions of COV Values on Subgrade and Base Layers at LTRC Site

Table 7.7.1 – Variability of Modulus-Based Technologies at 80% Confidence Level

Device	Coefficient of Variation of Triplicate Measurements	
	Base	**Subgrade**
Ultrasonic Surface Wave (PSPA)	18%	20%
Electro-Mechanical Stiffness (Geogauge)	16%	26%
LWD (Dynatest)	38%	19%
LWD (Zorn)	24%	10%
DCP	8%	18%

7.8 Acceptance Scenarios for Construction Quality Control

Figure 7.8.1 compares the conventional approach of comparing the NDG dry densities of the subgrade layer with a 95% MDD acceptance limit. All sections pass the defined acceptance limit.

A typical acceptance scenario of the subgrade layer with the ultrasonic surface wave (PSPA) technology is depicted in Figure 7.8.2. The optimum and wet sections did not achieve the desired acceptance limits, while the dry section marginally passed the specified target modulus. The anticipated moduli for each moisture condition based on the laboratory FFRC results are also shown in Figure 7.8.2. The PSPA moduli are greater than moisture-adjusted anticipated modulus (red dashed line) for the wet section, are similar for the optimum section and are less for the dry section.

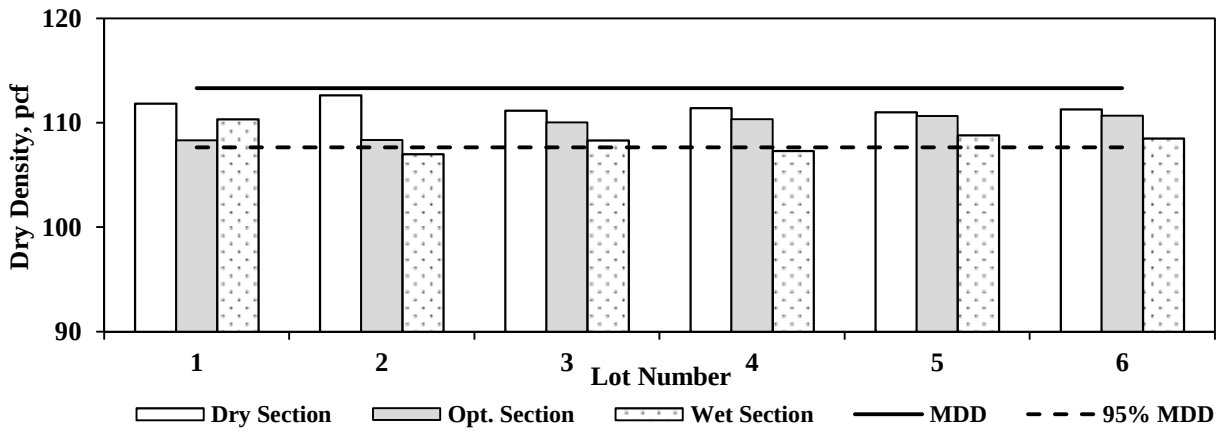

Figure 7.8.1 – Quality Acceptance based on NDG Density Criterion for Subgrade Layer at LTRC Site

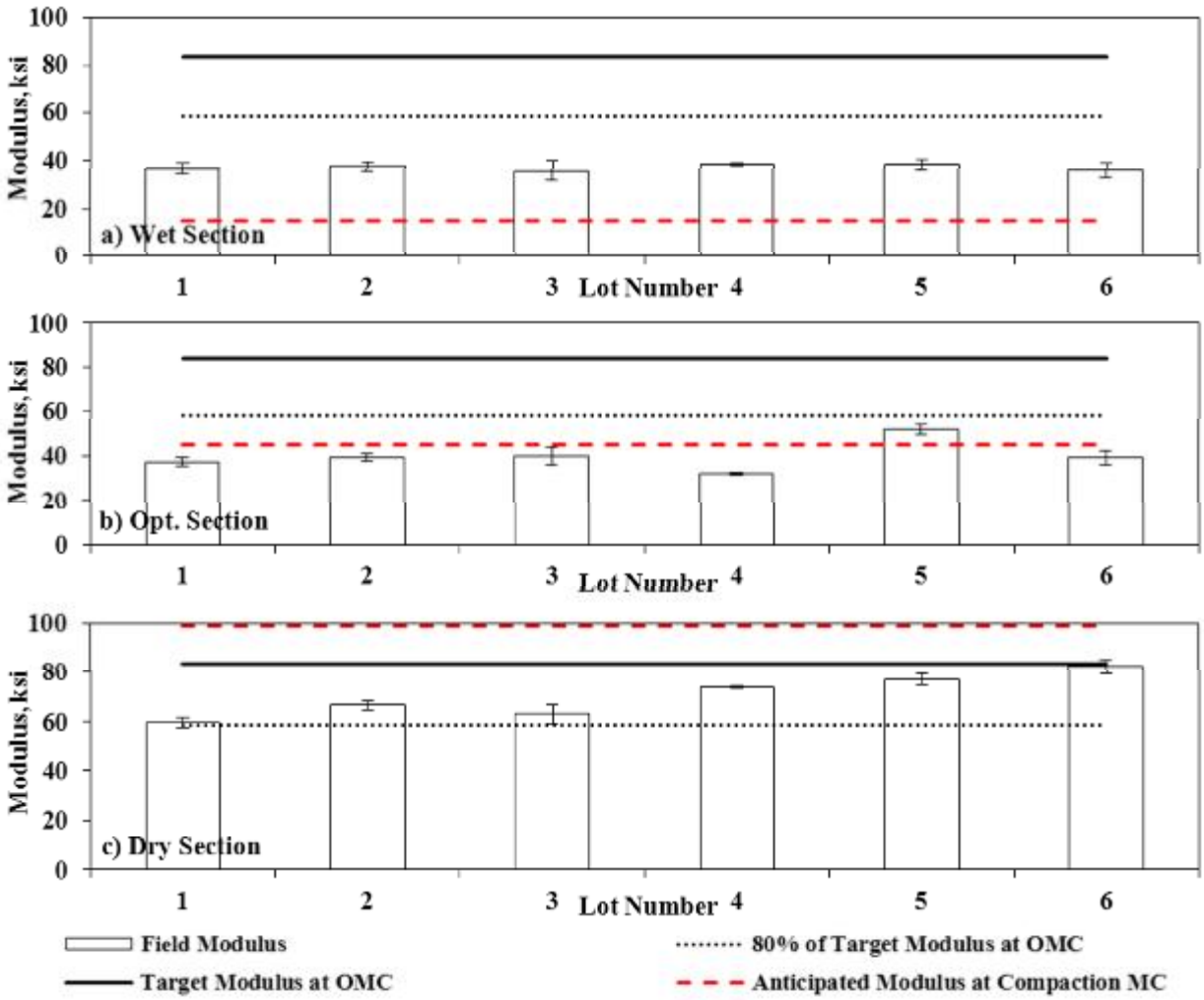

Figure 7.8.2 – Quality Acceptance based on PSPA Modulus Criterion for Subgrade Layer (Poisson's Ratio=0.40)

One of the factors influencing the modulus-based acceptance criteria is the Poisson's ratio of the compacted soil. The acceptance limits (based on established target modulus) and moisture-adjusted anticipated field moduli in Figure 7.8.2 were calculated based on an assumed Poisson's ratio of 0.4 for all subgrade sections. It is well known that the Poisson's ratio of a material increases as its moisture content increases. To study the impact of the Poisson's ratio on the established acceptance criteria, the target moduli based on the target moisture content of OMC were recalculated based on a Poisson's ratio of 0.35. The moisture-adjusted anticipated field moduli were also recalculated based on Poisson's ratios of 0.35 for dry and optimum sections and 0.45 for the wet section. The results of such adjustments are depicted in Figure 7.8.3. The anticipated field moduli (adjusted for field moisture contents) are reasonably close to the actual field moduli. Furthermore, all testing lots of the dry section now pass the modulus-based acceptance limit (even after adjustments based on the difference between compaction and testing conditions). One of the lots of the optimum section is also satisfying the acceptance criterion. Still none of the lots in wet section reaches the acceptance limit.

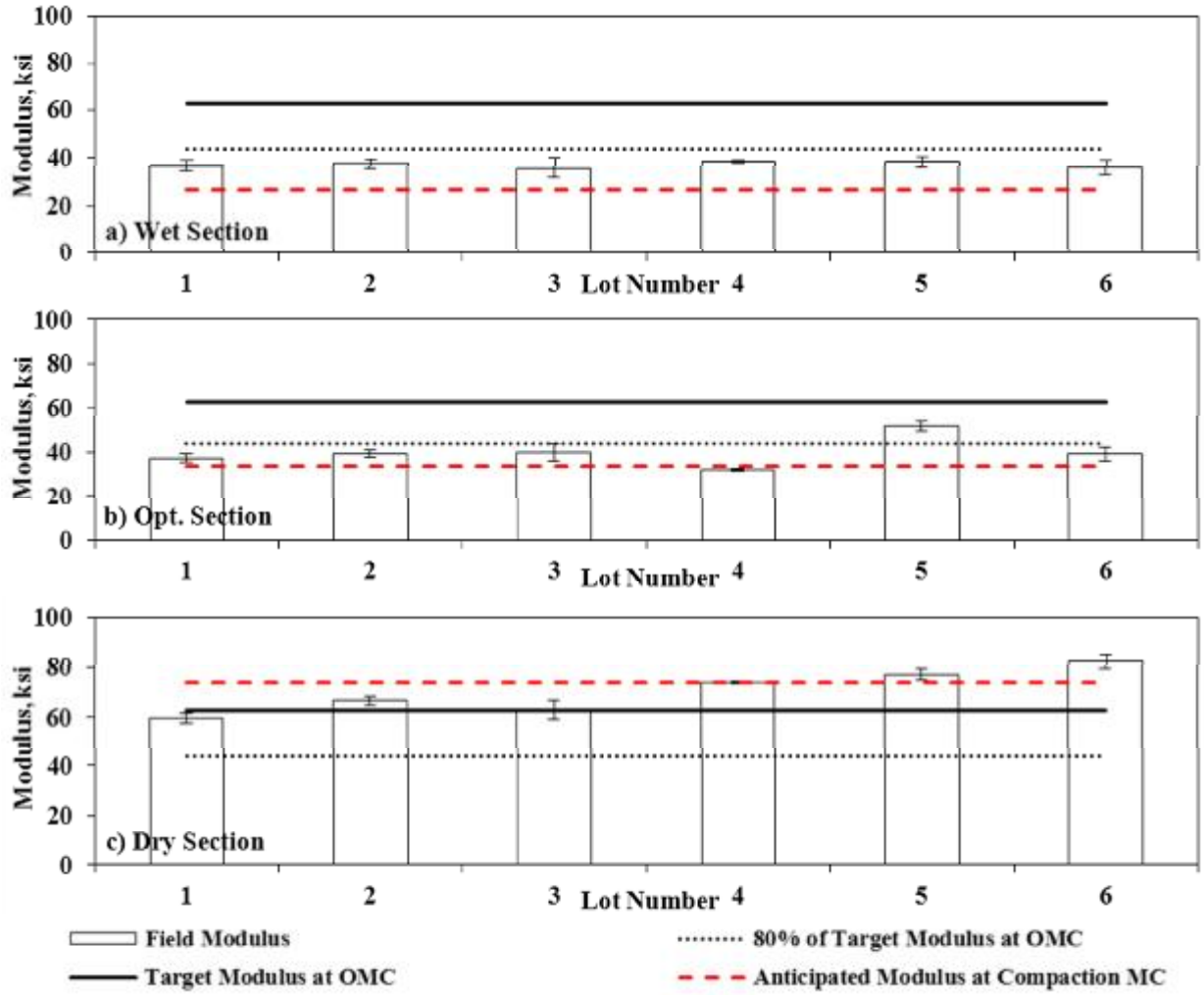

Figure 7.8.3 – Quality Acceptance based on PSPA Modulus Criterion for Subgrade Layer (Poisson's Ratio=0.35)

Figure 7.8.4 summarizes the acceptance scenarios based on the Zorn LWD field measurements. Half of the test spots in dry section pass acceptance limit based on the established target modulus. None of the other sections (optimum, wet and saturated sections) achieves the acceptance limit. The estimated field moduli corrected for the compaction moisture content (the black dashed line) are close to the actual field

LWD modulus at saturated and wet section but overestimate the field modulus in optimum and dry sections.

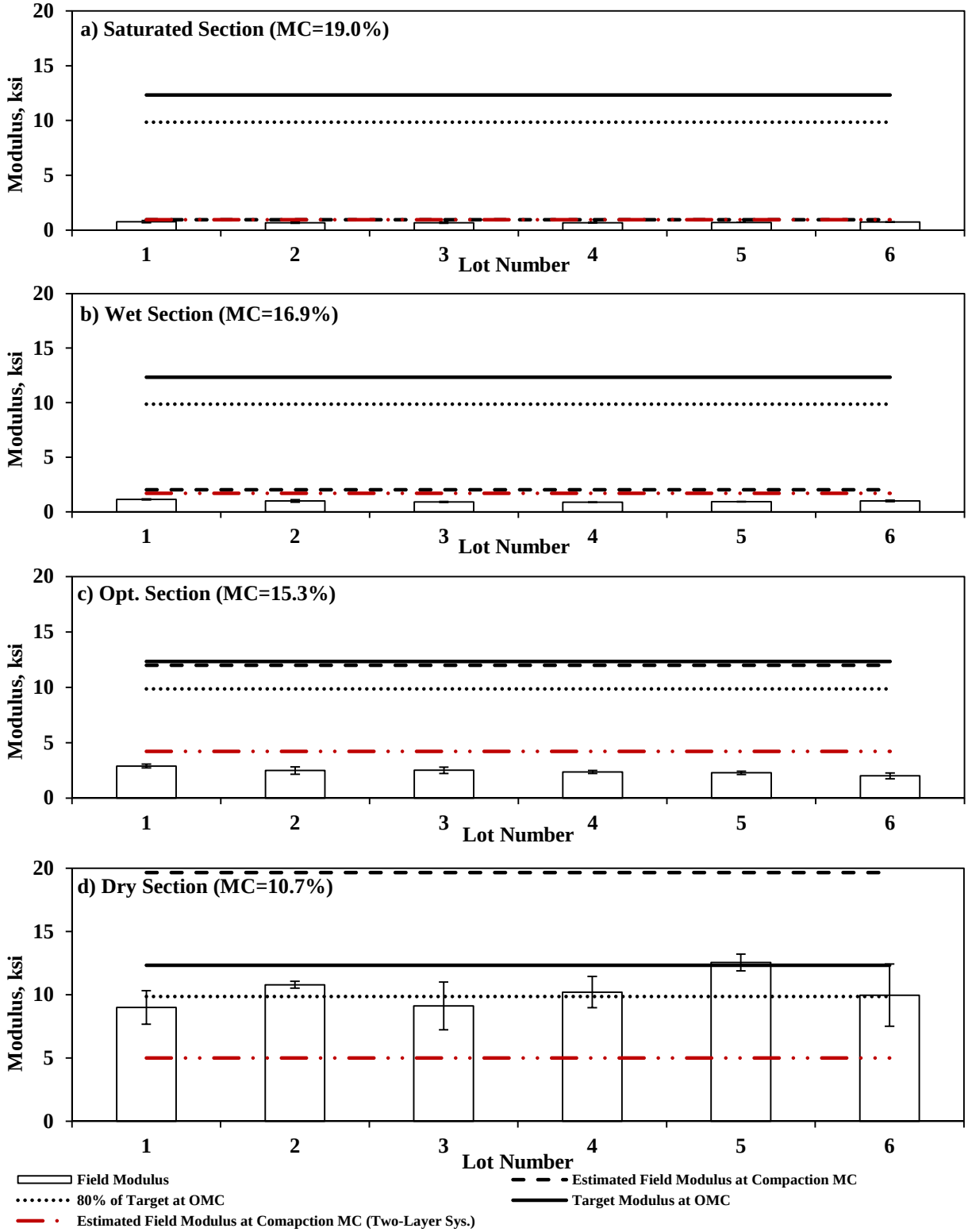

Figure 7.8.4 – Quality Acceptance based on Zorn LWD Modulus Criterion for Subgrade Layer (Poisson's Ratio=0.40)

Such estimated field moduli are calculated utilizing the algorithm discussed in Section 6.2 assuming a one-layer system (only subgrade soil). Since LWD measures the composite modulus of the compacted layers, the stiffness of the underlying embankment layer may also affect the measured moduli. To calculate an estimate of the composite LWD modulus, the two-layer algorithm in Section 6.2 was employed. The dashed-dotted red lines in Figure 7.8.4 represent the estimated composite field moduli at compaction moisture contents using a two-layer system. The latter approach yields closer results to the actual field LWD moduli. Considering the 80% of the established target modulus as the acceptance criterion, none of the test spots along the saturated, wet and optimum sections achieves the desired moduli. Only 67% of the test spots of the dry section pass the modulus-based acceptance criteria.

The selection of Poisson's ratio not only affects the ultrasonic surface wave (PSPA)-based modulus acceptance but also the LWD-based process. The Zorn LWD field moduli illustrated in Figure 7.8.4 were calculated using a Poisson's ratio of 0.40. Figure 7.8.5 contains two other sets of LWD field moduli calculated based on Poisson's ratios of 0.30 and 0.35. As an example, at the dry section, 33% of the test spots pass the modulus-based acceptance limit, and 33% are marginally acceptable (between 70% and 80% of the established target modulus) when a Poisson's ratio of 0.40 is assumed. By assuming a Poisson's ratio of 0.35, 67% of the test spots pass the acceptance criterion. Furthermore, using a Poisson's ratio of 0.3 yields an 83% passing rate with additional 17% of the spots passing marginally. Such an experiment indicates the importance of proper Poisson's ratio selection on the acceptance scenarios based on the LWD results.

A detailed evaluation of the acceptance scenarios for different technologies and devices over base and subgrade layers is included in Appendix G. To compare the conventional density-based criteria with the modulus-based acceptance limits, the percent of lots either passing each criterion, or considered as marginally acceptable (between 70% and 80% of the established target moduli) are summarized in Table 7.8.1 for both the subgrade and base layers. The impact of Poisson's ratio on the acceptance criteria is also reflected in Table 7.8.1. Based on the NDG results, almost all subgrade and base test sections (except for the dry section of the base layer) pass the 95% MDD acceptance limit.

None of the test lots of the wet subgrade section passes the acceptance limit based on the ultrasonic surface wave (PSPA) technology. None of the test lots of the optimum sections passes the acceptance criterion with Poisson's ratio of 0.4, while 17% pass when the Poisson's ratio of 0.35 is assumed. With an assumption of a Poisson's ratio of 0.40, 50% of the lots for the dry section pass the criterion; while with a Poisson's ratio of 0.35, all test lots achieve the modulus-base acceptance limit.

For the base layer, all test lots along the dry and optimum sections (assuming both Poisson's ratios of 0.35 and 0.40) pass the criterion. Although based on the NDG results 100% of the lots along the wet section pass the density criteria, 83% of the lots achieve the acceptance limit based on the PSPA moduli with a Poisson's ratio of 0.40. Such PSPA-based acceptance rate would have changed to 100% if the Poisson's ratio were changed to 0.35.

As summarized in Table 7.8.1, the acceptance rates for the Zorn LWD are different from those of the Dynatest LWD. As an example, for the dry section of subgrade, 100% of the lots pass the modulus acceptance limit based on the Dynatest LWD results while 50% pass using a Zorn LWD. This pattern is primarily due to the differences in the way that these two devices measure the deflections (Dynatest LWD measures the deflection of the soil while Zorn LWD measures the deflection of the plate) and furthermore, the loading conditions are different between two devices.

Based on a normally accepted Poisson's ratio of 0.4 for the dry section of subgrade, 50% of the lots pass the Zorn LWD acceptance limit while changing the Poisson's ratio to 0.35 yields 67% passing rate. Such variations show the importance of Poisson's ratio on the acceptance criteria based on LWD results.

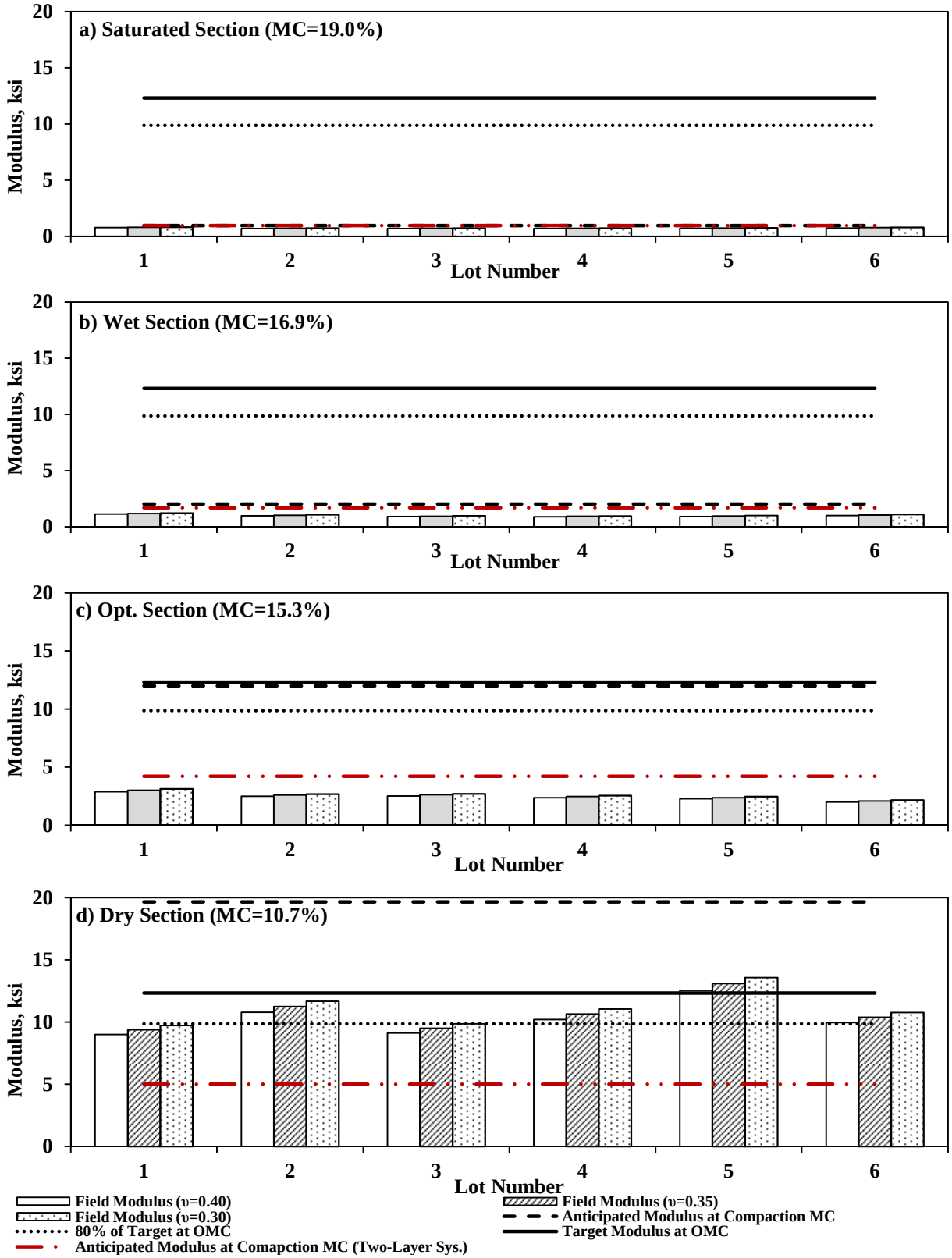

Figure 7.8.5 – Quality Acceptance based on Zorn LWD Modulus Criterion for Subgrade Layer with Variable Poisson's Ratio

Table 7.8.1 – Quality Acceptance based on Modulus Criterion for Subgrade and Base Layer*

Section		Poisson's Ratio	Acceptance Approach	% Passing	% Marginal	% Not Passing
Subgrade	Dry		**NDG Dry Density**	**100**	**0**	**0**
		0.40	PSPA Mod.	50	50	0
		0.35	PSPA Mod.	100	0	0
		0.40	Dynatest LWD Mod.	100	0	0
		0.40	Zorn LWD Mod.	50	17	33
		0.35	Zorn LWD Mod.	67	33	0
		0.30	Zorn LWD Mod.	100	0	0
	Opt		**NDG Dry Density**	**100**	**0**	**0**
		0.40	PSPA Mod.	0	0	100
		0.35	PSPA Mod.	17	0	83
		0.40	Dynatest LWD Mod.	0	0	100
		0.40	Zorn LWD Mod.	0	0	100
		0.35	Zorn LWD Mod.	0	0	100
		0.30	Zorn LWD Mod.	0	0	100
	Wet		**NDG Dry Density**	**100**	**0**	**0**
		0.40	PSPA Mod.	0	0	100
		0.35	PSPA Mod.	0	0	100
		0.40	Dynatest LWD Mod.	0	0	100
		0.40	Zorn LWD Mod.	0	0	100
		0.35	Zorn LWD Mod.	0	0	100
		0.30	Zorn LWD Mod.	0	0	100
Base	Dry		**NDG Dry Density**	**67**	**0**	**33**
		0.40	PSPA Mod.	100	0	0
		0.35	PSPA Mod.	100	0	0
		0.40	Dynatest LWD Mod.	33	33	34
		0.40	Zorn LWD Mod.	0	0	100
		0.35	Zorn LWD Mod.	0	0	100
		0.30	Zorn LWD Mod.	0	0	100
	Opt		**NDG Dry Density**	**100**	**0**	**0**
		0.40	PSPA Mod.	100	0	0
		0.35	PSPA Mod.	100	0	0
		0.40	Dynatest LWD Mod.	100	0	0
		0.40	Zorn LWD Mod.	0	0	100
		0.35	Zorn LWD Mod.	0	0	100
		0.30	Zorn LWD Mod.	0	0	100
	Wet		**NDG Dry Density**	**100**	**0**	**0**
		0.40	PSPA Mod.	83	17	0
		0.35	PSPA Mod.	100	0	0
		0.40	Dynatest LWD Mod.	17	17	66
		0.40	Zorn LWD Mod.	0	0	100
		0.35	Zorn LWD Mod.	0	0	100
		0.30	Zorn LWD Mod.	0	0	100

*The Poisson's ratio to determine the target modulus assumed as 0.40 and 0.35 for subgrade and base materials, respectively.

The lessons learned from this field study can be summarized as follows. the electrical impedance spectroscopy technology (SDG) exhibited high variability in moisture and density estimations especially on the base layer. The electro-mechanical stiffness technology (Geogauge) exhibited high uncertainty in estimating the field modulus. The ultrasonic surface wave (PSPA), LWD and DCP technologies perform reasonably well with some caveats. The PSPA exhibited the highest variability but provided the most reasonable layer-specific trends. The two LWDs reported different moduli at the same test spots, so the specification should clearly state which device should be used. It is also important to consider the properties of the underlying layers, in setting the target value, especially when the layer of interest is overlying a layer with significantly different modulus. The DCP results were not very sensitive to moisture content changes.

The modulus-moisture correlations recommended from the laboratory and small-scale studies are for the most part reasonable. The proposed model of correlating normalized modulus (M/M_{opt}) with normalized moisture content [(MC-OMC)/OMC] matched the field data better.

The estimated target moduli from the process proposed in Chapter 6 seem reasonable. However, the limits need to be fine-tuned based on testing at more sites. The Poisson's ratio of the layer plays a role in the acceptance process and it should be standardized in the specification. The density seems to have a week correlation to quality as judged by the modulus of a layer. This case study confirmed the importance of a reasonable process control in terms of moisture content during compaction.

Based on the small-scale and these field tests, the use of the electrical impedance spectroscopy, electro-mechanical stiffness, and DCP (on unbound aggregates) technologies was de-emphasized in most of the actual field tests for the next phase of the project.

CHAPTER 8 – OBSERVATIONS FROM IMPLEMENTATION OF SPECIFICATION

8.1 Introduction

To evaluate the specification discussed and presented in Appendix A, five construction sites were visited. Three of these sites were tested by the research team (Stage I), and two others were tested in close collaboration with the agencies' personnel (Stage II). The results from these site visits are discussed comprehensively in Appendices H through L and are summarized below. Figure 8.1.1 presents aerial views of the different testing sites. The test sites for Stage I are the following:

Site I.1. ***US 67 in Dublin, TX (see Appendix H)***: The project was five miles long with extensive embankment and subgrade work with two different fine-grained materials and unbound aggregate base. The contract required the use of intelligent compaction.

Site I.2. ***IH 35 W, Tarrant County, TX (see Appendix I)***: The project was one mile long with subgrade work. The contract required the use of intelligent compaction.

Site I.3. ***Route 22, Bridgewater Township, NJ (see Appendix J)***: This work included the placement of a clayey shale subgrade, unbound aggregate subbase, and dense-graded aggregate base materials mixed with reclaimed asphalt pavement.

The selected construction sites for Stage II are as follows.

Site II.1. ***FAA Facility, Atlantic City, NJ (see Appendix K):*** Field evaluation was carried out at the National Airport Pavement Testing Facility (NAPTF) of the U.S. Federal Aviation Administration (FAA) located at the William J. Hughes Technical Center. Two 30 ft×300 ft subgrade sections were tested during the week of August 12, 2103. The subbase and base layers were prepared and tested by the NAPTF personnel during November 2013 and May 2014, respectively.

Site II.2. ***US-50, North Vernon, IN (see Appendix L):*** The subgrade was tested in collaboration with INDOT staff. The subgrade layer was placed at 8 in. lifts and compacted along a candidate section. The INDOT staff collected the LWD (the device that they prefer) data on a subbase at the site.

8.2 Laboratory Results

The index properties of all geomaterials encountered are summarized in Table 8.2.1, and their gradation curves are presented in Figure 8.2.1. The classification of each geomaterial, as per Unified Soil Classification System (USCS), is reported in Table 8.2.1 as well. The optimum moisture contents and maximum dry unit weights obtained as per standard Proctor tests (AASHTO T99) for the subgrades and as per modified Proctor tests (AASHTO T180) for subbase and base materials are reported in Table 8.2.1.

The resilient modulus (MR) and FFRC tests were performed on laboratory specimens prepared at the OMC, dry of OMC and wet of OMC. The results of these laboratory tests at OMC are summarized in Table 8.2.2. The expanded results are included in Appendices H through L. Figures 8.2.2 and 8.2.3 summarize the variations of the FFRC moduli and representative MR values with moisture content for the subgrades and bases/subbases, respectively.

a) Site I.1 - US 67 in Dublin, Texas

b) Site I.2 - IH 35 W, Tarrant County, Texas

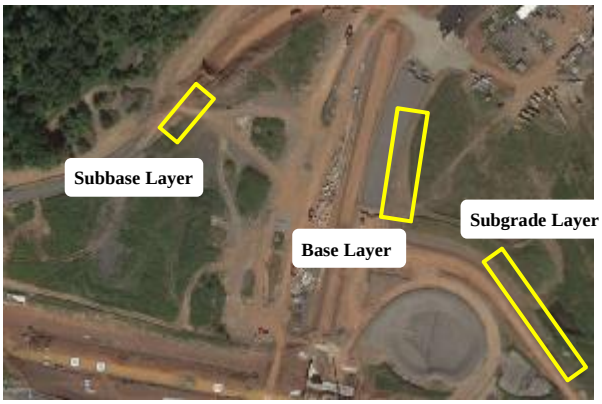

c) Site I.3 - Route 22Bridgewater, NJ

d) Site II.1 - FAA Facility in Atlantic City, NJ

e) Site II.2 - US-50, North Vernon, IN

Figure 8.1.1 – Aerial Views of Field Evaluation Sites

Table 8.2.1 - Index Properties of Field Evaluation Geomaterials

Site No.	Soil Type	Gradation %				USCS Class.	Specific Gravity	Atterberg Limits			Moisture/Density	
		Gravel	Coarse Sand	Fine Sand	Fines			LL	PL	PI	OMC,* %	MDUW,** pcf
I.1	Subgrade A	0	4	10	86	CL	2.75	41	14	27	16.7	107.0
	Subgrade B	0	5	11	84	CL	2.75	36	13	23	16.9	109.0
	Base	52	29	15	5	GW	2.68	28	16	12	10.4	120.4
I.2	Subgrade	0	8	3	89	CH	2.76	55	15	40	21.2	101.1
I.3	Subgrade	12	20	13	55	CL	2.68	32	18	14	12.2	127.7
	Subbase	63	26	10	1	GW	2.65	Non-Plastic			4.8	147.5
	Base	59	32	7	1	GW	2.65	Non-Plastic			4.6	147.3
II.1	Subgrade	5	4	2	89	CL	2.65	48	15	33	24.0	97.9
	Subbase	0	79	18	3	SP	2.65	0	0	0	8.9	132.0
	Base	50	35	13	2	GW	2.65	0	0	0	5.4	152.0
II.2	Subgrade	5	8	22	65	CL	2.73	27	11	16	16.4	111.9
	Subbase	56	34	10	1	GW	2.65	0	0	0	5.8	143.8

*OMC = Optimum Moisture Content, **MDUW = Maximum Dry Unit Weight

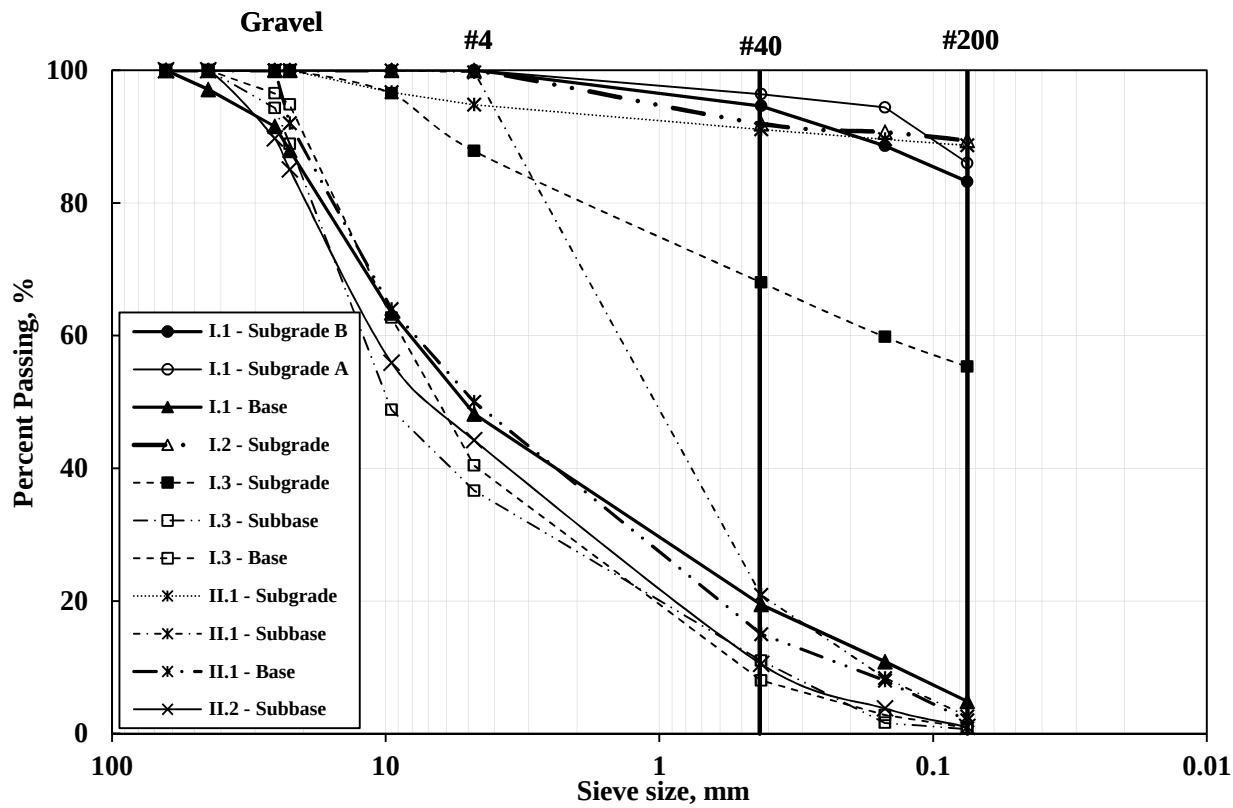

Figure 8.2.1 – Gradation Curves of Field Evaluation Geomaterials

Table 8.2.2 – Laboratory Results of MR and FFRC Tests of Field Evaluation Geomaterials at their Corresponding Optimum Moisture Contents

Site No.	Type	Actual Moisture Content, %	Dry Density, pcf	FFRC Modulus, ksi	Nonlinear Parameters			Representative MR, ksi*
					k'_1	k'_2	k'_3	
I.1	Subgrade A	16.7	108.6	38	935	0.17	-0.35	14.2
	Subgrade B	16.9	108.2	25	829	0.23	-0.71	12.3
	Base	11.5	126.0	30	875	0.74	-0.23	27.1
I.2	Subgrade	21.5	102.0	23	795	0.30	-2.91	8.0
I.3	Subgrade	12.6	125.2	24	437	1.12	-3.00	7.3
	Subbase	4.8	149.7	55	883	0.74	-0.05	29.2
	Base	4.6	147.0	35	982	0.71	-0.05	31.6
II.1	Subgrade	24.3	98.5	30	1217	0.12	-2.85	11.3
	Subbase	Cylindrical laboratory samples were instable to perform the resilient modulus test						
	Base	5.4	152.6	43	811	0.78	-0.10	27.6
II.2	Subgrade	16.5	108.0	37	667	0.65	-1.67	10.7
	Subbase	5.8	148.3	24	665	0.52	-0.05	17.1

* from Eq. 3.2.1 based on τ_{oct} and θ values of 7.5 psi and 31 psi for base and 3 psi and 12.4 psi for subgrades as recommended by NCHRP Project 1-28A.

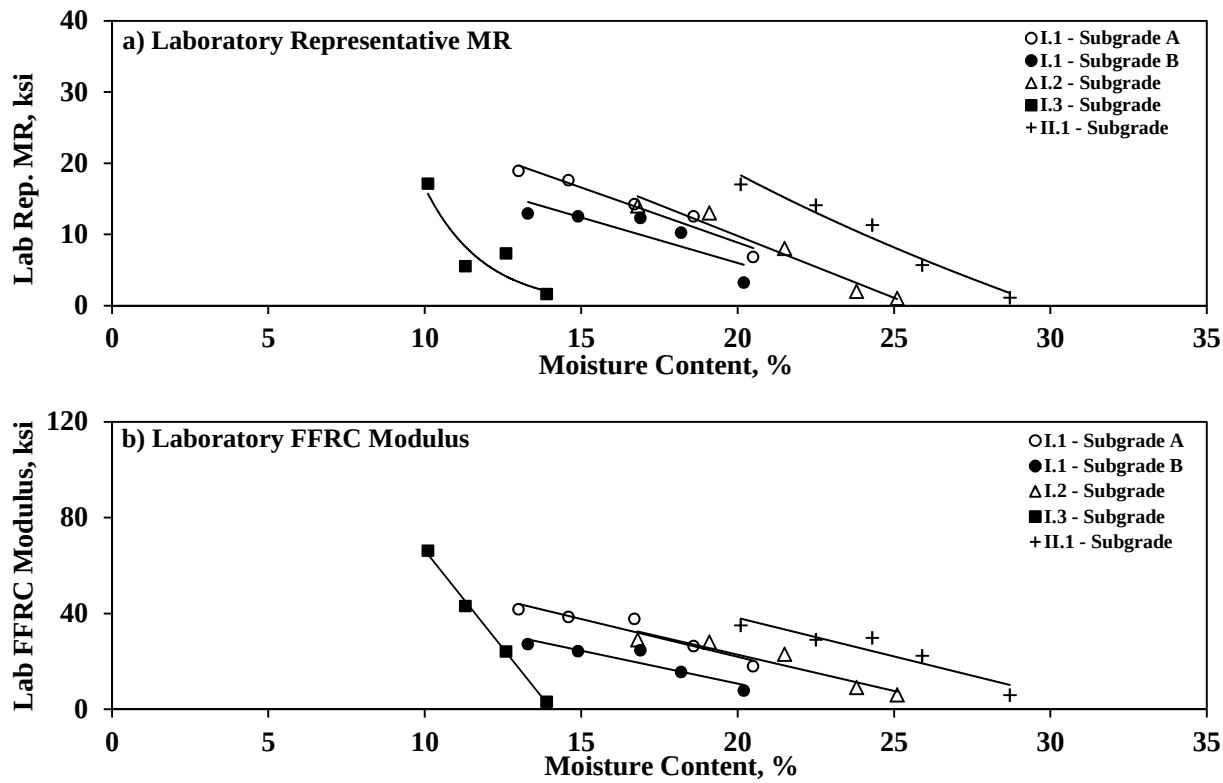

Figure 8.2.2 – Variations of Laboratory MR and FFRC Moduli with Moisture Content (Subgrade)

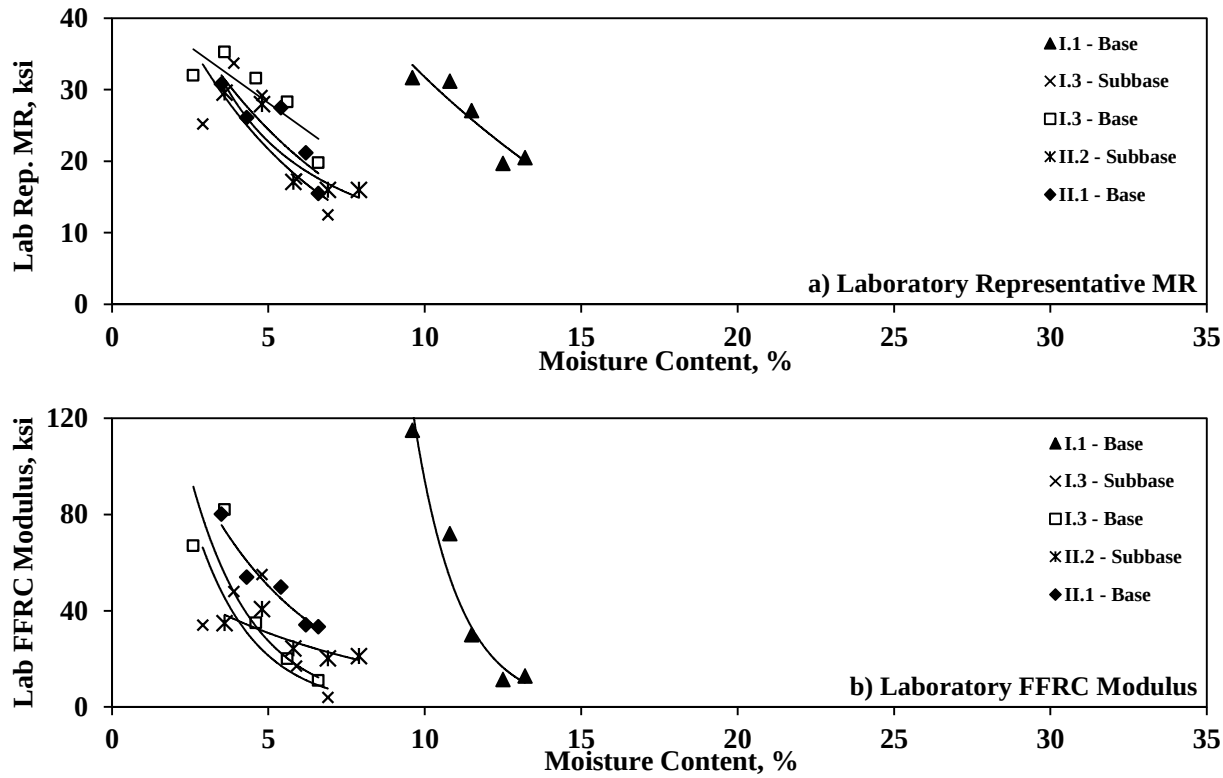

Figure 8.2.3 – Variations of Laboratory MR and FFRC Moduli with Moisture Content (Base)

The laboratory FFRC moduli are compared with the representative MR moduli of various subgrade geomaterials in Figure 8.2.4.a. The laboratory representative MR values are globally 0.37 times of the laboratory FFRC moduli with some scatter. This trend is similar to the one observed from the subgrade soils used in Phase II laboratory studies as discussed in Chapter 3. Figure 8.2.4b summarizes the laboratory moduli for the base and subbase (unbound aggregate) materials from Phase II and Phase III. More scatter in the data is evident. However, the trends are similar. The limited number of base materials used in this study does not represent a wide range of material properties. More variety of unbound aggregate sources is required to evaluate these geomaterials more rigorously.

As discussed in Section 3.2, incorporating the index properties of the subgrade soils along with moisture-density parameters could improve the observed correlation between the laboratory representative MR and FFRC moduli (see Equation 3.2.3). The predicted representative MR values from Equation 3.2.3 are compared with the measured ones in Figure 8.2.5. For softer soils (at saturated conditions), the proposed model is inaccurate because of the buildup pore pressure during the resilient modulus testing. For the unsaturated specimens, the model yields reasonable results. In order to propose an improved prediction model, all the subgrade data from the laboratory studies (Chapter 3) and the laboratory results from the field validation sites (this chapter) were combined to develop Equation 8.2.1 based on all the data for subgrade soils.

$$MR = -0.28(MC) - 0.08(DD) + (0.3)FFRC + 0.53(Fine) - 0.10(PI) + 0.43(Sand) - 29.51 \qquad (8.2.1)$$

where *MC* = moisture content (%), *DD* = dry density (pcf), *FFRC* = laboratory FFRC modulus (ksi), *Fine* = percent passing sieve #200 (%), *Sand* = percent passing sieve #4 (%), and *PI* = plasticity index. The predicted MR values are compared with the measured ones in Figure 8.2.6 along with 95% confidence and prediction limits. Equation 8.2.1 predicts the laboratory representative MR better than Equation 3.2.3.

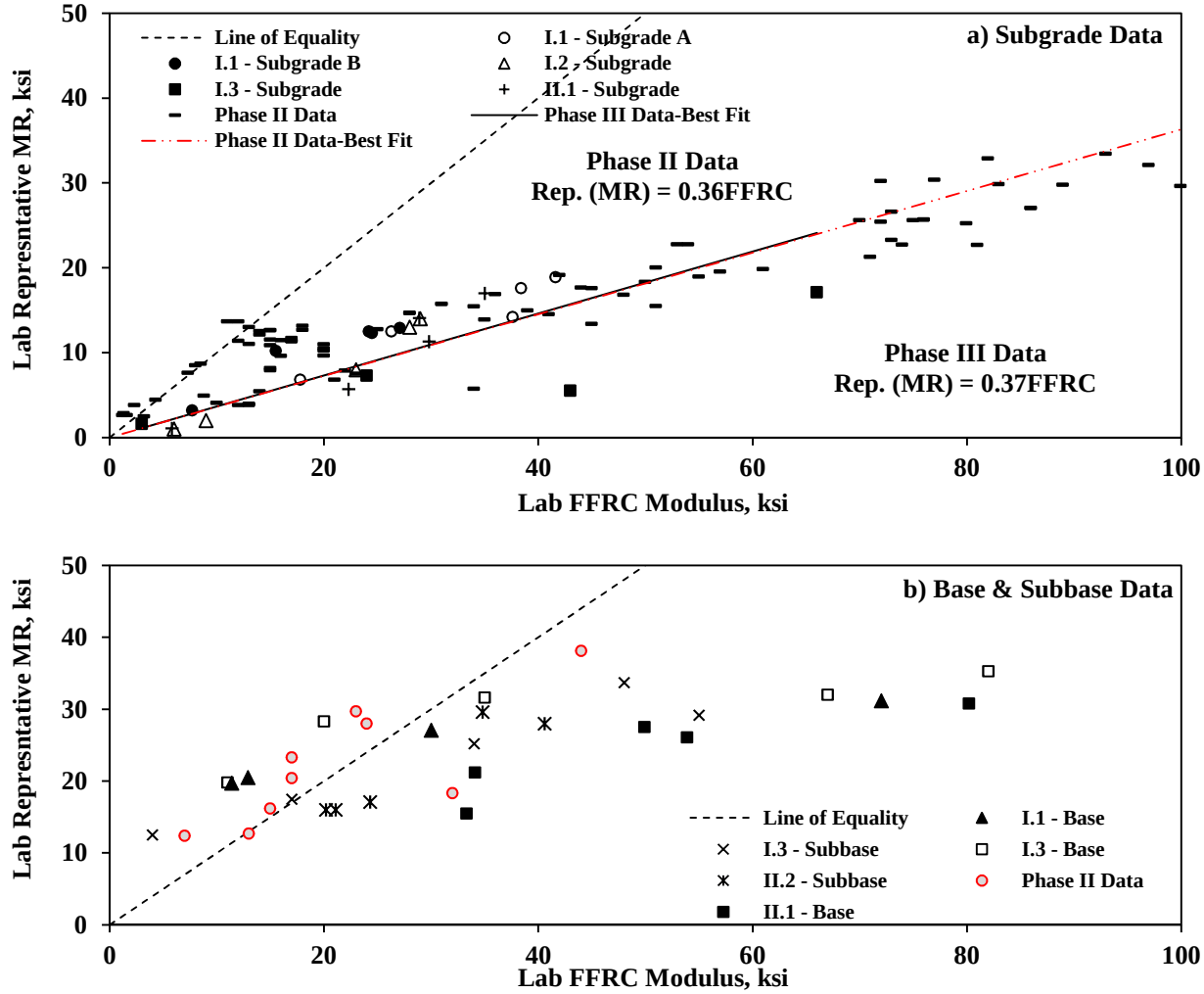

Figure 8.2.4 – Correlation between Laboratory MR and FFRC Moduli

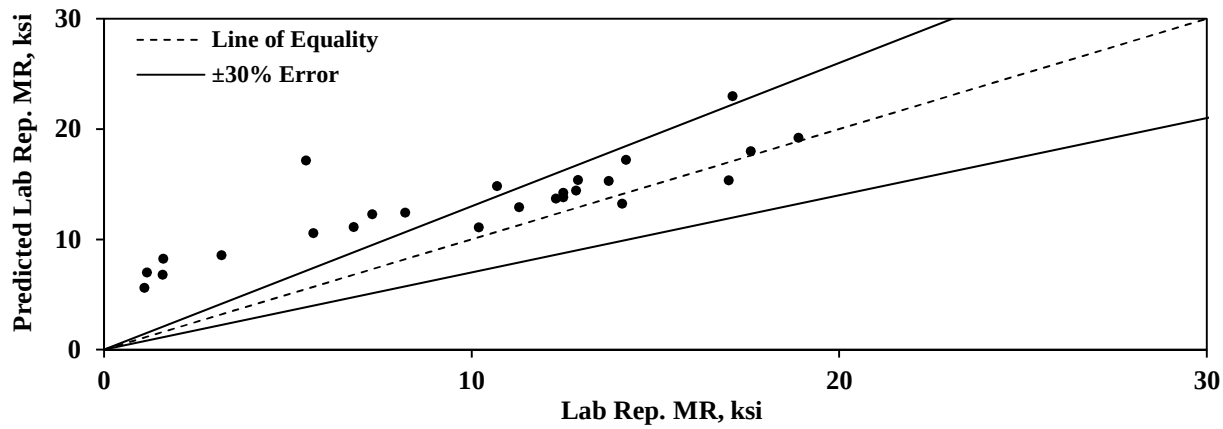

Figure 8.2.5 – Prediction of Laboratory Representative MR using Equation 3.2.3 for Phase III Subgrade Soils

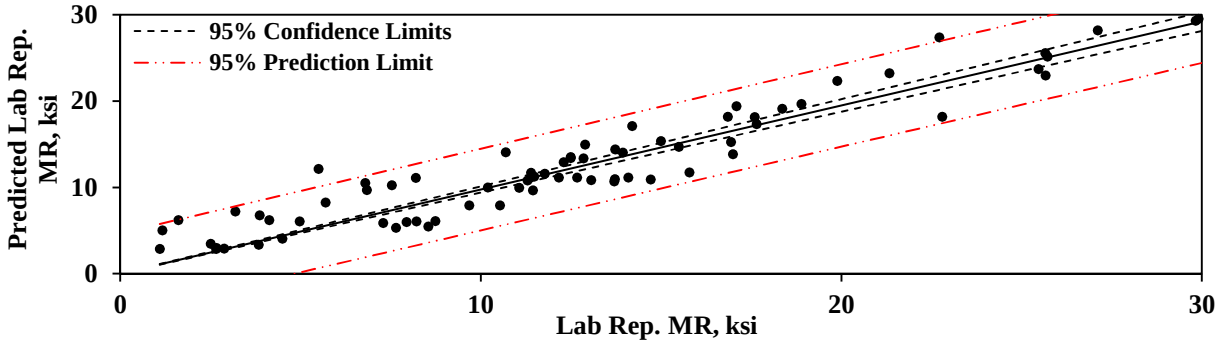

Figure 8.2.6 – Evaluation of Equation 8.2.1 in Predicting Laboratory Representative MR for Phase II and Phase III Subgrade Soils

8.3 Field Testing Program

Test sections at different sites are illustrated in Figures 8.3.1 and 8.3.2. Table 8.3.1 contains a list of field tests carried out at each site. In addition, soil samples were extracted from the compacted layer at most test spots to estimate their oven-dry moisture contents. The results from the Geogauge are discussed in the appendices but are not included herein due to the uncertainty in the results.

8.4 Evaluation of Moisture-Density Technologies

Subgrade Layer: Comprehensive discussions of moisture-density results from all field evaluation sites are included in Appendices H through L. The moisture contents measured with the nuclear density and electrical impedance spectroscopy technologies (NDG and SDG devices, respectively) during Phase III are compared with the oven-dry moisture contents in Figures 8.4.1a and 8.4.1b, respectively. The uncertainties associated with the NDG-oven moisture contents are reasonably random. Figure 8.4.1b indicates that the SDG results are not very sensitive to the changes in moisture content in a number of occasions. Since NDG tests are not a part of routine quality control process of INDOT anymore, only the SDG data were available for that site. Limited number of sand-cone and drive cylinder tests was performed to evaluate the in-situ dry density. Soil samples were also extracted at the same locations to estimate the oven-dry moisture content.

The cumulative distributions of the differences between the values measured with the two field devices and oven moisture contents are shown in Figure 8.4.1c. The NDG exhibits less variability in moisture readings as compared to the SDG. Even though the NDG and SDG seem to have similar error distributions, the correlation coefficients of the NDG readings relative to the oven moisture contents are generally greater than the correlation coefficients for the SDG readings (see Table 8.4.1). This observation suggests that the NDG estimated the moisture contents more accurately on this project.

Figure 8.4.2 compares the density measurements using the SDG and NDG. The dry densities estimated by the SDG in many occasions are greater than the NDG densities (especially for Site I.3).

Base/Subbase Layer: The performance of the moisture-density devices on the base/subbase layers is summarized in Figure 8.4.3. The NDG moisture contents for Site I.1 compare well with the oven-dry moisture contents (Figure 8.4.3a); comparison of the SDG moisture contents are shown in Figure 8.4.3b. Judging from the oven moisture contents, neither the NDG nor the SDG are sensitive to the changes in moisture content of the clean (less than 1% passing 200 sieve) base material used at Site 1.3. Comparing Figures 8.4.1a with 8.4.3a, the NDG exhibits less variability on the base materials as compared to the subgrade soils. Figure 8.4.3c contains the cumulative error distributions of the NDG and SDG for the base materials.

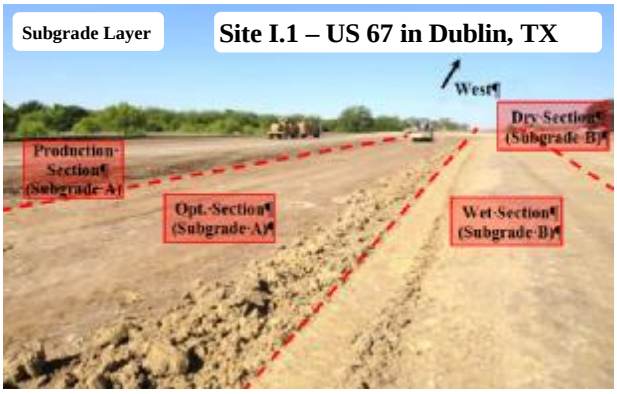

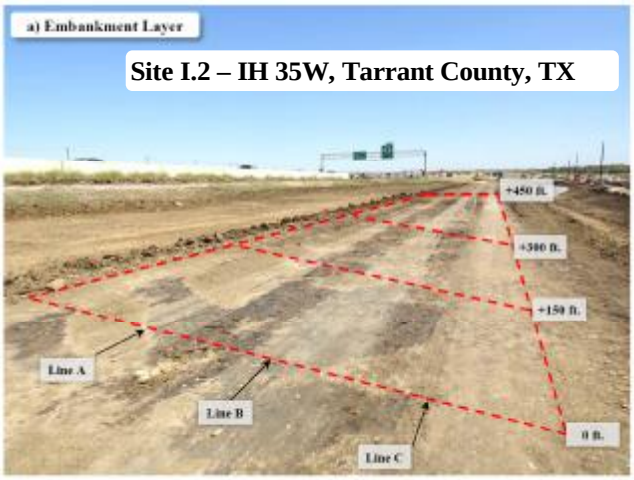

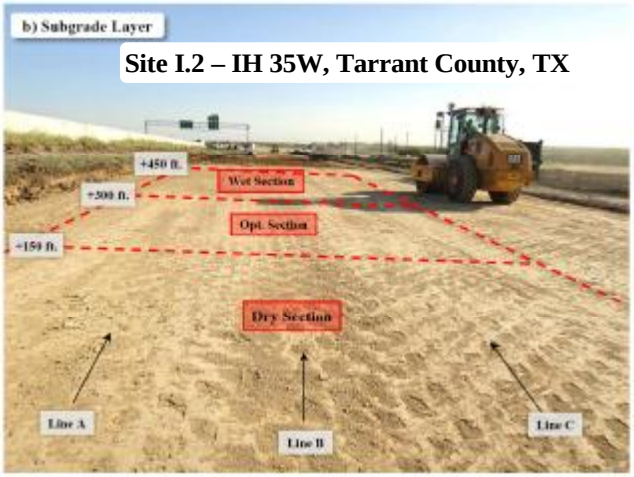

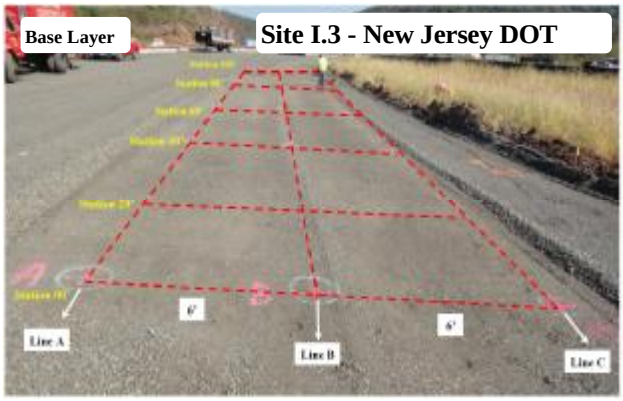

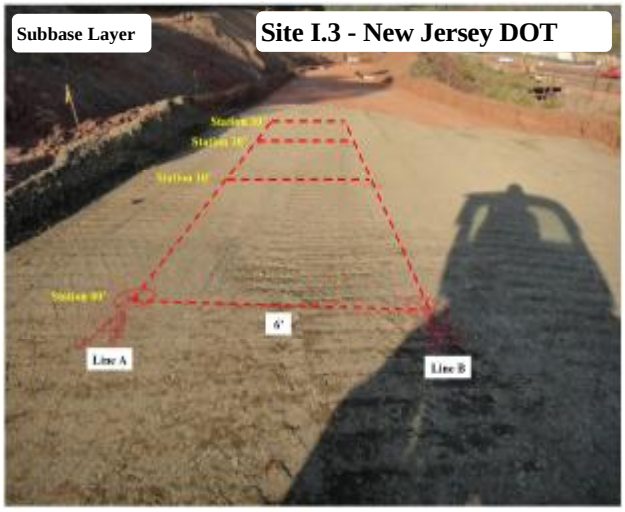

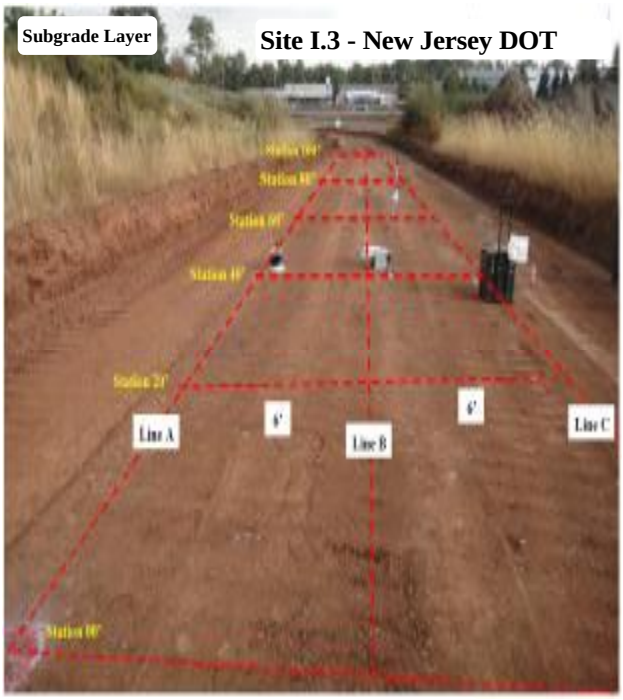

Figure 8.3.1 – Illustration of Test Sections on Field Evaluation Sites (Stage I)

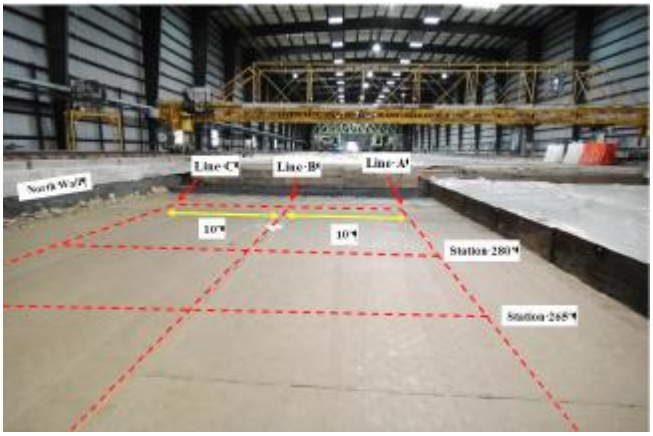

a) Site II.1 - FAA Facility in Atlantic City, NJ

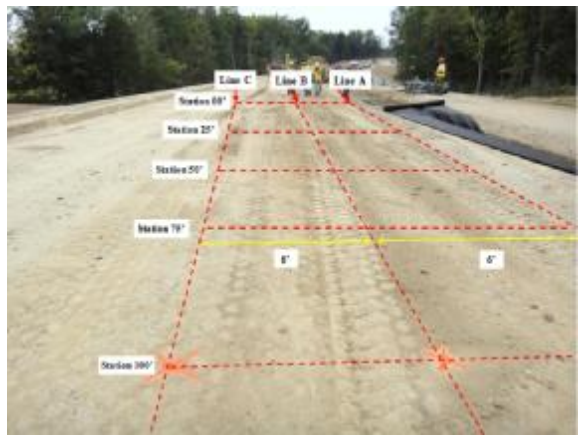

b) Site II.2 - Indiana DOT

Figure 8.3.2 – Illustration of Test Sections on Field Evaluation Sites (Stage II)

Table 8.3.1 – Quantities of Field Tests Carried out at each Site with Different Devices

Site No.	Type	SDG	NDG	LWD	PSPA	DCP	Oven Moisture Content
I.1	Subgrade A	86	110	212	306	33	26
	Subgrade B	77	69	178	202	32	25
	Base	63	80	93	374	26	32
I.2	Subgrade	63	114	156	458	64	52
I.3	Subgrade	-	31	72	126	18	36
	Subbase	-	15	48	54	18	16
	Base	-	30	72	121	8	36
II.1	Subgrade	36	-	108	244	36	6
	Subbase	-	-	108	244	36	3
	Base	-	36	108	244	-	-
II.2	Subgrade	15	-	30	52	27	-
	Subbase	5	-	5	-	-	2

Table 8.4.1 – Comparison of Correlation between Device Moisture Measurements and Oven Moisture Contents

Site	Correlation Coefficient	
	NDG	SDG
I.1	0.73	0.00
I.2	0.74	0.68
I.3	0.62	0.38

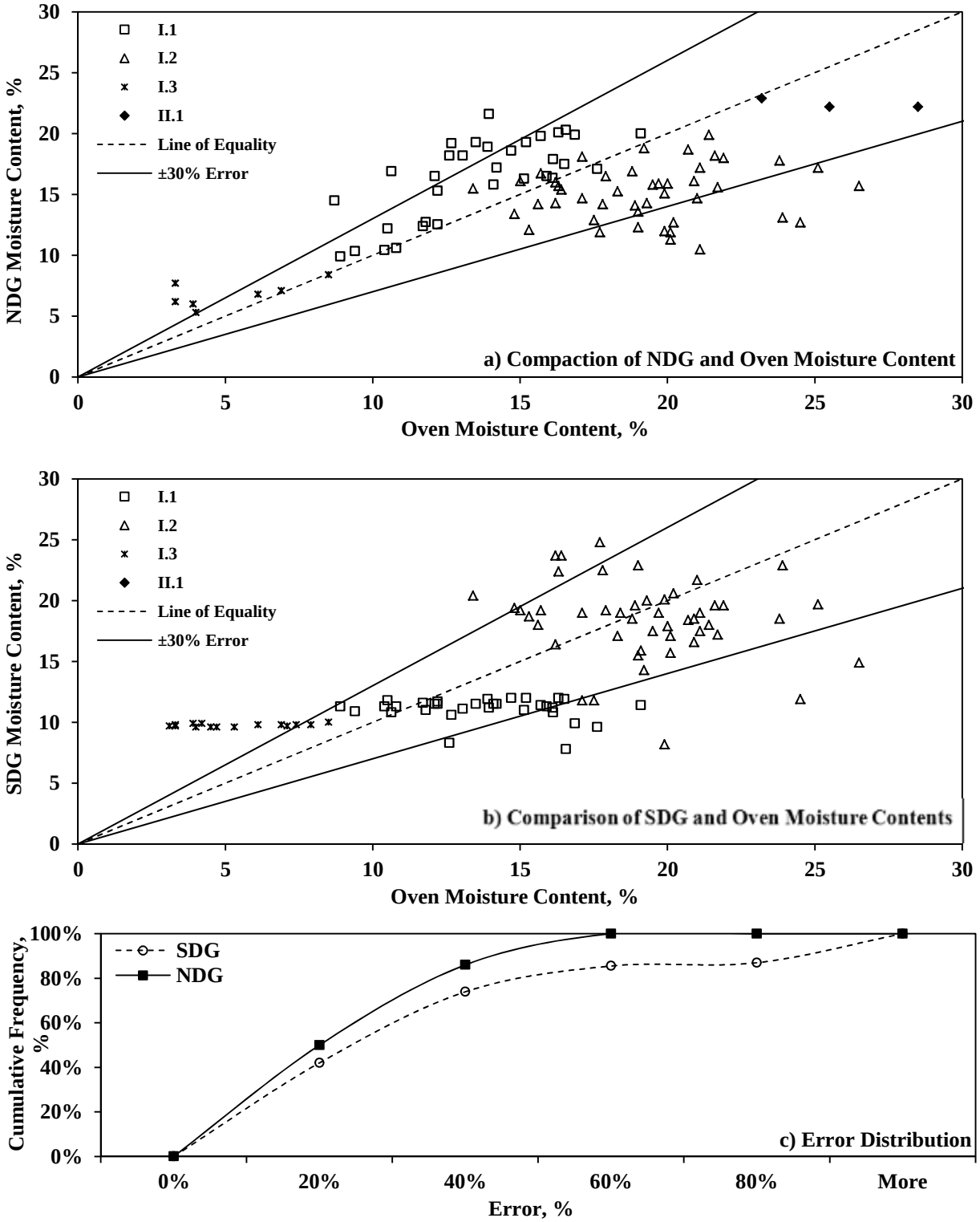

**Error is defined as (Device MC-Oven MC)/(Oven MC) where MC=Moisture Content*

Figure 8.4.1 – Comparison of NDG, SDG and Oven-Dry Moisture Contents for Field Evaluation Sites (Subgrade Layer)

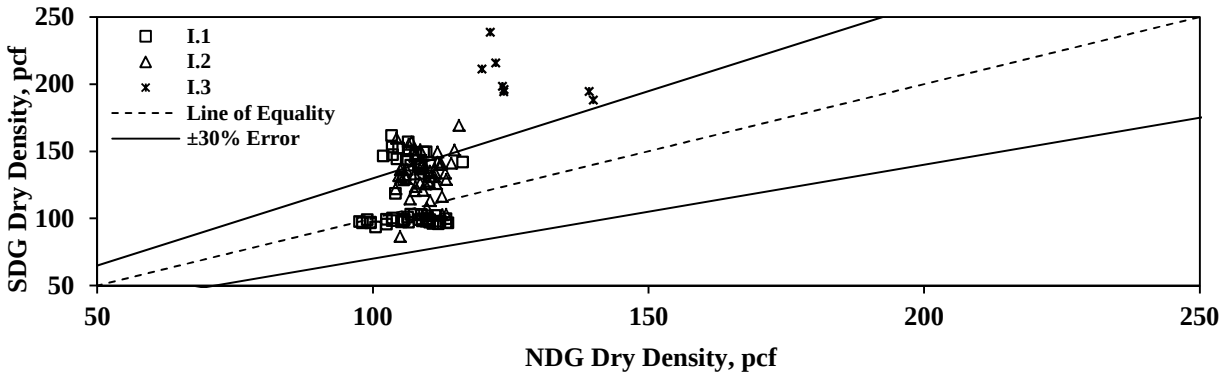

Figure 8.4.2 – Comparison of NDG and SDG Dry Densities for Subgrade Layers

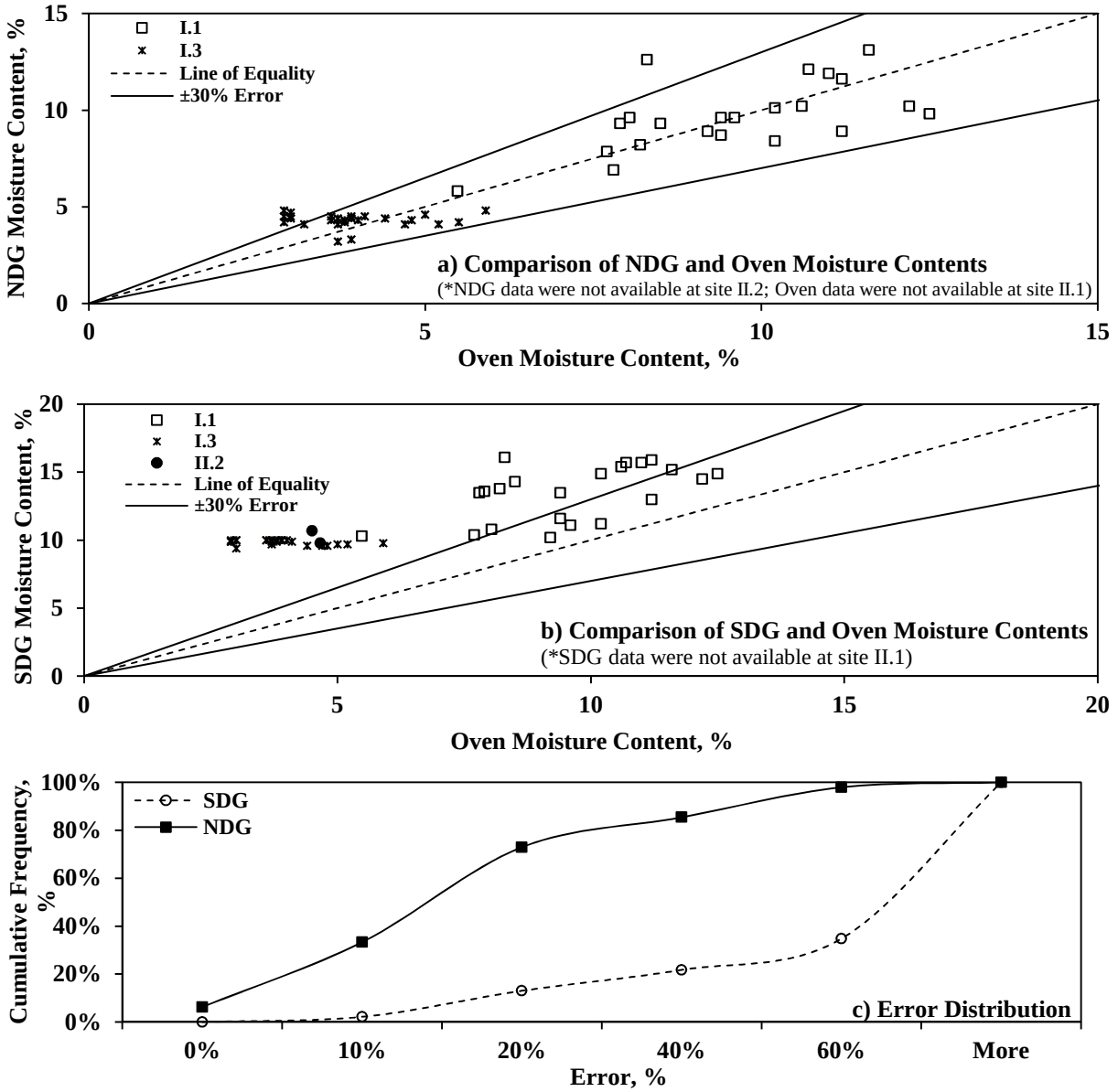

Figure 8.4.3 – Comparison of NDG and SDG Moisture Contents for Field Evaluation Sites (Base/Subbase Layer)

Figure 8.4.4 compares the dry densities of compacted base layers estimated with the SDG and NDG. While the two estimated densities are reasonably close for one site, they are systematically different for the other. These case studies along with those in Phase II of the project shed light on uncertainties associated with the well-established density-based methods. Well-qualified technicians carried out all the NDG tests with well-calibrated devices. The performance of the modulus-based technologies and devices should be considered with those uncertainties in mind.

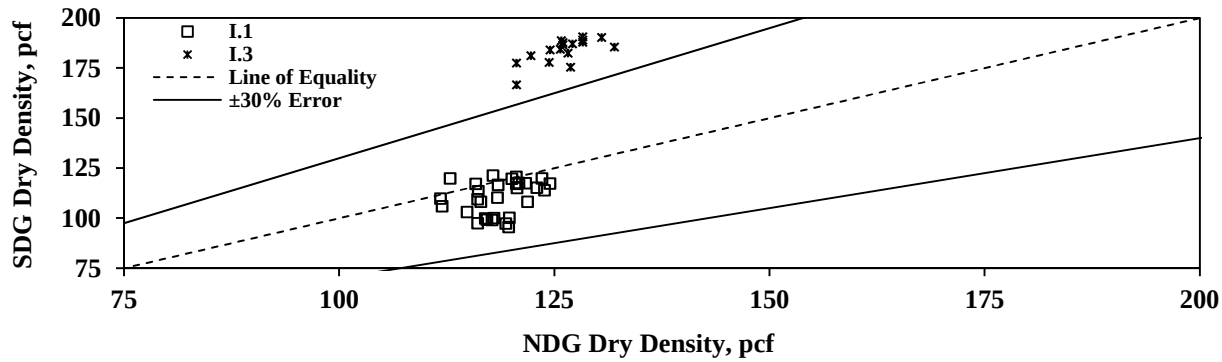

Figure 8.4.4 – Comparison of NDG and SDG Dry Densities for Field Evaluation Sites (Base Layer)

8.5 Evaluation of Modulus-Based Technologies

Subgrade Layer: As discussed earlier, test sections for the first two sites (I.1 and I.2) were prepared at three different moisture contents (dry of OMC, OMC and wet of OMC) to evaluate the modulus-based technologies under different moisture conditions. Figure 8.5.1 compares the average oven-dry moisture contents with their target values set based on their laboratory OMC values. The standard deviation of the oven-dry moisture contents at each section is also depicted as error bar in Figure 8.5.1. The oven-dry moisture contents are on average 3.6% less than their nominal target values for Site I.1 primarily due to the differences between the OMC used by the contractor and the actual OMC of the materials obtained from the materials retrieved at the site on the day of testing. Such offsets from the target moisture contents would affect the process of modulus-based quality control. For Site I.2, the differences between the target and average oven-dried moisture contents are less than Site I.1. However, despite the NDG readings, the average oven-dried moisture content of the optimum section is similar to the dry section. The routine construction processes were followed for the other three sites. The subgrade at Site I.3 was compacted at 6.8% less than the laboratory OMC as discussed in Appendix J. The oven-dry moisture contents from the field samples at Sites II.1 was 1.7% more than OMC and at Site II.2 was 1.2% less than its corresponding laboratory OMC.

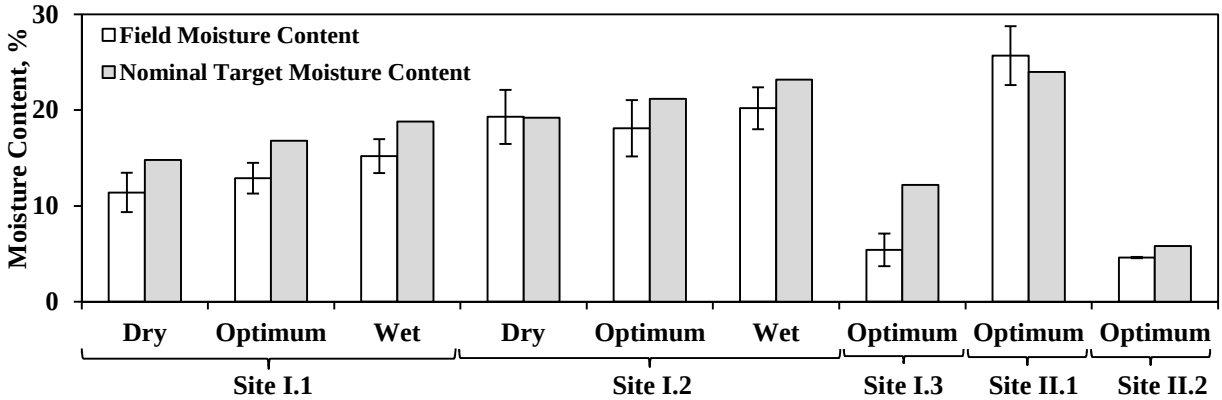

Figure 8.5.1 – Comparison of Field Oven-Dry Moisture Contents with Nominal Moisture Contents of Subgrades

The detailed evaluations of the modulus/stiffness technologies at various sites are included in Appendices H through L. The results from the devices based on ultrasonic surface wave (PSPA), LWD, and DCP technologies are summarized in Figures 8.5.2 through 8.5.4, respectively. Since the subgrade material at Site I.1 was placed and compacted at three different moisture contents (dry of OMC, OMC and wet of OMC) a clear pattern could be observed from the field modulus measurements (dry sections is expectedly stiffer than optimum and wet section). The same variation of moisture content was also applied during construction of Site I.2. As shown in Figure 8.5.1, except for the dry section, the sections were not placed very close to their designated target moisture contents. The variability in modulus results between the three sections (dry, optimum and wet) observed in Site I.2 in Figures 8.5.2 through Figure 8.5.4 is due to such moisture offsets.

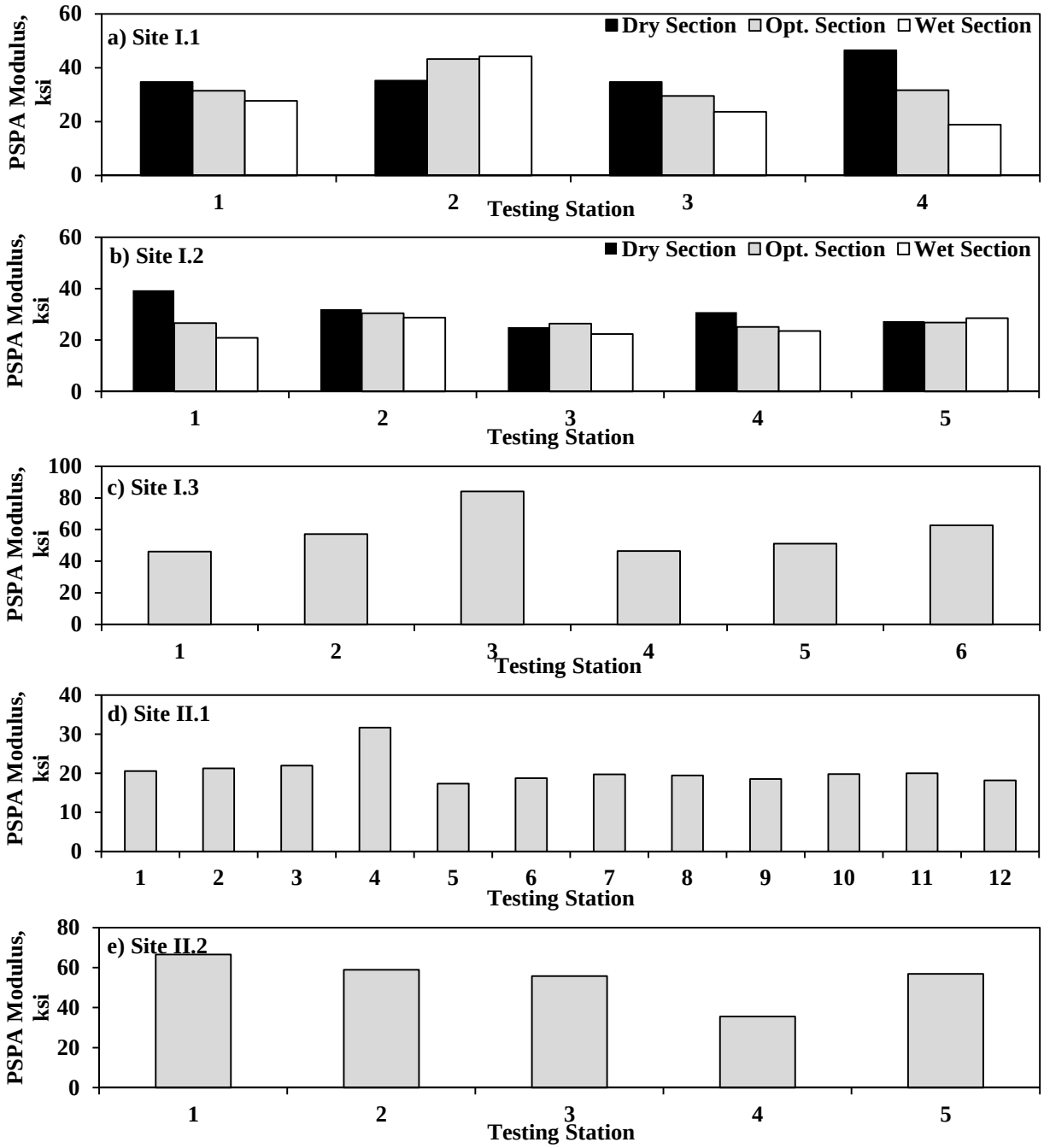

Figure 8.5.2 – Summary of Average PSPA Measurements for Subgrades at Different Sites

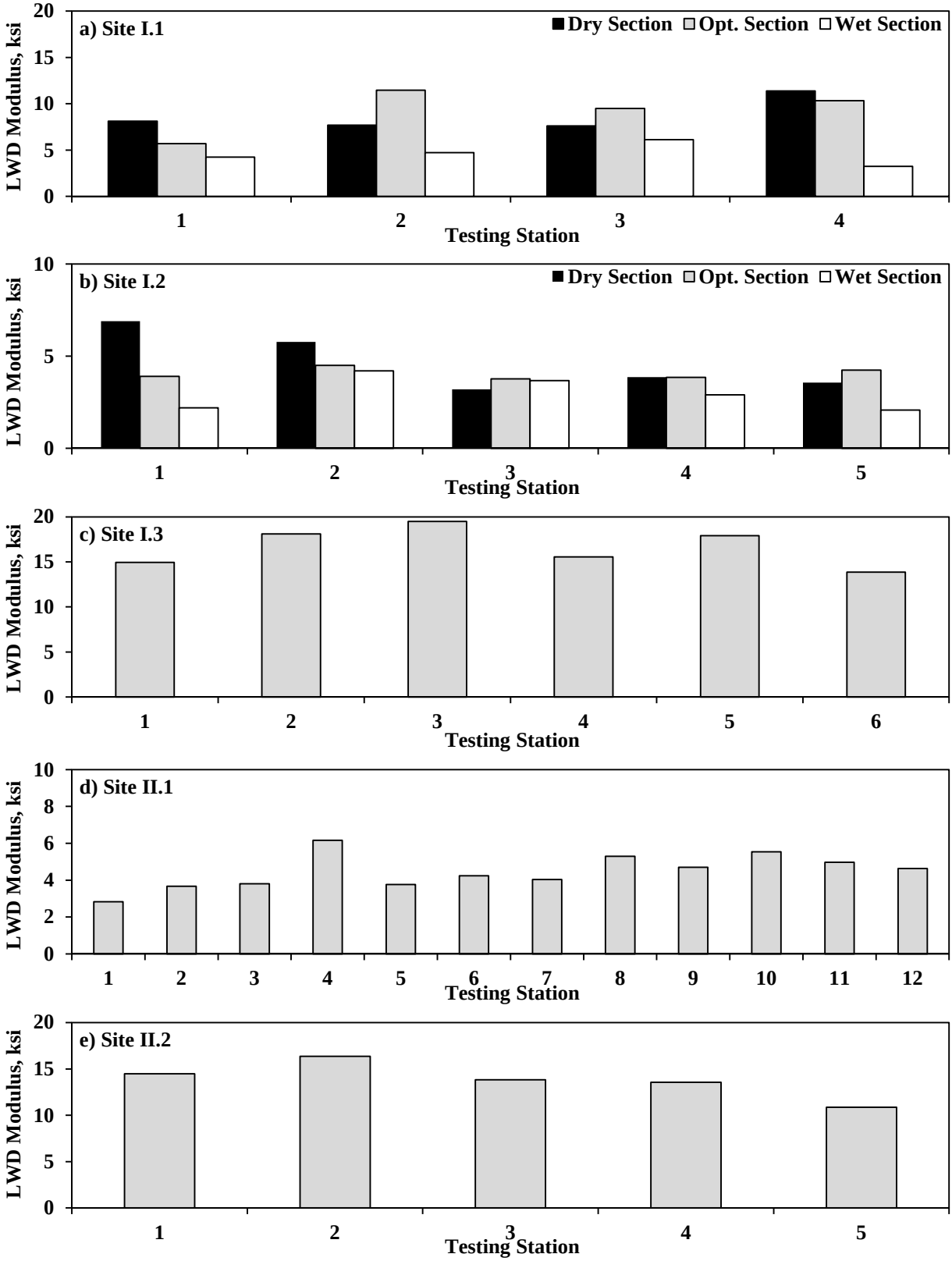

Figure 8.5.3 – Summary of Average Zorn LWD Measurements for Subgrades at Different Sites

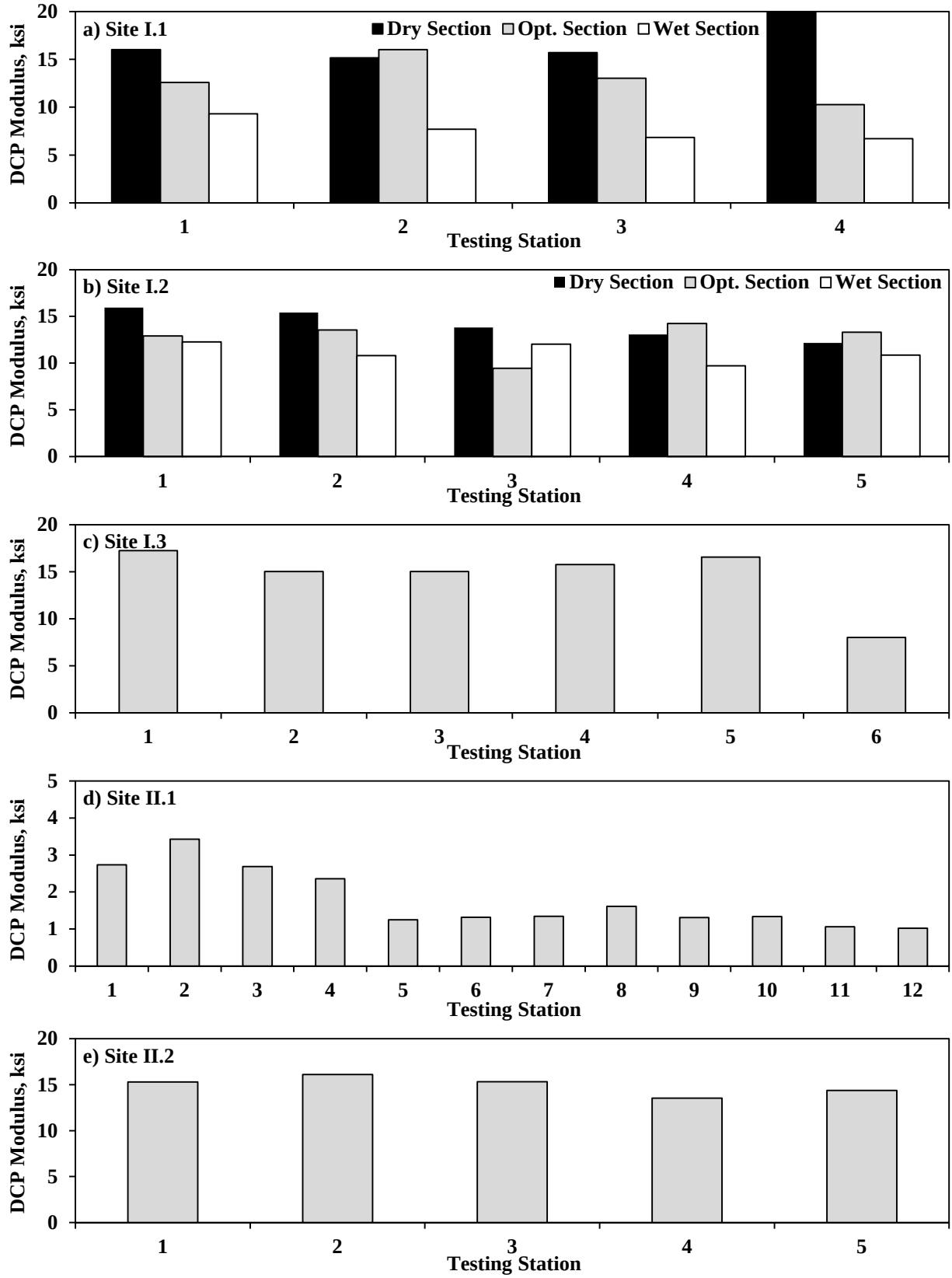

Figure 8.5.4 – Summary of Average DCP Measurements for Subgrades at Different Sites

Base Layer: Four sites (I.1, I.3, II.1 and II.2) contained base/subbase layers. Limited number of oven-dry moisture samples was collected on Site II.1 (three subbase material samples that extracted for sand cone test) and II.2 (two samples on subbase layer). Figure 8.5.5 compares the oven-dry moisture contents of the materials sampled during the testing of the base/subbase layers with their nominal target moisture contents. The differences between the two moisture contents in some cases are significant. The site-related variability in moisture contents (as judged by the error bars) is high for Site I.1.

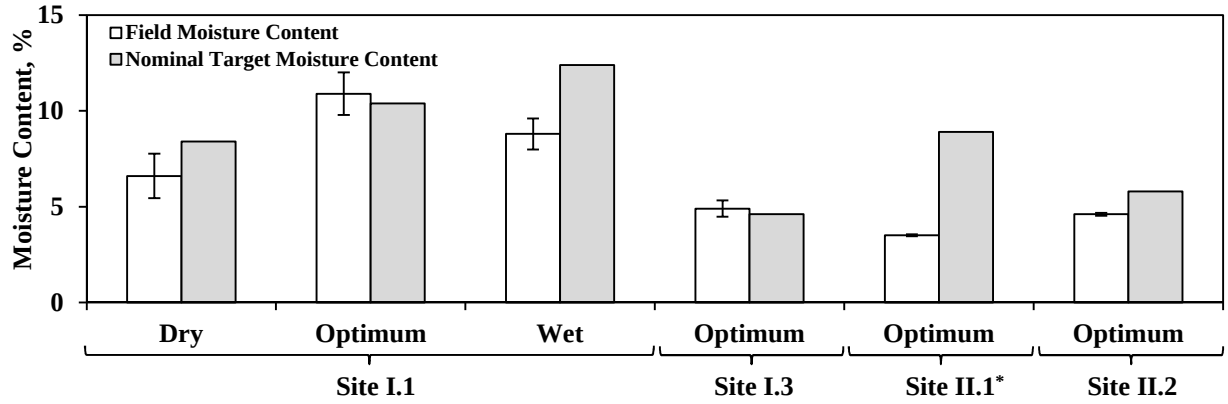

*These data correspond to subbase layer of Site II.1. Oven-dry moisture data were not collected after compaction of base layer at Site II.1 (only NDG data was available).

Figure 8.5.5 – Comparison of Field Oven-Dry Moisture Content with Laboratory OMC (Base/Subbase)

Figure 8.5.6 summarizes the average PSPA measurements on compacted base/subbase layers. The average PSPA moduli for the dry, optimum and wet sections of Site I.1 were 76, 74 and 51 ksi, respectively (with the corresponding standard deviations of 14, 9 and 15 ksi). Similar results but for the LWD are summarized in Figures 8.5.7. A Zorn LWD device was used on all base/subbase layers except for Site II.1 where the agency utilized a Dynatest LWD as a part of their routine quality control process. The average LWD moduli for the dry, optimum and wet sections of Site I.1 were 19.2, 18.7 and 12.4 ksi, respectively (with the corresponding standard deviations of 1.2, 1.1 and 2.9 ksi). Those trends are similar to the trends observed with the PSPA. Figure 8.5.8 summarizes the measured field DCP moduli, which suggest that the DCP results are not sensitive to the moisture content of the compacted base layer of Site I.1 as reflected in Figure 8.5.8a. Poisson's ratios of 0.40 and 0.35 were used for subgrade and base/subbase materials, respectively. The average DCP moduli for the dry, optimum and wet sections are 24, 26 and 26 ksi, respectively.

8.6 Modulus-Moisture Correlations

The modulus-moisture correlations for all sites are included in Appendix H through L. Figure 8.6.1 summarizes the relation between the measured field moduli from different devices and corresponding oven-dry moisture contents for all subgrades. The PSPA, LWD and DCP exhibit reasonable site-by-site trends. However, a global correlation for all different sources of materials cannot be ascertained.

The normalized measured moduli (M/M_{opt}) are plotted against the normalized degree of saturation ($S\text{-}S_{opt}$) in Figure 8.6.2 for all subgrade soils. The Cary and Zapata (2010) and MEDPG (2004) models are superimposed on the figure. Irrespective of the device used, neither of the two relationships can explain the field data for degrees of saturation greater than the S_{opt}. The data from the LWD exhibit more scatter than the other two devices. Considering the scatter in the data, the field results from the three devices match the MEPDG model better for the degrees of saturation less than S_{opt}.

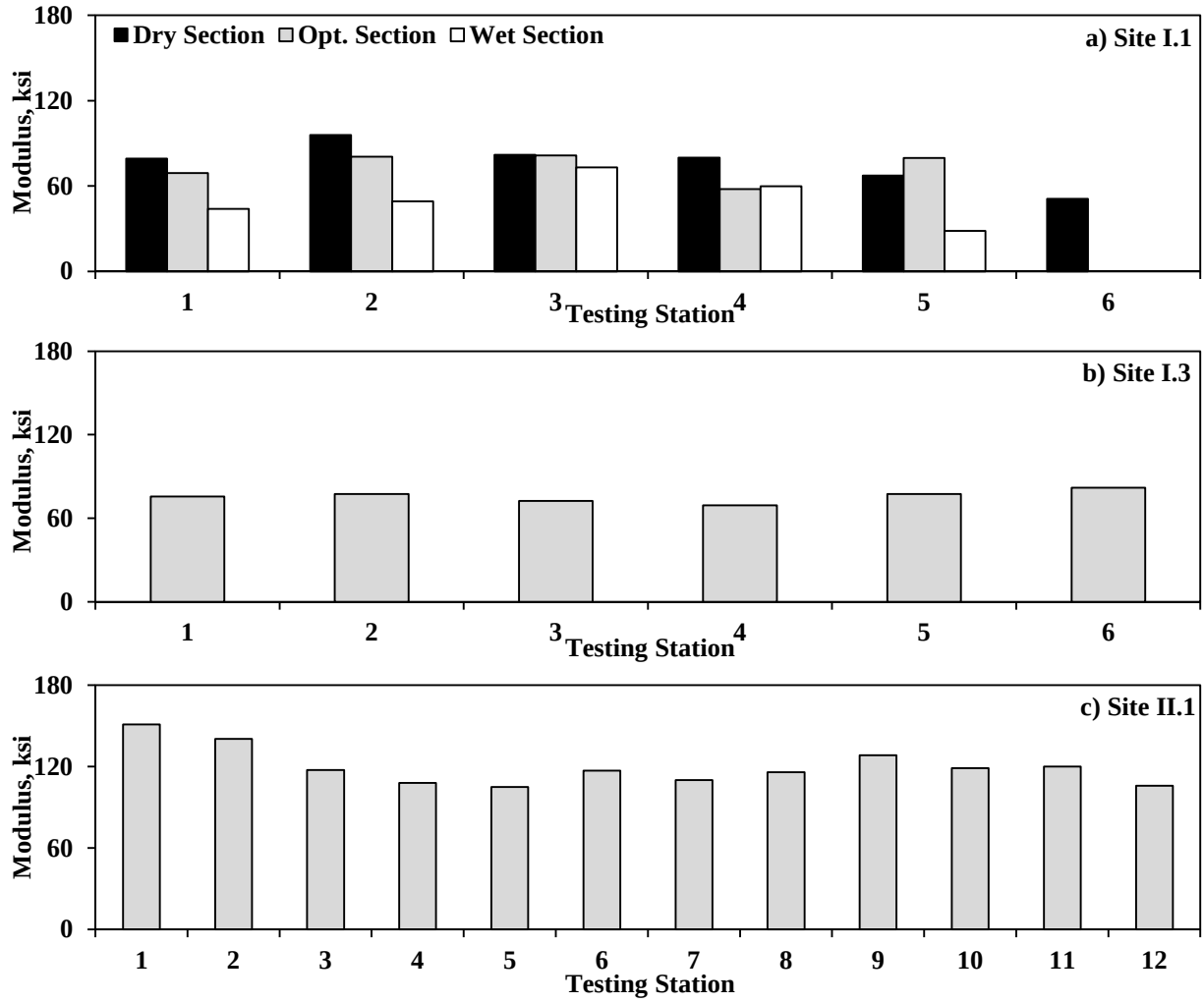

Figure 8.5.6 – Summary of Average PSPA Measurements for Base/Subbase at Different Sites

As discussed in Section 3.3 (see Figure 3.3.7), the normalized laboratory moduli could be correlated to the normalized moisture content [(MC-OMC)/OMC]. Figure 8.6.3 summarizes the normalized field moduli with respect to normalized oven-dry moisture contents for different devices. The trends from Figure 3.3.7 are also superimposed on the field results. The field data are mostly bracketed between the FFRC and MR laboratory models for all three devices. For most devices, the FFRC laboratory model seems to explain the field data slightly better.

As reflected in Figure 8.6.4, limited field data are currently available for the evaluation of modulus-moisture relationships for the unbound aggregate (base/subbase) materials. The field moduli from Site I.1 show some correlation with the oven-dry moisture contents. The field moduli from Site I.3 base layer and Sites II.1 and II.2 subbase layer do not exhibit a clear trend because their variations in the moisture content was small.

The LWD shows the best correlation between the measured field moduli and oven-dry moisture contents for Site I.1. Investigation of additional sources of base materials is necessary to study the modulus-moisture correlation on compacted base layers.

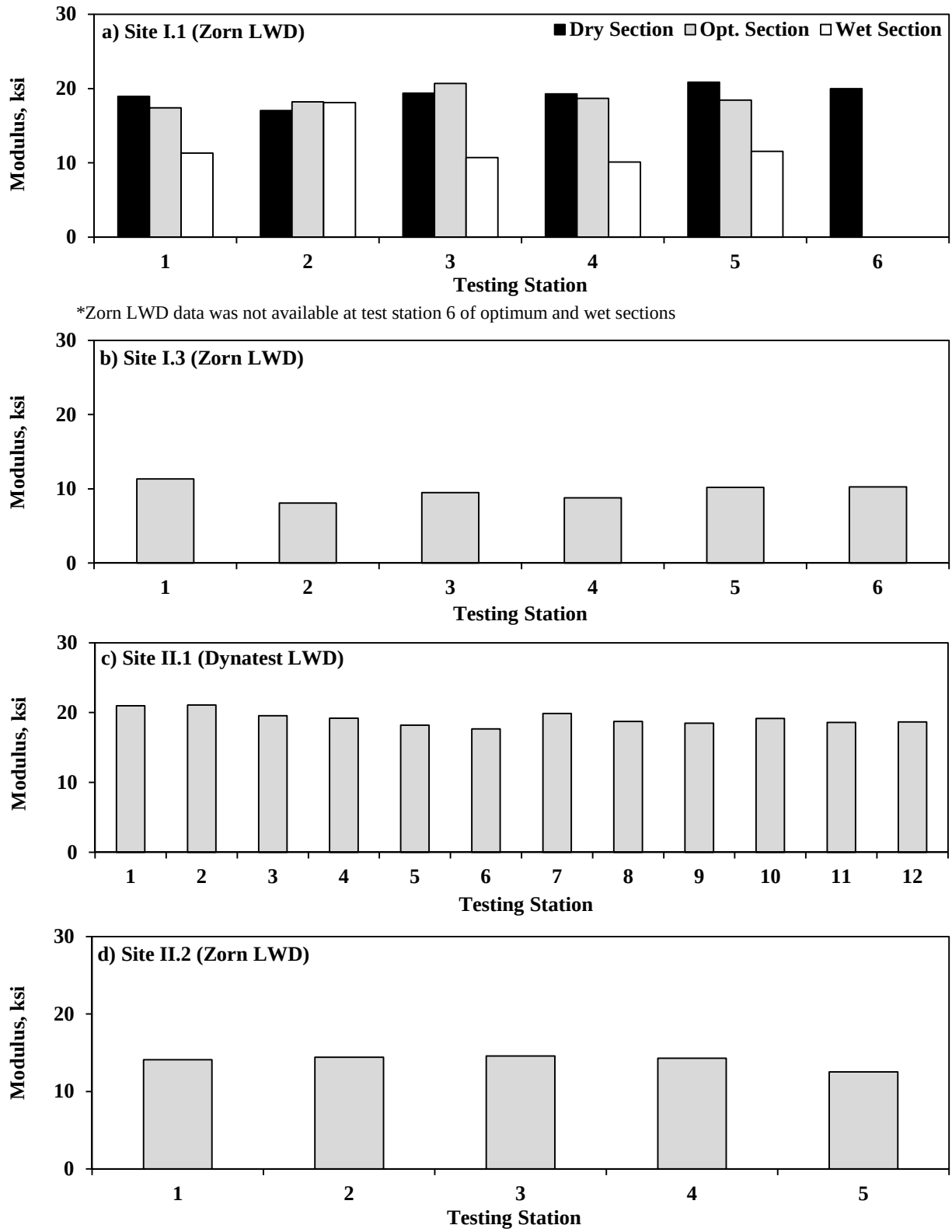

Figure 8.5.7 – Summary of Average LWD Measurements for Base/Subbase at Different Sites

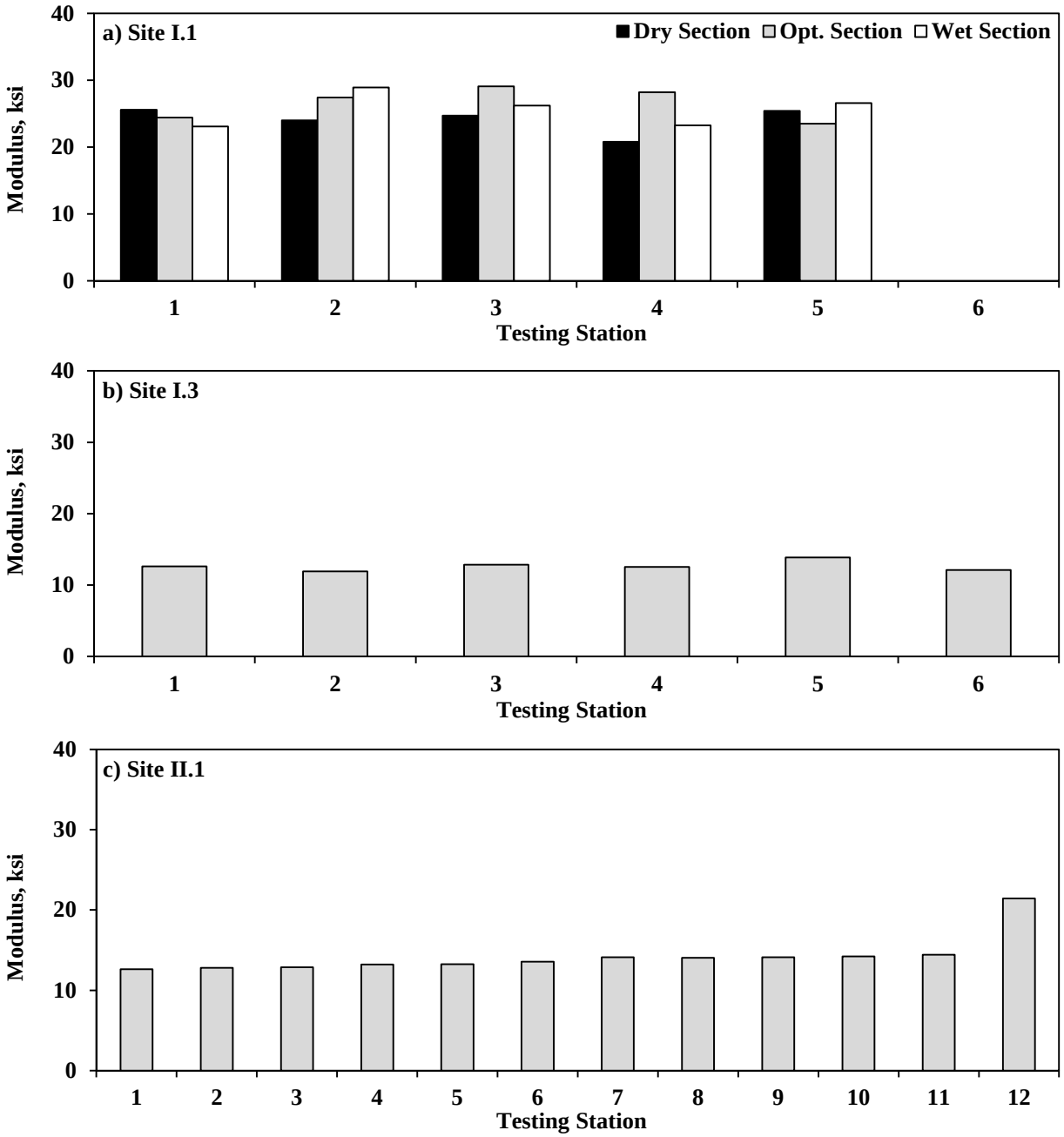

*DCP data were not collected on subbase layers of Sites Site II.1 and II.2

Figure 8.5.8 – Summary of Average DCP Measurements for Base/Subbase at Different Sites

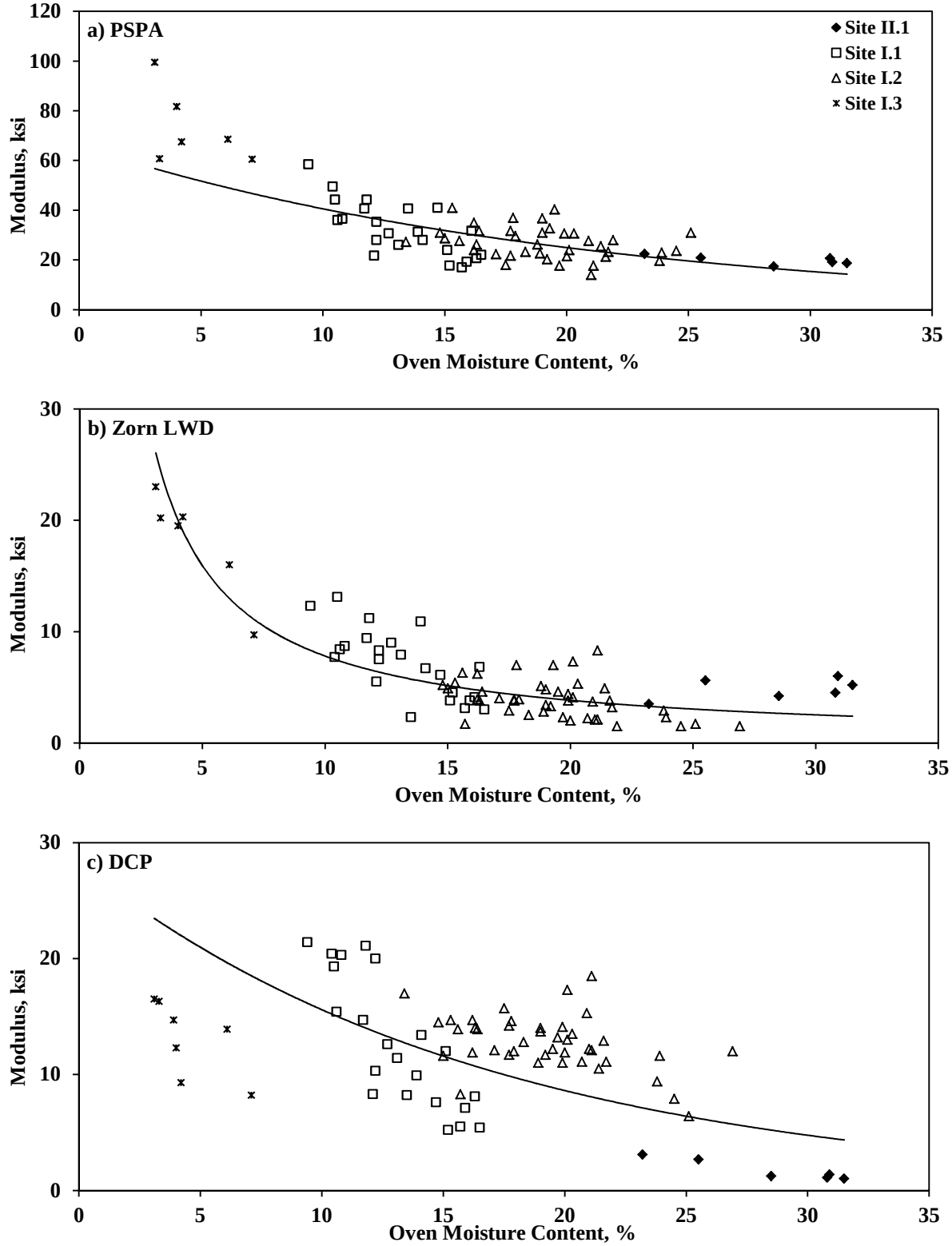

*Oven moisture data were not available on subgrade layer of Site II.2

Figure 8.6.1 – Field Modulus-Moisture Correlations based on Oven-Dry Moisture Contents

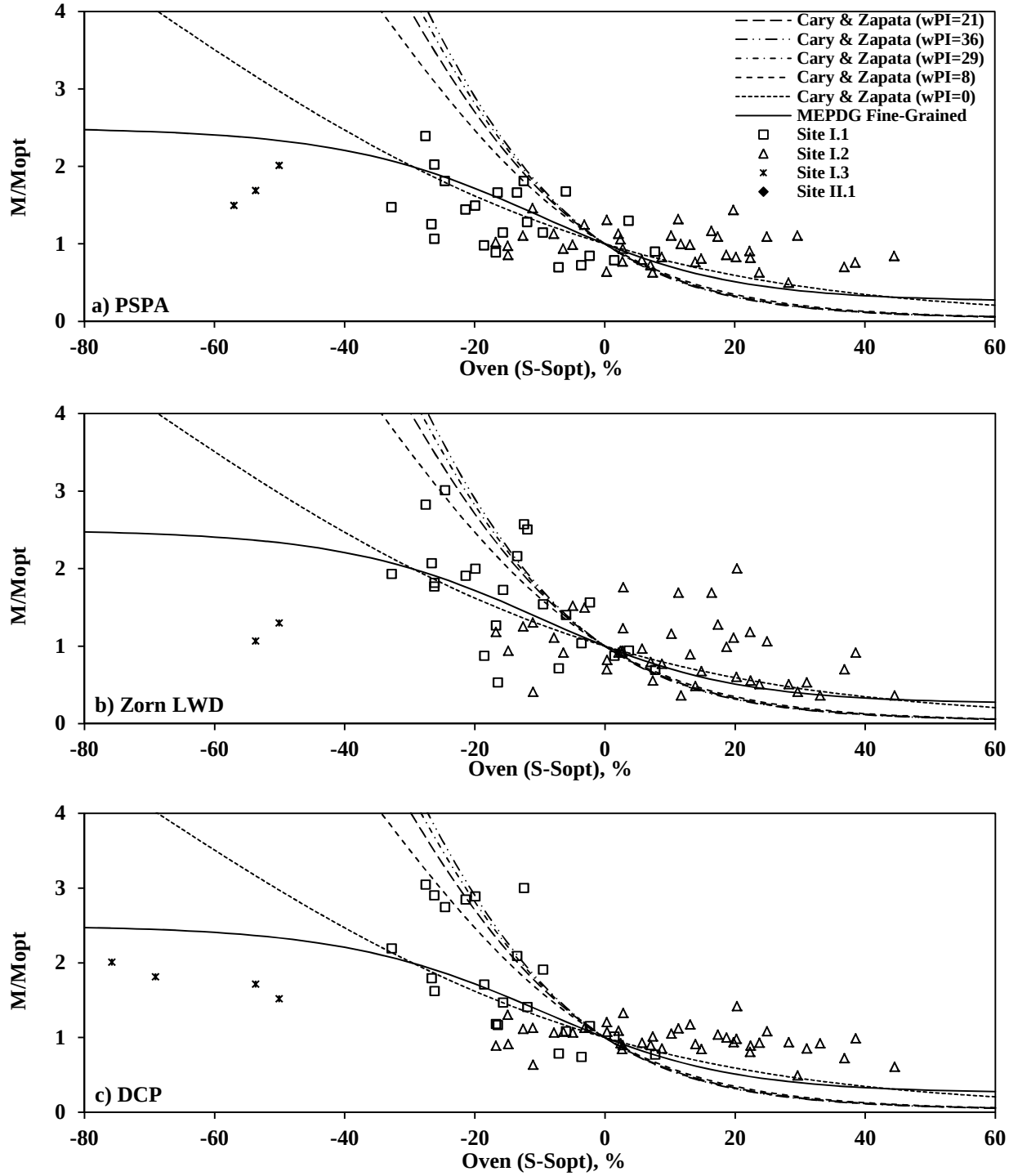

Figure 8.6.2 – Correlation of Normalized Field Moduli with Normalized Degree of Saturation (using Oven-Dry Moisture Contents)

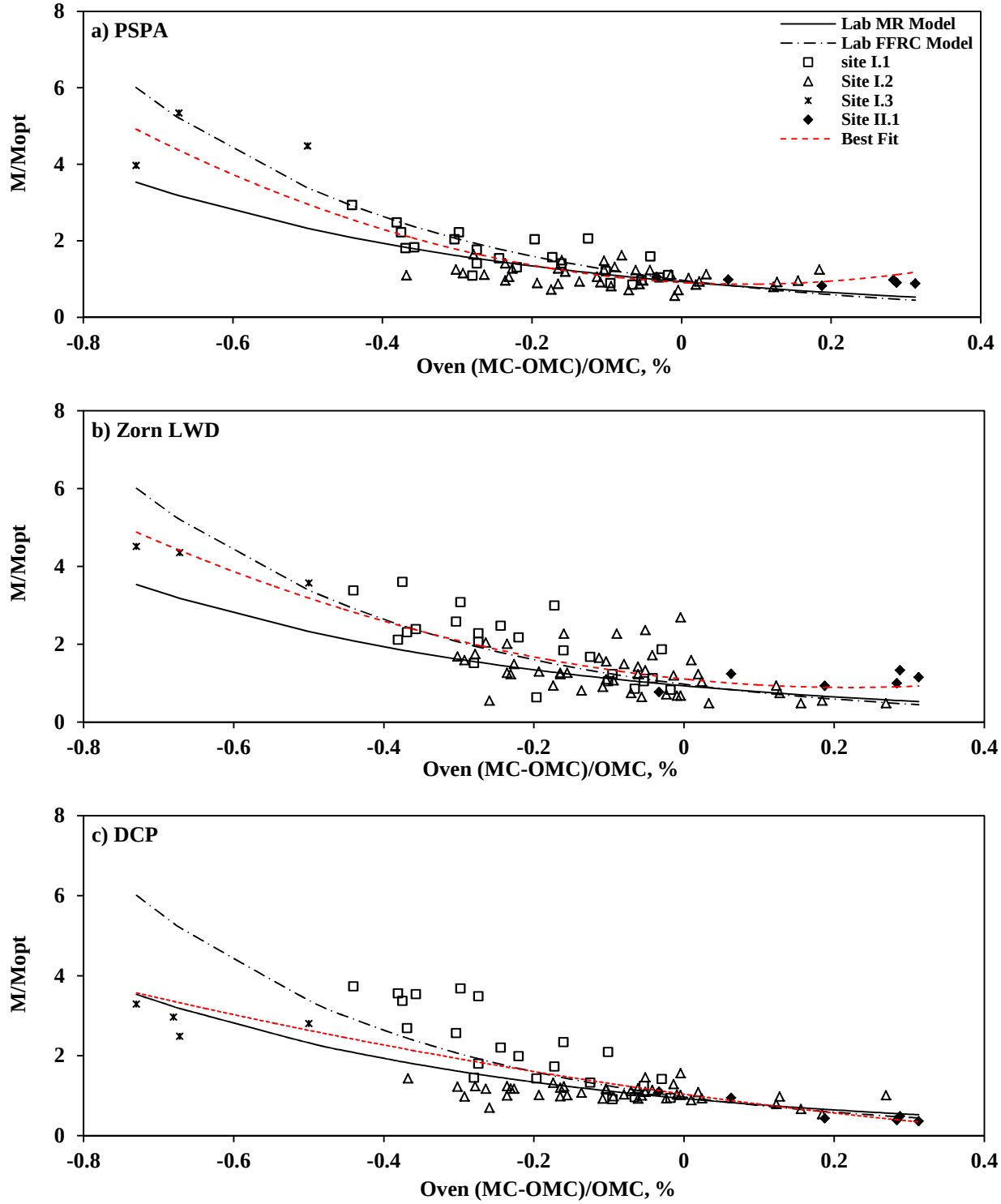

Figure 8.6.3 – Correlation of Normalized Field Moduli with Normalized Oven-Dry Moisture Contents

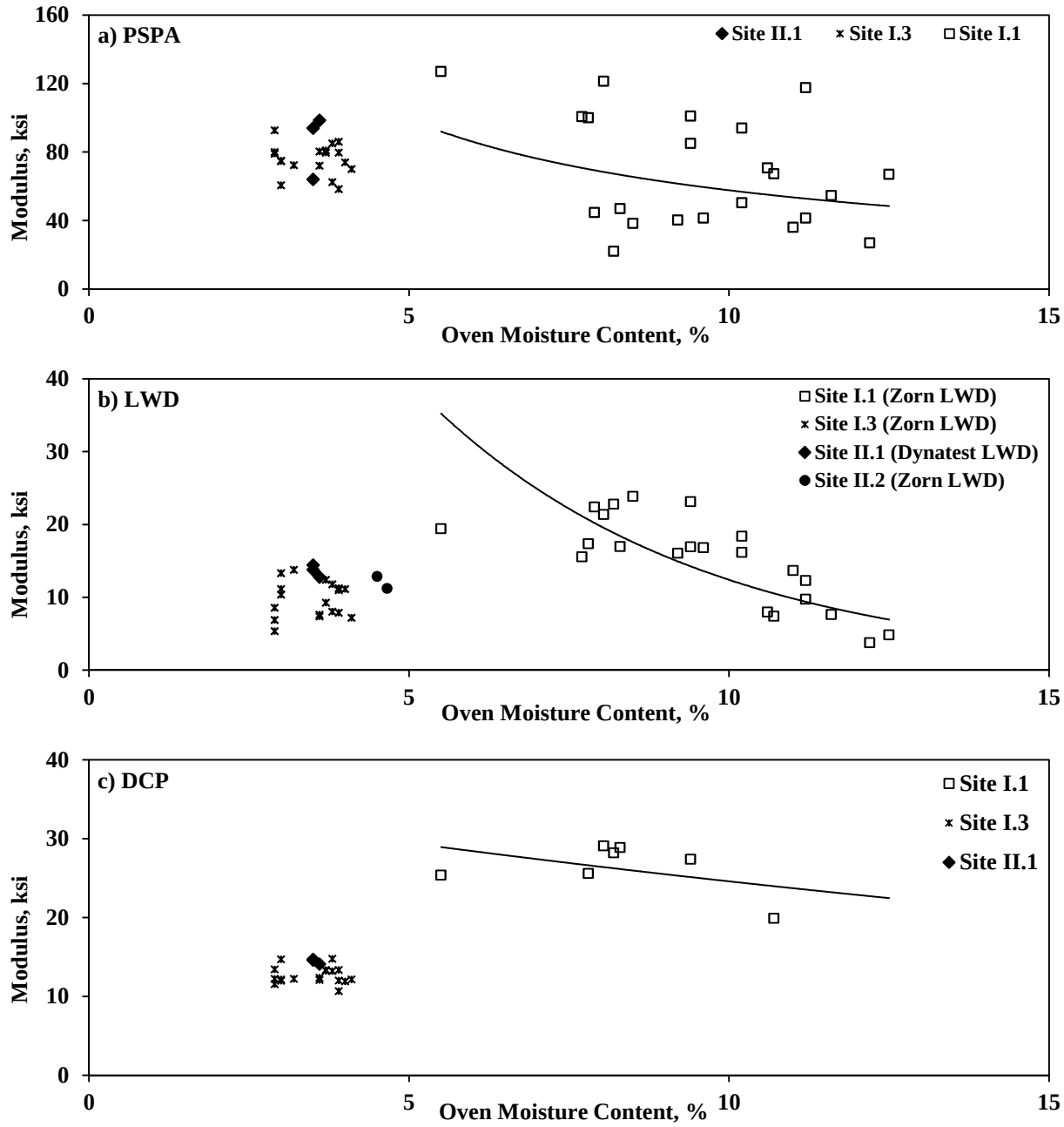

Figure 8.6.4 – Modulus-Moisture Correlations of Base Layer using Oven-Dry Moisture Contents

The modulus-moisture content relationships for the subgrade materials from laboratory and field tests are compared in Figure 8.6.5. As reflected in Figure 8.6.5a, the field PSPA modulus-moisture correlation and the adjusted laboratory FFRC modulus-moisture relationship (as discussed in Section 6.4) are for the most part closer than the same results for the other two devices. As explained in Section 6.5, the representative MR values from laboratory tests do not relate to the LWD moduli measured in the field at the same moisture contents (see Figure 8.6.5b). The DCP moduli and laboratory MR trends (Figure 8.6.5c) are in general agreement with significant scatter. The somewhat better relationships for the PSPA and DCP relative to LWD can be because they are layer-specific tests.

Similar results for the bases are summarized in Figure 8.6.6. The modulus-moisture trends for field and laboratory data are summarized separately for each geomaterial. The trends from the laboratory and field data are not as close as the ones observed for subgrade soils. The most favorable comparison is between the ultrasonic surface wave technology (PSPA device) moduli and the adjusted FFRC moduli within the limited ranges of laboratory moisture contents.

8.7 Variability of Modulus-Based Technologies

Triplicate tests were carried out with the PSPA and LWD at each test spot to quantify the variability of the devices. The variations of the COV of the triplicate measurements with measured average field modulus for different devices on the subgrade are summarized in Figure 8.7.1. A clear pattern cannot be observed from the results. As reflected in Figure 8.7.2, the COV of the PSPA measurements are as high as 74% with an average of 16%. The average COV of the LWD measurements is 13% with a maximum of 37%. At 80% confidence level, the PSPA exhibits a COV of 25% while the LWD has a COV of 20%.

The same methodology was repeated for the base/subbase measurements. As reflected in Figure 8.7.3, the COV values from the PSPA measurements on bases are as high as 51% with and average value of 16%. The COV values of the LWD measurements exhibit an average of 9% with a maximum of 25% (if the data from Site I.1 is ignored). Figure 8.7.4 summarizes the distributions of the COV values on the base layers. At 80% confidence limit, the COVs of the PSPA and LWD are 20% and 10%, respectively.

8.8 Acceptance Scenarios for Quality Control Process

Detailed acceptance scenarios for each site are included in Appendices H through L. Since the intelligent compaction (IC) technology was used at some sites, a summary of the IC results for Site I.1 along with the relevant modulus-based acceptance scenarios are discussed in this section first. The detailed discussion of such results for Site I.2 is included in Appendix I.

The IC roller drum and the soil interaction to compaction process were captured using the Compaction Meter Value (CMV). The CMV technology uses an accelerometer to measure the roller drum vibration in response to the soil behavior during the compaction. Figure 8.8.1 presents typical distributions of the CMVs with the number of roller passes for the three sections of subgrade at Site I.1.

The CMV distribution for the dry section tends toward higher values with increase in compaction effort. The CMV values for the OMC section do not change much after six and nine roller passes. On the contrary, the CMV values on the wet section decrease with more passes of IC roller passes.

Figure 8.8.2 compares the color maps of CMV distributions before placement and compaction of the subgrade layer and after the final pass of the IC roller on the compacted subgrade layer. More areas achieve higher compaction after compaction of the subgrade layer but some of them indicate lower CMV values after compaction of subgrade layer as compared to the embankment layer. The CMV distributions before (called mapping) and after compaction of the subgrade layer are summarized in Figure 8.8.3. The CMV values before and after the compaction of the subgrade layer are similar except for the wet section. The trends from the wet section clearly show the ineffectiveness of compaction for that section.

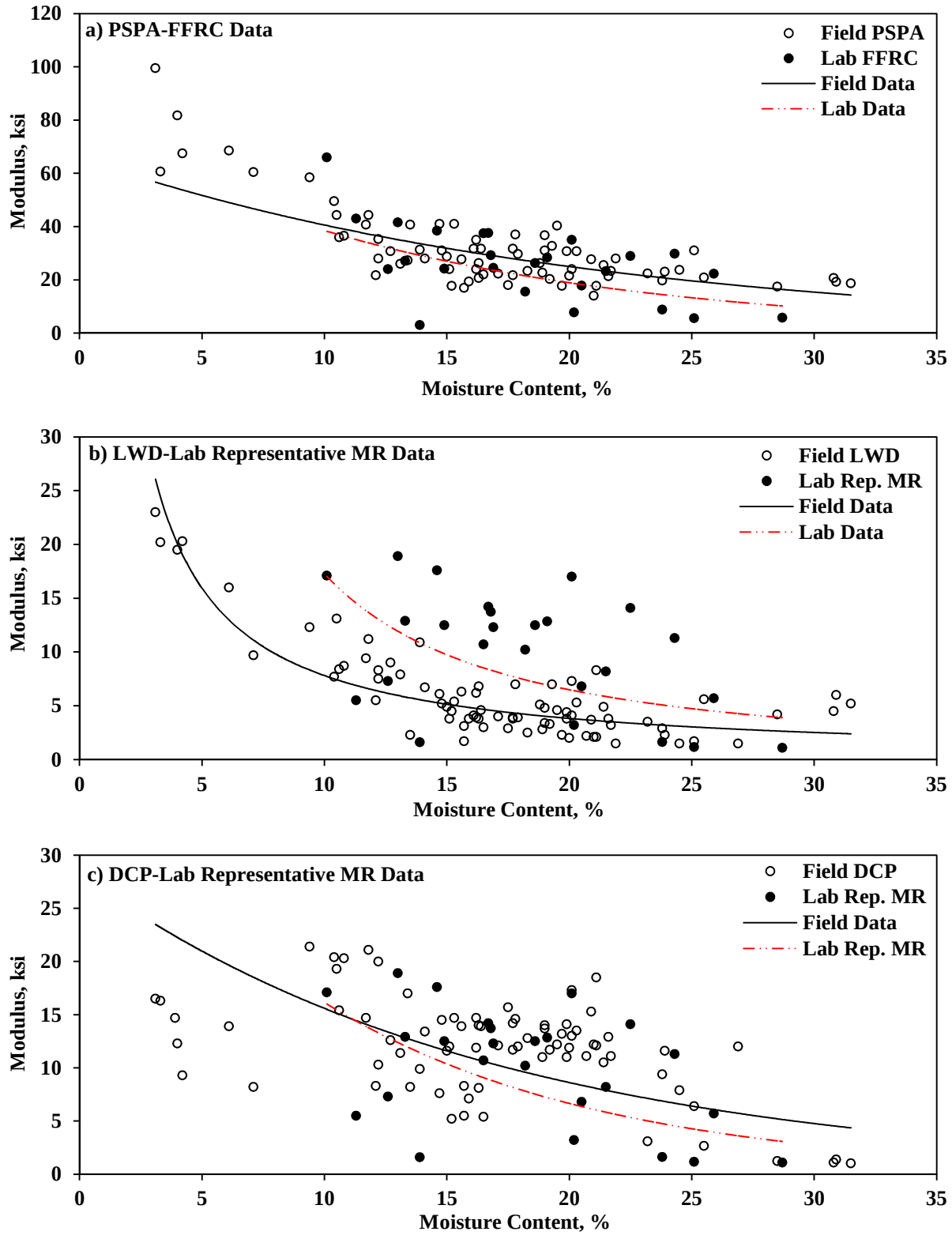

Figure 8.6.5 – Comparison of Modulus-Moisture Correlation between Field and Laboratory Data (Subgrade)

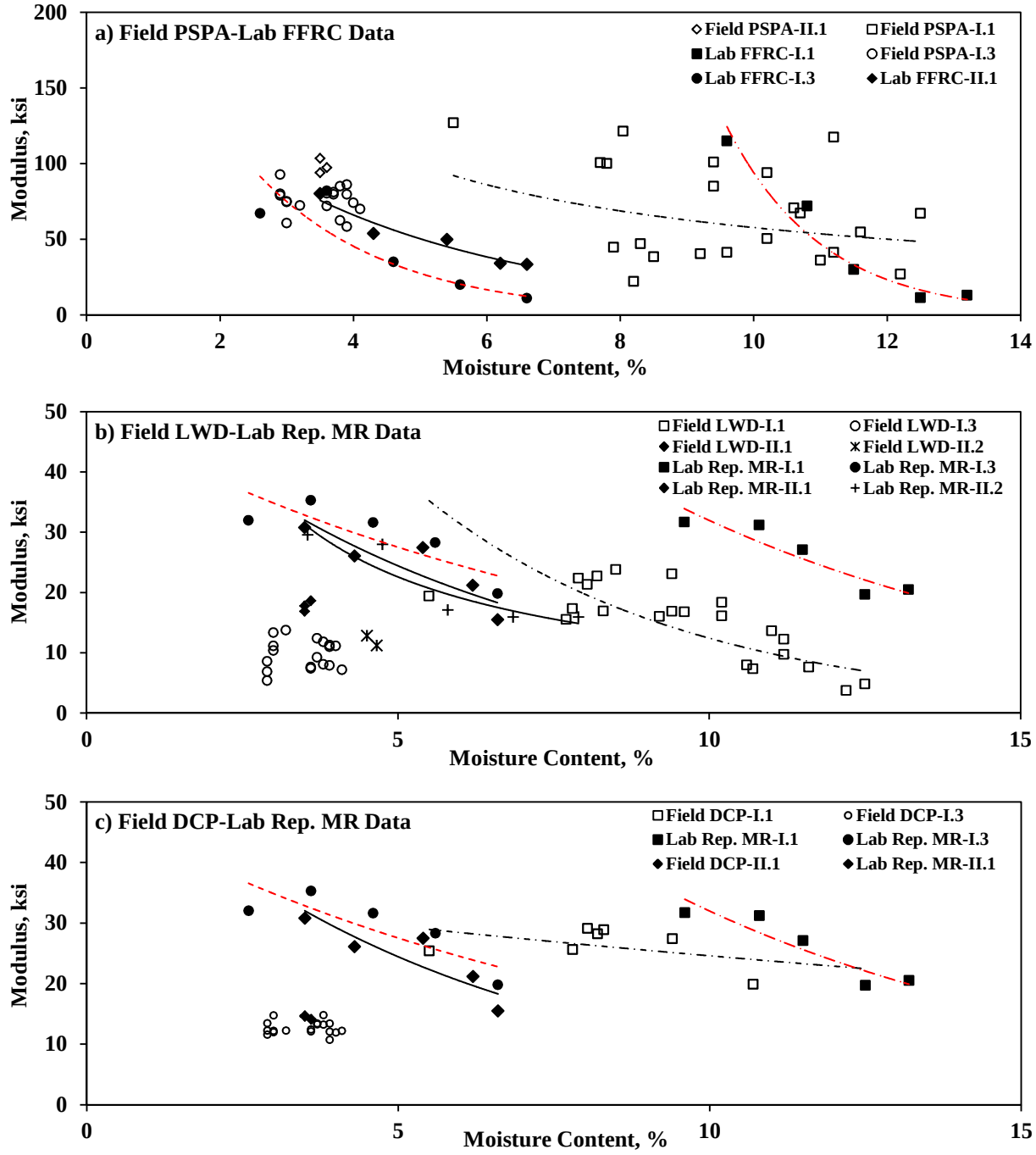

*Field DCP data at Site II.1 in this figure collected from subbase layer since no DCP data were available on base layer; the laboratory representative MR data at Site II.1 were available only for base materials due to instability of subbase laboratory samples.

Figure 8.6.6 – Comparison of Modulus-Moisture Correlation between Field and Laboratory Data (Base/Subbase)

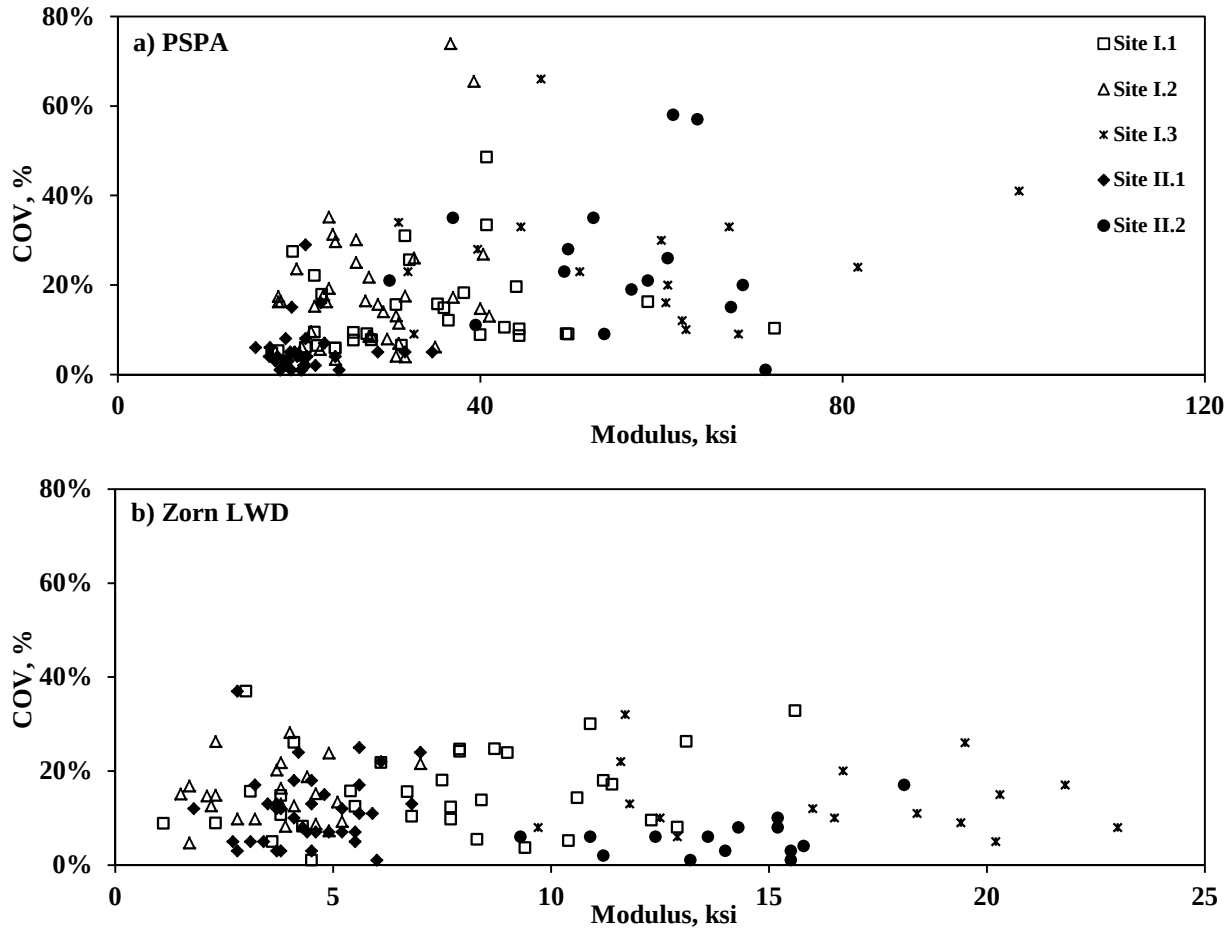

Figure 8.7.1 – Variations in COV of Modulus-based Devices (Subgrade Layer)

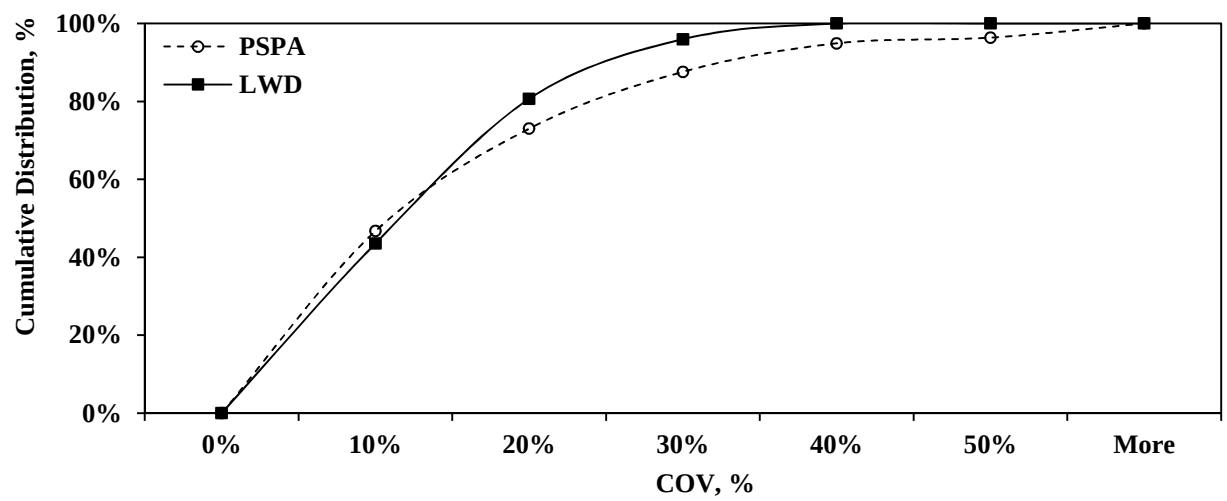

Figure 8.7.2 – Distributions of COV Values for Modulus-Based Devices (Subgrade Layer)

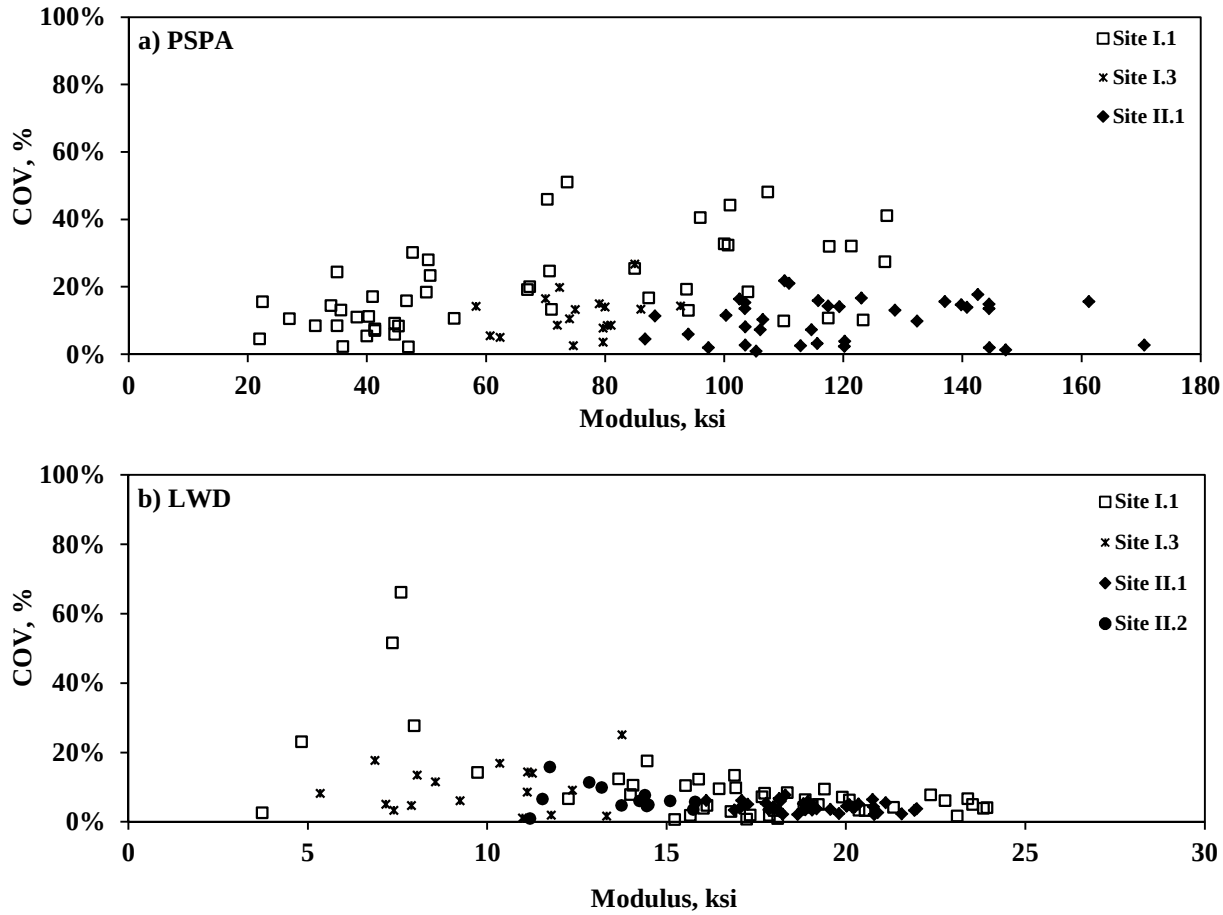

Figure 8.7.3 – Variations in Coefficient of Variation (COV) of Modulus-Based Devices (Base/Subbase Layer)

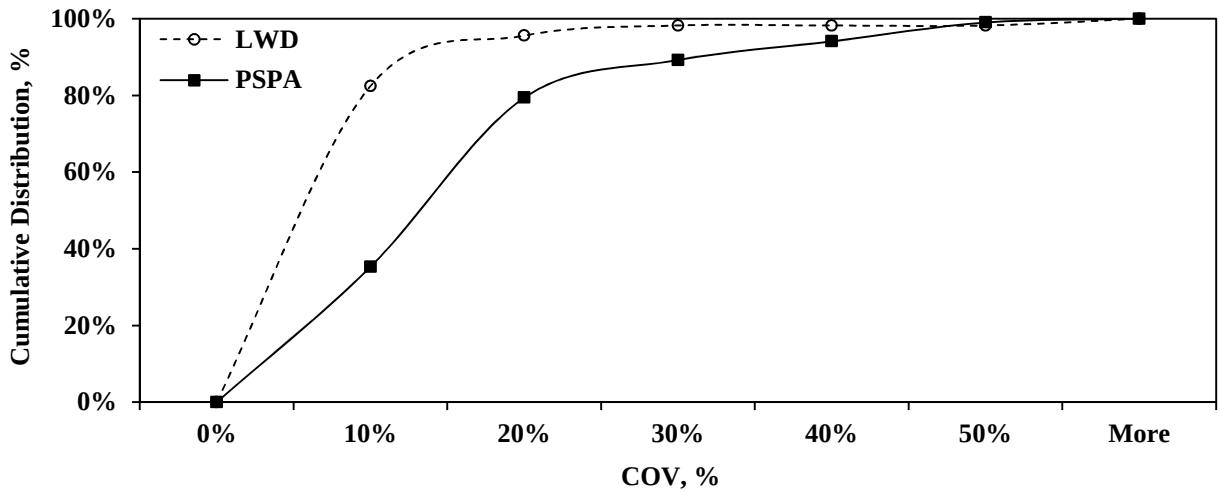

Figure 8.7.4 – Distribution of COV Values for Modulus-Based Devices (Base/Subbase Layer)

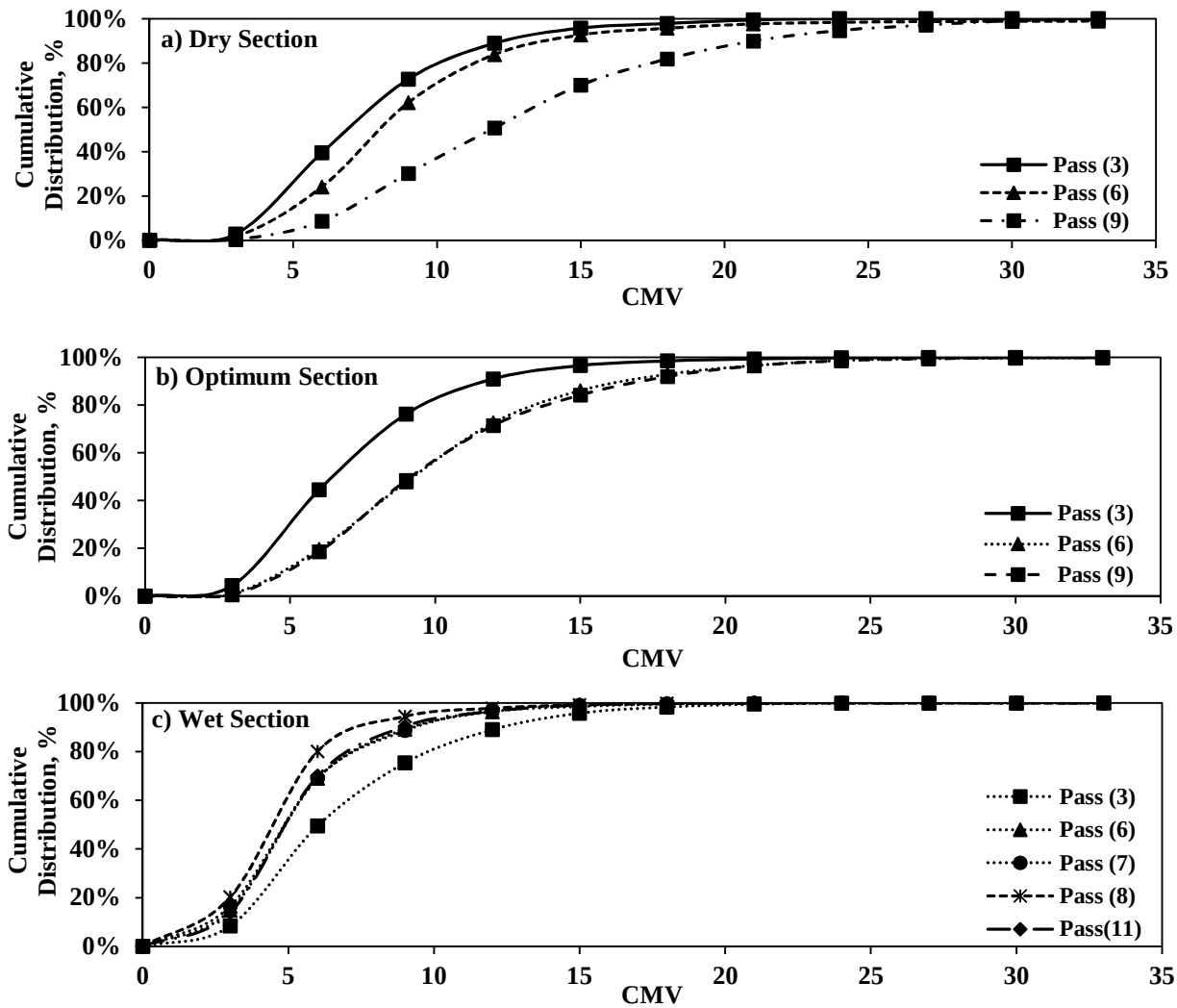

Figure 8.8.1 – Distributions of CMVs with Passes for Different Subgrade Sections (Site I.1)

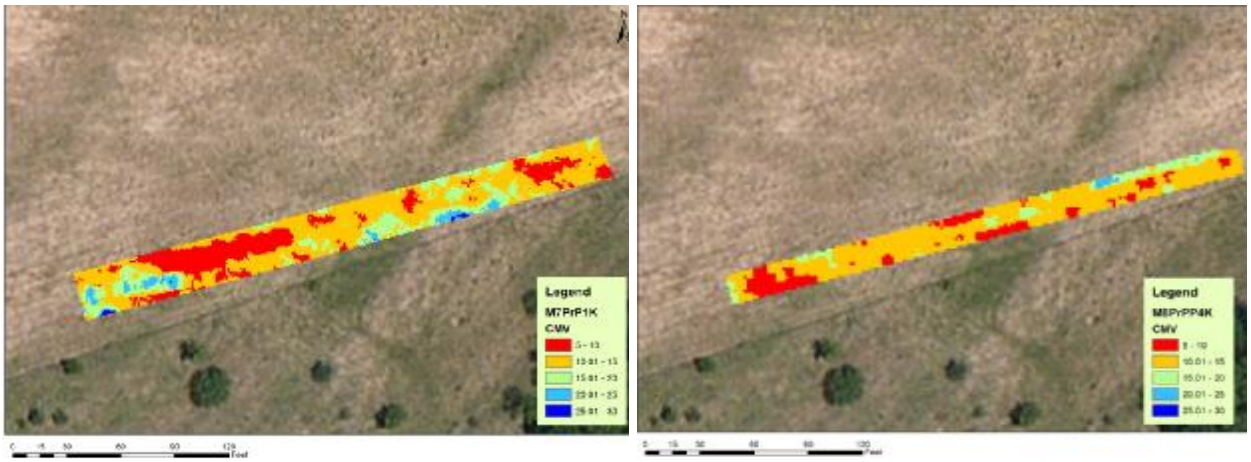

Figure 8.8.2 – Variations of CMV before and after Compaction of Subgrade

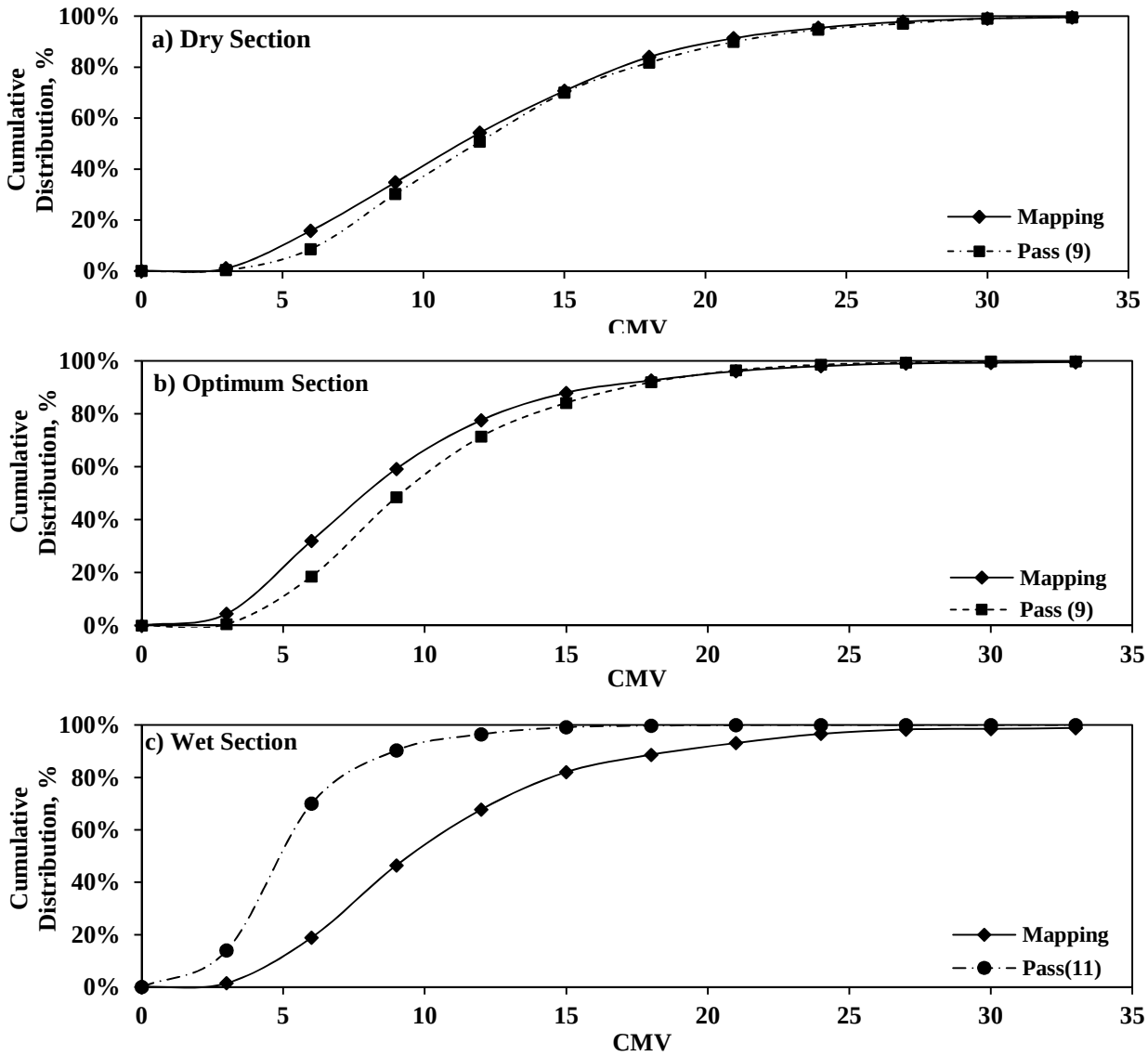

Figure 8.8.3 – Impact of Subgrade Placement after Compaction of the Embankment Layer

Figure 8.8.4 summarizes the dry densities from the NDG and the CMV values from the IC roller at different sections of subgrade layer at Site I.1. It seems that there is not a strong correlation between these two values. In that context, the acceptance scenarios are evaluated next.

Figure 8.8.5 summarizes the traditional density-based quality control process of the subgrade sections at Site I.1. The dry and wet sections achieve the 95% MDD criterion while the optimum section marginally fails the density requirements.

Figure 8.8.6 summarizes the acceptance scenarios based on the PSPA moduli at Site I.1. The dry section marginally and the optimum and wet sections substantially fail the acceptance criterion of 80% of the target modulus at OMC. The estimated moisture-corrected field moduli using the laboratory FFRC data overestimate the measured field moduli for the dry and optimum sections and are reasonably close to the field moduli for the wet section. The reason for this pattern is the assumption of the same Poisson's ratio for the three test sections as explained in Chapter 7.

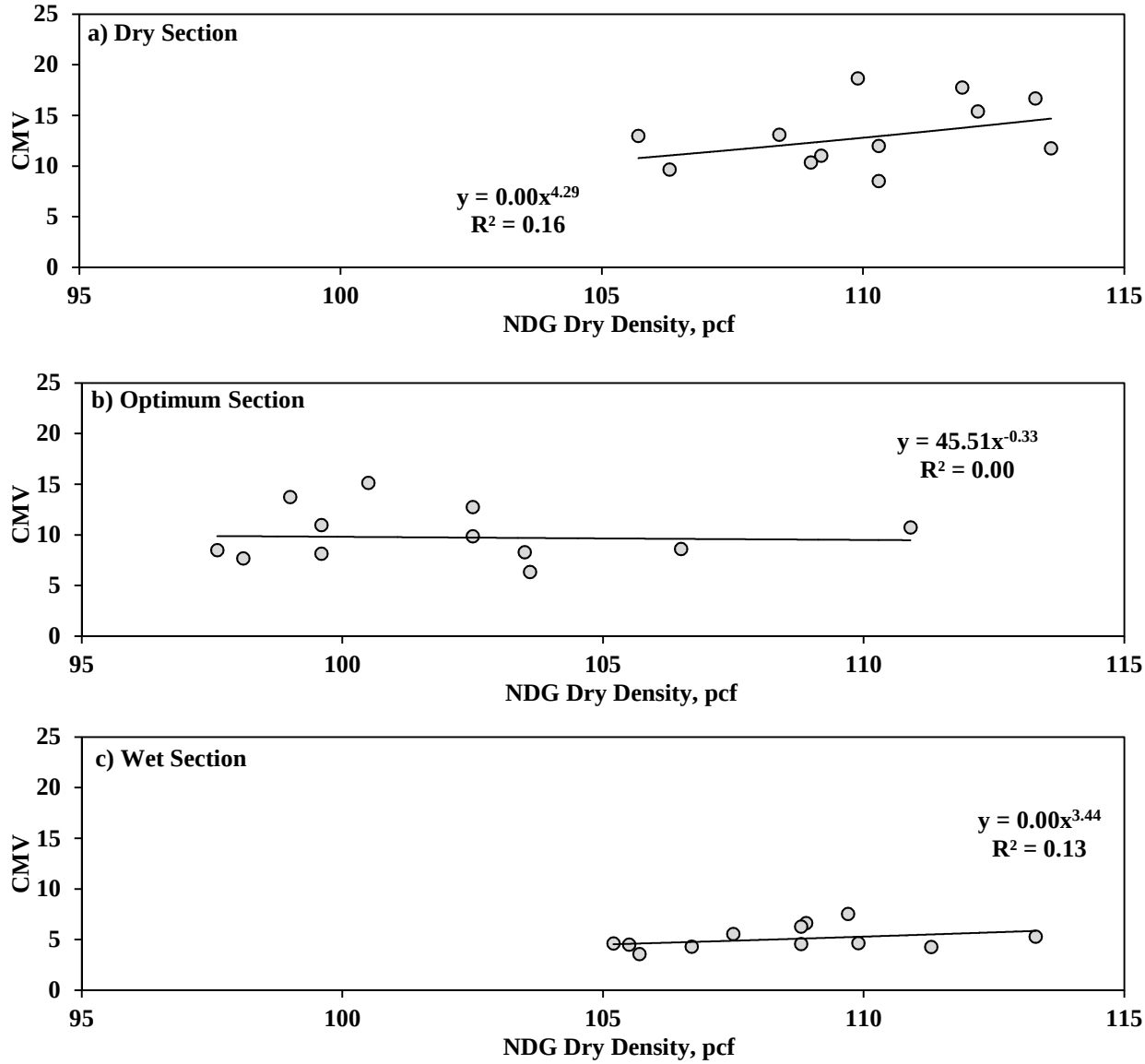

Figure 8.8.4 – Correlation of CMV and Dry Density for Subgrade Layer (Site I.1)

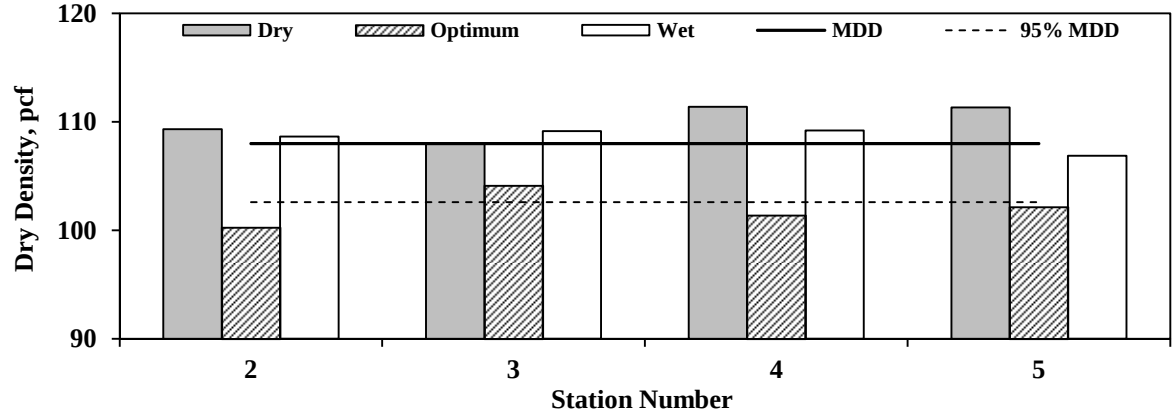

Figure 8.8.5 – NDG Dry Densities after Compaction of Subgrade Sections at Site I.1

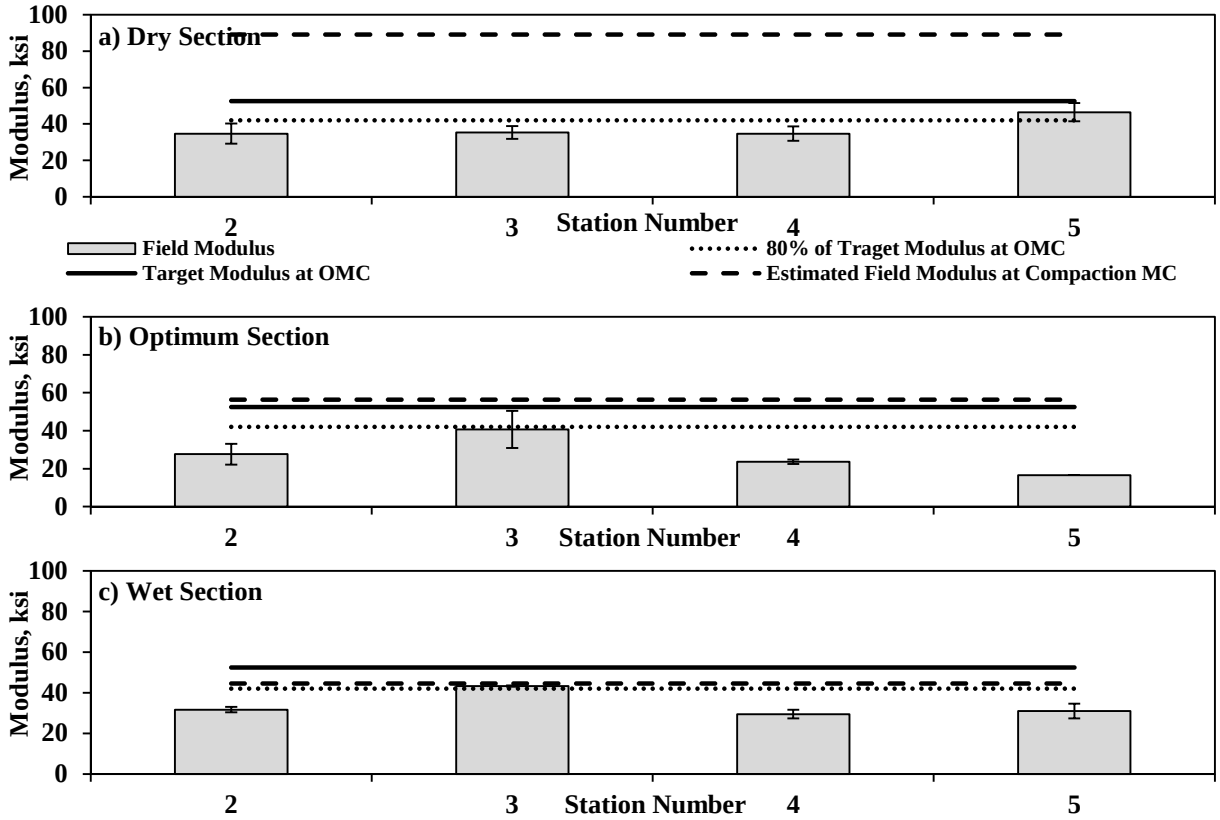

Figure 8.8.6 - Acceptance Scenarios for PSPA Modulus of Subgrade Sections at Site I.1

Figure 8.8.7 illustrates the Zorn LWD-based acceptance scenarios at Site I.1. In this case, the dry and wet sections marginally and the optimum section significantly fail the established criteria. The estimated moisture-corrected field moduli follow the PSPA patterns.

As a part of the evaluation process at Site I.1, an independent test section that followed the routine construction procedure (labeled as Production section) was also tested. The details of this section are included in Appendix H. Figure 8.8.8 summarizes the distributions of the moisture content and dry density along with the modulus measurements at the production section. The moisture contents vary between 14% and 24% while the densities vary from 102 pcf to 114 pcf. As reflected in Figure 8.8.8c, such variations have significant impact on the modulus of the compacted layer.

Figure 8.8.9 summarizes the acceptance scenarios for the production section for the PSPA and LWD moduli. The section fails according to the PSPA and passes according to the LWD. Aside from the issue of selecting the proper Poisson's ratio, the inherent difference between the LWD- and PSPA-based acceptance scenarios is due to the influence depths of the devices. As discussed in Appendix H, the embankment layer at this site was quite stiff. While the LWD measures a composite modulus, the PSPA is a layer-specific device and measures the low-strain elastic modulus of the intended top layer.

Figure 8.8.10 compares the average field dry densities at Sites I.2 and I.3 (from NDG tests) and II.1 (from Drive Cylinder tests-ASTM D2937) with their corresponding density-based acceptance limits (95% of laboratory MDD). The NDG data were not collected at Site II.2 since it was not a part of the routine operation of the agency. The compacted subgrade layers at all sections of Site I.2, Site I.3 and Site II.1 achieve the density-based acceptance criteria. Standard deviation of density measurements was 1.7, 2.1 and 1.5 pcf at the dry, optimum and wet sections of Site I.2 (for NDG tests), 7.6 and 0.2 pcf for NDG and Drive Cylinder tests at Sites I.3 and II.1, respectively.

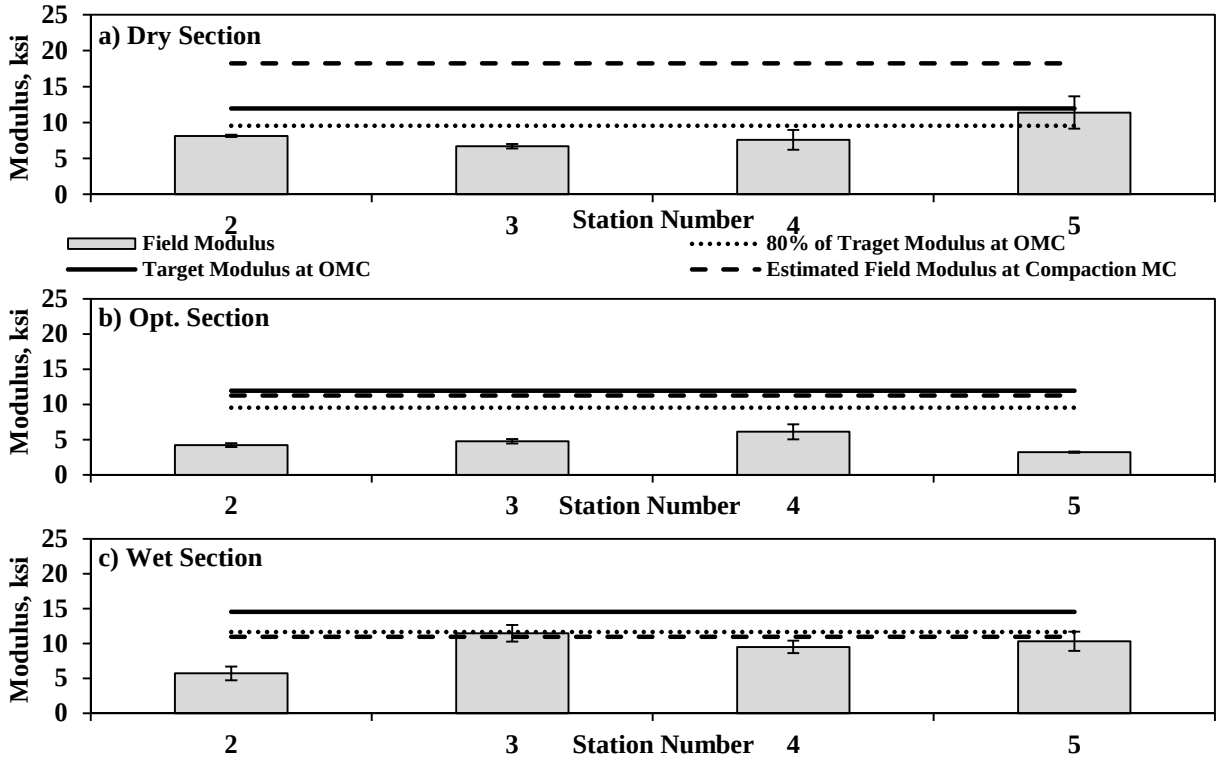

Figure 8.8.7 - Acceptance Scenarios for Zorn LWD Modulus of Subgrade Sections at Site I.1

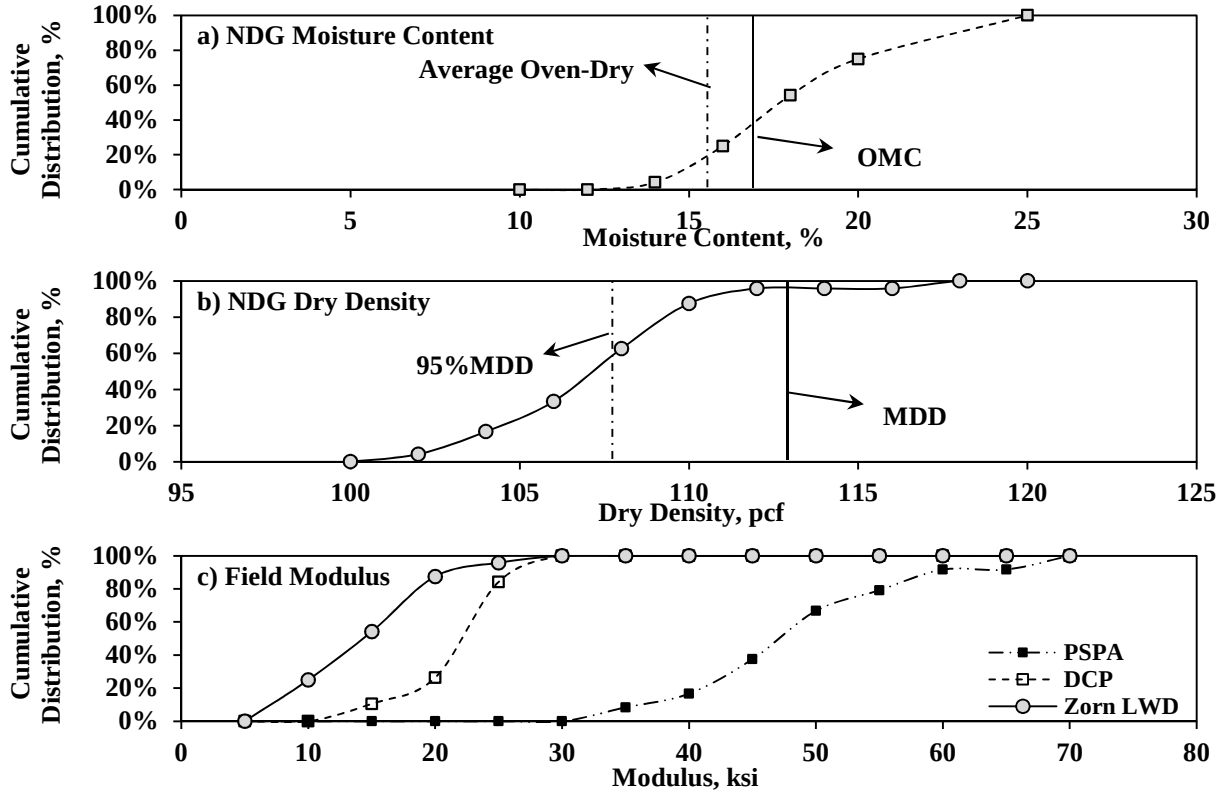

Figure 8.8.8 – Distribution of Moisture, Density and Modulus Measurements on Subgrade Production Section (Site I.1)

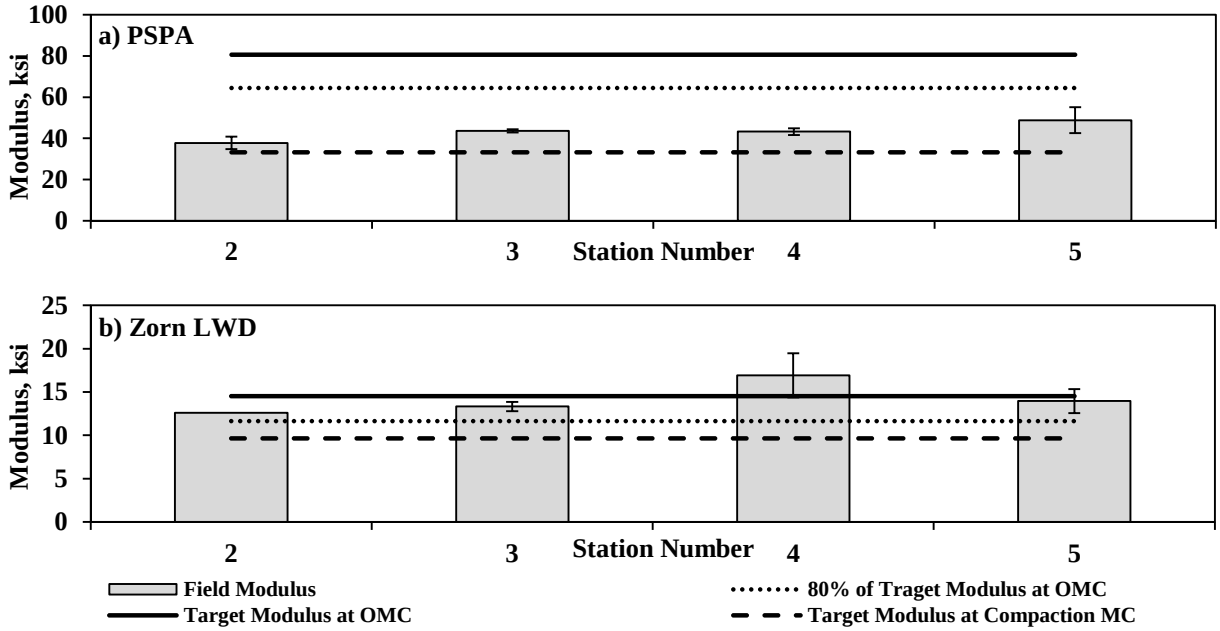

Figure 8.8.9 – Acceptance Scenarios for Production Section of Subgrade at Site I.1

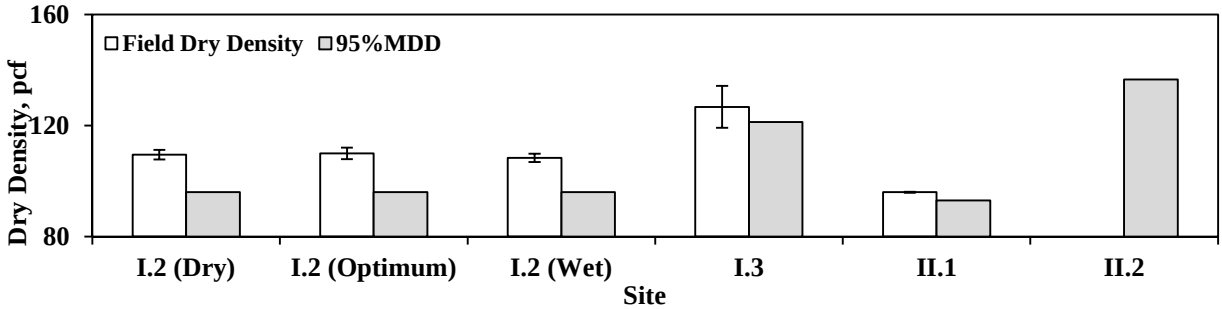

Figure 8.8.10 – Comparison of Field NDG Dry Density with Density-Based Acceptance Limit of Subgrade Sections

Figure 8.8.11 summarizes the average field dry densities of the base layer at Site I.1 (dry, optimum and wet sections), base layer of Site I.3 and base layer of Site II.1. Except for the base layer at Sites I.3 and II.1, all the other sites pass the density-based acceptance criteria (dry section of base layer at Site I.1, marginally achieve the 95%MDD limit).

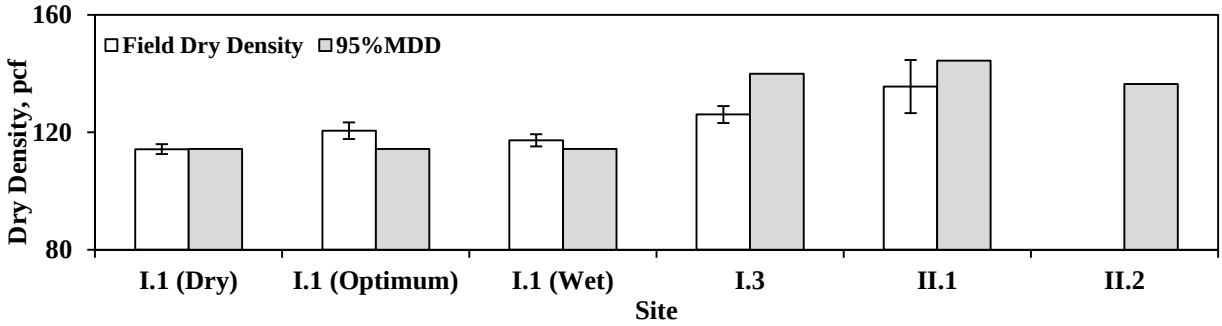

Figure 8.8.11 – Comparison of Field NDG Dry Density with Density-Based Acceptance Limit of Base/Subbase Sections

Table 8.8.1 compares the modulus-based quality acceptance scenarios for subgrade and base/subbase sections at different sites with density-based acceptance criteria. In most cases, even though the sections passed the density-based criterion, they did not pass (or only marginally pass) the modulus-based acceptance limit. Furthermore, the selected modulus technology and associated device also affects the acceptance rate (as discussed in details earlier in this report).

Lessons learned from the implementation of modulus-based specification are summarized in the following paragraphs:

- The NDG moisture estimations are closer to the oven-dry moisture contents than the moisture contents estimated with the electrical impedance spectroscopy technology (SDG device). The results with the SDG device are less sensitive to the variation of moisture content in the field. The variability of the NDG device is less on base/subbase geomaterials than on subgrade soils.
- Among modulus/stiffness-based technologies, the ultrasonic surface wave technology (PSPA device) and LWD technology appear more promising in terms of sensitivity to variations in field moisture content and reasonableness of the modulus estimations. However, there are some inherent differences in the way that these two devices estimate the modulus of a compacted unbound aggregate layer.
- Reasonably strong correlations between the measured field moduli and moisture contents are observed. Such correlations are in reasonable agreement with the modulus-moisture models proposed by Cary and Zapata (2010). However, the normalized field moisture content, $(MC_{Field}-OMC)/OMC$, seems to explain the variations in the subgrade field moduli better. Such correlations for base/subbase geomaterials are not as strong as subgrade soils.
- A comprehensive evaluation of both density-based and modulus-based acceptance approaches shed some light towards an effective quality control process. Even though most layers achieved the desired density, not all of them met the established limits for target modulus.
- Acceptance scenarios among different technologies and associated devices are different. Generally, the acceptance trends from different devices are complementary since DCP and PSPA make layer-specific measurements, while the LWD measures a composite modulus of both top and underlying layers.

Table 8.8.1 – Quality Acceptance based on Modulus Criterion for Subgrade and Base Layer

Section		Device	Acceptance Level		
			% Passing	% Marginal	% Not Passing
Subgrade	I.2 (Dry)	**NDG Dry Density**	**100**	**0**	**0**
		PSPA Mod.	0	20	100
		Zorn LWD Mod.	40	20	40
	I.2 (Optimum)	**NDG Dry Density**	**100**	**0**	**0**
		PSPA Mod.	0	0	100
		Zorn LWD Mod.	20	40	40
	I.2 (Wet)	**NDG Dry Density**	**100**	**0**	**0**
		PSPA Mod.	0	0	100
		Zorn LWD Mod.	20	0	80
	I.3	**NDG Dry Density**	**100**	**0**	**0**
		PSPA Mod.	100	0	0
		Zorn LWD Mod.	100	0	0
	II.1	**NDG Dry Density**	**100**	**0**	**0**
		PSPA Mod.	0	0	100
		Zorn LWD Mod.	8	25	67
	II.2	**NDG Dry Density**	No NDG data collected		
		PSPA Mod.	0	60	40
		Zorn LWD Mod.	100	0	0
Base/Subbase	I.1 (Dry)	**NDG Dry Density**	**67**	**0**	**33**
		PSPA Mod.	17	50	33
		Zorn LWD Mod.	17	67	16
	I.1 (Optimum)	**NDG Dry Density**	**80**	**0**	**20**
		PSPA Mod.	0	60	30
		Zorn LWD Mod.	17	63	20
	I.1 (Wet)	**NDG Dry Density**	**100**	**0**	**0**
		PSPA Mod.	0	0	100
		Zorn LWD Mod.	0	0	100
	I.3	**NDG Dry Density**	**0**	**0**	**100**
		PSPA Mod.	100	0	0
		Zorn LWD Mod.	0	0	100
	II.1	**NDG Dry Density**	**8**	**67**	**25**
		PSPA Mod.	100	0	0
		Zorn LWD Mod.	100	0	0
	II.2	**NDG Dry Density**	NDG and PSPA data not collected at the desire of the agency		
		PSPA Mod.			
		Zorn LWD Mod.	100	0	0

CHAPTER 9 - FRAMEWORK OF A MODULUS-BASED SPECIFICATION

9.1 Summary of Activities

This research started with a thorough literature review of national and international state of practice in modulus-based quality control and quality acceptance process. The results of an online survey revealed that the state DOTs are interested in implementing a practical modulus-based specification. However, the incorporation of unsaturated soil mechanics principles or laboratory resilient modulus tests was not perceived positively.

The actual work phases in this study included laboratory, small-scale, and field activities. Three fine-grained soils (CL, CH and ML), two sandy materials (SC, and SM), and two unbound granular base materials (GW and GP) were initially used. Based on the outcomes of the laboratory and small-scale studies along with development of a structural analysis algorithm (to establish the target modulus), a draft specification was proposed. The draft specification was tested at several construction projects to identify its practical restrictions, update the developed models, and improve the proposed quality control process. The updated version of the modulus-based specification was then implemented at five different construction projects to evaluate its practicality and reasonableness by the research team and highway agencies.

9.2 General Conclusions

The general conclusions based on evaluation of the proposed modulus-based specification are the following:

- The adaption of the modulus-based specification needs to be approached in the context of the levels of uncertainty associated with the current well-established density criteria (especially when nuclear density gauges are used). It has been shown on many occasions in this study that achieving quality compaction (defined as achieving adequate layer modulus) is only weakly associated with achieving density.
- Among the modulus/stiffness-based technologies, devices based on the ultrasonic surface wave, lightweight deflectometer, and dynamic cone penetrometer technologies (PSPA, LWD, and DCP devices, respectively) perform reasonably well with the following caveats:
    - The PSPA exhibits the highest variability and needs the most training, but provides the most reasonable layer-specific information.
    - Different LWDs estimate different moduli at the same test spot. As such, the specification should be clear which LWD should be used. It is also important to consider the properties of the underlying layers in setting the LWD target values, especially when the layer of interest is overlying a layer with a significantly different modulus.
    - The DCP is simple to use and inexpensive. However, since DCP strictly measures the strength not the modulus of the layer, setting its target should be done with care. The DCP results were not very sensitive to moisture content and material changes.
- Among the modulus-based technologies evaluated, the LWD is recommended. This decision was partly made based on the familiarity of the highway agencies with the deflection concept, the ease of use of the device, and the availability of a network of providers of LWDs throughout the world.
- Among the moisture-measurement technologies, the pressure rise technology (e.g., the Speedy Moisture Tester) appears most appropriate for subgrade while a “well-calibrated” nuclear density gauge appears most appropriate for base. Even though not evaluated directly here, the utilization of microwave oven approach based on Berney et al. (2011) may be considered.

- The Cary and Zapata (2010) modulus-moisture model and its variations are reasonable. The proposed model of correlating normalized modulus (M/M_{opt}) with normalized moisture content [(MC-OMC)/ OMC] gave a better match to the field data.

9.3 Major Components of Specification

Appendix A presents a proposed specification for modulus-based acceptance entitled "Standard Specification for Modulus-Based Quality Management of Earthwork and Unbound Aggregates." Two test methods are also provided to supplement the specification with device-specific protocols. The specification addresses the following four major items:

1. Relating Acceptance to Structural Design Algorithm
2. Acceptance of Materials for Durability and Constructability
3. Select Target Modulus, and
4. Perform Field Measurements and Acceptance.

This section describes how these four items are addressed in the proposed specification and the rationale behind these proposals.

9.3.1 Relating Acceptance to Structural Design Algorithm

The structural response algorithms used in this study are discussed in Chapter 6. Those response algorithms are quite similar to the response algorithms contained in the MEPDG. The MEPDG advocates two structural models (layered elastic and nonlinear finite element). As demonstrated in Section 6.2, the nonlinear algorithm seems more appropriate for estimating the behavior of compacted geomaterials under several modulus-based devices. A nonlinear structural model that approximates the response of layered geomaterials under most modulus-based devices has been recommended and calibrated for LWDs and Plate Load tests (see Chapter 6).

Aside from the structural response algorithms, the material models proposed by the MEPDG are of interest to this study. A modified version of the MEPDG nonlinear material model (Ooi et al, 2004) in the form of Equation 9.3.1 seems to yield more representative responses of the modulus-based devices than the model recommended by the MEPDG in Equation 9.3.2.

$$MR = k_1^{'} P_a \left(\frac{q}{P_a} + 1 \right)^{k_2^{'}} \left(\frac{t_{oct}}{P_a} + 1 \right)^{k_3^{'}} \tag{9.3.1}$$

$$MR = k_1 \, P_a \left(\frac{q}{P_a} \right)^{k_2} \left(\frac{t_{oct}}{P_a} + 1 \right)^{k_3} \tag{9.3.2}$$

Understanding the practical problems that this change may cause for highway agencies that utilize the MEPDG material model, relationships have been provided in Appendix D to convert parameters k_1 through k_3 recommended by the MEPDG to k'_1 through k'_3 utilized in this study.

One important item that should be emphasized is that different resilient modulus test protocols (e.g., T 307-03 and NCHRP 1-28A) may yield different nonlinear parameters k_1 through k_3. The relationships provided here are based on AASHTO T 307-03. The proposed relationships in the specification and test methods should be recalibrated by highway agencies that use other test protocols.

9.3.2 Acceptance of Materials for Durability and Constructability

Achieving an adequate modulus does not guarantee a durable compacted geomaterial. To ensure durability, the selection of the material to be used in a construction project should be based on parameters such as hardness, gradation, and plasticity of the material. The requirements espoused by different highway agencies for this purpose are extremely diverse (see https://fhwapap04.fhwa.dot.gov/nhswp/

searchSpecifications.jsp). Different agencies can incorporate their own requirements since they can add their wealth of local experience with the available geomaterials and construction practices.

9.3.3 Selecting Target Modulus

Sections 6.5 and 6.6 contain a process to select target moduli for devices that measure the response of the geomaterials. The nonlinear algorithm described in Section 6.2 was used to develop straightforward relationships for estimating field target moduli from resilient modulus parameters (k_1 through k_3) for a uniform layer of compacted geomaterial.

The MEPDG proposes a three-tier approach (Level I through Level III). The proposed modulus-based specification is perhaps more appropriate for Levels I and II where some laboratory effort has been incorporated in estimating the material properties. Parameters k_1 through k_3 should preferably be determined from laboratory tests on the geomaterial sampled from the site. Understanding the constraints that this activity may bring to the operations of highway agencies, an option for estimating these parameters from index properties of the geomaterial is also provided in the specification.

A neural network algorithm is provided for estimating the target moduli of two-layer systems. However, the most appropriate approach (especially for multi-layer earthwork) is to utilize directly the nonlinear algorithm described in Section 6.2.

9.3.4 Perform Field Measurements and Acceptance

One of the main concerns in the pavement community with the modulus-based devices is the variability of the measurements. Measured moduli from well-controlled small-scale studies are compared with the corresponding target moduli in Figure 9.3.1 to demonstrate such variability. The sources of variability can be traced to the following parameters:

1. Inherent variability of the devices,
2. Moisture content at the time of compaction,
3. Moisture content at the time of testing,
4. Relative compaction of the compacted geomaterial, and
5. Differences in the laboratory and field moduli when specimens are prepared at same density and moisture content.

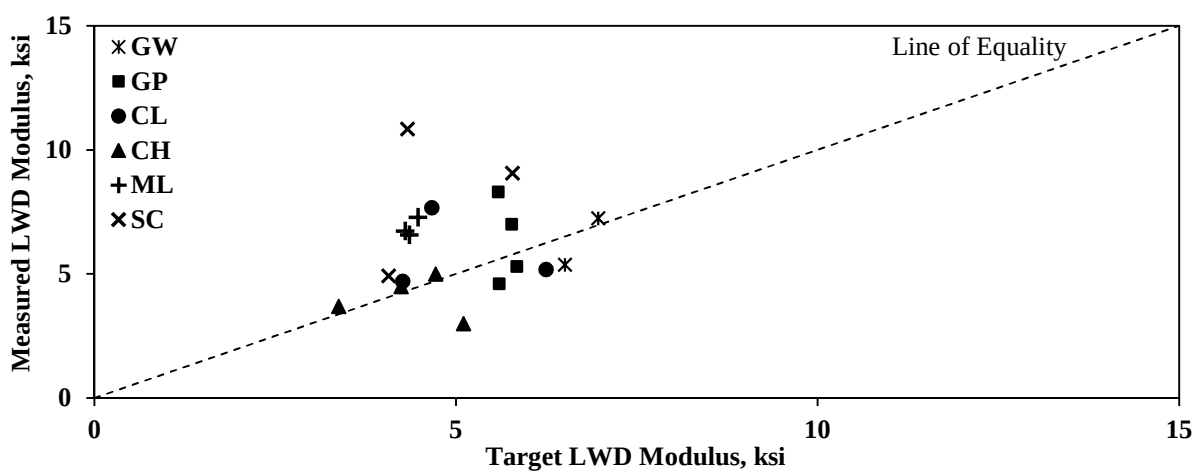

Figure 9.3.1 - Comparison of Target and Field Moduli for LWD

The inherent variability of each modulus-based technology and associated device is reported in Table 5.2.2. Based on tests on 20 independent specimens, the repeatability of devices is better than 15% and their reproducibility is better than 12%. Based on Table 5.2.3, more than 70% of variability measured with these devices can be attributed to the variation in the properties of the materials. Based on that

analysis, the acceptance threshold is preliminarily set at 80% of the target modulus calculated as described in Section 5.2. According to Table 5.2.3, the repeatability of the device at a 95% confidence level when the operator-device-specimen interactions are ignored is 20%. However, this level may have to be adjusted based on more experience.

The moisture content at compaction significantly influences the modulus of the geomaterials as demonstrated in Section 3.3. Depending on the type of geomaterial, a ±2% variation in the compaction moisture content may result in a variation of up to a factor of 3 in modulus.

Evidence of the importance of considering the moisture content at the time of testing relative to the moisture content at the time of compaction is provided in Section 3.4. Figure 3.4.4 includes preliminary relationships to adjust the measured field moduli to a reference moisture content. The proposed relationships become less effective when the compaction moisture content significantly deviates from the OMC (especially when the material is placed wet of OMC), and when the field test is delayed significantly (significant difference between the compaction and testing moisture contents).

9.4 Recommendations Related to Specification

The specification and test methods in Appendix A contain suggestions about the areas that the SHAs may modify to match them to their needs and institutional policies. Some guidance in implementing the specifications is given here.

9.4.1 Material Selection

Adequate stiffness does not guarantee adequate durability of the material. The following items should be considered in specifying the types and nature of the geomaterials for different layers:

- Depending on the geographical location and the availability of materials, different highway agencies have different gradation and index property requirements for the geomaterials to be used in their areas. Different agencies should supplant Section 4 of the specification with their own definitions of the types of geomaterial permissible.
- The moisture-density (M-D) information of a geomaterial is a piece of information that has been used for decades by the contractors and DOTs to achieve reasonable quality of earthwork. Different SHAs use different compaction methods or energy to obtain the M-D curve. The specification should clearly define the compaction method and energy for different materials. The same compaction method should be used for preparing specimens for subsequent strength/modulus tests.

9.4.2 Placing and Mixing of Materials

One of the attractions of the modulus-based specifications to some SHAs is not having to deal with nuclear density gauges since density and moisture content requirements are supplanted with achieving adequate modulus/stiffness. One of the impediments to implementing modulus-based specifications indicated by the SHAs is that the contractors know how to achieve a certain density but they do not know how to achieve a certain modulus. Based on these perceptions, the following remarks are offered:

- Modulus of a layer is a more rational and sensitive indicator of the quality of construction. A number of material-related and construction-related parameters influence the modulus of a layer. Based on the field study carried out in this project, a reasonably rigid process control will go a long way toward achieving a uniform and acceptable quality compacted layer.
- Until the contractors become experienced enough with modulus specifications, it may be prudent to use the density and moisture content as process control items.
- The moisture content at the time of compaction has a significant influence on the modulus of the compacted geomaterials (see Chapter 8). It is important to control the moisture content before the compaction as discussed in Section 6.4 of the specification.

- It is also prudent to achieve a certain density before acceptance testing. Less rigid density requirements (as compared to densities used for acceptance) are proposed in Section 6.5 of the specification.
- One prudent means of process control is the use of the intelligent compaction technology instead of the density. That technology, if used properly, ensures the uniformity of the layer.
- The fastest way to obtain uniform and acceptable quality is to ensure that the first layer of the embankment or pavement foundation is compacted uniformly and solidly. The lack of uniformity of the first layer will propagate throughout the lifts placed at a job site, especially when the devices that measure the system response (such as LWDs) are used.

9.4.3 Quality Acceptance

Several inter-related aspects of quality acceptance require further comment.

- The timing of the modulus-based acceptance testing relative to the completion of the compaction is much more critical than for density-based acceptance testing. As demonstrated in Chapter 3, the modulus of the compacted geomaterial increases significantly with time, as the material becomes drier. As such, modulus-based testing should be carried out as close to the completion to compaction as possible. To discourage delay between the time of testing and compaction, the concept of moisture-adjusted modulus is introduced to adjust the modulus to one reference moisture content (i.e., moisture content at the time of compaction). In addition, some limits are proposed for the delay in testing in terms of reduction in moisture content of the material.
- The minimum number of tests for acceptance has been set based on limited precision and bias tests. These values can be modified based on the experience of the SHAs.
- The acceptance method and basis for payment should be specified by each SHA based on their institutional preference and shadow specification of several trial projects.

9.4.4 Selecting Target Modulus

A new algorithm has been proposed for setting the target modulus. This algorithm considers the nonlinear parameters of the geomaterial being tested in a way that is comparable with the design process. The following advices can be provided based on our experience:

- The accuracy of the target modulus is directly related to the sophistication of the response model used in the design and the effort placed in characterizing the materials in the laboratory.
- Considering the MEPDG-proposed three-tier design approach (Level I through Level III), the proposed modulus-based specification is perhaps the most appropriate for Level I where laboratory efforts has been incorporated in estimating the material properties (especially parameters k_1 through k_3 from MR tests).
- The method should also work reasonably well when a Level II type analysis is considered with material properties either estimated from a catalogue of most common materials or other sources.
- The proposed process should be used with caution by the SHAs that conduct pavement design using empirical methods or use the default material models provided in the mechanistic-empirical design methods. In those cases, the concept of using a test strip to set the target modulus empirically can be entertained. One should be aware that this approach would provide the potential modulus of the layer that may not be the same as the design modulus.
- In the course of this study, it was found that the Poisson's ratio of the material can influence the target modulus and as such the acceptance rate. The specification provides a set of recommended Poisson's ratios that are directly compatible with the MEPDG recommendations. The SHAs should evaluate these values for compatibility with their materials. As a general guideline, the assumed Poisson's ratio should be increased if the contractor tends to place the material wet of optimum moisture content and decreased if the contractor tends to place the material dry of optimum moisture content.

9.5 Feedback from Participating States during Phase III

As indicated in Chapter 8, five different groups were involved in the assessment of the specifications. During each project, feedback was sought from the technicians and engineers affiliated with the owner agencies and the contractors. Upon completion of each project, a detailed report (see Appendices H through L) was prepared and shared with the owner agencies' representatives to provide feedback and suggestions to improve the process. All groups found the exercise informative and reasonable. The large variation of moisture content within each project and the level of changes in the modulus with the change in placement moisture content were deemed informative by most parties. Based on these interactions, the following items should be strongly emphasized as part of the dissemination of the specification:

- Modulus-based acceptance should be implemented in conjunction with a strict process control since reasonably small changes in the moisture content will have significant impact on measured moduli.
- Perhaps the density and moisture measurements can be considered as process control items, with modulus-based measurements being used for quality acceptance. Highway agencies should consider incorporating the moisture content of the loose material before compaction as a process control item in their specifications.
- The best results are obtained, when a moisture content measurement is carried out in conjunction with the modulus-based measurement. Of the moisture-measurement technologies and devices considered in this study, the SDG based on electrical impedance spectroscopy technology or a nuclear density gauge (with a thorough calibration) may be reasonable alternatives.

9.6 Future Activities

This study clearly demonstrates the technical benefits and the challenges that are related to the implementation of the modulus-based specification. Even though all aspects of the development of the protocols are thoroughly and comprehensively demonstrated, the number of geomaterials used is limited. The future activities can be categorized in the following manner:

9.6.1. Gaining Experience

As indicated in Section 9.3.2, the current specifications for quality management of compaction of geomaterials vary significantly among different SHA's. In this study, a set of protocols and procedures were selected and uniformly implemented. The proposed protocols and specification should be adjusted to the local practices of a number of SHAs and should be applied to a number of different projects to understand better the limitations of the process.

9.6.2. Documenting Cost-Benefit of New Specification

Based on our interaction with the SHAs that did and did not participate in Phase III of this project, the investments that they have to make in terms of acquiring equipment, training, and operational costs are evident. However, the benefits achieved in terms of longer lasting pavements have not been documented. It would be desirable to construct and monitor the performance of several test sections using the existing specification and the one proposed in this study to demonstrate the tangible benefits achieved. As part of this cost benefit study, the benefits of conduction of the laboratory tests proposed in the study (as opposed to using presumed values) should also be documented.

9.6.3. Dissemination of Information

The findings of the research should be disseminated in a balanced way to the community. The presentations should not only emphasize the benefits of the specifications, but should enumerate the changes in day-to-day operations of the SHAs and means of adapting them in their operations in a gradual and manner.

REFERENCES

- Abdallah, I., Meshkani, A., Yuan, D. and Nazarian, S. (2005), "Design Modulus Values Using Seismic Moduli (SMART User's Manual)," TXDOT Report No. 0-1780-5, The University of Texas at El Paso, El Paso, TX.
- Amiri, H., Nazarian, S. and Fernando, E. (2009), "Investigation of Impact of Moisture Variation on Response of Pavements through Small-Scale Models," ASCE Journal of Materials in Civil Engineering, Vol. 21, No. 10, pp. 553-560.
- Anderson, D.G., Woods, R.D. (1975), "Comparison of Field and Laboratory Shear Moduli," Proceedings, Conference on In situ Measurement of Soil Properties," Specialty Conference of the Geotechnical Engineering Division, ASCE, Raleigh, North Carolina, Vol. 1, pp. 69-92.
- Bishop, A.W. (1959), "The Principle of Effective Stress," Teknisk Ukeblad I Samarbeide Med Teknikk, Oslo, Norway, Vol. 106, No. 39, pp. 859-863.
- Berney, I.V., Ernest, S., and Wahl, R.E. (2011), "Device Comparison for Determining Field Soil Moisture Content," US Army Corps of Engineers, Report No. ERDC/GSL-TR-08-3, Washington, D.C.
- Booth, J., Keeton, G.P., and Gosling, R.C. (2008), "Some Observations on Determining CBR and the Use of Stiffness as an Alternative," Proceedings of 1st International Conference in Transportation Geotechniques, pp. 701-706, Nottingham, U.K.
- Briaud, J.L., Li, Y., and Rhee, K. (2006), "BCD: a Soil Modulus Device for Compaction Control." Journal of Geotechnical and Geoenvironmental Engineering, Vol. 132, No. 1, pp. 108-115.
- Brown, S. F. (1996), "Soil Mechanics in Pavement Engineering," 36th Ranking Lecture of the British Geotechnical Society, Geotechnique, Vol. 46, No. 3, pp. 383-426.
- Burati, J. L., Weed, R. M., Hughes, C.S., Hill, H.S. (2003), "Optimal Procedures for Quality Assurance Specifications," Report No. FHWA-RD-02-095, Federal Highway Administration (FHWA), pp. 57-59
- Cary, C. E., and Zapata, C. E. (2010), "Enhanced Model for Resilient Response of Soils Resulting from Seasonal Changes as Implemented in Mechanistic-Empirical Pavement Design Guide," Transportation Research Record: Journal of the Transportation Research Board, No. 2170, pp. 36-44.
- Celaya, M., Nazarian, S., and Yuan, D., (2008), "Implementation of Quality Management of Base Materials with Seismic Methods: Case Study in Texas," Transportation Research Record: Journal of Transportation Research Board, No. 2057, pp. 99-106.
- Fredlund, D.G., and Rahardjo, H. (1993), "Soil Mechanics for Unsaturated Soils," John Wiley and Sons Inc., New York.
- Fredlund, D. G., and Xing, A. (1994), "Equations for the Soil-Water Characteristic Curve," Canadian Geotechnical Journal, Vol. 31, No. 4, pp. 521-532.
- Gupta, S., Ranaivoson, A., Edil, T., Benson, C., Sawangsuriya, A. (2007), "Pavement Design Using Unsaturated Soil Technology," Report No. MN/RC-2007-11, Final Research Report submitted to Minnesota Department of Transportation, University of Minnesota, St. Paul, MN.
- Hansen, B. J., and Nieber, J. L. (2013), "Performance-Based Measurement of Optimum Moisture for Soil Compaction," Research Report No. MN/RC 2013-28, Sponsored by Minnesota Department of Transportation, University of Minnesota, St. Paul, MN.
- Highways Agency (2009), "Design Guidance for Road Pavement Foundations," Interim Advice Note 73, Highways Agency, London.
- Ke, L., Nazarian, S., Abdallah, I., and Yuan, D. (2001), "A Sensitivity Study of Parameters Involved in Design with Seismic Moduli," Research Report No. 1780-2, Center for Highway Materials Research, the University of Texas at El Paso, El Paso, TX.
- Khoury, N. N., and Zaman, M. M. (2004), "Correlation between Resilient Modulus, Moisture Variation, and Soil Suction for Subgrade Soils," Transportation Research Record: Journal of Transportation Research Board, No. 1874, pp. 99-107.

- Khoury, N. N., and Zaman, M. M. (2007), “Influences of Various Cementitious Agents on the Performance of Stabilized Aggregate Base Subjected to Wet-Dry Cycles,” International Journal of Pavement Engineering, Vol. 8, No. 4, pp. 265-276.
- Kim, J. R., Kang, H. B., Kim, D., Park, D. S., and Kim, W. J. (2007), “Evaluation of in Situ Modulus of Compacted Subgrades Using Portable Falling Weight Deflectometer and Plate-bearing Load Test,” Journal of Materials in Civil Engineering, Vol. 19, No. 6, pp. 492-499.
- Liang, R. Y., Al-Akhras, and K. Rabag’ah, S. (2006), “Field Monitoring of Moisture Variations Under Flexible Pavement,” Transportation Research Record: Journal of Transportation Research Board, No. 1967, pp. 160-172.
- Liang, R.Y., Rabag’ah, S., and Khasawneh, M. (2008), “Predicting Moisture-Dependent Resilient Modulus of Cohesive Soils Using Soil Suction Concept,” Journal of Transportation Engineering, Vol. 134, No. 1, pp. 34-40.
- Ling, J., Guo, R., and Yuan, J. (2006), “A Method to Monitor and Evaluate Seasonal Variation in Resilient Modulus of Pavement Subgrade,” ASCE, Pavement Mechanics and Performance 2006, GSP 154.
- Lu, N. and Likos, W. J. (2004), “Unsaturated Soil Mechanics,” John Wiley & Sons, Inc., NJ.
- Meshkani, A., Abdallah, I., and Nazarian, S. (2002), “Determination of Nonlinear Parameters of Flexible Pavement Layers from Nondestructive Testing,” Research Report 1780-3, Center for Highway Materials Research, the University of Texas at El Paso, TX.
- Mitchell, J. K., and Soga, K. (2005), “Fundamentals of Soil Behavior,” John Wiley and Sons, Inc., NJ.
- Mooney, M.A., Rinehart, R.V., Facas, N.W., Musimbi, O.M., White, D.J. and Vennapusa, P.K.R. (2010), “Intelligent Soil Compaction Systems,” NCHRP Report 676, National Cooperative Highway Research Program, Transportation Research Board, Washington, D.C.
- Moré, J. J. (1978), “The Levenberg-Marquardt algorithm: implementation and theory,” Numerical analysis, pp. 105-116.
- Nazarian, S., Yuan, D., Tandon, V., and Arellano, M. (2003a), “Quality Management of Flexible Pavement Layers with Seismic Methods,” Research Report 1735-3F, Center for Highway Materials Research, The University of Texas at El Paso, El Paso, TX.
- Nazarian, S., Yuan, D., and Williams, R. R. (2003b), “A Simple Method for Determining Modulus of Base and Subgrade Materials,” ASTM STP No. 1437, ASTM, pp. 152-164.
- Nazarian, S., Yuan, D. (2008), “Variation in Moduli of Base and Subgrade with Moisture," ASCE Geotechnical Special Publication, Vol. 178, pp. 570-577.
- Nazarian, S., Abdallah, I., Mohammad, L.N., Abu-Farsakh, M., Puppala, A.J., Bulut, R. (2011), “Modulus-Based Construction Specification for Compaction of Earthwork and Unbound Aggregates,” NCHRP 10-84 Project, Draft Phase I Report.
- Nazzal, M. (2014), “Non-Nuclear Methods for Compaction Control of Unbound Materials,” NCHRP Synthesis 456, National Cooperative Highway Research Program, Transportation Research Board, Washington, D.C.
- Oh, J. H. and Fernando, E. G. (2011), “Development of Correction Factors between Lab and Field Modulus,” Report No. BDL76-1, Submitted to the Florida Department of Transportation, Texas Transportation Institute, College Station, TX.
- Oh, W. T., Vanapalli, S. and Puppala, A.J. (2009), “A Semi-Empirical Model for the Prediction of Modulus of Elastic for Unsaturated Soil,” Canadian Geotechnical Journal, Vol. 46, pp. 903-914.
- Oloo, S. Y., and Fredlund, D. G. (1998), “The Application of Unsaturated Soil Mechanics Theory to the Design of Pavements,” Proceedings of the 5th International Conference on the Bearing Capacity of Roads and Airfields, pp. 1419-1428, Trondheim, Norway,.
- Ooi, P. S. K., Archilla, A. R., and Sandefur, K. G. (2004), “Resilient Modulus Models for Compacted Cohesive Soils,” Transportation Research Record: Journal of the Transportation Research Board, No. 1874, pp. 115-124.

- Pacheco, L.G., Nazarian, S. (2011), "Impact of Moisture Content and Density on Stiffness-Based Acceptance of Geomaterials," Transportation Research Record: Journal of Transportation Research Board, No. 2212, pp. 1-13.
- Puppala, A.J. (2008), "Estimating Stiffness of Subgrade and Unbound Materials for Pavement Design," NCHRP Synthesis 382, National Cooperative Highway Research Program, Transportation Research Board, Washington, D.C.
- Richter, C. (2006), "Seasonal Variations in the Moduli of Unbound Pavement Layers," Publication No. FHWA-HRT-04-079, Turner – Fairbanks Highway Research Center, McLean, VA.
- McClelland, J. L., Rumelhart, D. E., and the PDP Research Group (1986), "Parallel distributed processing," Explorations in the microstructure of cognition, Vol. 1, pp. 272-318.
- Sawangsuriya, A., Edil, T. B., Benson, C. H. (2009), "Effect of Suction on Resilient Modulus of Compacted Fine-Grained Subgrade Soils," Transportation Research Record: Journal of the Transportation Research Board, No. 2101, pp. 82-87.
- Sebesta, S. D., Scullion, T., Taylor, R. J., Frazier, J. T. (2012), "Alternative Methods of Flexible Base Compaction Acceptance," Research report No. 0-6587-1, Texas Transportation Institute, The Texas A&M University System, College Station, TX.
- Siekmeier, J. A. (2011), "Unsaturated Soil Mechanics Implementation during Pavement Construction Quality Assurance," Proceedings of 59th Annual Geotechnical Engineering Conference, St. Paul, MN.
- Terzaghi, K., Peck, R. (1967), "Soil Mechanics in Engineering Practice," Wiley and Sons, New York.
- Tutumluer, E. (2013), "Practices for Unbound Aggregate Pavement Layers," NCHRP Synthesis 445, National Cooperative Highway Research Program, Transportation Research Board, Washington, D.C.
- Vanapalli, S. K., and Fredlund, D. G. (2000), "Comparison of Different Procedures to Predict Unsaturated Soil Shear Strength," Proceedings of Sessions of Geo-Denver 2000, Advances in Unsaturated Geotechnics, ASCE, Geotechnical Special Publication, No. 99, pp. 195-209.
- Vennapusa, P. K., and White, D. J. (2009), "Comparison of Light Weight Deflectometer Measurements for Pavement Foundation Materials," ASTM geotechnical Testing Journal, Vol. 32, No. 3, pp. 239-251.
- Von Quintus, H. L., and Killingsworth, B. (1998), "Analyses Relating to Pavement Material Characterizations and Their Effects on Pavement Performance," FHWA-RD-97-085, Federal Highway Administration, McLean, Va.
- Von Quintus, H. L., Rao, C., Minchin, R. E., Nazarian, S., Maser, K.R., and Prowell, B. (2009), "NDT Technology for Quality Assurance of HMA Pavement Construction," NCHRP Report 626, National Cooperative Highway Research Program, Transportation Research Board, Washington, D.C.
- Von Quintus, H. L., Rao, C., Bhattacharya, B., Titi, H., and English, R. (2010), "Evaluation of Intelligent compaction technology for Densification of Roadway Subgrades and Structural Layers," Submitted to the Wisconsin Highway Research Program (WHRP), Draft Final Report, WHRP Study No. 00092-08-07, Applied Research Associates, Inc., University of Wisconsin at Milwaukee.
- Wheeler, D. J. (2009), "An Honest Gauge R&R Study," ASQ/ASA Fall Technical Conference, SPC Press.
- Yang, R. R., Huang, W. H., and Tai, Y.T. (2005), "Variation of Resilient Modulus with Soil Suction for Compacted Subgrade Soils," Transportation Research Record: Journal of Transportation Research Board, No. 1913, pp. 99–106.
- Yang, S. R., Lin, H. D., Kung, Johnson H. S., and Huang, W.H. (2008), "Suction-Controlled Laboratory Test on Resilient Modulus of Unsaturated Compacted Subgrade Soils," Journal of Geotechnical and Geo-environmental Engineering, Vol. 134, No. 9, pp. 1375-1384.
- Zapata, C.E., Perera, Y.Y., Houston, W.N. (2009), "Matric Suction Prediction Model in New AASHTO Mechanistic-Empirical Design Guide," Transportation Research Record: Journal of the Transportation Research Board, No. 2101, pp. 53-62.
- Zapata, C.E. and Houston, W.N. (2008), "Calibration and Validation of the Enhanced Integrated Climatic Model for Pavement Design," NCHRP Report 602, National Cooperative Highway Research Program, Transportation Research Board, Washington, D.C.